Geographical Variation and Evolution in the Middle Devonian Brachiopod, *MUCROSPIRIFER*

by

Delpfine Ellen Welch

Dissertation submitted to the Faculty of the

Virginia Polytechnic Institute and State University

in partial fulfillment of the requirements for the degree of

Doctor of Philosophy

in

Department of Geological Sciences

APPROVED:

Richard K. Bambach, Co-chairperson

Norman L. Gilinsky, Co-chairperson

E. Fred Benfield

Dewey M. McLean

Bruce Wallace

February 20, 1991

Blacksburg, Virginia

c.2

Geographical Variation and Evolution in the Middle Devonian Brachiopod, *MUCROSPIRIFER*

by

Delpfine Ellen Welch

Richard K. Bambach, Co-chairperson

Norman L. Gilinsky, Co-chairperson

Department of Geological Sciences

(ABSTRACT)

The Middle Devonian brachiopod, *Mucrospirifer*, was studied over most of its geographical and stratigraphical range in order to test the theory of punctuated equilibria. Punctuated equilibria holds that most evolution is concentrated in rapid speciation events and that the subsequent lifespan of a species is then characterized by approximate morphological stasis. Although many fossil lineages have been studied since the theory of punctuated equilibria was proposed, very few have included broad geographical coverage. To study a species adequately through time, the extent of its morphological variation in space must be known.

Specimens of *Mucrospirifer* were collected from New York, Ontario, Michigan, Pennsylvania, Maryland, and West Virginia from sandstones, siltstones, mudstones, calcareous shales, and limestones spanning 5-7 million years of geological history. Although many species of *Mucrospirifer* have been proposed, the most recent taxonomic work reduced the number to two and found that the overall shape of the shell and the shape of the fold and sulcus were the best criteria to distinguish species of *Mucrospirifer*. These same two criteria were applied in this study. Overall shape was examined by Fourier analysis of the outline of each usable adult specimen employing a video digitizing system assembled for this project. Selection of harmonics that contribute most to the shape of *Mucrospirifer* was aided by stepwise discriminant analysis, and only these harmonics were used in subsequent statistical analyses.

Shape differences among adult specimens cannot be attributed to allometry which was not significant when linear regression of log-transformed data for harmonic 0 (size) vs

harmonic 2 (shape) was applied. Using cluster analysis, polar ordination, and principal component analysis extensive continuous morphological variation of *Mucrospirifer* was detected over its geographical range as well as within populations, so that only a single polytypic species, *Mucrospirifer mucronatus*, could be identified. Although no strong correlation between morphology and lithology was found over the entire study area, using linear regression an east-west trend of increasing roundness was identified in New York state. This trend may be due to an adaptation to water turbulence that decreases from the nearshore in the east to the offshore in the west or to sediment type which becomes finer grained going from east to west. Using principal component analysis and linear regression, no significant directional change in overall shape could be detected. Therefore, morphological stasis characterizes the 5-7 million-year history of *Mucrospirifer mucronatus* in the study area. These findings lend substantial support to the theory of punctuated equilibria.

Acknowledgements

I thank my advisors, Richard Bambach and Norman Gilinsky, for their unfailing confidence in my abilities. Their "hands off" approach allowed me to choose and develop my own project and carry it through to its conclusion. I went down many blind alleys along the way, but am grateful for what it taught me. Thanks also to my committee members Fred Benfield, Dewey McLean, and Bruce Wallace. Niles Eldredge generously loaned me his field journal and encouraged me to pursue this project. I am grateful to John Costain who gave freely of his time to help me access the IMSL Fourier subroutines on the mainframe. Eric Smith of the Department of Statistics deserves special mention for his valuable advice on statistical procedures. Jim Light helped me sort out problems with the video digitizing system and Dan Smith built the "bat cave" in which it is housed. Cahit Çoruh generously loaned me his Tektronics 4107 terminal when mine "blew up" at a most inopportune time. Thanks also to Dean Heffner who kept me supplied with mainframe computer funds and solved other financial problems as they arose. Karen Hunt always knew what to do and then did it. Thanks to Llyn Sharp for keeping things running in the paleo lab and for help with photography. Sharon Chiang's drafting advice improved the quality of my slides and figures. Thanks to Belinda Pauley, Linda Bland, and Carolyn Williams for help when I needed it. My brother Dan spent a week with me each field season making an otherwise lonely and arduous affair almost fun.

My graduate student colleagues and friends, too numerous to mention by name, helped enrich my stay at Virginia Tech. Particular appreciation goes to special friends Linda Mae, Terry, and Rick who know me better than most and who were always there for me. Steve Miller encouraged me to persevere and helped me through the hard times. I thank my family for enstilling in me the importance of education.

Funding for this research was provided by Sigma Xi, the Scientific Research Society; the Geological Society of America; the Virginia Tech Graduate Research Development Committee; and the Appalachian Basin Industrial Associates (ABIA). The College of Arts and Sciences, Department of Geological Sciences, and ABIA provided funding for the video digitizing system. Fred Read generously loaned a video camera and tv monitor.

Table of Contents

List of Illustrations

List of Tables

INTRODUCTION

Almost two decades have elapsed since Eldredge and Gould (1972) proposed the theory of punctuated equilibria and challenged the hegemony of phyletic gradualism in evolutionary theory, yet considerable disagreement still exists (see Gould, 1985; Fortey, 1985; Gingerich, 1985; Gould and Eldredge, 1986). Much of the debate now centers on the relative importance of these two models for evolutionary change and the identification of factors that yield one or the other (Gould, 1985). The controversy has inspired many empirical studies of fossil lineages (e.g. Stanley and Yang, 1987; Geary, 1987; Wei and Kennett, 1988; Lich, 1990). However, very little work has included broad geographical coverage. The aim of this project is to test the theory of punctuated equilibria by studying a selected brachiopod lineage over as much of its preserved geographical and stratigraphical range as possible.

Eldredge and Gould (1972) maintained that the theory of phyletic gradualism, described as the origin of new species by the slow steady transformation of an ancestral population over a large part of its geographical range, has dictated paleontology's outlook on speciation. Under this theory, paleontologists have labored to find "unbroken fossil series" linking ancestor to descendant while attributing all morphological breaks in a purported lineage to an imperfect record. Eldredge and Gould (1972; Gould and Eldredge, 1977) asserted that most evolution is instead concentrated in very rapid speciation events that episodically

punctuate homeostatic equilibria. Punctuated equilibria holds that many breaks in the fossil record are not only real but are to be expected and that the norm for a species during its existence is morphological stasis or minor nondirectional fluctuations.

Punctuated equilibria is a theory of macroevolution, or the deployment of species in geological time, and is not constrained by a particular mode of speciation (Gould, 1982, 1985). Eldredge and Gould (1972) originally formulated their theory of punctuated equilibria as the expected geological consequence of the allopatric mode of speciation. In allopatric speciation a new species develops from a small subpopulation of the ancestor in an isolated, peripheral portion of the ancestral species' geographical range (Mayr, 1954, 1963). Speciation, then, would be largely an ecological and geographical process involving adaptation to local conditions, the development of isolating mechanisms, and alterations in the genome. In recent years, many evolutionists have come to believe that local demes within the geographical range of a species may have the required independence, like peripheral isolates, for potential speciation and in fact may be a more common method of speciation than the traditional allopatric mode (Gould, 1980). Other new models of speciation treat reproductive isolation as primary and nonadaptive, such as those based on chromosomal alterations (Bush, 1975, 1981; White, 1978; Carson, 1971, 1975, 1976; Templeton, 1980; Carson and Templeton, 1984). All of the above modes of speciation are compatible with the theory of punctuated equilibria (Gould, 1980, 1982).

Gould and Eldredge (1977) offered a protocol for the further testing of punctuated equilibria that included studying the geographical variation of individual species over their entire preserved ranges, not just in local sections. Simply examining local sections disregards the potential migration of populations with a shift in environmental conditions. A conclusion of phyletic evolution from observing a local section may therefore be unwarranted. When geographical variation is studied and is found to be slight compared to temporal change, a claim for gradualism may have credence. However, if geographical variation is more pronounced than temporal, an observed temporal "trend" may be insignificant.

Gould and Eldredge (1977; Gould, 1982) have repeatedly maintained that of the two claims of punctuated equilibria--geologically rapid origins and morphological stasis within established species--they regard stasis as the more important. Gradualistic bias has led to the neglect of stasis as data even though the phenotypic stability of an established species has been the basis of biostratigraphy (Gould and Eldredge, 1977). However, stasis is available for study and its documentation is critical for the potential validation of the theory of punctuated equilibria (Gould, 1982).

The Middle Devonian brachiopod, *Mucrospirifer*, fulfills several criteria necessary for a spatiotemporal study of evolution: it is well preserved; easily collectable; has a long history; and is found over a broad geographical range spanning many different environments. *Mucrospirifer* is common in the Middle Devonian rocks of the Appalachian and Michigan basins. Its morphology is highly variable and a dozen different species of *Mucrospirifer* have been proposed. However, previous semiquantitative work on specimens from Michigan, Ontario, and Ohio found an overlap in the range of variation suggesting that only two species, *M. mucronatus* and *M. thedfordensis* are valid and that the others are variations of these two. Although *M. mucronatus* from the Hamilton Group of New York is the type species and is considered an "index fossil" for the Middle Devonian, it has not been studied in detail in the Appalachian states.

I collected specimens of *Mucrospirifer* from its reported geographical range in Maryland, Michigan, New York, Ontario, Pennsylvania, and West Virginia from strata spanning 5-7 million years of its geological history. This is part of the same geographical and stratigraphical range over which Eldredge (1971, 1972) studied the trilobite genus *Phacops* which helped lead him to question the model of gradual phyletic evolution (Eldredge, 1971) and to propose the theory of punctuated equilibria (Eldredge and Gould, 1972). For each usable adult specimen I collected information on two species-discriminating features: overall shape of the shell and shape of the fold or sulcus. Overall shape was determined using Fourier analysis of each shell outline. Harmonics that contribute significantly to the shape of

Mucrospirifer were identified through stepwise discriminant analysis. Only these significant harmonics were used in subsequent statistical analyses.

Linear regression of log-transformed data for size (harmonic 0) vs shape (harmonic 2) led me to conclude that adult size has no significant effect on overall shape. Therefore, any observed shape differences can be attributed to geographical variation or evolution. Using cluster analysis, polar ordination, and principal component analysis, only a single, highly variable, polytypic species can be distinguished, *Mucrospirifer mucronatus*. Intrapopulational variation is as great as interpopulational variation. No directional change in overall shape was observed through linear regression and principal component analysis, even when each rock type was analyzed separately. There is a correlation between the more elongate forms and nearshore habitats and between the rounder forms and offshore habitats in New York state. Morphological stasis appears to characterize the 5-7 million-year history of *Mucrospirifer mucronatus* in the study area.

BACKGROUND

STRATIGRAPHY

Middle Devonian stratigraphy in the Appalachian and Michigan basins is complex. This is due both to differing approaches of state surveys, i.e. biostratigraphical vs lithostratigraphical correlation, as well as to extensive facies changes and repetition of units (Sevon and Woodrow, 1985). Cooper et al. (1942) assembled the first useful regional stratigraphical correlation chart for the Devonian of North America. Currently, the "Committee on Stratigraphic Units of North America" of the American Association of Petroleum Geologists is in the process of tabulating another. Sanford (1967), as part of the International Symposium on the Devonian System, published a stratigraphical correlation chart for Michigan and Ohio. Subsequently, Appalachian Basin stratigraphy was updated in 1969 by Oliver et al. and in 1985 by Sevon and Woodrow (Oliver et al., 1969; Sevon and Woodrow, 1985). Rickard (1975, 1981, 1984) has not only updated New York stratigraphy for the New York State Geological Survey, but has used borehole information to correlate the subsurface of southwestern Ontario, southeastern Michigan, northwestern Pennsylvania, northwestern Ohio, and western New York. Berg et al. (1983) have recently reissued a new state correlation chart for the Pennsylvania Geological Survey.

For the two stratigraphic correlation charts included here (Figure 1 and Figure 2), I have synthesized information from a number of sources (Baird, 1979; Berg et al., 1983; Brett et al., 1986; Cooper, 1942; Kesling et al., 1976; Rickard, 1975, 1984; Sanford, 1967; Sevon and Woodrow, 1985). The transect illustrated in Figure 1 extends from northern Michigan (lower peninsula) to southwestern Ontario through New York up to the Catskill Delta front. The transect illustrated in Figure 2 runs from westcentral Virginia through northeastern West Virginia to western Maryland and Pennsylvania to eastcentral New York.

Figure 3 shows the preserved outcrop of Middle Devonian rocks in the study area. The most extensive exposure is in New York where Middle Devonian rocks crop out from Albany to Buffalo. The New York section has been studied for over 100 years and formed the reference standard for North America until the middle of this century (Oliver and Klapper, 1981). Rickard (1981) commented that perhaps nowhere else in the world is the Devonian section as complete, undisturbed, well exposed and well studied as in New York. Consequently, stratigraphical correlation for New York is more refined than for the other states.

In New York the Hamilton Group is divided by thin limestone units (Stafford-Mottville, Centerfield, and Tichenor-Menteth) into four formations: the Marcellus, Skaneateles, Ludlowville, and Moscow (Figure 1 and Figure 2). These formations are further subdivided into members, most of which extend only over a limited area (Rickard, 1975, 1981, 1984). In far eastern New York, the lower Marcellus is composed of dark-gray sandy shale and is overlain by cross-bedded sandstone and shaly sandstone. The Skaneateles, Ludlowville, and Moscow consist of red and green sandstones with interbedded conglomerate (Cooper, 1957). This nonmarine part of the section was not included in my study and is not covered in the correlation chart. In central New York (Rochester to Cooperstown) the Marcellus is composed principally of black and gray shale with minor dark limestones. The Skaneateles is also primarily composed of dark shales with minor siltstone and sandstone and with a limestone unit at its base (Cooper, 1957; Rickard, 1975). The Ludlowville also begins with a thin limestone followed by dark shales overlain by silty and sandier units (Cooper, 1957; Rickard, 1975). Cooper (1957) described the Moscow as being principally composed of mostly somewhat silty

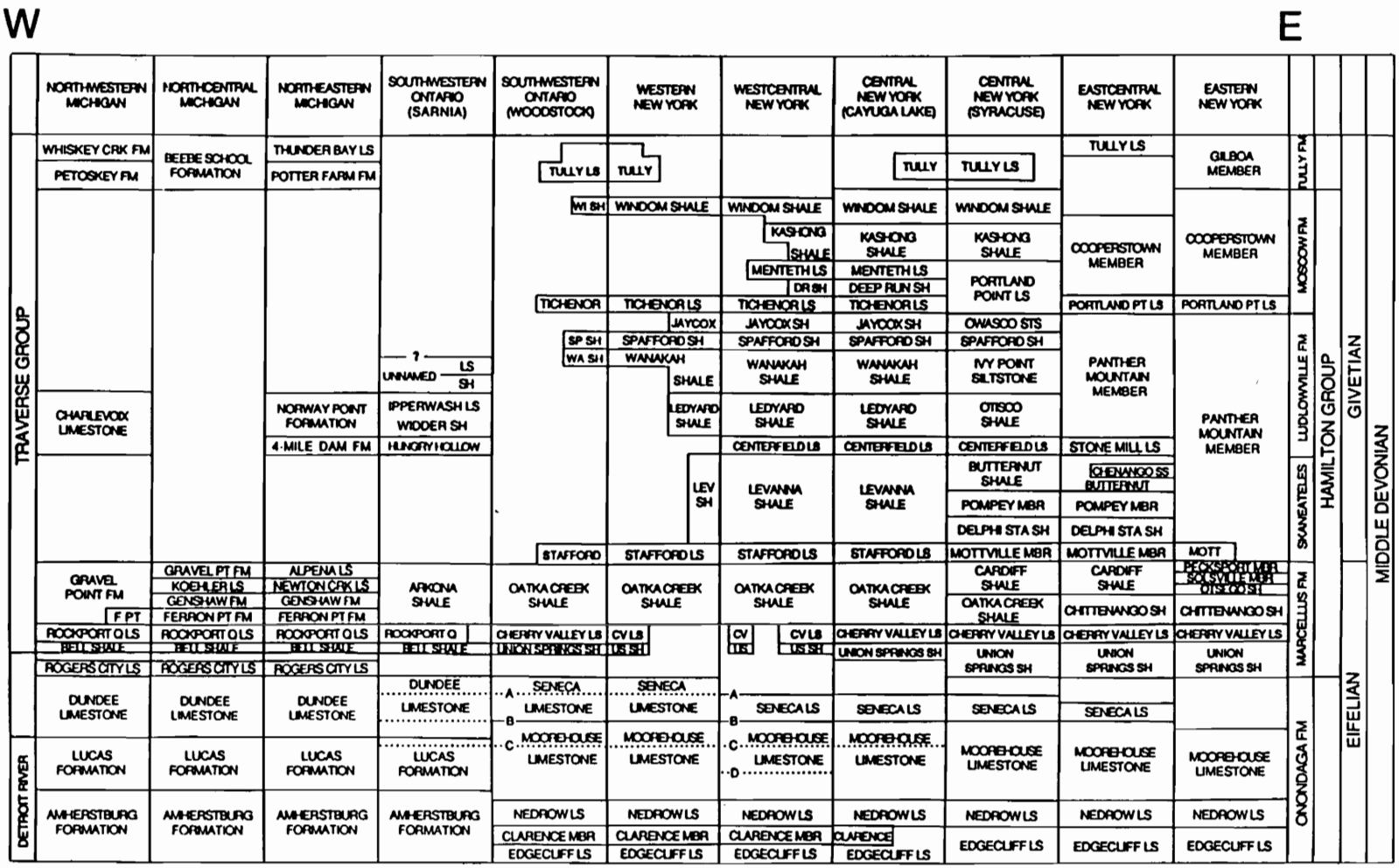

Figure 1. Stratigraphical correlation chart for Michigan, Ontario, and New York: Compiled from Baird (1979), Brett et al. (1986), Cooper (1942), Kesling et al. (1976), Rickard (1975, 1984), Sanford (1967).

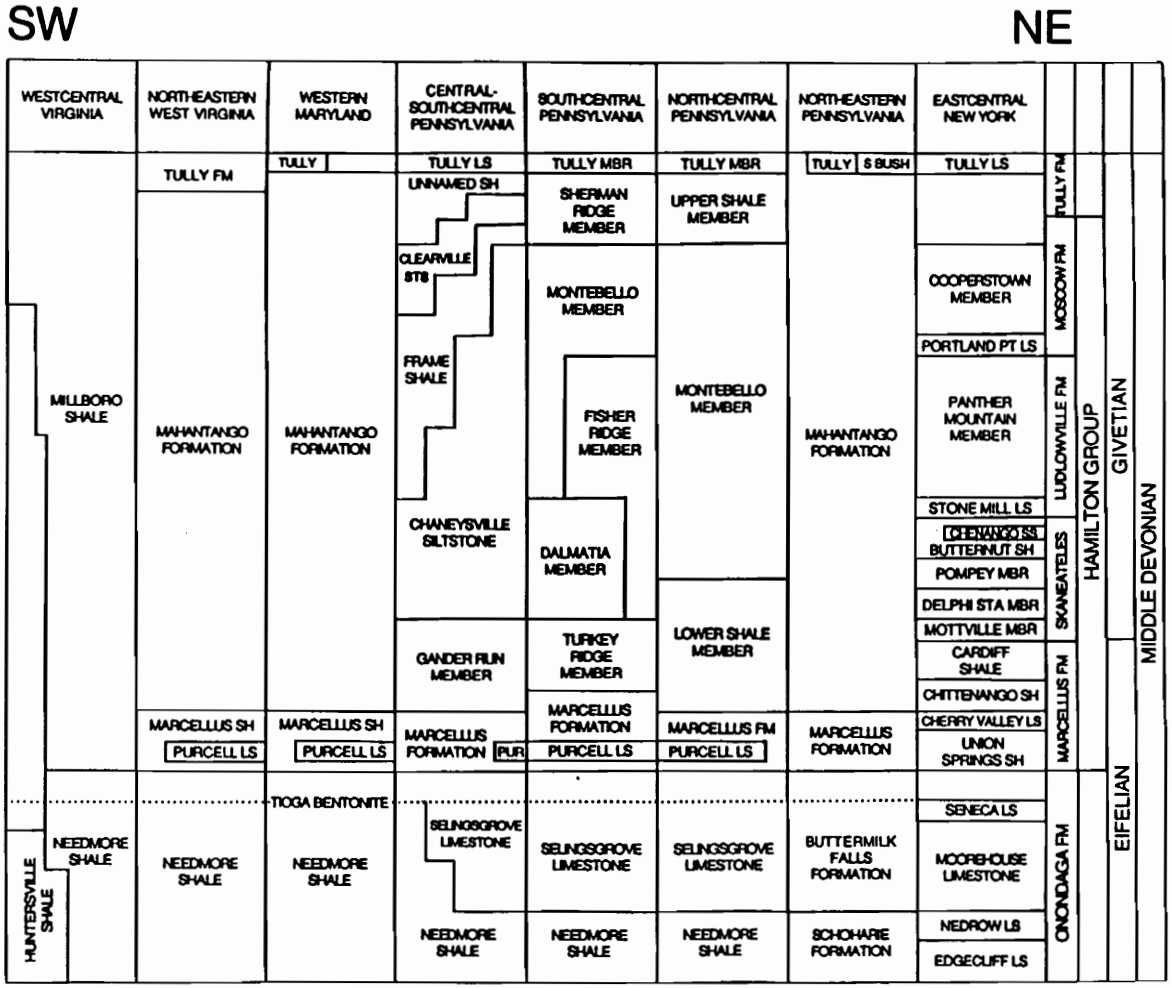

Figure 2. Stratigraphical correlation chart for Virginia, West Virginia, Maryland, and Pennsylvania: Compiled from Berg et al. (1983), Rickard (1984), Sevon and Woodrow (1985).

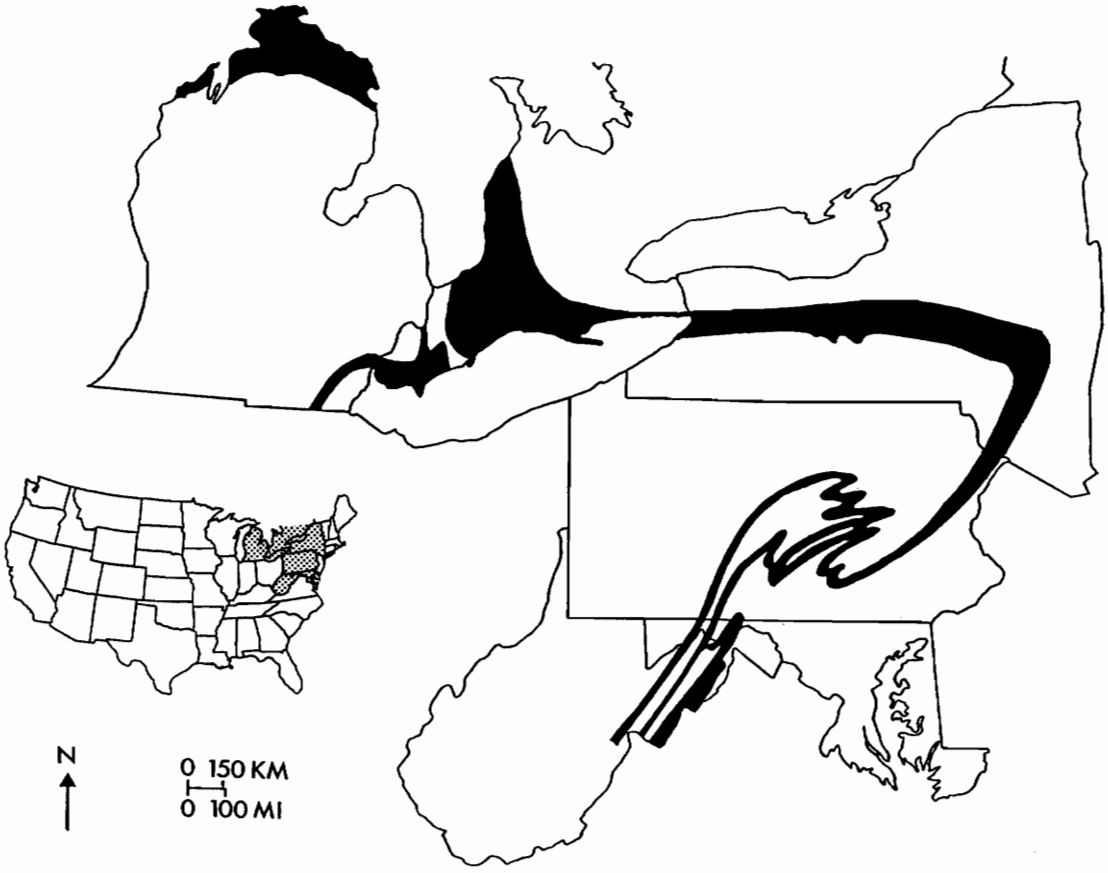

Figure 3. Outcrop pattern of Middle Devonian rocks in the study area (from Cooper, 1957).

shale. In western New York the Marcellus is composed entirely of black shale. The Skaneateles contains a limestone at its base, but otherwise is mostly dark shale, as is also true for the Ludlowville. The Moscow is much thinner in western New York and is mostly gray shale with a limestone at its base (Cooper, 1957).

Beneath Lake Erie, Rickard (1984) has traced the Union Springs Shale, Cherry Valley Limestone, and Oatka Creek Shale Members of the Marcellus into the Bell Shale, Rockport Quarry Limestone, and Arkona Shale of southwestern Ontario (Figure 1). The shales in Ontario are blue-gray and mainly calcareous (Sanford, 1967). The Skaneateles equivalent is missing in southwestern Ontario where the Arkona Shale is directly overlain by the crinoidal and coral-bearing Hungry Hollow Limestone. Cooper et al. (1942) correlated the Hungry Hollow with the Centerfield Limestone of New York based on fossil content (Figure 1). Rickard's later work (1984) neither confirms nor denies this correlation. Other Ludlowville equivalents are the calcareous gray Widder Shale and Ipperwash Limestone. The upper Ludlowville and Moscow equivalents are missing in southwestern Ontario (Cooper et al., 1942; Rickard, 1984).

In Michigan, the Hamilton Group equivalents are known as the Traverse Group; however, the uppermost units correlate with the overlying Tully Formation in New York (Figure 1). The Bell Shale and Rockport Quarry Limestone continue from Ontario into Michigan. The rest of the Marcellus equivalents--Gravel Point Formation, Ferron Point Formation, Koehler Limestone, Genshaw Formation, Alpena Limestone, Newton Creek Limestone--are composed of alternating limestones and calcareous shales (Sanford, 1967). The Skaneateles equivalents are not present. The lower Ludlowville equivalents are represented by the Charlevoix Limestone; the Norway Point Formation, alternating gray limestone and calcareous shale; and the Four-Mile Dam Formation, brownish-gray skeletal limestone alternating with shale (Sanford, 1967; Kesling et al., 1974). As in Ontario, the upper Ludlowville and Moscow equivalent rocks are missing from the section in Michigan (Cooper et al., 1942) (Figure 1).

In West Virginia, Maryland, and Pennsylvania, the Hamilton Group equivalents are known as the Marcellus Shale or Formation, which generally correlates with the lower half of the New York Marcellus Formation; and the Mahantango Formation, which in parts of Pennsylvania is further divided into members (Figure 2). The uppermost Mahantango correlates with the Tully Formation of New York and the lowermost with the Marcellus Formation of New York. The Mahantango Formation as originally described by Willard in 1935 consists mainly of dark gray to brown shale to fine-grained dark shaly sandstone (Ellison, 1965). In northcentral Pennsylvania, sixty percent of the formation is sandstone, confined almost wholly to the Montebello Sandstone Member. In central to southcentral Pennsylvania, the median unit is siltstone and shale, rather than sandstone (Ellison, 1965).

GEOLOGIC SETTING AND DEPOSITIONAL ENVIRONMENTS

During the Middle Devonian the Appalachian and Michigan basins were located at approximately 20-25°S (Scotese and McKerrow, 1990; Kent and Van Der Voo, 1990). The climate was warm to hot with geographically variable rainfall, comparatively high evaporation rates, and predominantly easterly winds (Woodrow et al., 1973).

Volcanism represented by the Tioga ashfall probably signalled the start of the Middle Devonian Acadian Orogeny (Faill, 1985). The ash beds can be traced across New York (Rickard, 1975, 1984), in the subsurface of northwestern Pennsylvania (Rickard, 1984) and in outcrops in the Valley and Ridge (Dennison and Textoris, 1978), in the subsurface of northeastern Ohio (Rickard, 1984), beneath Lake Erie, and in the subsurface of Michigan and Ontario (Sanford, 1967). Ettensohn (1985a) describes the Acadian Orogeny as a product of oblique convergence and periodic collision along a sinistral strike-slip fault zone between the North American craton and the Avalon Terrane which formed part of the larger Armorica plate. Major zones of deformation and topographical relief migrated southwest with each successive collision of the Avalon Terrane with a promontory of North America (Ettensohn, 1985a).

Ettensohn (1985a) refers to these periods of increased convergence or collision and associated delta development as "tectophases," with the second tectophase of the Acadian Orogeny in the Middle Devonian culminating in the collision of Avalon with the New York promontory.

According to Quinlan and Beaumont (1984), the Appalachian Basin is a multistage foreland basin developed by lithospheric downwarp under the loads of the Taconic, Acadian, and Alleghanian thrust sheets that formed the Appalachian Mountains. The flexural interactions between the Appalachian Basin and the intracratonic Michigan and Illinois basins formed the interbasin arches (Kankakee, Findlay, Algonquin, Cincinnati) and domes (Jessamine and Nashville). In this interpretation the foreland basin is the flexural downwarp and the arch or dome is the associated peripheral bulge. Quinlan and Beaumont (1984) consider that the load of the orogenic thrust sheets may have been sufficient to depress the lithosphere over a wide enough area to incorporate an adjacent intracratonic basin into the foreland basin. The arches and domes were episodically either emergent or submergent, resulting in the alternating yoking together and decoupling of the foreland basin and intracratonic basins. Episodes of uplift of the interbasin arches are associated with orogenic quiescence while episodes of submergence of the arches are associated with emplacement of overthrust loads on the margin (Quinlan and Beaumont, 1984; Quinlan, 1987; Beaumont et al., 1988). During the second tectophase, the Appalachian foreland basin expanded and migrated westward (Ettensohn, 1985a); the Findlay and Algonquin arches were depressed and the Michigan Basin was linked to the Appalachian Basin (Quinlan, 1987; Beaumont et al., 1988).

During the second tectophase of the Acadian Orogeny the Late Eifelian-Givetian sediments of the Hamilton Group in New York and its equivalents elsewhere in the Appalachian and Michigan basins were deposited, recording 5-7 million years of geological history (Ettensohn, 1985a; Rickard, 1975, 1984; Sevon and Woodrow, 1985). In the Appalachian Basin the Hamilton Group is an eastward thickening and coarsening wedge of marine shales, siltstones, and sandstones punctuated by thin widespread carbonates (Rickard, 1975, 1981). In New York the Hamilton Group ranges in thickness from 80 m (260 ft) at Lake Erie to over

850 m (2800 ft) at the Catskill Delta Front (Hudson River) (Rickard, 1981). The muddy sediments of western New York gradually slope eastward toward the structural basin in westcentral New York and the coarser-grained sediments of eastern New York slope westward (Brett and Baird, 1985). The deposits thin going southwest from New York and Pennsylvania and east to Tennessee, and change from coarser marine clastics to finer gray and black marine shales. Faill (1985) noted that the absence of coarse detritus in the southern part of the basin suggests that the Acadian Orogeny did not extend further than Virginia in the Middle Devonian. In Michigan, the Hamilton Group equivalents (the shales and limestones of the Traverse Group) are thickest in central and northwestern Michigan (210-240 m, 700-800 ft) and thin to the south and east. The equivalent strata in Ontario are 90 m (300 ft) thick near Lake Huron and slope gradually eastward to where they thin to 30 m (100 ft) beneath central Lake Erie (Sanford, 1967).

Ettensohn (1985a) recognizes four stages in the second tectophase. The first stage is marked by the onset of tectonism. Uplift of the Appalachian Mountains creates an orogenic barrier which decreases precipitation on the western side of the mountains. Subsidence in the foreland basin outstrips sedimentation, creating a deep basin with restricted vertical and horizontal circulation, and resulting in deposition of organic-rich black or dark shales. These relatively unfossiliferous rocks are referred to as the "Marcellus Facies" (Rickard, 1981). The dysaerobic to anaerobic dark shales intertongue westward with and replace the aerobic carbonates below (Ettensohn, 1985a, 1985b).

Increased collision and decreased subsidence highlight stage 2. Sedimentary subcycles within this stage change upward from dark shales to blue-gray and gray-green shales to siltstones and fine-grained sandstones to limestones. This stage is correlated with the fossiliferous marine rocks of the "Hamilton" and "Moscow" facies. These facies were deposited on the subtidal shelf in a number of different environments (Rickard, 1981). The inferred environments represent a change from somewhat anaerobic to dysaerobic in the prodelta, to aerobic in the delta front and delta platform, to shallow water delta destruction as water depth decreased and oxygenation increased. There are four of these subcycles in the New York

Hamilton Group, essentially equivalent to the four formations (Ettensohn, 1985a). On the western edge of the Michigan Basin, a back reef restricted environment of scattered lagoons and sabkhas is indicated (Gardner, 1974; Nunn and Sleep, 1984; Fisher et al., 1988).

Stage 3 is marked by a regional disconformity due to collision and uplift, while stage 4 begins a period of tectonic quiesence represented by carbonate deposition in slowly transgressing waters. Rocks of the Late Givetian Tully Limestone characterize stage 4 and mark the end of Hamilton Group deposition (Ettensohn, 1985a).

PALEOECOLOGY

Mucrospirifer (Figure 4) is a common brachiopod in the Middle Devonian Hamilton Group strata in the Appalachian and Michigan basins. It can be found in a wide range of rocks including clastics varying in coarseness from clay- to sand-sized grains, and carbonates varying from calcareous shale to relatively pure limestone. Cooper (1957) noted that *Mucrospirifer* is common in all marine environments, except in black shale where it is rare. The faunal associations of *Mucrospirifer* are also varied. In a synthesis of previous paleoecological studies which named over 70 fossil "communities" in the Hamilton Group of New York and incorporating unpublished work, Brett et al. (1986) recognized seven biofacies, three of which include *Mucrospirifer* as a dominant member. Each community is of moderate species diversity (30-50 species).

Mucrospirifer is common in the *Athyris* Biofacies which also includes the brachiopods *Athyris* and *Devonochonetes*, stereolasmatid corals, fenestellid bryozoans, medium-sized protobranch, modiomorphoid, and endobyssate pterioid bivalves, archaeogastropods, phacopid trilobites, and some flexible and adunate crinoids. This biofacies is typical in medium-gray claystones to silty mudstones and often has shell-rich beds. It is characterized by moderate water depths of 30-50 m in the lower storm wave base (Brett et al., 1986). How-

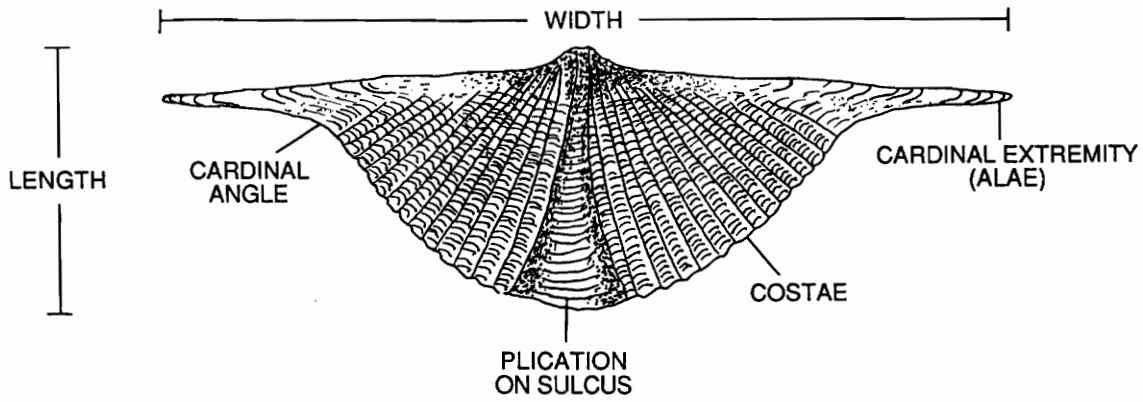

Figure 4. Morphological terminology applied to *Mucrospirifer*.

ever, they were normally quiet waters with fairly low turbidity. Although the bottom waters were aerobic, the upper sediments were dysaerobic.

A second biofacies, the *Mucrospirifer*-chonetid Biofacies, is often dominated by *Mucrospirifer* and *Devonochonetes* and/or minor trilobites. This biofacies is common in medium-gray silty mudstones and muddy siltstones. The *Mucrospirifer*-chonetid Biofacies interfingers with the *Athyris* Biofacies. The water depths of the two biofacies were similar, but the *Mucrospirifer*-chonetid Biofacies was characterized by a higher sedimentation rate, greater amounts of silt, and high turbidity. Shallow burrowing was abundant and the substrate was probably unstable.

The *Tropidoleptus* Biofacies is dominated by brachiopods including *Tropidoleptus, Devonochonetes, Longispina, Mucrospirifer, Athyris, Meristella,* and *Spinocyrtia. Pseudoatrypa* and some strophomenids are rare. Bivalves such as *Cypricardella, Modiomorpha, Ptychopteria,* and *Glyptodesma* are also common. The tabulate coral *Pleurodictyum* may be large and common. Also present are ramose and fistuliporoid bryozoans, phacopid and proetid trilobites, platycerid gastropods, crinoids, and blastoids. This biofacies is found in medium to light bluish gray, soft, bioturbated, blocky, and moderately to sparsely fossiliferous mudstones or muddy siltstones. Coquinites may be present, some with grading, and gutter casts. Water depths for the *Tropidoleptus* Biofacies are interpreted typically to have been 20-30 m (Brett et al., 1986). The muddy to silty bottom was aerobic and often swept by epeiric storm waves.

Mucrospirifer (Figure 4), like most other articulate brachiopods, is an epifaunal suspension feeder. It is often described as free lying or reclining (Grasso, 1981; Brower et al., 1978). However, *Mucrospirifer* was pedunculate until late in its ontogeny. Cowen (1968) studied the delthyrial cover of *Mucrospirifer mucronatus* using well-preserved specimens collected from the Traverse Group, Michigan, and housed in the Sedgwick Museum, Cambridge, England. He found a unique delthyrial structure which he named stegidial plates. Stegidial plates are independent plates secreted by and held in place by the mantle, unlike deltidial

plates which are continuations of the interarea and are therefore integral parts of each valve. The stegidial plates join medially to form a pedicle foramen and later in ontogeny the ventral plates extend completely around the pedicle at which point the pedicle must have ceased to grow in absolute size. Shell material continued to be added to the ventral plates facing the foramen and the opening decreased in size. Cowen (1968) noted that the development of delthyrial structures and the hinge line are closely related. At the same time that alae were formed by accretion at the cardinal angles, the pedicle became surrounded by the stegidial plates. Cowen (1968) suggested that the alae must have helped stabilize the shell on the sediment surface since the development of this secondary stabilizing structure coincides with the decline of the primary stabilizing structure, the pedicle. Rudwick (1970) suggested that spiriferids like *Mucrospirifer*, without a large flat interarea to rest on, used the alae like skis to stabilize the shell in soft sediment.

From study of living brachiopods, Thayer (1981) found that the attachment strength of the pedicle is not closely correlated with the size of the pedicle foramen because anchorage is often by rootlets. Since the nature of the pedicle in *Mucrospirifer* is not known, it can be postulated to have had a similar pedicle. Thayer (1981) also suggested that many brachiopods may have attached to nonpreservable "hard" objects (such as worm tubes) when young. Schumann (1967) found that *Mucrospirifer* did live attached to dead corals or bryozoans. Schumann (1967) determined the life position and feeding currents of *Mucrospirifer reidfordi* from the location of commensal *Cornulites* on its shell and the disruption of marginal shell growth. Incurrent water entered the shell laterally and exited medially.

PALEONTOLOGY OF *MUCROSPIRIFER*

Mucrospirifer is biconvex, generally highly alate with cardinal extremities commonly mucronate (extended into sharp points), having numerous lateral costae, and bald fold and sulcus or with a median ridge in the sulcus and a median groove in the fold (Figure 4).

Growth begins at the beak and continues anteriorly and laterally. Growth lines are strongly imbricated. Late in ontogeny the viscera withdraw from the cardinal extremities and shell material is instead deposited at the cardinal angles. Casts made from interior molds clearly show the later growth lines at the cardinal angles (Figure 5). Perhaps the fact that most specimens of *Mucrospirifer* are found without the cardinal extremities is partly due to the differential between the weaker cardinal extremity and stronger cardinal angle. The cardinal angle becomes a natural breakpoint.

Raymond (1904) studied the ontogeny of *Mucrospirifer mucronatus* from New York by constructing a series representing the shell in all stages of growth. The protegulum is circular, somewhat convex, with a curved hinge. As growth continues the shell becomes more oval and remains smooth. The sulcus and fold are then added with two initial costae on each side. Costae continue to be added in pairs outside of the older ones. The hinge line continues to widen and the cardinal extremities become accuminate. By the time what Raymond (1904) refers to as "adolescence" is reached, strong mucronate points have developed.

PREVIOUS SYSTEMATIC WORK

In 1841 in the Fifth Annual Report on the Paleontology of the State of New York, T. A. Conrad proposed the new species, *Delthyris mucronatus*. Since that time, the generic name for the species has been referred to first as *Spirifer*, then *Mucrospirifer*, and a dozen different species have been proposed. James Hall illustrated the range of morphologies for *Mucrospirifer* in New York, reproduced here as Figure 6.

Shimer and Grabau (1902) named *Spirifer mucronatus* var *arkonensis* and *S. mucronatus* var *thedfordensis* based on their work in the Hamilton Group equivalents of the Thedford region, Ontario. They described *S. mucronatus* var *arkonensis* from the lower Hamilton as extremely elongate, reaching a width as great as 75 mm and a height of 18 mm. It differs from *S. mucronatus* of New York by being attenuated at the cardinal extremities in the

Figure 5. Cast of specimen N1104 showing growth lines of shell material deposited at the cardinal angle.

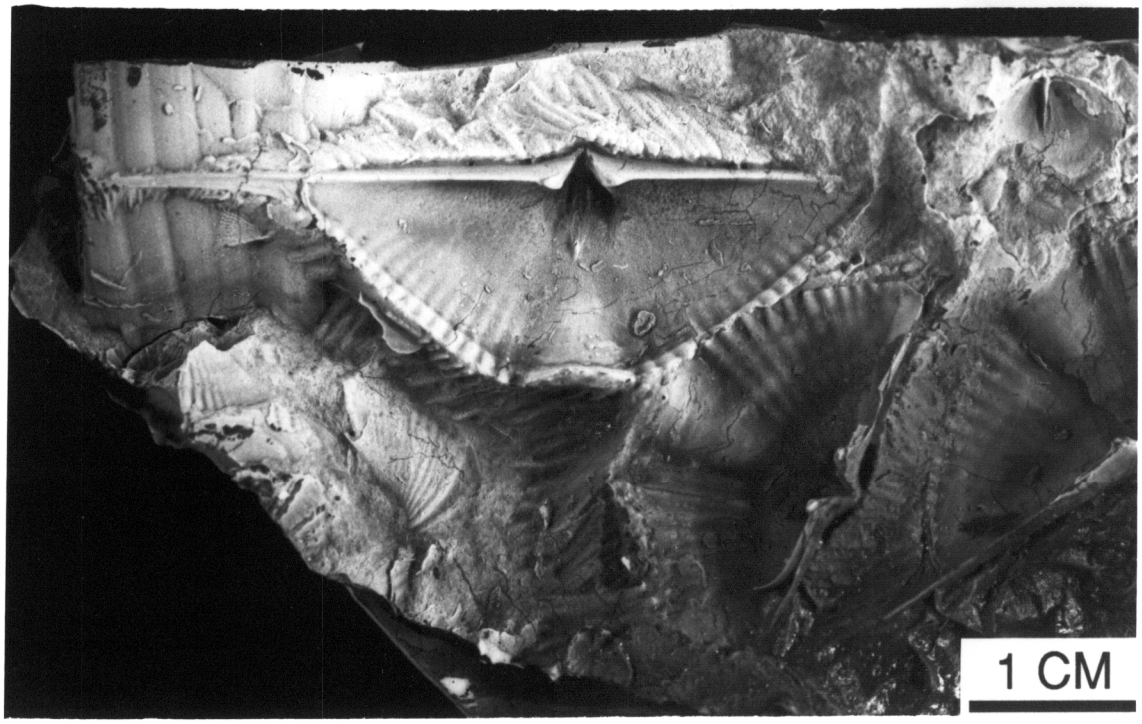
1 CM

Figure 6. Range of morphologies of *Mucrospirifer* in the Hamilton Group of New York (from Hall, 1867).

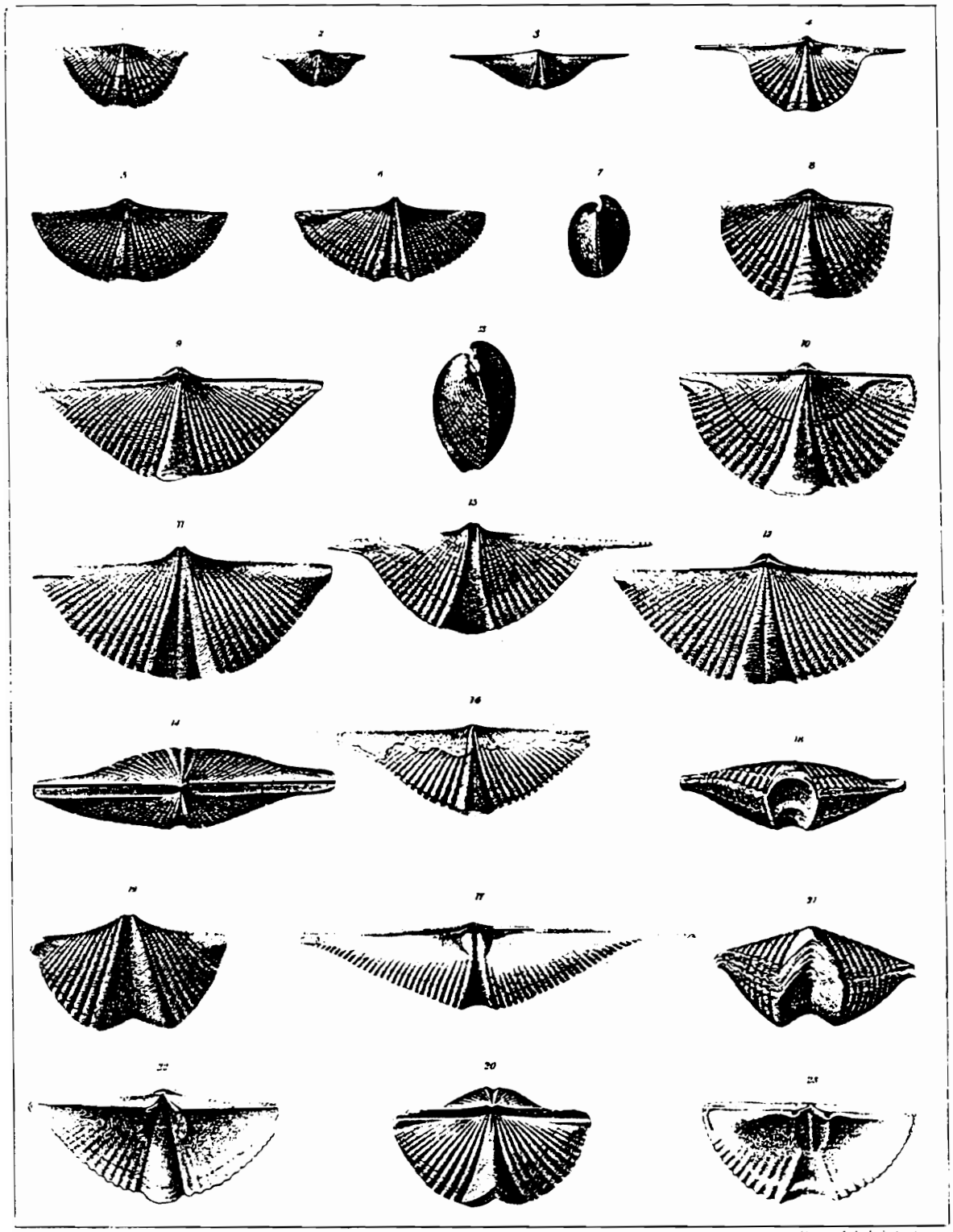

adult stage, rather than being mucronate. They noted, however, that *S. mucronatus* var *arkonensis* is strongly mucronate immediately prior to the adult stage when additional lamellae are added.

S. mucronatus var *thedfordensis*, a variety with much variation, was proposed by Shimer and Grabau (1902) from specimens collected in the upper Hamilton and based on a study of its development (ontogeny). As an adult, it is robust with pronounced fold, sulcus, costae, and concentric growth lines. Shimer and Grabau (1902) contrasted *S. mucronatus* var *thedfordensis* with *S. mucronatus* of New York which they felt is less robust with less pronounced and regular growth lines and retains a sulcus with a medial ridge and a fold with a medial groove throughout its development.

In 1910, Grabau and Reed named one species, two varieties, and two "mutations" from the Hamilton Group equivalent rocks in Ontario and Michigan. The designations were based on shell indices determined by dividing the length of the pedicle valve by the width, indicated in parentheses as follows: *S. profundus* Grabau (2-1), *S. profundus* mut. *intermedia* Grabau (1.58-1.41), *S. profundus* mut *lata* Grabau (2), *S. mucronatus* var *attenuatus* Grabau (3.27-1.76), *S. mucronatus* var *multiplicatus* Grabau (2.12-1.27).

Mook (1915) used length/width ratios in a study of variation in four previously described "mutations" of *S. mucronatus* from Michigan and the Thedford region of Ontario (*multiplicatus, profundus, thedfordense, attenuatus*), and a fifth described for the first time in his paper and credited to Grabau (*alpenense*). *S. mucronatus alpenense* occurs in the lowest shale beds of the Michigan Hamilton Group; *S. mucronatus multiplicatus* in the limestones above or alternating with the *alpenense* shales; *S. mucronatus profundus* and *S. mucronatus attenuatus* co-occur in the upper Michigan shales; *S. mucronatus thedfordense* is found in the upper Hamilton shales of the Thedford region. He concluded that the primitive *S. mucronatus* gave rise to two lines of evolution: one deriving *profundus* and *thedfordense* from *alpense* and the other including *attenuatus* and *multiplicatus*. Both lines show a reduction in shell index, number of costae and shell width, a loss of groove and ridge on fold and sulcus, a strengthening of growth lines and costae, and a deepening of the sulcus (Mook, 1915).

Stewart (1927) described *S. mucronatus* var *prolificus* from the Silica Shale, a Hamilton Group equivalent, in Lucas County, Ohio. Although this variety is very similar to *S. mucronatus* var *thedfordense*, it differs in rarely having a ridge developed in the sulcus and commonly retaining a groove in the fold, although either situation can be found in specimens of *S. mucronatus* var *thedfordense*. Stewart remarks that specimens here assigned to *S. mucronatus* var *prolificum* exhibit such a range in their characteristics that she found it difficult to arrive at satisfactory conclusions regarding its common features.

In 1956, Stumm published revised descriptions and illustrations of Grabau's species based on the original specimens from the Traverse Group and elevated them to species rank (*Mucrospirifer alpenensis, M. multiplicatus, M. attenuatus, M. profundus, M. grabaui, M. latus*). He also described and illustrated *M. prolificus* Stewart from the Silica Shale of Ohio and the Traverse Group of Michigan. Stumm stated that several nonconspecific species from the Ludlowville and Moscow formations of the Hamilton Group of New York and the Appalachian region have been assigned to *M. mucronatus*. He suggested limiting *M. mucronatus* only to the very short wide form with a medial groove in the sulcus and a medial ridge in the fold and an average of 20 costae on either side of the fold or sulcus.

Stumm (1956) divided Grabau's species into three lineaages that are characterized by the nature of the fold and sulcus. The *M. alpenensis* lineage is distinguished by a wide and shallow sulcus with a flat base and no medial ridge. The fold is low and relatively flat, generally without a medial groove. The species included in this lineage are *M. alpenensis* and *M. prolificus* Both are found in the calcareous shales of the lower Traverse Group of Michigan while *M. prolificus* also occurs in the Silica Shale of northwestern Ohio and southeastern Michigan. The two species are identical except that *M. prolificus* has a wider interarea between the beaks and a narrower apical angle in the delthyrium. The *M. multiplicatus* lineage is marked by a fold and sulcus with distinct medial ridge and groove, respectively (Stumm, 1956). *M. multiplicatus* and *M. attenuatus* are placed in this lineage. *M. multiplicatus* is found in the Genshaw Formation and *M. attenuatus* occurs in the Norway Point Formation, both in the Thunder Bay region. *M. attenuatus* differs from *M. multiplicatus* in having a narrower

interarea, and a shorter and thinner shell with finer costae. Stumm (1956) noted that species of this lineage closely resemble the *M. mucronatus* type species from New York, except that *M. multiplicatus* does not have distinct mucronate points at the cardinal extremities and its shell is thicker with fewer and coarser costae.

The *M. profundus* lineage is characterized by a low, convex fold and a deep, V-shaped sulcus (Stumm, 1956). *M. profundus, M. grabaui* (formerly *S. profundus* var *intermedia*), and *M. latus* are placed here. *M. profundus* occurs in the Norway Point, Potter Farm, and lower Petoskey formations. *M. grabaui* is found in the Four-Mile Dam, Potter Farm, Gravel Point, and lower Petoskey formations. *M. grabaui* var *A* is confined to the lower blue shale of the Gravel Point Formation in Bell Quarry. *M. latus* occurs in the Alpena Limestone and the Norway Point and Potter Farm formations. *M. profundus* lacks wings and mucronate points, is relatively narrow, and has a small number of coarse costae. It is quite distinct from the other species in the lineage. *M. grabaui* is larger than *M. profundus* and is more variable. *M. grabaui* var *A* differs in being alate rather than mucronate. *M. latus* has more and finer costae than *M. grabaui* as well as more gradually tapering mucronate points (Stumm, 1956).

The most recent systematic work is that of Tillman (1964) who studied the variation of *Mucrospirifer* from the Middle Devonian rocks of Michigan, Ontario, and Ohio by measuring previously described species and constructing histograms for each set of measurements. Tillman studied characters emphasized in previous descriptions: number of costae, width of costae, length of interarea, presence or absence of medial ridge in the sulcus and medial groove on the fold, presence or absence of mucronate points at the cardinal extremities, size of shell, width/length ratios, and the shape of the fold and sulcus.

Tillman (1964) concluded that number of costae depends on the age and/or size of the individual, as does length of interarea. Width of costae was not constant even within a given population. Development of the medial ridge and groove in the sulcus and fold, respectively, was quite variable except in specimens from the Arkona Shale and Genshaw Formation where they are usually well formed. In observing growth lines on individual specimens, Tillman found that all previously described specimens of *Mucrospirifer* are mucronate at some stage

in their development. This includes specimens from the Arkona Shale which as adults do not appear mucronate because of the addition of lamellae that decrease the degree of deflection at the anterior border at the cardinal extremities and increase the shell thickness without significantly changing the length or width of the specimen. Because the cardinal extremities are rarely preserved and the growth lines are very difficult to trace, Tillman determined width/length ratios to be of doubtful value. He found that as the angle made by the plane of commissure at the fold increases, the height of the fold decreases, and he also found that angle to be highly variable in all populations.

The shape of the fold and sulcus and the shape and general proportions of the shell were the characters determined by Tillman (1964) to be most useful in distinguishing species. Because he observed such an overlap among the species in the range of variation for the characters studied, Tillman felt that no more than two species could be identified. Tillman retained the species *M. mucronatus* and *M. thedfordensis* and considered all the rest to be variations of these two. He placed *arkonensis, attenuatus, multiplicatus, alpenensis,* and *prolificus* into synonymy with *M. mucronatus*; and *thedfordensis, profundus, intermedia, latus,* and *grabaui* into synonymy with *M. thedfordensis.*

Tillman (1964) states that *"M. mucronatus* (Conrad) differs from *M. thedfordensis* (Shimer and Grabau) in having a broadly U-shaped sulcus with flattened floor and subangular edges and a gently convex to flattened fold"; *"M. thedfordensis* (Shimer and Grabau) differs from *M. mucronatus* (Conrad) in having a U-shaped to V-shaped sulcus, never with a flattened floor; a low moderately convex fold, never with a flattened surface." Tillman also described a new species, *M. norwoodensis*, from a small number of poorly preserved specimens that closely resemble *M. consobrinus* d'Orbigny.

METHODS

FIELD COLLECTION

Specimens of *Mucrospirifer* were collected from a variety of litho- and biofacies from Hamilton Group rocks in New York, and from equivalent strata in southwestern Ontario, northern Michigan (lower peninsula), Pennsylvania, western Maryland, and northeastern West Virginia. Figure 7 shows the geographical distribution of samples used in this study. Table 1 lists localities and numbers of specimens. Collecting sites were chosen primarily from published locality lists. No single locality exposes the entire stratigraphical section. Each site instead represents a small portion of Hamilton and equivalent strata. Because of the differences in stratigraphical resolution among regions and also because of differences in completeness of section, the study area is divided into four horizons: A, B, C, and D, equivalent to the four formations of the Hamilton Group of New York. Stratigraphical location of samples and lithology of the enclosing rock is displayed in Figure 8. Lithologies include sandstones, siltstones, and mudstones in the Appalachian Basin; calcareous shales and limestones in the Michigan Basin. A locality register is given in Appendix A.

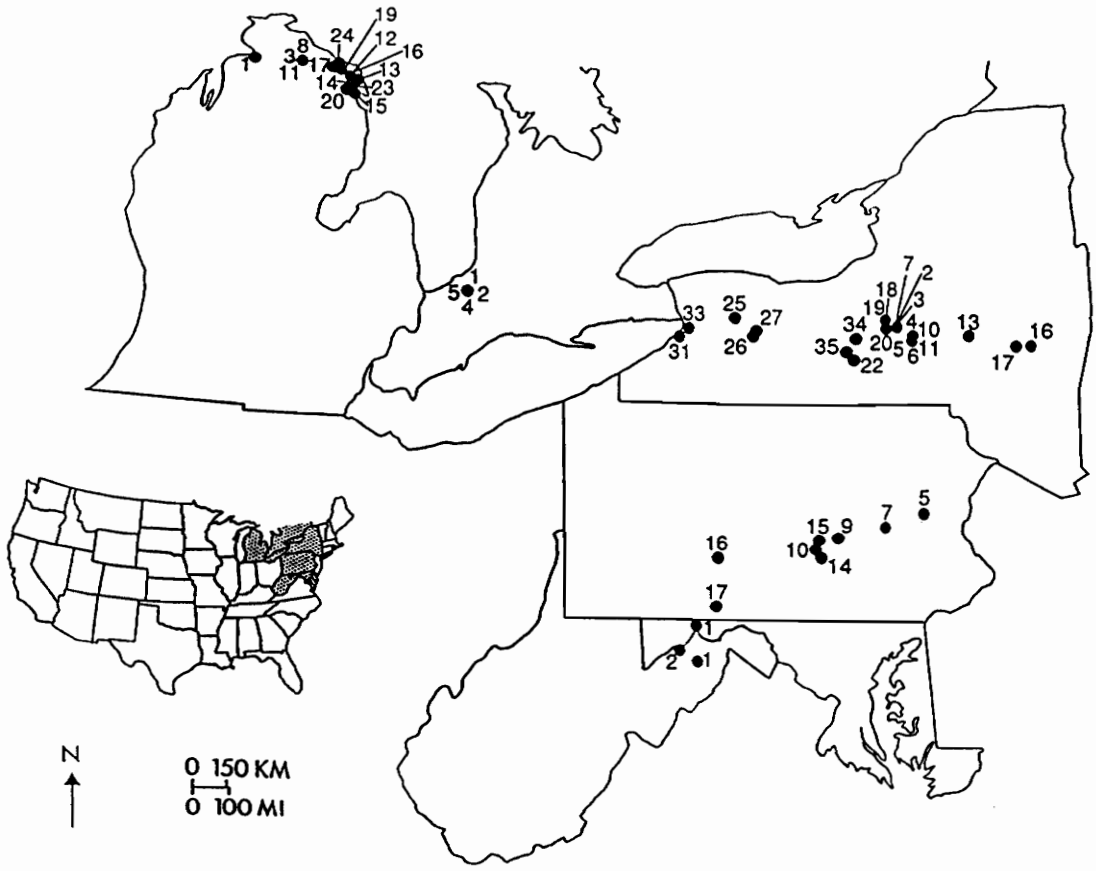

Figure 7. Geographical location map: Collection sites indicated by dots and locality numbers.

Table 1. List of localities and numbers of specimens for each locality.

LOCALITY	SPECIMENS
NEW YORK	
N02	25
N03	22
N04	11
N05A	20
N05B	14
N06	15
N07	18
N10	24
N11	22
N13	09
N16	01
N17	24
N18	17
N19	11
N20	17
N22A	03
N22B	10
N22C	02
N22D	07
N25	02
N26	02
N27	05
N31	20
N33	17
N34A	09
N34B	03
N34C	13
N34D	03
N34E	02
N34F	06
N34G	10
N35A	01
N35B	08
TOTAL = 373	

LOCALITY	SPECIMENS
ONTARIO	
O01A	18
O02A	04
O02C	22
O04	10
O05	15
TOTAL = 69	
MICHIGAN	
M01	20
M03	07
M08	04
M11	03
M12	05
M13	05
M14	04
M15	07
M16	01
M17	04
M19	03
M20	02
M23	10
M24	02
TOTAL = 77	
MARYLAND/WEST VIRGINIA	
D01	03
D02	07
W01	09
TOTAL = 19	
PENNSYLVANIA	
P05	06
P07	03
P09	01
P10	06
P14	09
P15	02
P16	02
P17	05
TOTAL = 34	
GRAND TOTAL = 572	

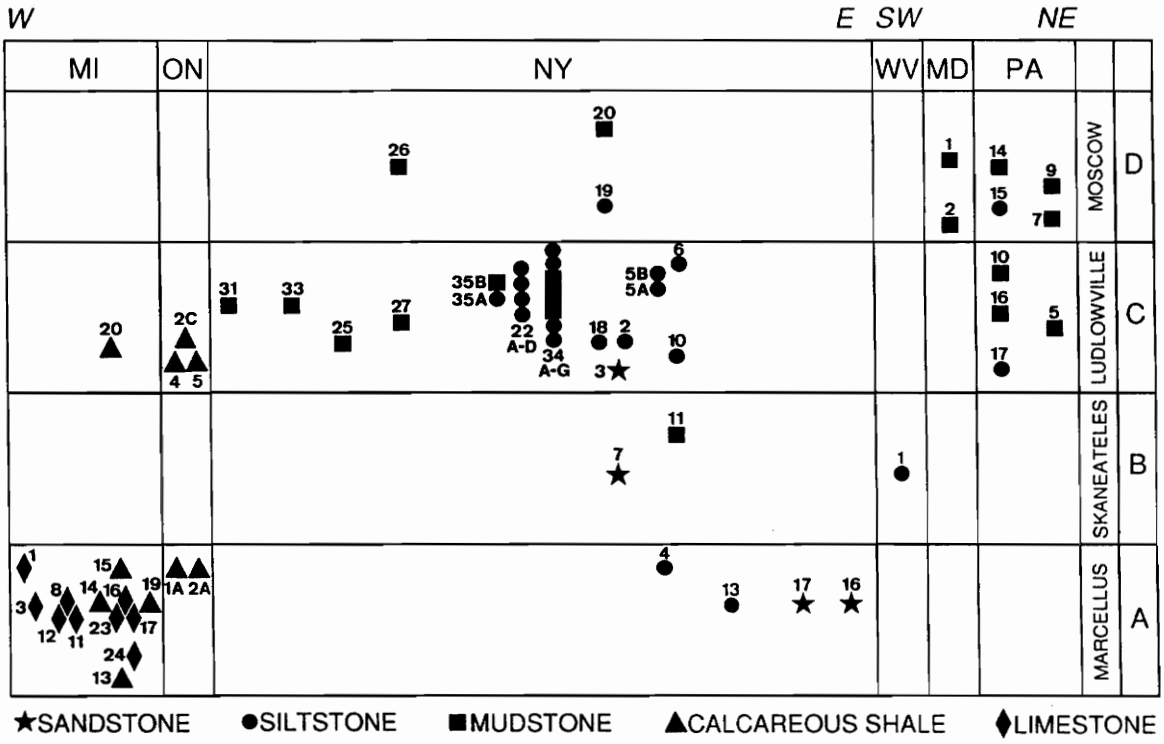

Figure 8. Stratigraphical location chart: All sampling localities plotted according to stratigraphic and geographic distribution. Symbols refer to lithologies of localities as given in the figure.

LAB PREPARATION

Collected specimens include both molds and the original whole shell. Preservation by internal and external molds was more common for specimens from the Appalachian Basin while the original whole shell, free from the rock matrix, was often found in the Michigan Basin. All specimens were washed and scrubbed. Where necessary, rocks were split to expose molds of the valves. A vibrotool and wheel-type dental saw were used to remove rock covering the valves. Where the mold was obscured by shell material, the rock was soaked in HCl to remove the shell and expose the mold. Casts of silicone rubber were made of molds of selected specimens.

MORPHOMETRIC DATA COLLECTION

I collected two pieces of morphometric data for each specimen: the overall shape of the shell, as expressed in its outline; and the shape of the fold and/or sulcus. These are the two features of *Mucrospirifer* that Tillman (1964) determined to be most useful in distinguishing species. For the shape of the fold and/or sulcus, Tillman's two categories were used: (1) broadly U-shaped and subangular, possibly with a flattened floor; and (2) U- or V-shaped, never with a flattened floor. All specimens were examined by eye and placed in one of the two categories. Overall shape was determined for each specimen by Fourier analysis of the outline. Traditionally, shell dimensions and point-to-point linear measurements have been used in morphometric studies. However, as Scott (1980) pointed out, this was probably due more to instrument limitations and to precedent than to theoretical restrictions. With the advent of microprocessors and electronic digitizers and their widespread availability, it is now possible to quickly and inexpensively quantify the complexity of organic shape. The outline

of the shell is here taken to be the best two-dimensional planar representation of overall shape.

Outline data were collected using a video digitizing system assembled in the course of this project (Figure 9). The system consists of a Compaq Deskpro 286 personal computer equipped with a math coprocessor (80287), an Imaging Technology PCVISION*plus* frame grabber, and the Jandel Scientific video analysis software, JAVA version 1.31; a high resolution Panasonic CT-1320M monitor; a Cohu 5182 video camera with lens and extension tubes mounted on a copy stand; a Jandel Scientific 12 x 12 high resolution electromagnetic digitizing tablet and puck; and assorted lights. The computer was linked to the mainframe IBM 3090 for direct transfer of data.

To prevent ontogenetic allometry from biasing results only adult specimens were measured. Each specimen was oriented under the camera with the plane of commissure parallel to the focal plane of the lens and the hinge line closest to the operator. Where necessary to increase detail, the specimen was blackened with a graphite compound and then whitened with magnesium oxide. A grid on transparent film was placed over each specimen in order to scale for size while calibrating. The brachial valve was measured when possible since it is somewhat less convex than the pedicle valve and should therefore cause less distortion. Otherwise, the pedicle valve was used. The half of the valve that retained the greatest portion of its original morphology was measured.

In preparation for Fourier analysis, the outline of the valve was digitized in polar coordinates in stream mode from the center of the fold or sulcus at the commissure, along the commissure to the tip of the preserved portion of the cardinal extremity at the hinge line (Figure 10). Each measurement is the radius from the center of the beak at the hinge line to a point on the commissure. If the right half was measured, radii begin at 90° and end at 0°; if the left half was measured, radii begin at 90° and end at 180°. These measurements were then submitted to a computer program that selected radii at equiangular intervals, a requirement of the fast Fourier transform.

Figure 9. Video digitizing system assembled for this project: See description in text.

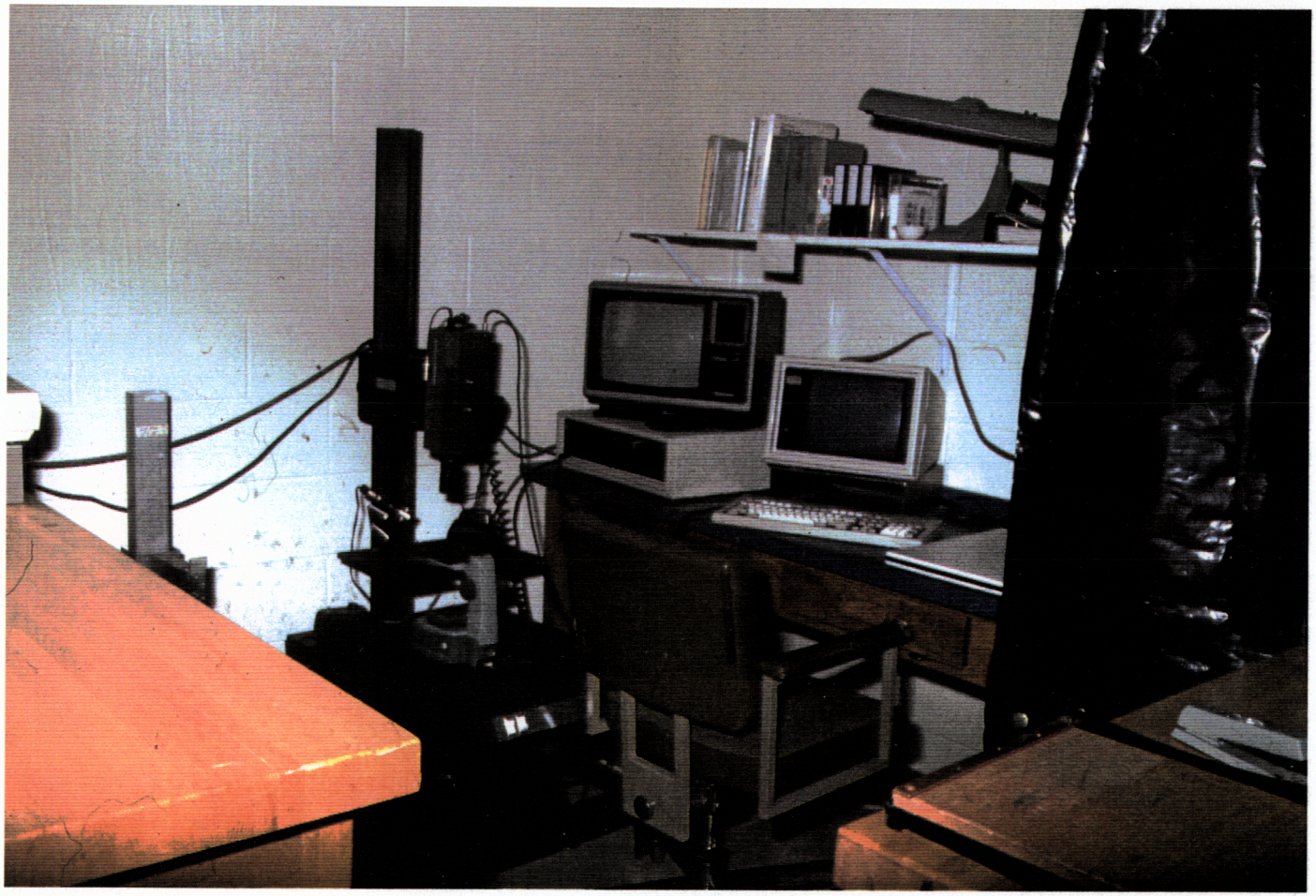

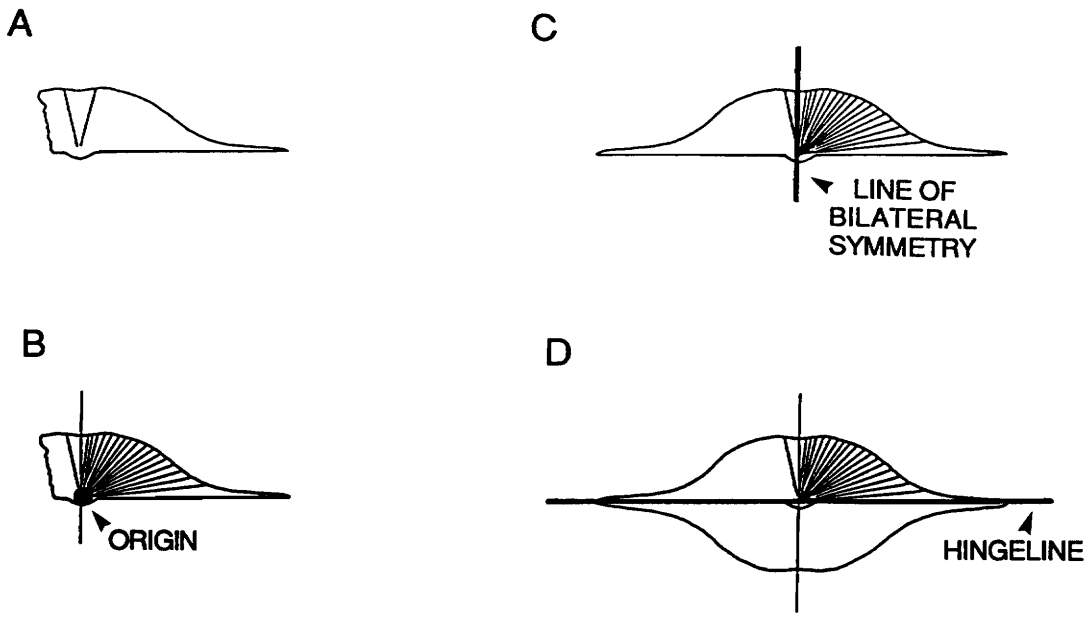

Figure 10. Morphometric data collection: **(A)** A typical specimen. **(B)** Measurements of radii were made in polar coordinates at 5° intervals from the origin to the commissure beginning at the center of the fold or sulcus and ending at the hingeline. **(C)** A mirror image of the measured portion was made along the line of bilateral symmetry in order to create a whole valve. **(D)** A mirror image of the valve was made using the hingeline as the line of symmetry in order to create a closed form.

FOURIER ANALYSIS

Fourier analysis in closed form to study shape was first applied by Ehrlich and Weinberg (1969) and Schwarcz and Shane (1970) in their work on sand grains. Since then it has proven useful in paleontological studies of morphology on a variety of organisms including ostracodes (Kaesler and Waters, 1972; Younker and Ehrlich, 1977; Dick et al., 1987), bryozoans (Anstey and Delmet, 1973; Delmet and Anstey, 1974; Anstey and Pachut, 1980), miospores (Christopher and Waters, 1974), bivalves (Gevirtz, 1976), foraminafera (Healy-Williams and Williams, 1981), blastoids (Waters, 1977), and trilobites (Foote, 1989). Canfield and Anstey (1981) examined cephalopod sutures using Fourier series in open form.

The utility of Fourier analysis derives from the fact that any simple curve can be described mathematically as the sum of a series of sine and cosine curves. The resultant curve can then be defined completely by the period, amplitude, and displacement of a series of sine and cosine curves of incrementally decreasing wavelength (Christopher and Waters, 1974). Fourier series applied to shape analysis resolves the total shape into a series of shape components, harmonics, with the relative amplitude values reflecting changes in shape. The mathematical model that results is the discrete harmonic amplitude spectrum and describes each specimen uniquely. A given shape can be reproduced as precisely as required by the inclusion of a sufficient number of terms in the equation (Younker and Ehrlich, 1977).

The basic expression of a Fourier series is as follows (Gevirtz, 1976):

$$r(\theta) = \frac{a_0}{2} + \sum_{n=1}^{\infty} a_n \cos(n\theta) + \sum_{n=1}^{\infty} b_n \sin(n\theta)$$

Using trigonometric identities for multiple angle relationships (Gevirtz, 1976), the above equation can be put in the amplitude-phase form which states that the radius, r, as a function of the polar angle, θ, at which it is measured, is given by the sum of the mean radius, c_0, plus n harmonics, and offset by the appropriate phase angle, ϕ (Ehrlich and Weinberg, 1969):

$$r(\theta) = c_0 + \sum_{n=1}^{\infty} c_n \cos(n\theta - \phi_n)$$

where each harmonic consists of an amplitude (a_n and b_n are the Fourier coefficients of the cosine and sine terms),

$$c_n = \sqrt{a_n^2 + b_n^2}$$

and its associated phase angle,

$$\phi = \frac{1}{\tan}\left(\frac{b_n}{a_n}\right)$$

The phase angle orients the harmonic form with respect to the coordinate system (Younker and Ehrlich, 1977).

The Fourier series for a specimen is obtained by measuring radii at a given angle in polar coordinates from the center of the specimen to points on the margin (Figure 10). Since all peripheral points must be visible from the center, the shapes must be convex and each radius must have only one value (Gevirtz, 1976). Previous morphological studies applying Fourier analysis have either used a biological landmark as the origin (Kaesler and Waters, 1972; Waters, 1977; Rohlff and Archie, 1984) or a computed center of gravity (Younker and Ehrlich, 1977; Dick et al., 1987; Anstey and Delmet, 1973; Delmet and Anstey, 1974; Anstey and Pachut, 1980; Christopher and Waters, 1974; Gevirtz, 1976; Healy-Williams and Williams, 1981; Foote, 1989). To compute a center of gravity, an arbitrary origin is first chosen and radii measured. From this information the true center of gravity is computed and the radii recalculated by interpolation, most often using the method of Ehrlich and Weinberg (1969).

For this study, an easily identifiable biological landmark, the center of the beak at the hingeline, was chosen as the origin. This landmark is presumably homologous in all specimens. A ray extended from the origin through the midline of the fold or sulcus to the commissure is the line of bilateral symmetry dividing the right from the left side of the valve

(Figure 10). In order to increase the number of usable specimens, because many are incomplete, only one side is measured and a mirror image of the other side is computed with a FORTRAN program written for this purpose. Canfield and Anstey (1981) in their study of cephalopod sutures measured a half suture and created a mirror image to produce the whole, as does Foote (1989) in his work on trilobite cranidia. Canfield and Anstey (1981) used the full suture because using half did not reduce the root mean square error as well. Also, using the full symmetrical suture, or whole valve as in this study, reduces the sine coefficient to zero and the series becomes a simple cosine series with the phase angles reduced to $\pm 90°$ (Canfield and Anstey, 1981). In addition, for this study, a closed form with an exactly located centroid was created by making a mirror image of the whole valve with the line of symmetry about the hingeline (Figure 10). With this step, all odd harmonics drop out, the morphological information becomes concentrated in the amplitudes of the even harmonics, and the phase angles can be ignored.

If the specimen being analyzed contains power beyond the cutoff wave number corresponding to the Nyquist frequency, whose wavelength is two times the distance between sample points, then aliasing will result (Boon et al., 1982; Davis, 1986). With aliasing, high frequencies with wavelengths less than two times the distance between successive observations will be irresolvable from low frequencies. To avoid the problem of aliasing, enough points should be digitized so that the cutoff wave number lies outside of the area encompassing significant power values. In practice, this means that the sampling interval should be small enough to account for all observed variation (Boon et al., 1982). For this study it was felt that by computing radii every 5°, the original shape of the specimen was preserved and aliasing was avoided. Since the cardinal extremities are frequently broken, the measurement at 10°/170° was repeated for the 5°/175° and 0°/180° measurements in further analyses.

The number of terms in a discrete Fourier series is equal to one half the number of measurements. In the present study, the 72 measurements for each specimen would then give 36 harmonic amplitudes. However, due to the symmetry about the hingeline which eliminates the odd harmonics, only amplitudes for the even harmonics 0 through 36 result.

Each harmonic amplitude measures the rotational symmetry indicated by the harmonic number. For example, harmonic 6 measures six-fold rotational symmetry; harmonic 4 measures four-fold rotational symmetry; harmonic 2 measures two-fold rotational symmetry, or elongation (Figure 11). The zeroth harmonic is the mean radius and as such is a sensitive measure of size. All higher harmonics were divided by the zeroth to provide size-independent data. Each harmonic is independent of and orthogonal to the others; therefore, the shape contribution made by a particular harmonic can be evaluated without regard to any other harmonic (Christopher and Waters, 1974).

The lower harmonics measure the gross shape of the specimen, whereas the higher harmonics measure the finer-scaled details. If morphological complexity is not great, i.e., if the outline of the specimen is fairly smooth, then more overall shape information will be contained in the lower harmonics (Canfield and Anstey, 1981). Although all harmonics are necessary to fully describe the shape of a specimen, some may carry redundant information, others may provide unique information, and some may relay relatively unimportant information (Younker and Ehrlich, 1977). In addition, random error is associated with digitization either due to limits of the instrumentation or operator error. This results in spuriously raising amplitudes of the higher harmonics without increasing the actual shape information (Boon et al., 1982; Gevirtz, 1976; Younker and Ehrlich, 1977). Therefore, it is important to determine which harmonics contribute most to the total shape description and use only these harmonics in further analyses so as not to obscure morphologically meaningful information. Harmonic amplitudes for the harmonics determined to contribute most to the overall shape of *Mucrospirifer* were used as the raw data in all statistical analyses. Fourier transformed data are included in Appendix B.

Fourier series were computed using the discrete fast Fourier transform of IMSL on an IBM 3090. The reverse discrete transform was called to construct shape plots given the Fourier coefficients. Programs written to access the IMSL subroutine are given in Appendix C.

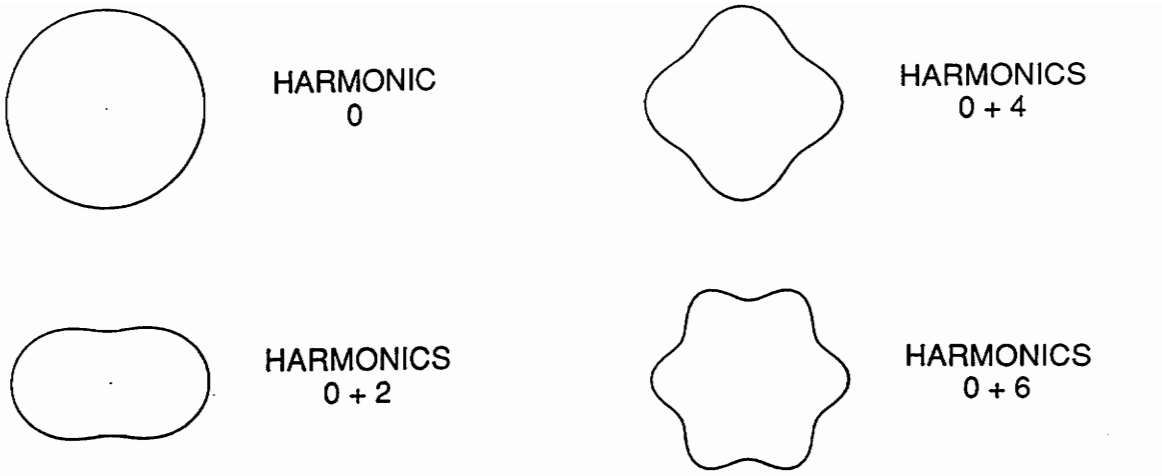

Figure 11. Rotational symmetry of Fourier harmonics: Harmonic numbers indicate amount of rotational symmetry.

STATISTICAL TECHNIQUES

HYPOTHESIS TESTING

Many of the techniques described below test a null hypothesis that will be either rejected or accepted (fail to reject) based on a probability (p value) determined by the test. If the result has a very small probability under the conditions of the null hypothesis, then there is little confidence in its correctness. In order to balance the chances of keeping a false hypothesis with throwing away a true one, the probability that is demanded before a hypothesis can be rejected must be neither too small nor too large. By convention, a probability of 0.05 is considered to be a small enough chance of rejecting the null hypothesis when it is true and a large enough chance of not rejecting the null hypothesis when it is false (Zar, 1984). Unless otherwise stated, all statistical testing was done at the 0.05 significance level.

STEPWISE DISCRIMINANT ANALYSIS

The primary method used to determine which harmonics contribute significantly to overall shape is stepwise discriminant analysis. Procedure STEPDISC of the SAS/STAT software package was used on an IBM 3084, as were all other statistical procedures. Stepwise discriminant analysis is a variable selection technique that identifies a subset of quantitative variables that best reveals differences among the groups under study. The procedure STEPDISC was run with the option of stepwise selection. Stepwise selection begins with no variables in the model. At each step, if the variable already entered that contributes least to the discriminatory power of the model (as measured by Wilks' lambda) fails to meet the criterion to stay, then that variable is removed; otherwise, the variable not in the model that contributes most is entered. The procedure stops when variables can neither be entered nor

removed. Variables are chosen to enter or leave the model based on the significance level of an F test from an analysis of covariance (see below) where the variables already in the model act as covariates and the variable under consideration is the dependent variable (SAS Institute, 1988). A liberal significance level of $\alpha = 0.15$, the default value, was used.

LINEAR REGRESSION

Linear regression was used in several parts of the study: to examine the relationship between size and shape where unnormalized, log-transformed data for harmonic 0 was regressed against harmonic 2; to determine if a correlation exists between shape and time and between shape and environment; and to determine the correlation between distance from shore and the amplitude of harmonic 2. The procedure REG of the SAS/STAT software package was employed in all cases. In linear regression the magnitude of one variable, the dependent variable, is assumed to be a function of the magnitude of another variable, the independent variable (Zar, 1984). The simple linear regression equation, the general equation for a straight line, is given as:

$$Y_i = \alpha + \beta X_i$$

where β is the regression coefficient, or slope of the best fit regression line, and α is the Y intercept. The best fit regression line is determined using the concept of least squares, where the sum of the squares of the vertical deviation of each point from the line is at a minimum. For the size/shape study, an F test was conducted to determine if the slope differed significantly from 1. The F test for the other studies tested if the slope differed significantly from 0. In all cases, plots were made using the predicted values of Y.

CLUSTER ANALYSIS

Cluster analysis using the FORTRAN program PLANTS2 written by Whitehurst (Plants, 1977), revised by Miller and Rounds in 1981, and by Rounds (1982), was applied to group specimens or localities. Cluster analysis is a numerical method for grouping objects based on their similarity. The similarity measure used in both cluster analysis and in polar ordination (see below) is the quantified Czekanowski coefficient, also known as the Dice coefficient (Sepkoski, 1974):

$$C = \frac{2\sum_{k=1}^{n} \min(x_{ik}, x_{jk})}{\sum_{k=1}^{n} x_{ik} + \sum_{k=1}^{n} x_{jk}}$$

where

n = total number of harmonics in the two localities being compared,

x_{ik} = amplitude of the kth harmonic in one locality being compared,

x_{jk} = amplitude of the kth harmonic in the other locality being compared,

$\min(x_{ik}, x_{jk})$ means to select the minimum of the two values enclosed in parentheses.

A similarity matrix was computed by comparing all possible pairs of samples using the Czekanowski coefficient.

The algorithm of PLANTS2 is based on the unweighted pair-group method using arithmetic averages (UPGMA). UPGMA is an agglomerative hierarchical technique that operates on the computed similarity matrix. In general, the clustering process begins by treating each sample as a separate group and then repeatedly combining the two most similar groups until only one remains. The groups themselves are arranged into a hierarchy (Digby and Kempton, 1987). The UPGMA algorithm computes the average similarity of a new group to another, weighting each element of the group equally (Sneath and Sokal, 1973). A dendogram is produced which graphically illustrates the results of the clustering process.

Cluster analysis can give an objective and useful preliminary classification. However, cluster analysis forces partitioning into discrete groups that may or may not be natural. To evaluate if natural groupings exist or if variation is continuous, it is helpful to combine cluster analysis with an ordination.

POLAR ORDINATION

Polar, or Bray-Curtis, ordination using the FORTRAN program POLAR2 written by Sharry and Sepkoski in 1976, revised by Sepkoski in 1980, and modified by Rounds (1982), was employed in conjunction with cluster analysis and principal component analysis to establish and evaluate groupings of specimens or localities. Ordination is the process of arranging samples in relation to one or more gradients or axes. Indirect ordination techniques, like polar ordination, order samples with information that emerges from the data (Whittaker, 1973). In polar ordination a dissimilarity, or distance, matrix is first constructed, where

$$DISTANCE = 1 - SIMILARITY$$

The measure of similarity used in this study is the quantified Czekanowski coefficient, as in cluster analysis, and described above. POLAR2 selects endpoints based on variances in distance between samples which are computed from the dissimilarity matrix. One endpoint is the sample showing the highest variance while the other endpoint is the most distant sample from it. Ordination values are then computed for all remaining samples with the equation (Gauch, 1982):

$$X = \frac{d^2 + a^2 - b^2}{2d}$$

where

X = distance along the axis of the sample being plotted;

d = distance between endpoints;

a = distance of the sample from one endpoint;

b = distance of the sample from the other endpoint.

Polar ordination may be carried out in several dimensions, so that in a three-dimensional graph the position of each sample can be seen relative to all others.

Bray and Curtis (1957) introduced polar ordination in a study of plant distribution. It has since been widely used in other ecological studies (Gauch, 1982) and in some paleoecological work (Shaffer and Wilke, 1965; Cisne and Rabe, 1978; Miller, 1988). In the present study, the axes represent gradients in shape rather than in environmental factors or community composition as in previous work.

PRINCIPAL COMPONENT ANALYSIS

Principal component analysis using the SAS/STAT procedure PRINCOMP aided in the selection of significant harmonics, was employed in conjunction with cluster analysis and polar ordination to establish and evaluate groupings of specimens or localities, and was used to assess the relationships among shape, time, and environment. Principal component analysis, like polar ordination, is an indirect ordination method. The purpose of principal component analysis is to transform original variables to a smaller number of new variables, or principal components, with the least possible distortion. Each principal component is a linear combination of the old variables and each accounts successively for as much of the total variance as possible. The first principal component captures the most variance, the second accounts for the maximal remaining variance, and so on until all variance is accounted for when all principal components are computed (Davis, 1986). The result is a sequence of axes of diminishing importance. Principal component analysis is an eigenanalysis problem. The principal components are eigenvectors of the covariance matrix and yield the orientation of the principal axes of a multidimensional ellipsoid. Eigenvalues represent the lengths of each

of the major and minor axes and the variance accounted for by that axis. The axes are orthogonal because the matrix is symmetrical (Gauch, 1982).

ANALYSIS OF VARIANCE

Analysis of variance was employed as one means of evaluating groupings of specimens and localities developed through cluster analysis, polar ordination, and principal component analysis. It was also used to test the association between time, lithology, and the amplitudes of the significant harmonics. Analysis of covariance is an integral part of stepwise discriminant analysis. Regression analysis also applies the *F* statistic. The SAS/STAT procedure GLM with the MANOVA statement was used. In analysis of variance more than two means are compared and an *F* test determines if the means are significantly different from one another (Zar, 1984):

$$F = \frac{\text{GROUPS MS}}{\text{ERROR MS}}$$

where

$$\text{GROUPS MS} = \frac{\sum_{i=1}^{k} n_i(\overline{X}_i - \overline{X})^2}{k-1} \quad \begin{matrix}\text{(GROUPS SS)} \\ \text{(GROUPS DF)}\end{matrix}$$

and

$$\text{ERROR MS} = \frac{\sum_{i=1}^{k}\left[\sum_{j=1}^{n_i}(X_{ij} - \overline{X}_i)^2\right]}{N-k} \quad \begin{matrix}\text{(ERROR SS)} \\ \text{(ERROR DF)}\end{matrix}$$

The significance of F was determined at $\alpha = 0.05$. Including the MANOVA statement results in the computing of several multivariate tests using Wilks' criterion, Pillai's trace, Hotelling-Lawley trace, and Roy's maximum root criterion (SAS Institute, 1988).

DISCRIMINANT ANALYSIS

Discriminant analysis using the procedure DISCRIM of the SAS/STAT software package was used as one means of evaluating groupings of specimens and localities developed through cluster analysis, polar ordination, and principal component analysis. Discriminant analysis assigns an observation of unknown origin to one of any number of defined groups on the basis of one or more quantitative variables (Lachenbruch, 1975). Procedure DISCRIM uses a measure of generalized squared distance to compute a linear discriminant function. In this study, a multivariate normal distribution for each group is assumed and parametric methods are invoked. The "within" covariance matrices are used in the discriminant function if the chi-square value is significant at the 0.10 level; otherwise, a pooled covariance matrix is used. The discriminant function also takes into account the prior probabilities of the groups. Each observation is assigned to the group from which it has the smallest generalized squared distance. The generalized squared distance from group x to group t is given as:

$$D_t^2(x) = d_t^2(x) + g_1(t) + g_2(t)$$

where

$d_t^2(x)$ is the squared distance from group x to t;

$g_1(t) = \log_e|S_t|$ if the within-group covariance matrices are used, or

$g_1(t) = 0$ if the pooled covariance matrix is used;

$g_2(t) = -2\log_e(q_t)$ if the prior probabilities are not all equal, or

$g_2(t) = 0$ if the prior probabilities are all equal;

S_t is the covariance matrix within group t;

$|S_t|$ is the determinant of S_t;

q_t is the prior probability of membership in group t.

Procedure DISCRIM also computes the posterior probability of an observation belonging to each group using the equation:

$$p(t|x) = \frac{\exp(-0.5D_t^2(x))}{\sum_u \exp(-0.5D_u^2(x))}$$

An observation is assigned to group u if $t = u$ yields the largest posterior probability value or the smallest generalized squared distance (SAS Institute, 1988).

FISHER EXACT TEST

A two-tailed Fisher exact test was used in a contingency table analysis to test the association between shape and environment and between shape and time. When the expected frequencies expressed in the null hypothesis of the variable under study are too small to use the chi-square statistic, the Fisher exact test may be used in its place to test whether the row and column categories are independent of each other. The resulting probability is that of observing a table that gives at least as much evidence for association as the table originally observed. The probability of a 2 x 2 contingency table is given as (Zar, 1984):

$$P = \frac{\frac{R_1!R_2!C_1!C_2!}{n!}}{f_{11}!f_{12}!f_{21}!f_{22}!}$$

where f is the observed frequency with f_{12} being that in row 1 and column 1, f_{12} being that in row 1 and column 2, f_{21} being that in row 2 and column 1, f_{22} being that in row 2 and column 2; R_1 and R_2 are the row totals of observed frequencies; C_1 and C_2 are the column totals of observed frequencies; and n is the total of rows and columns. The SAS procedure FREQ was used with the option EXACT to test for tables that are larger than 2 x 2 (SAS Institute, 1988).

MEASURES OF VARIABILITY AND DISPERSION

R^2 and the coefficient of variation were used in conjunction with linear regression and analysis of variance to assess the strength of the tests. In linear regression the coefficient of determination, R^2, measures the proportion of total variation in Y that is explained by the fitted regression line (Zar, 1984):

$$R^2 = \frac{\text{TOTAL SS - ERROR SS}}{\text{TOTAL SS}}$$

Also known as goodness of fit, R^2 in analysis of variance is the proportion of variation in the dependent variable explained by the model. The better the fit, the closer R^2 is to 1. A poor fit may be caused by high variance in the dependent variable or the fitting of an inappropriate model (Davis, 1986).

The coefficient of variation measures dispersion or variability relative to the mean of the sample (Zar, 1984):

$$CV = 100 \cdot \frac{\text{STANDARD DEVIATION}}{\text{MEAN}}$$

Because both the numerator and denominator are in the same units, the coefficient of variation is dimensionless. As a relative measure it makes possible the comparison of the dispersion and variability of variables of different absolute mean sizes (Simpson et al., 1960).

RESULTS

SELECTION OF SIGNIFICANT HARMONICS

Harmonics 2, 4, and 6 have the greatest discriminatory power and contribute most to the overall shape of *Mucrospirifer*. Stepwise discriminant analysis, knowledge of the data, and realization of the limits of the instrumentation were used to make this determination. Figure 12 is a reconstruction of a single specimen using the Fourier coefficients to illustrate graphically that the bulk of the shape is captured by harmonics 0, 2, 4, 6. As more harmonics are added to the series, the overall shape change is not biologically meaningful. A three-dimensional plot of the mean amplitudes for all harmonics for all localities is given in Figure 13. The absolute drop in amplitudes after harmonic 6 shows how little the higher harmonics contribute.

When stepwise discriminant analysis was run by locality using all specimens, the first three variables to enter the model are harmonics 2, 6, and 4, in that order. Harmonic 2 stands out with an *F* statistic in the model summary considerably higher than any others (Table 2). In order to reduce the effect of localities with a small number of specimens and to determine if these harmonics still have discriminating power using different geographical groupings of specimens, STEPDISC was also run by basin, region, and state. Basin refers to the

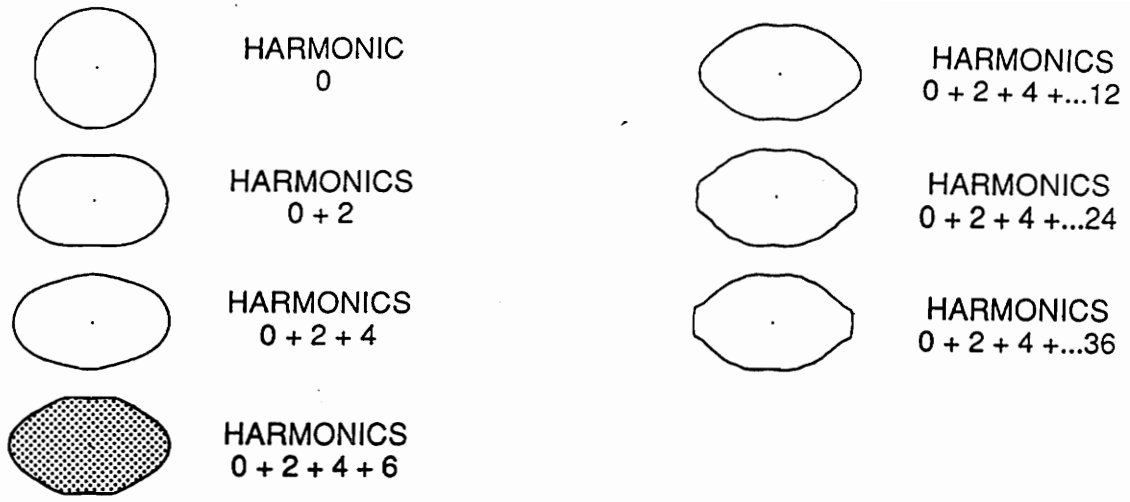

Figure 12. Reconstruction of single specimen: Stippled plot shows shape when the amplitudes of harmonics 0, 2, 4, and 6 were used. These harmonics were determined to be significant and were the ones used in further analyses.

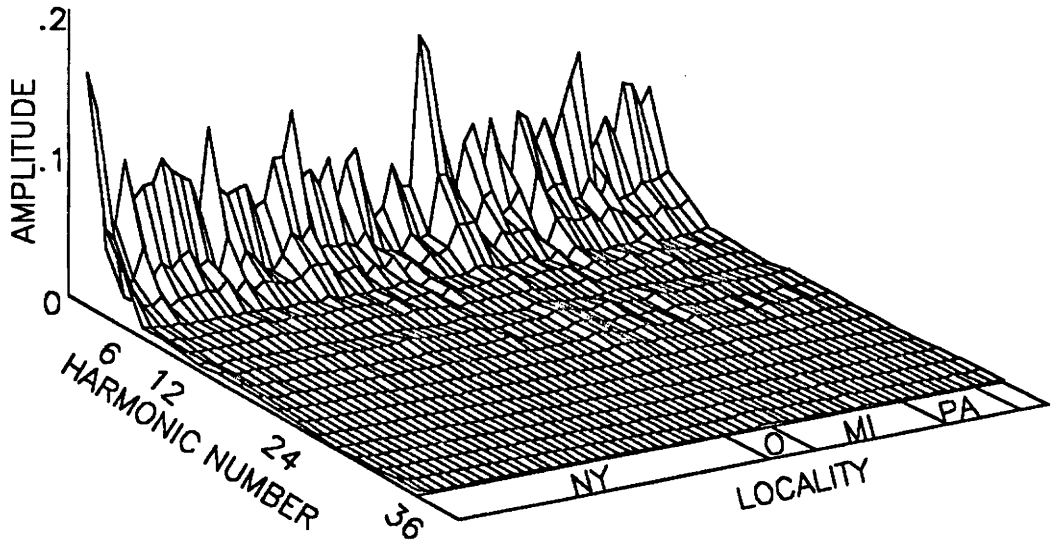

Figure 13. Three-dimensional plot of mean amplitude vs harmonic number vs locality: Note drop in amplitude after harmonic 6.

Appalachian and Michigan basins with specimens from New York, Pennsylvania, Maryland, and West Virginia placed in the Appalachian Basin and those from Michigan and Ontario in the Michigan Basin. For the regional analysis three regions were established: New York; Pennsylvania-Maryland-West Virginia; and Michigan-Ontario. Because of the small number of localities, Maryland and West Virginia were grouped together for the state analyses.

By basin, harmonics 6, 2, and 4 are entered into the model in steps 1, 2, and 4. The *F* statistics for harmonics 6 and 2 are almost two times the value for the next highest. By region, harmonics 6, 2, and 4 are selected in steps 1, 2, and 6, although the final *F* statistic for harmonic 4 places it third. By state, harmonics 6, 2, and 4 come in 1, 2, and 3 (Table 2).

Harmonics 12, 14, 18, 24, and 28 are the other harmonics common to all four analyses. Harmonics 24 and 28 were disregarded due to their high harmonic number. Their shape contribution could be due to random error associated with the resolution capability of the instrument or operator error. Given the simple shape of *Mucrospirifer*, it was also felt that the higher harmonics do not contribute any meaningful biological information. In addition, harmonic 24 has a low value for the *F* statistic compared to harmonics 2, 4, and 6 as do harmonics 12, 14, and 18.

IDENTIFICATION OF MORPHOLOGICAL TYPES

OVERALL SHAPE

Cluster analysis, polar ordination, and principal component analysis were applied to analyze the overall shape of *Mucrospirifer* as captured in harmonics 2, 4, and 6 of the Fourier series.

Cluster analysis on the mean values of significant harmonics for each locality identified four groupings and potential morphs: clusters 1, 2, 3, and 4, highlighted in four different

Table 2. Results of stepwise discriminant analysis by locality, basin, region, and state. Significance level to enter and to stay in the model is 0.15. No variables were removed after entering.

STEP	VARIABLE ENTERED	PARTIAL R^2	F STATISTIC	PROB > F	WILKS' LAMBDA	PROB < LAMBDA	AVERAGE SQUARED CANONICAL CORRELATION	PROB > ASCC
				LOCALITY				
				DF = 62, 497				
1	HAR2	0.6320	14.100	0.0001	0.3680	0.0001	0.0102	0.0001
2	HAR6	0.3636	4.680	0.0001	0.2342	0.0	0.0159	0.0
3	HAR4	0.3179	3.811	0.0001	0.1598	0.0	0.0197	0.0
4	HAR14	0.2233	2.346	0.0001	0.1241	0.0	0.0231	0.0
5	HAR10	0.2188	2.281	0.0001	0.0969	0.0	0.0265	0.0
6	HAR12	0.1765	1.742	0.0007	0.0798	0.0	0.0291	0.0
7	HAR16	0.1541	1.478	0.0137	0.0675	0.0	0.0315	0.0001
8	HAR34	0.1516	1.447	0.0186	0.0573	0.0	0.0339	0.0001
9	HAR28	0.1474	1.397	0.0301	0.0488	0.0	0.0362	0.0001
10	HAR18	0.1408	1.321	0.0589	0.0420	0.0	0.0384	0.0001
11	HAR8	0.1373	1.280	0.0825	0.0362	0.0	0.0405	0.0001
12	HAR24	0.1333	1.236	0.1170	0.0314	0.0	0.0425	0.0001
				BASIN				
				DF = 1, 560				
1	HAR6	0.0634	38.591	0.0001	0.9366	0.0001	0.0634	0.0001
2	HAR2	0.0545	32.820	0.0001	0.8855	0.0001	0.1145	0.0001
3	HAR28	0.0316	18.505	0.0001	0.8576	0.0001	0.1424	0.0001
4	HAR4	0.0257	14.984	0.0001	0.8355	0.0001	0.1645	0.0001
5	HAR12	0.0176	10.116	0.0016	0.8208	0.0001	0.1792	0.0001
6	HAR14	0.0081	4.624	0.0320	0.8142	0.0001	0.1858	0.0001
7	HAR24	0.0064	3.630	0.0573	0.8089	0.0001	0.1910	0.0001
8	HAR32	0.0066	3.745	0.0535	0.8036	0.0001	0.1964	0.0001
9	HAR18	0.0054	3.059	0.0808	0.7993	0.0001	0.2007	0.0001
10	HAR22	0.0053	3.012	0.0832	0.7950	0.0001	0.2050	0.0001
				REGION				
				DF = 2, 558				
1	HAR6	0.0680	20.768	0.0001	0.9320	0.0001	0.0340	0.0001
2	HAR2	0.0546	16.396	0.0001	0.8811	0.0001	0.0596	0.0001
3	HAR28	0.0323	9.462	0.0001	0.8526	0.0001	0.0738	0.0001
4	HAR14	0.0298	8.685	0.0002	0.8272	0.0001	0.0885	0.0001
5	HAR12	0.0307	8.953	0.0001	0.8018	0.0001	0.1020	0.0001
6	HAR4	0.0345	10.063	0.0001	0.7742	0.0001	0.1164	0.0001
7	HAR18	0.0120	3.408	0.0338	0.7650	0.0001	0.1217	0.0001
8	HAR24	0.0103	2.920	0.0548	0.7571	0.0001	0.1262	0.0001
9	HAR32	0.0106	3.011	0.0501	0.7491	0.0001	0.1305	0.0001
10	HAR10	0.0088	2.489	0.0839	0.7424	0.0001	0.1347	0.0001
11	HAR16	0.0124	3.501	0.0308	0.7332	0.0001	0.1404	0.0001
				STATE				
				DF = 4, 558				
1	HAR6	0.0696	10.604	0.0001	0.9304	0.0001	0.0174	0.0001
2	HAR2	0.0731	11.166	0.0001	0.8623	0.0001	0.0348	0.0001
3	HAR4	0.0425	6.269	0.0001	0.8257	0.0001	0.0444	0.0001
4	HAR14	0.0338	4.926	0.0007	0.7978	0.0001	0.0526	0.0001
5	HAR12	0.0404	5.930	0.0001	0.7656	0.0001	0.0616	0.0001
6	HAR28	0.0290	4.190	0.0024	0.7434	0.0001	0.0677	0.0001
7	HAR18	0.0155	2.209	0.0668	0.7319	0.0001	0.0712	0.0001
8	HAR24	0.0135	1.910	0.1074	0.7220	0.0001	0.0744	0.0001
9	HAR36	0.0122	1.733	0.1412	0.7132	0.0001	0.0770	0.0001

patterns in Figure 14. Similarity coefficients for the dendogram branches are given in Table 3. The mean shape for each cluster is also illustrated in Figure 14. Cluster 2 contains localities with the most elongate specimens; cluster 3 contains localities with elongate specimens, but slightly less so; cluster 4 includes localities with rounder specimens; and cluster 1 has localities with the roundest. Clusters 1, 3, and 4 include localities from a range of states, horizons, and lithologies while cluster 2 is more limited (Table 4).

Cluster 1 is the most dissimilar from the other three, adding on at a low similarity coefficient of 0.54. The cluster itself is fairly disparate, not forming until 0.76, a level much lower than the other clusters. Ten localities from New York (N11, N13, N20, N22D, N25, N31, N33, N34C, N34D, N35B), two from Ontario (O02C, O05), three from Michigan (M14, M15, M24), and two from Pennsylvania (P10, P16) are included here. Localities from all four time horizons are included. The predominant lithology is mudstone, although three localities are composed of siltstone and one of limestone. Cluster 2 is limited to horizon a and includes only four localities: N16 and N17 from New York and O01A and O02A from Ontario. The New York localities are composed of sandstone but the Ontario localities are made up of calcareous shale. The cluster forms at a similarity coefficient of 0.93 while as a unit it is quite dissimilar from other clusters with a similarity level of 0.67. Cluster 3 contains localities from New York (N04, N18, N22C), Michigan (M13, M17), and Pennsylvania (P07, P09). These localities span horizons a, c, and d and include lithologies of siltstone, mudstone, calcareous shale, and limestone. Except for P09 which has only one specimen and chains on late, cluster 3 forms at a similarity coefficient of 0.90 and joins other clusters at a level of 0.76. Cluster 4 consists of four subclusters which join to each other at similarity coefficients of 0.91, 0.87, and 0.81. Together they form a cluster at 0.79. Localities from all states make up cluster 4: New York (N02, N03, N5A, N5B, N06, N07, N10, N19, N22A, N22B, N26, N27, N34A, N34B, N34E, N34F, N34G, N35A); Ontario (O04); Michigan (M01, M03, M08, M11, M12, M16, M19, M20, M23); Maryland (D01, D02); West Virginia (W01); and Pennsylvania (P05, P14, P15, P17). Horizons b, c, and d are represented and all lithologies are included.

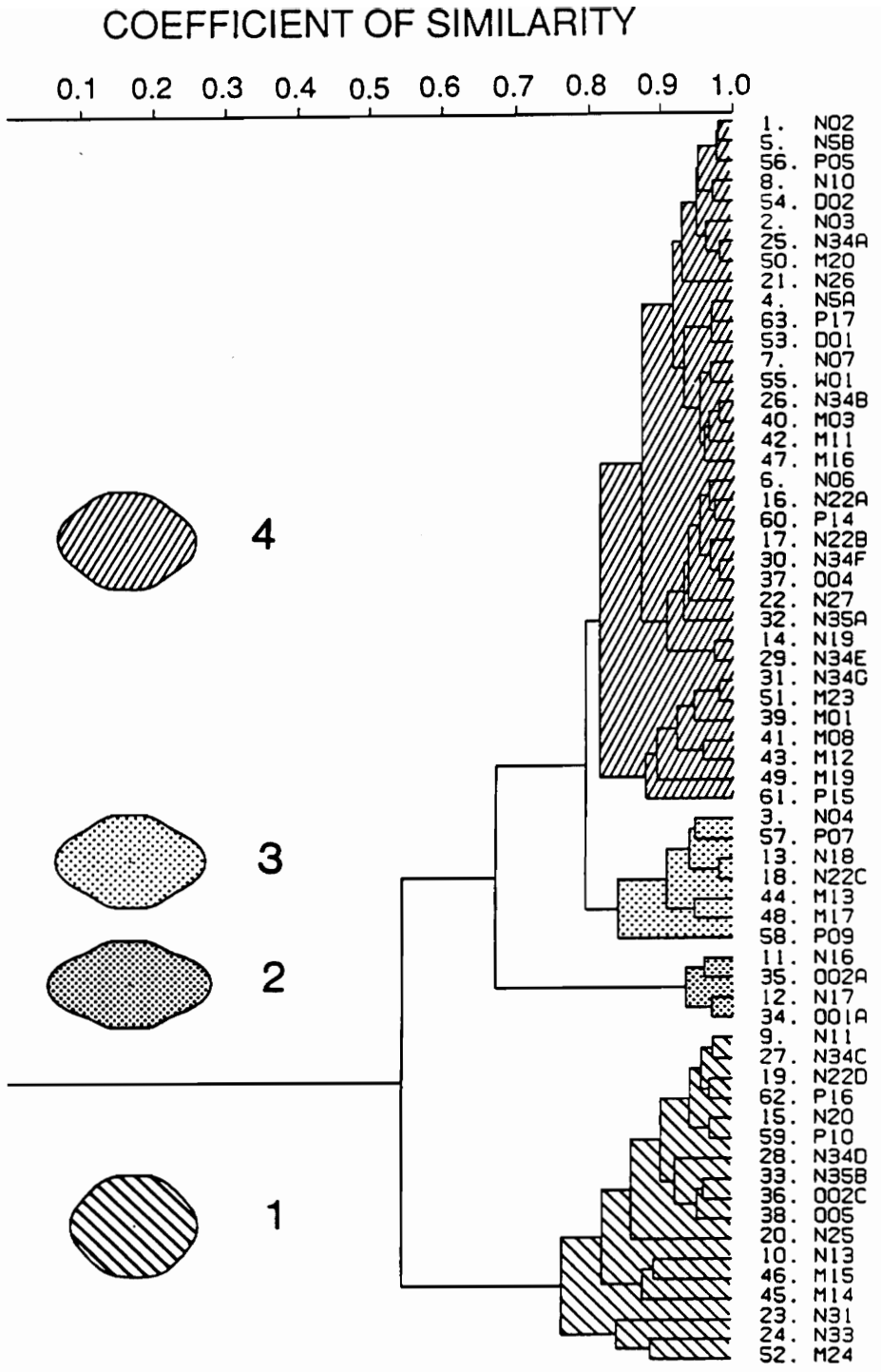

Figure 14. Cluster dendogram: Four clusters were identified when mean amplitudes for all specimens in each locality were used. A mean shape for each cluster is also shown. Cluster 1 shown in left line pattern; cluster 2 in heavy dot pattern; cluster 3 in light dot pattern; and cluster 4 in right line pattern.

Table 3. Similarity coefficient values for dendogram branches.

25.	=	N34A	50.	=	M20	0.982
31.	=	N34G	51.	=	M23	0.982
13.	=	N18	18.	=	N22C	0.981
26.	=	N34B	40.	=	M03	0.981
30.	=	N34F	37.	=	O04	0.981
1.	=	N02	5.	=	N5B	0.981
1.	=	N02	56.	=	P05	0.978
14.	=	N19	29.	=	N34E	0.976
16.	=	N22A	60.	=	P14	0.975
9.	=	N11	27.	=	N34C	0.973
8.	=	N10	54.	=	D02	0.973
12.	=	N17	34.	=	O01A	0.972
4.	=	N5A	63.	=	P17	0.971
4.	=	N5A	53.	=	D01	0.970
15.	=	N20	59.	=	P10	0.970
17.	=	N22B	30.	=	N34F	0.969
19.	=	N22D	62.	=	P16	0.969
7.	=	N07	55.	=	W01	0.969
6.	=	N06	16.	=	N22A	0.968
26.	=	N34B	42.	=	M11	0.967
2.	=	N03	25.	=	N34A	0.963
11.	=	N16	35.	=	O02A	0.961
33.	=	N35B	36.	=	O02C	0.961
26.	=	N34B	47.	=	M16	0.960
41.	=	M08	43.	=	M12	0.960
9.	=	N11	19.	=	N22D	0.957
6.	=	N06	17.	=	N22B	0.954
7.	=	N07	26.	=	N34B	0.954
1.	=	N02	8.	=	N10	0.952
33.	=	N35B	38.	=	O05	0.952
1.	=	N02	2.	=	N03	0.950
3.	=	N04	57.	=	P07	0.948
44.	=	M13	48.	=	M17	0.947
31.	=	N34G	39.	=	M01	0.947
9.	=	N11	15.	=	N20	0.941
3.	=	N04	13.	=	N18	0.940
6.	=	N06	22.	=	N27	0.939
11.	=	N16	12.	=	N17	0.935
6.	=	N06	32.	=	N35A	0.932
4.	=	N5A	7.	=	N07	0.932
1.	=	N02	21.	=	N26	0.929
31.	=	N34G	41.	=	M08	0.923
28.	=	N34D	33.	=	N35B	0.921
1.	=	N02	4.	=	N5A	0.917
6.	=	N06	14.	=	N19	0.909
3.	=	N04	44.	=	M13	0.909
9.	=	N11	28.	=	N34D	0.902
31.	=	N34G	49.	=	M19	0.895
10.	=	N13	46.	=	M15	0.892
24.	=	N33	52.	=	M24	0.887
31.	=	N34G	61.	=	P15	0.879
10.	=	N13	45.	=	M14	0.875
1.	=	N02	6.	=	N06	0.873
9.	=	N11	20.	=	N25	0.859
3.	=	N04	58.	=	P09	0.840
23.	=	N31	24.	=	N33	0.839
9.	=	N11	10.	=	N13	0.818
1.	=	N02	31.	=	N34G	0.815
1.	=	N02	3.	=	N04	0.795
9.	=	N11	23.	=	N31	0.763
1.	=	N02	11.	=	N16	0.672
1.	=	N02	9.	=	N11	0.544

Table 4. States, horizons, and lithologies found in each cluster.

	CLUSTER 1	CLUSTER 2	CLUSTER 3	CLUSTER 4
STATE	NY ON MI PA	NY ON	NY MI PA	NY ON MI PA MD WVA
HORIZON	A B C D	A	A C D	B C D
LITHOLOGY	MUDSTONE SILTSTONE CALC. SHALE LIMESTONE	SANDSTONE CALC. SHALE	SILTSTONE MUDSTONE CALC. SHALE LIMESTONE	SANDSTONE SILTSTONE MUDSTONE CALC. SHALE LIMESTONE

To examine whether the groupings from cluster analysis are natural, or if variation is actually continuous, polar ordination was run on the means of the significant harmonics for each locality. Figure 15 is a three-dimensional plot of axes 1, 2, and 3. The four groupings identified through cluster analysis are indicated on the plot by the four symbols. Correlation coefficients for each locality for the three axes are given in Table 5. For axis 1, locality N16 of cluster 2 forms one endpoint (correlation coefficient of -0.031) and locality M24 of cluster 1 forms the other (correlation coefficient of 0.706). Axis 1 apparently represents the shape gradient of elongation where the most elongate have the lowest value and the roundest have the highest. No interpretation can be made for the other two axes. The endpoints for axis 2 are both localities in cluster 4: N35A (0.242) and P15 (0.000). For axis 3, localities in cluster 3 form the endpoints: M17 (0.177) and P09 (0.000).

Cluster 2 remains a distinct grouping in polar ordination. Localities in this cluster have low correlation coefficients for all three axes and similar values for each locality (axis 1, -0.031 to 0.015; axis 2, 0.119 to 0.120; axis 3, 0.085 to 0.086). This results in a grouping with almost no dispersion in any direction. Cluster 1 spans a range of roundness on axis 1 with correlation coefficients from 0.379 to 0.706. Axis 2 shows slight dispersion for cluster 1 indicated by values of 0.083 to 0.148, while there is almost none on axis 3 (0.088-0.094). Cluster 1 is distinct in three-dimensional space. Cluster 3 has virtually no spread on axis 2. Except for P09, which again appears to be aberrant as in cluster analysis, all axis 2 correlation values for cluster 3 are 0.121. The dispersion of cluster 3 on axis 1 is small with values from 0.092 to 0.125. Cluster 3 has the most breadth on axis 3, even discounting P09, with values ranging from 0.066 ot 0.177. Cluster 3 is a distinct grouping. Cluster 4 is the most disperse of the four clusters. The bulk of the dispersion is along axis 2 where correlation values range from 0 to 0.242. It is the only cluster with considerable breadth on axis 2. The spread of cluster 4 on axes 1 and 3 is moderate. Correlation coefficients on axis 1 for cluster 4 range from 0.172 to 0.389, intermediate between the other clusters, and for axis 3 from 0.088 to 0.158.

Principal component analysis was run both on the means of significant harmonics for each locality (Figure 16) and for all specimens (Figure 17). The four cluster analysis

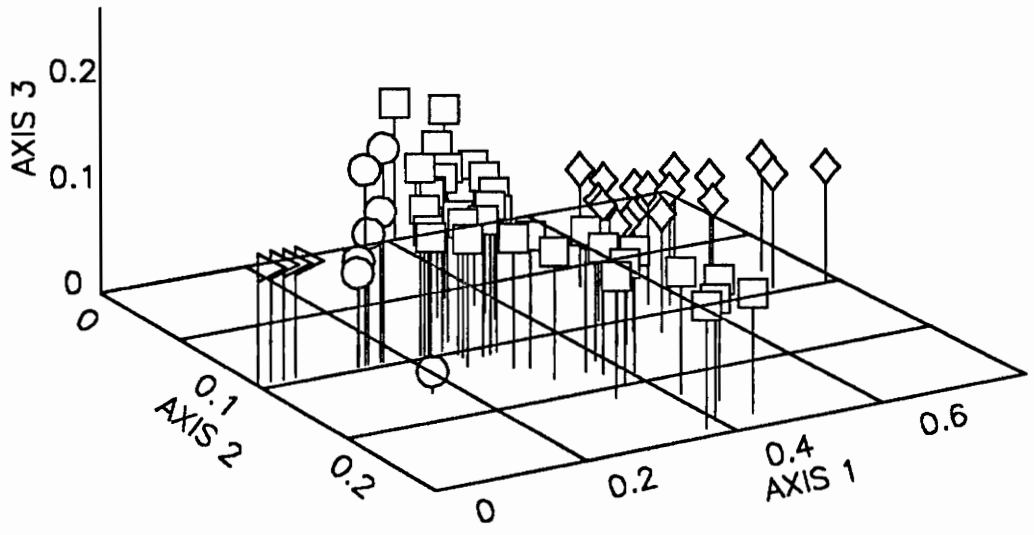

Figure 15. Polar ordination of the mean amplitude for all specimens in each locality: Diamonds are localities in cluster 1. Flags/triangles are localities in cluster 2. Circles are localities in cluster 3. Squares are localities in cluster 4.

Table 5. Polar ordination correlation coefficients for axes 1, 2, and 3. Cluster to which locality belongs is also given.

LOCALITY	AXIS1	AXIS2	AXIS3	CLUSTER
N02	0.260	0.168	0.095	4
N03	0.231	0.133	0.104	4
N04	0.121	0.121	0.118	3
N5A	0.172	0.127	0.098	4
N5B	0.256	0.153	0.100	4
N06	0.341	0.236	0.089	4
N07	0.184	0.121	0.127	4
N10	0.241	0.133	0.117	4
N11	0.397	0.128	0.094	1
N13	0.548	0.098	0.088	1
N16	-0.031	0.119	0.085	2
N17	0.015	0.120	0.086	2
N18	0.093	0.121	0.076	3
N19	0.389	0.236	0.088	4
N20	0.447	0.143	0.089	1
N22A	0.315	0.173	0.095	4
N22B	0.355	0.205	0.090	4
N22C	0.092	0.121	0.066	3
N22D	0.379	0.148	0.090	1
N25	0.524	0.138	0.089	1
N26	0.287	0.197	0.089	4
N27	0.303	0.167	0.108	4
N31	0.639	0.120	0.088	1
N33	0.660	0.101	0.088	1
N34A	0.210	0.127	0.107	4
N34B	0.185	0.121	0.129	4
N34C	0.406	0.120	0.092	1
N34D	0.504	0.118	0.088	1
N34E	0.380	0.218	0.089	4
N34F	0.332	0.158	0.095	4
N34G	0.308	0.091	0.108	4
N35A	0.318	0.242	0.090	4
N35B	0.476	0.108	0.088	1
O01A	0.000	0.120	0.086	2
O02A	-0.015	0.119	0.086	2
O02C	0.459	0.095	0.088	1
O04	0.348	0.177	0.091	4
O05	0.485	0.113	0.088	1
M01	0.307	0.099	0.098	4
M03	0.186	0.121	0.128	4
M08	0.254	0.087	0.141	4
M11	0.200	0.121	0.140	4
M12	0.221	0.113	0.141	4
M13	0.101	0.121	0.160	3
M14	0.569	0.112	0.089	1
M15	0.450	0.083	0.091	1
M16	0.172	0.121	0.153	4
M17	0.125	0.121	0.177	3
M19	0.295	0.069	0.158	4
M20	0.209	0.131	0.103	4
M23	0.312	0.081	0.112	4
M24	0.706	0.122	0.088	1
D01	0.199	0.140	0.096	4
D02	0.251	0.132	0.111	4
W01	0.176	0.122	0.114	4
P05	0.240	0.150	0.098	4
P07	0.106	0.121	0.100	3
P09	0.119	0.160	0.000	3
P10	0.420	0.137	0.089	1
P14	0.317	0.187	0.090	4
P15	0.350	0.000	0.113	4
P16	0.391	0.148	0.092	1
P17	0.173	0.128	0.092	4

groupings are identified on each plot. Values for covariances between harmonics, eigenvalues, and eigenvectors are given in Table 6. Values for scores of localities or specimens on each axis are listed in Appendix D and Appendix E.

Because 98.9% of the variance is encompassed by principal components 1 and 2 in the analysis using means, these two axes are plotted against each other (Figure 16). The second principal component accounts for a relatively small amount of the total variance (5.5%) while most rests with the first (93.4%). Because the second principal component is relatively short, it is plotted with an expanded axis in Figure 16. Harmonic 2 contributes most to the first principal component and harmonic 4 to the second. Therefore, principal component 1 can be considered to primarily represent "elongateness" while principal component 2 represents "squareness".

Ordination by principal component analysis using means of localities compares favorably with that found through polar ordination. However, because using means can be misleading since so much variation is lost in averaging amplitudes for specimens in a locality, principal component analysis was also run with all specimens. Using the amplitudes for significant harmonics for all specimens, 97.7% of the variance is included in the first and second principal components and these two axes are plotted. The second principal component contributes more to the total variance (7%) than with means, but due to its relative shortness its axis is expanded in all the following figures based on the analysis using all specimens. As with means, harmonic 2 contributes most to the first principal component and harmonic 4 most to the second. The first principal component represents elongation while the second represents squareness. The picture that emerges when all specimens are used is much different from that found using only means (Figure 17). Clusters 1 and 2 are separate from each other with the exception of one specimen. However, cluster 4 overlaps cluster 1 to a great extent and cluster 3 to a large degree as well. Cluster 4 and cluster 3 overlap with cluster 2 to a lesser extent.

To explore the intrapopulational variation, cluster analysis was run using the amplitudes for significant harmonics for all specimens (Figure 18). Thirteen clusters were identi-

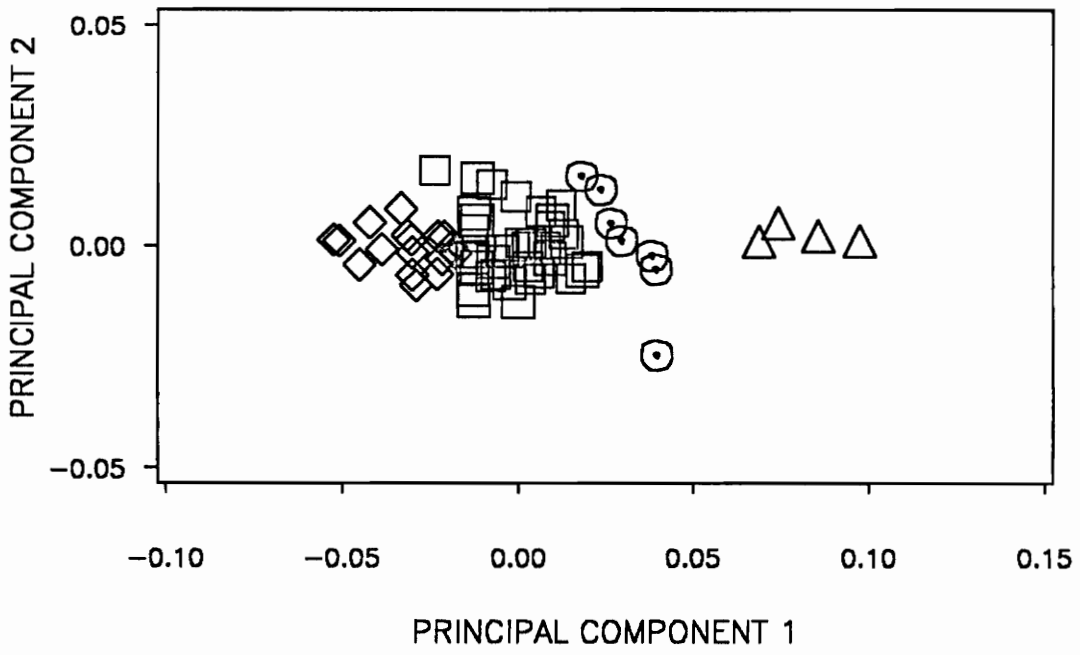

Figure 16. Principal component analysis of the mean amplitudes for all specimens in each locality: Diamonds are localities in cluster 1. Flags/triangles are localities in cluster 2. Circles are localities in cluster 3. Squares are localities in cluster 4.

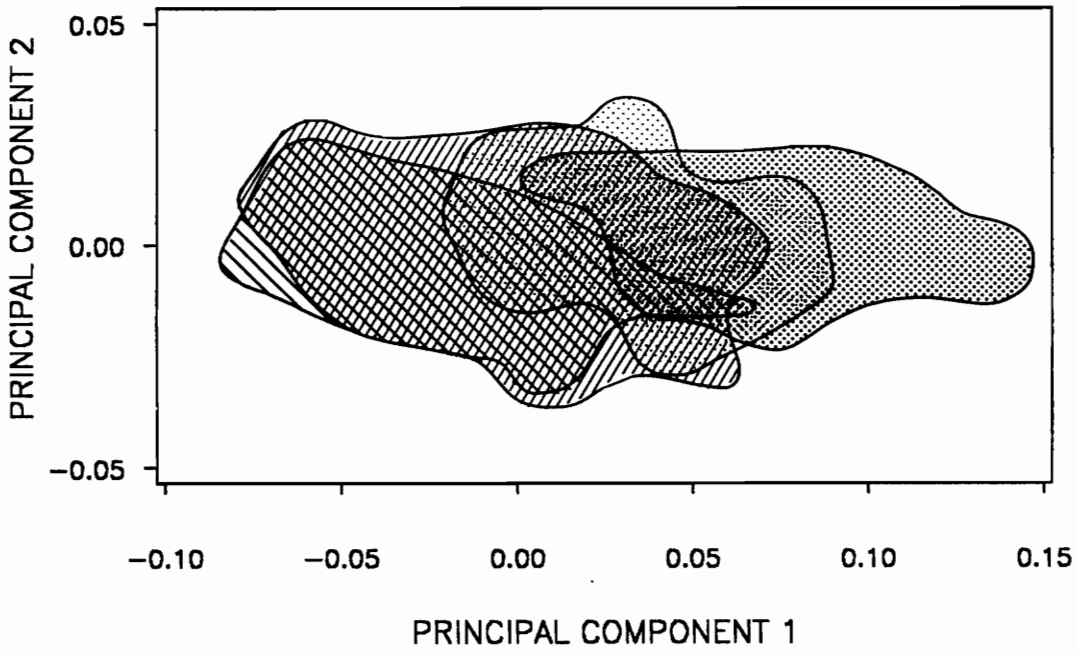

Figure 17. Principal component analysis for clusters 1, 2, 3, and 4 using amplitudes of all specimens: Patterns for each cluster are the same as used in Figure 14.

Table 6. Principal component analysis covariances, eigenvalues, and eigenvectors using means of amplitudes of harmonics 2, 4, 6 for all localities and using amplitudes of all specimens.

MEANS

	COVARIANCES			EIGENVECTORS		
	HAR2	**HAR4**	**HAR6**	**PRIN1**	**PRIN2**	**PRIN3**
HAR2	0.000797166	0.000274809	0.000136832	0.924217	-0.378993	-0.046768
HAR4	0.000274809	0.000152128	0.000064007	0.342970	0.877678	-0.334743
HAR6	0.000136832	0.000064007	0.000040128	0.167913	0.293335	0.941148

TOTAL VARIANCE = 0.000989422

	EIGENVALUE	DIFFERENCE	PROPORTION	CUMULATIVE
PRIN1	0.000924	0.000869	0.933885	0.93388
PRIN2	0.000055	0.000044	0.055440	0.98932
PRIN3	0.000011	.	0.010676	1.00000

ALL SPECIMENS

	COVARIANCES			EIGENVECTORS		
	HAR2	**HAR4**	**HAR6**	**PRIN1**	**PRIN2**	**PRIN3**
HAR2	0.001230714	0.000389004	0.000156247	0.937306	-0.341028	-0.071814
HAR4	0.000389004	0.000239356	0.000064543	0.324917	0.929631	-0.173822
HAR6	0.000156247	0.000064543	0.000058229	0.126039	0.139591	0.982155

TOTAL VARIANCE = 0.00152830

	EIGENVALUE	DIFFERENCE	PROPORTION	CUMULATIVE
PRIN1	0.001387	0.001280	0.907266	0.90727
PRIN2	0.000106	0.000071	0.069584	0.97685
PRIN3	0.000035	.	0.023151	1.00000

fied. In Figure 18 the vertical axis represents the 13 clusters with each identified by a horizontal black line. The clusters are ordered by elongation with the most round at the bottom and the most elongate at the top. Each locality, represented by a bar, is plotted on the x axis. A given bar connects all the specimens in a particular locality through the cluster to which it belongs. The patterns refer to the four groupings identified when cluster analysis was run using the mean amplitudes for each locality and are the same as in Figure 14. What is evident here is the tremendous intralocality or intrapopulational variation. What appeared to be distinct clusters when grouped by means, now overlap considerably. Only between the two end members, clusters 1 and 2, is the overlap minimal.

Discriminant analysis was run on clusters 1, 2, 3, and 4 as well as on combinations of these clusters to test their validity (Table 7). When class levels were defined as the four clusters, 37.6% of the observations were misclassified. That is, 37.6% of the specimens were placed in the wrong cluster. The misclassification is pronounced between clusters 1 and 4, 3 and 4, and less between 3 and 2. Clusters 1 and 2 are distinct from each other. When clusters 3 and 4 were grouped together and compared with cluster 1 and cluster 2, 26.6% were misclassified. Again, cluster 1 was confused with cluster 3/4 the most, 3/4 with 2 to a lesser extent, and 1 and 2 not at all. When cluster 1 and 4 were grouped together and compared with cluster 3 and cluster 2, 21.5% were misclassified. Cluster 1/4 overlapped with 3, 3 with 2, and 2 with 1/4 not at all. Percent misclassification drops to 11.7% when cluster 1/4 is compared to cluster 2/3. Percent misclassification is only 6.1% when cluster 1/4/3 is compared to cluster 2. Only one cluster 2 specimen is placed in the 1/4/3 class. When all specimens are used there appears to be no basis for designating discrete shape groups based on individual specimens of *Mucrospirifer*.

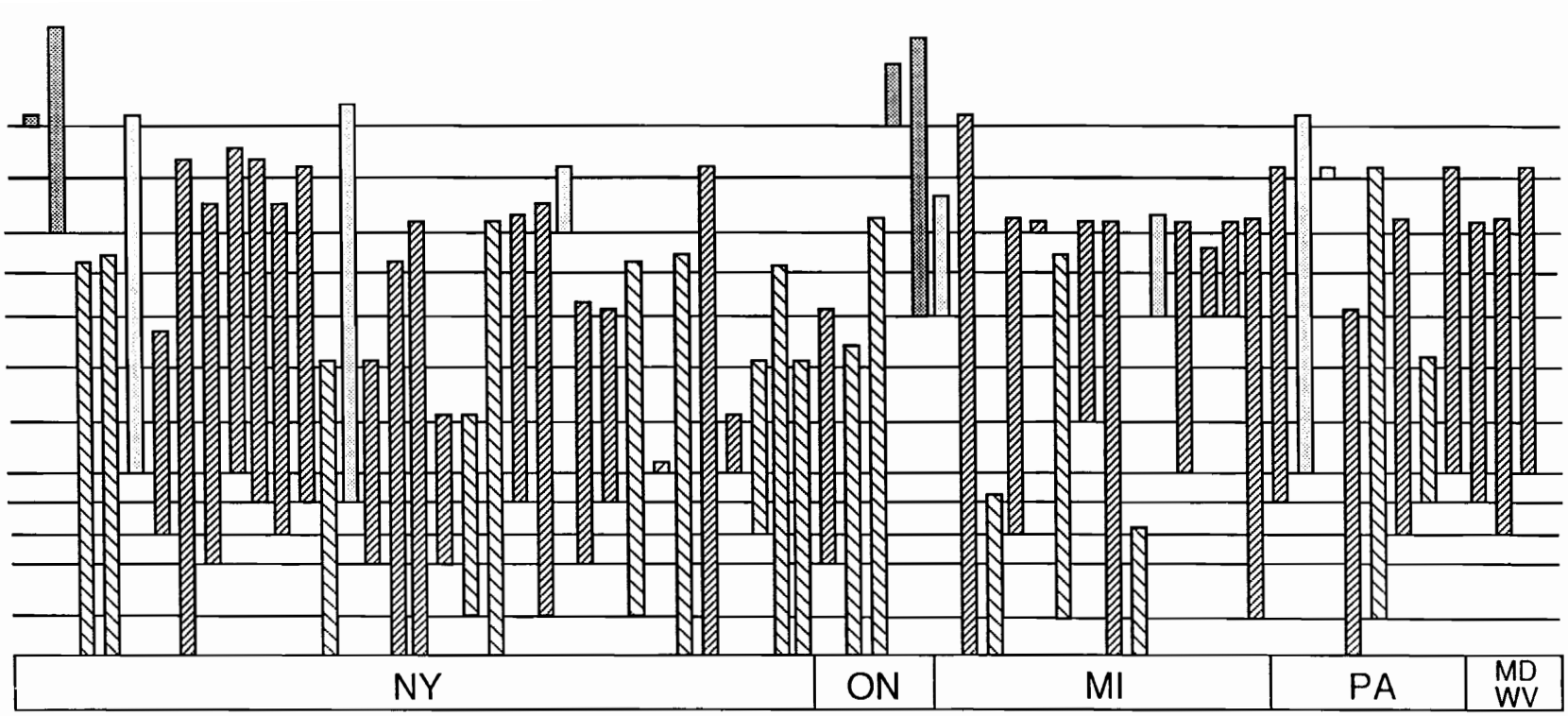

Figure 18. Cluster analysis using all specimens: Horizontal lines refer to each of the 13 clusters found when using all specimens. Localities, represented by a bar, are plotted on the x axis. Each bar connects specimens in a locality through the cluster to which it belongs. Patterns represent the four clusters identified when mean amplitudes were used and are the same as in Figure 10.

Table 7. Results of discriminant analysis on clusters 1, 2, 3, and 4; clusters 1, 3/4, and 2; clusters 1/4, 3, and 2; clusters 1/4 and 2/3; clusters 1/4/3 and 2.

FROM CLUSTER	NUMBER OF OBSERVATIONS AND PERCENTS CLASSIFIED INTO CLUSTER				
	1	**3**	**4**	**2**	**TOTAL**
1	131 74.43	4 2.27	41 23.30	0 0.00	176 100.00
3	0 0.00	26 60.47	11 25.58	6 13.95	43 100.00
4	72 23.53	70 22.88	160 52.29	4 1.31	306 100.00
2	0 0.00	7 14.89	0 0.00	40 85.11	47 100.00
TOTAL	203 35.49	107 18.71	212 37.06	50 8.74	572 100.00

	1	**3/4**	**2**	**TOTAL**
1	139 78.98	37 21.02	0 0.00	176 100.00
3/4	88 25.21	237 67.91	0 6.88	349 100.00
2	0 0.00	3 6.38	44 93.62	47 100.00
TOTAL	227 39.69	277 48.43	68 11.89	572 100.00

	1/4	**3**	**2**	**TOTAL**
1/4	378 78.42	100 20.75	4 0.83	482 100.00
3	6 13.95	31 72.09	6 13.95	43 100.00
2	0 0.00	7 14.89	40 85.11	47 100.00
TOTAL	384 67.13	138 24.13	50 8.74	572 100.00

	1/4	**2/3**	**TOTAL**
1/4	428 88.80	54 11.20	482 100.00
2/3	13 14.44	77 85.56	90 100.00
TOTAL	441 77.10	131 22.90	572 100.00

	1/4/3	**2**	**TOTAL**
1/4/3	491 93.52	34 6.48	525 100.00
2	1 2.13	46 97.87	47 100.00
TOTAL	492 86.01	80 13.99	572 100.00

SHAPE OF FOLD AND SULCUS

The second criterion that Tillman (1964) used to identify species of *Mucrospirifer* was the shape of the fold and sulcus. The shape of the fold and sulcus is highly variable in the study area. In addition, identification is obscured when only the internal mold of one valve is available or when the specimen is compressed, often making it difficult to place a specimen into one class or the other. In a given locality one type of fold or sulcus predominates. However, an occasional specimen of the other type is sometimes present and a few localities have a mixture of the two types. When the fold/sulcus types are grouped by locality and cluster, most of the cluster 1 localities have a V-shaped fold or sulcus; the cluster 4 localities are nearly equally divided; most of the cluster 3 localities have a flat fold or sulcus; all cluster 2 localities are flat (Table 8).

An analysis of variance (ANOVA) was run to test for a significant difference between the means of the flat and V-shaped types. Table 9 lists the results for harmonics 2, 4, and 6 and the results for the multivariate test on harmonics 2, 4, and 6 combined. The means were found to be significantly different for harmonics 2 and 4 and in the multivariate test. However, less than 9% of the total variation among amplitudes is explained by the model and the variation about the mean ranges from 48% to 57% (see Table 9 for R^2 values and coefficients of variation). The significance level is low because the small sum of squares is divided by the very large figure for degrees of freedom. The fact that the sum of squares is so small, yielding a miniscule difference between the means of the two groups, indicates instead that there is a great deal of overlap between the two groups and is evidence for lack of correlation between nature of the fold and sulcus and overall shape.

Table 8. Fold/sulcus types for localities within clusters.

CLUSTER	V	FLAT	FLAT & V	TOTAL
1	11	5	1	17
4	16	18	1	35
3	2	5	0	7
2	0	4	0	4
TOTAL	29	32	2	63

Table 9. Analysis of variance on flat vs V-shaped fold/sulcus types using General Linear Models Procedure. Two class levels, flat and V-shaped, and 555 observations.

DEPENDENT VARIABLE: HAR2

SOURCE	DF	SUM OF SQUARES	MEAN SQUARE	F VALUE	PR > F
MODEL	1	0.03781027	0.03781027	32.01	0.0001
ERROR	553	0.65322517	0.00118124		
CORRECTED	554	0.69103544			

R-SQUARE	C.V.	ROOT MSE	HAR2 MEAN
0.054715	47.8054	0.03436916	0.07189389

SOURCE	DF	TYPE I SS	F VALUE	PR > F
TYPE	1	0.03781027	32.01	0.0001

SOURCE	DF	TYPE III SS	F VALUE	PR > F
TYPE	1	0.03781027	32.01	0.0001

DEPENDENT VARIABLE: HAR4

SOURCE	DF	SUM OF SQUARES	MEAN SQUARE	F VALUE	PR > F
MODEL	1	0.01177068	0.01177068	54.18	0.0001
ERROR	553	0.12013594	0.00021724		
CORRECTED	554	0.13190662			

R-SQUARE	C.V.	ROOT MSE	HAR4 MEAN
0.089235	56.6622	0.01473920	0.02601241

SOURCE	DF	TYPE I SS	F VALUE	PR > F
TYPE	1	0.01177068	54.18	0.0001

SOURCE	DF	TYPE III SS	F VALUE	PR > F
TYPE	1	0.01177068	54.18	0.0001

DEPENDENT VARIABLE: HAR6

SOURCE	DF	SUM OF SQUARES	MEAN SQUARE	F VALUE	PR > F
MODEL	1	0.00020149	0.00020149	3.48	0.0627
ERROR	553	0.03202907	0.00005792		
CORRECTED	554	0.03223056			

R-SQUARE	C.V.	ROOT MSE	HAR6 MEAN
0.006251	52.8720	0.00761044	0.01439409

SOURCE	DF	TYPE I SS	F VALUE	PR > F
TYPE	1	0.00201497	3.48	0.0627

SOURCE	DF	TYPE III SS	F VALUE	PR > F
TYPE	1	0.00020149	3.48	0.0627

MANOVA TEST CRITERIA FOR THE HYPOTHESIS OF NO OVERALL TYPE EFFECT

WILKS' CRITERION	F(3,551)	PROB > F
0.89619364	21.27	0.0001

PILLAI'S TRACE	F(3,551)	PROB > F
0.10380636	21.27	0.0001

HOTELLING-LAWLEY TRACE	F(3,551)	PROB > F
0.11583028	21.27	0.0001

ROY'S MAXIMUM ROOT CRITERION	F(3,551)	PROB > F
0.11583028	21.27	0.0001

GROWTH AND FORM

Linear regression was employed to evaluate if the size of an adult specimen affects its shape. The power function, $y = bx^{\alpha}$, has been widely used in allometric studies due to its simplicity, interpretability, and adequate statistical fit. It is commonly called the equation of simple allometry (Gould, 1966). When the data are log transformed, the equation becomes

$$\log y = \alpha(\log x) + \log b$$

where y is the variable whose increase is considered relative to x, which measures size; α is the slope; and b is the y value at $x = 1$. The slope is a ratio of the specific growth rates of y and x. When log-transformed data are plotted in rectangular coordinates, a slope of 1 indicates isometric growth while a slope greater or less than 1 indicates allometric growth (Gould, 1966). In this study, log-transformed data for the amplitudes of harmonic 0, a measure of size, were regressed against harmonic 2. The original nonnormalized data were used, i.e. amplitudes were not divided by harmonic 0.

Using all specimens, a slope of 1.5488 was obtained and determined to be significantly different from 1 using the F statistic at a 0.05 level of significance ($p = 0.0001$) (Figure 19). In order to determine what factors contribute to the apparent allometry, harmonic 0 was regressed against harmonic 2 by locality, by cluster, and by lithology.

In the analysis by locality, no slopes were significantly different from 1 except those for localities N18 and O02C (Table 10). When specimens in localities N18 and O02C were examined they were found to include specimens spanning a range of sizes. The non-log-transformed amplitude of harmonic 0 for locality N18 ranges from 17.48 to 38.39 and for locality O02C from 20.11 to 36.13. Log-transformed figures are 1.27-1.59 for locality N18 and 1.30-1.56 for O02C. When the two smallest specimens were removed from the analysis for locality N18 and the three smallest were removed from the analysis for locality O02C, both slopes were not significantly different from 1 (N18, $p = 0.1045$, N=15; O02C, $p = 0.0680$, N=19). Therefore,

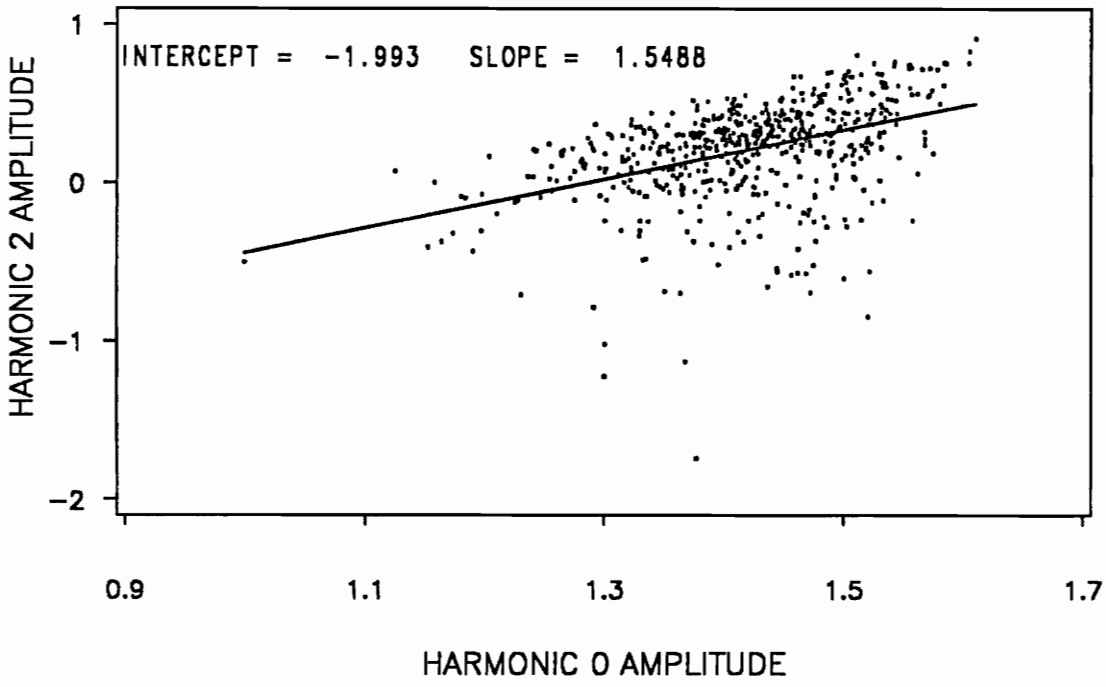

Figure 19. Linear regression of of log-transformed amplitudes of harmonic 0 vs harmonic 2 for all specimens: P = 0.0001.

no significant allometry was detected within localities. The lines of regression for each locality were compared in a homogeneity of slope model to determine if they could have come from the same population. Localities with only one or two specimens were eliminated because they give spurious results, as were localities N18 and O02C because of their significant allometry. No significant difference was found comparing the slopes of the remaining 49 localities ($p = 0.1428$) (Table 11).

No significant allometry was found when harmonic 0 was regressed against harmonic 2 for clusters 1, 2, 3, and 4 (1, $p = 0.3995$; 2, $p = 0.1105$; 3, $p = 0.1101$; 4, $p = 0.6012$) (Figure 20-Figure 23). In addition, no significant difference among the four slopes was found when they were compared in a homogeneity of slope model ($p = 0.4955$) (Figure 24, Table 12). Linear regression of specimens grouped by lithology found significant allometry for specimens in sandstone ($p = 0.0001$, N = 65) (Figure 25) and siltstone ($p = 0.0070$, N = 213) (Figure 26). Specimens in mudstone ($p = 0.7943$, N = 148) (Figure 27), calcareous shale ($p = 0.1873$, N = 90) (Figure 28), and limestone ($p = 0.8215$, N = 56) (Figure 29) did not show significant allometry. In a homogeneity of slope test, no significant difference was found among the slopes of the five regression lines ($p = 0.0622$) (Figure 30, Table 13). Since no significant allometry was detected among localities, clusters, or lithologies, shape differences among adult specimens of *Mucrospirifer* cannot be attributed to differences in size.

TIME, ENVIRONMENT, AND MORPHOLOGY

TIME

If the hypothesis is made that morphological shape is independent of time, then one would expect to find localities in each horizon evenly divided among the four clusters. As can be seen from Table 14, more localities from horizon c than would be expected fall in cluster

Table 10. Linear regression of harmonic 0 vs harmonic 2 on log-transformed data for each locality. Localities with fewer than three specimens omitted.

LOC	Y INTERCEPT	INTERCEPT SE	SLOPE	SLOPE SE	R^2	DF	NUMER.	DENOM.	F VALUE	PROB > F
D01	-2.33291079	1.09045462	1.90326497	0.77430934	0.8580	1,1	0.0286134	0.0210266	1.3608	0.4512
D02	-1.82457715	0.68258999	1.48669185	0.48612920	0.6516	1,5	0.0082367	0.0082176	1.0023	0.3627
M01	-1.01683864	1.32744894	0.82676358	0.95971288	0.0396	1,18	0.001074	0.032962	0.0326	0.8588
M03	-1.54356189	0.87448475	1.29615237	0.59014570	0.4910	1,5	0.0015802	0.0062749	0.2518	0.6371
M08	-0.65548858	2.54703537	0.62259265	1.70611320	0.0624	1,2	2.0E-04	0.0041778	0.0489	0.8455
M11	0.91796108	2.84665714	-0.39977208	1.95248698	0.0402	1,1	0.0033944	0.0066044	0.5140	0.6040
M12	-0.61398704	1.76933748	0.60399129	1.20015910	0.0779	1,3	0.0050512	0.0463944	0.1089	0.7631
M13	-0.62422054	0.31759186	0.69926989	0.22524337	0.7626	1,3	0.0041602	0.0023338	1.7826	0.2741
M14	-3.86699389	4.75933333	2.55459069	3.17975904	0.2440	1,2	0.0166831	0.0697964	0.2390	0.6733
M15	-1.08941933	2.30344854	0.74171381	1.67599353	0.0377	1,5	0.0010258	0.043192	0.0237	0.8836
M17	0.21103874	1.37551086	0.13441710	0.91980662	0.0106	1,2	0.0105489	0.0119119	0.8856	0.4460
M19	-4.96805336	49.75203687	3.42120815	33.76276582	0.0102	1,1	0.0027841	0.541381	0.0051	0.9544
M23	1.48847313	2.00533081	-0.88049385	1.35268954	0.0503	1,8	0.119456	0.06181	1.9326	0.2019
N02	-1.25073829	0.63634512	1.09764884	0.45124734	0.2046	1,23	5.2E-04	0.0111815	0.0468	0.8306
N03	-1.29238041	0.95835281	1.11120418	0.67409090	0.1196	1,20	2.8E-04	0.010112	0.0272	0.8706
N04	-1.26325836	0.31361294	1.16856641	0.21602128	0.7648	1,9	0.0018497	0.0030378	0.6089	0.4552
N05A	-0.81906175	0.38724172	0.84373443	0.27627299	0.3413	1,18	0.0022807	0.0071287	0.3199	0.5786
N05B	-1.69263048	0.77427796	1.41462244	0.56576097	0.3425	1,12	0.0081382	0.0151527	0.5371	0.4777
N06	-0.12609676	0.80301512	0.24230615	0.57580632	0.0134	1,13	0.0323878	0.0187045	1.7315	0.2109
N07	-0.63144169	1.35212294	0.66722175	0.96716559	0.0289	1,16	0.0025676	0.021688	0.1184	0.7353
N10	-1.96065314	0.68685101	1.59067883	0.49186848	0.3222	1,22	0.0250778	0.0173894	1.4421	0.2426
N11	0.55783859	1.20033123	-0.36510653	0.87091588	0.0087	1,20	0.117706	0.0479091	2.4569	0.1327
N13	-3.66681279	2.38140371	2.50789491	1.70798665	0.2355	1,7	0.13961	0.17912	0.7794	0.4066
N17	-1.72690133	0.56384237	1.56336770	0.37173357	0.4457	1,22	0.0131775	0.0057374	2.2968	0.1439
N18	-1.95748735	0.34969008	1.68681849	0.24379663	0.7614	1,15	0.087622	0.0110404	7.9365	0.0130
N19	-1.72359233	1.07723350	1.38001987	0.77277139	0.2616	1,9	0.0038722	0.0160119	0.2418	0.6347
N20	-1.68521664	0.70680212	1.30745100	0.58363160	0.2507	1,15	0.0140221	0.0505287	0.2775	0.6060
N22A	-4.28989624	1.25817973	3.36889591	0.95881167	0.9251	1,1	0.0358452	0.0058723	6.1042	0.2448
N22B	-1.97623747	1.51394777	1.53764889	1.06578696	0.2065	1,8	0.0052757	0.0207311	0.2545	0.6275
N22D	-1.18512439	1.98550473	0.93006178	1.36618734	0.0848	1,5	1.7E-04	0.0657483	0.0026	0.9612
N27	-3.44659970	1.55248868	2.51072978	1.04871728	0.6564	1,3	0.104869	0.0505346	2.0752	0.2453
N31	-2.17878610	2.39451519	1.39472339	1.61714955	0.0397	1,18	0.0076493	0.128392	0.0596	0.8099
N33	0.31123515	2.50954573	-0.50459060	1.84031473	0.0050	1,15	0.150414	0.225027	0.6684	0.4264
N34A	-1.07160373	1.01000384	0.96547426	0.70280739	0.2123	1,7	7.3E-05	0.0302307	0.0024	0.9622
N34B	0.13739801	0.97335891	0.08381296	0.71069322	0.0137	1,1	0.0266395	0.0160296	1.6619	0.4200
N34C	-3.35310477	1.14506180	2.36536767	0.78176925	0.4542	1,11	0.193486	0.0634317	3.0503	0.1085
N34D	13.23009060	4.86817496	-9.34319631	3.45027834	0.8800	1,1	0.103882	0.0115596	8.9867	0.2050
N34F	10.24257154	3.44520716	7.35166979	2.46385295	0.6900	1,4	1.04575	0.157355	6.6458	0.0615
N34G	-3.62782069	1.39435977	2.64840706	0.97075652	0.4820	1,8	0.121632	0.0421831	2.8834	0.1279
N35B	-2.57712319	1.30463003	1.85998547	0.97155395	0.3792	1,6	0.0569399	0.0726722	0.7835	0.4101
O01A	-1.51647338	0.61018308	1.42943550	0.40139297	0.4422	1,16	0.0092816	0.008109	1.1446	0.3006
O02A	-0.01674635	0.59850992	0.47328115	0.39149981	0.4222	1,2	0.0013459	7.4E-04	1.8101	0.3107
O02C	2.11916978	1.09617778	-1.44532410	0.75405645	0.1552	1,20	0.56304	0.0535395	0.5164	0.0041
O04	-0.09993716	0.69569795	0.20906576	0.48948287	0.0223	1,8	0.0324097	0.0124128	2.6110	0.1448
O05	-1.53318903	2.13705717	1.08147431	1.45939363	0.0405	1,13	3.1E-04	0.098204	0.0031	0.9563
P05	-1.92095797	0.56531341	1.59801512	0.41177116	0.7901	1,4	0.0167296	0.0079318	2.1092	0.2201
P07	0.28009695	2.46036297	0.09530998	1.72312978	0.0031	1,1	0.0064868	0.0235325	0.2757	0.6922
P10	-5.41696831	2.98496073	3.99675108	2.23719303	0.4438	1,4	0.287172	0.160047	1.7943	0.2514
P14	0.02854436	1.62117179	0.13880804	1.15386808	0.0021	1,7	0.0138544	0.0248714	0.5570	0.4798
P17	0.40342027	2.87383165	0.02373285	1.93277420	0.0001	1,3	0.0038921	0.0152548	0.2551	0.6483
W01	-0.62283285	0.90595067	0.67899014	0.62440583	0.1445	1,7	0.0062785	0.023755	0.2643	0.6230

Table 11. Test for significant difference among slopes of localities. Localities N18, O02C and those with less than three specimens omitted giving 49 localities and 513 observations.

SOURCE	DF	SUM OF SQUARES	MEAN SQUARE	F VALUE	PR > F
MODEL	97	32.38353502	0.33385088	7.47	0.0001
ERROR	415	18.54028844	0.04467539		
CORRECTED	512	50.92382346			

R-SQUARE	C.V.	ROOT MSE	HAR2 MEAN
0.635921	103.0387	0.21136555	0.20513218

SOURCE	DF	TYPE I SS	F VALUE	PR > F
HAR0	1	10.82334181	242.27	0.0001
LOCALITY	48	18.90857093	8.82	0.0001
HAR0*LOCALITY	48	2.65162227	1.24	0.1428

SOURCE	DF	TYPE III SS	F VALUE	PR > F
HAR0	1	0.43040650	9.63	0.0020
LOCALITY	48	2.73074975	1.27	0.1127
HAR0*LOCALITY	48	2.65162227	1.24	0.1428

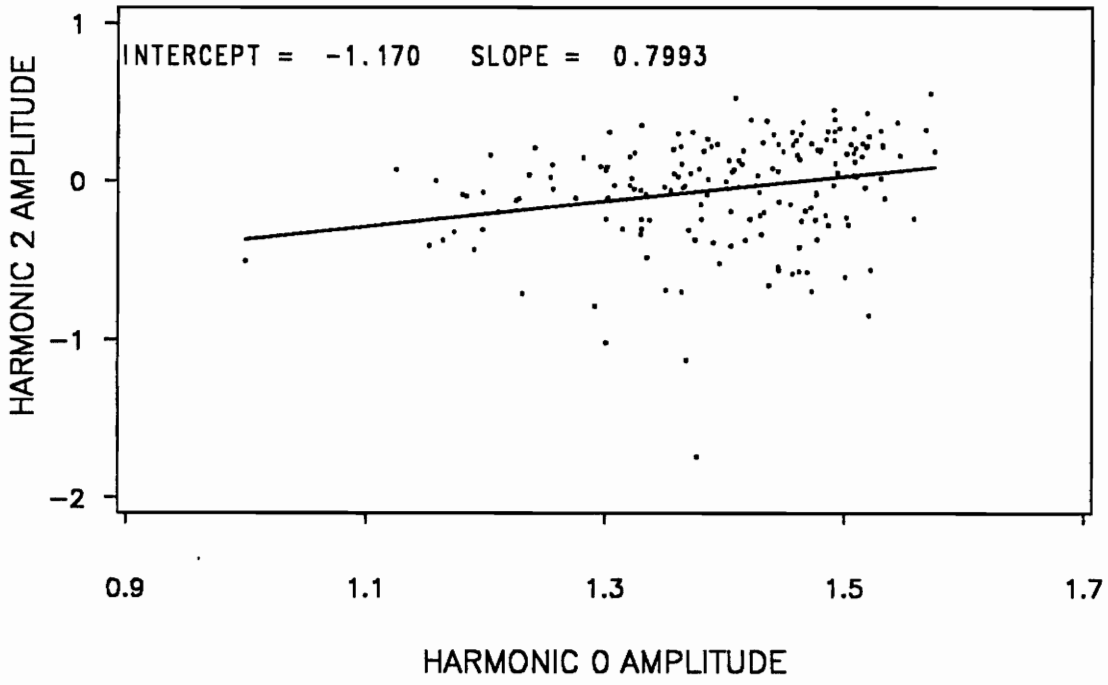

Figure 20. Linear regression of of log-transformed amplitudes of harmonic 0 vs harmonic 2 for all specimens in cluster 1: P = 0.3995; 176 specimens in 17 localities.

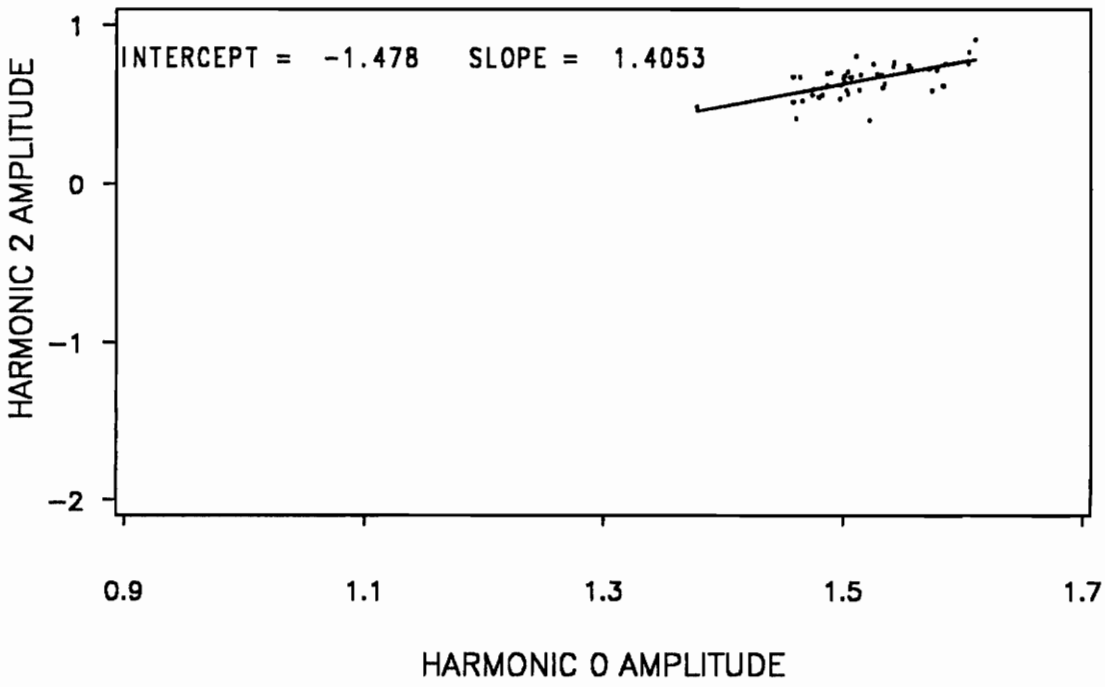

Figure 21. Linear regression of of log-transformed amplitudes of harmonic 0 vs harmonic 2 for all specimens in cluster 2: P = 0.1105; 47 specimens in 4 localities.

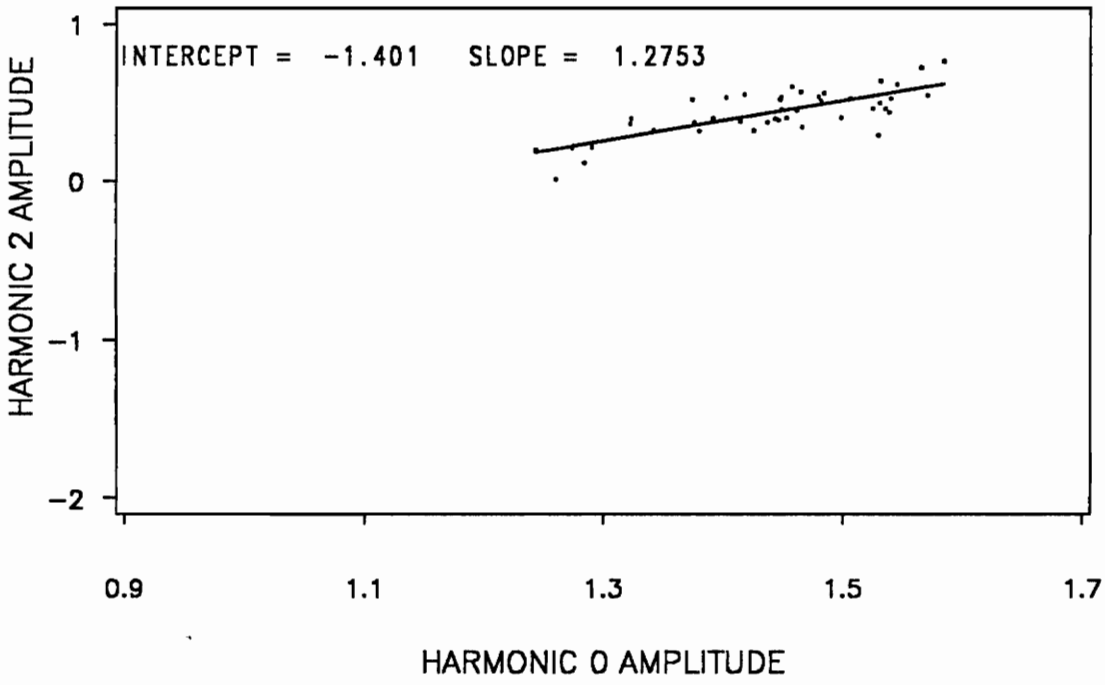

Figure 22. Linear regression of of log-transformed amplitudes of harmonic 0 vs harmonic 2 for all specimens in cluster 3: P = 0.1101; 306 specimens in 35 localities.

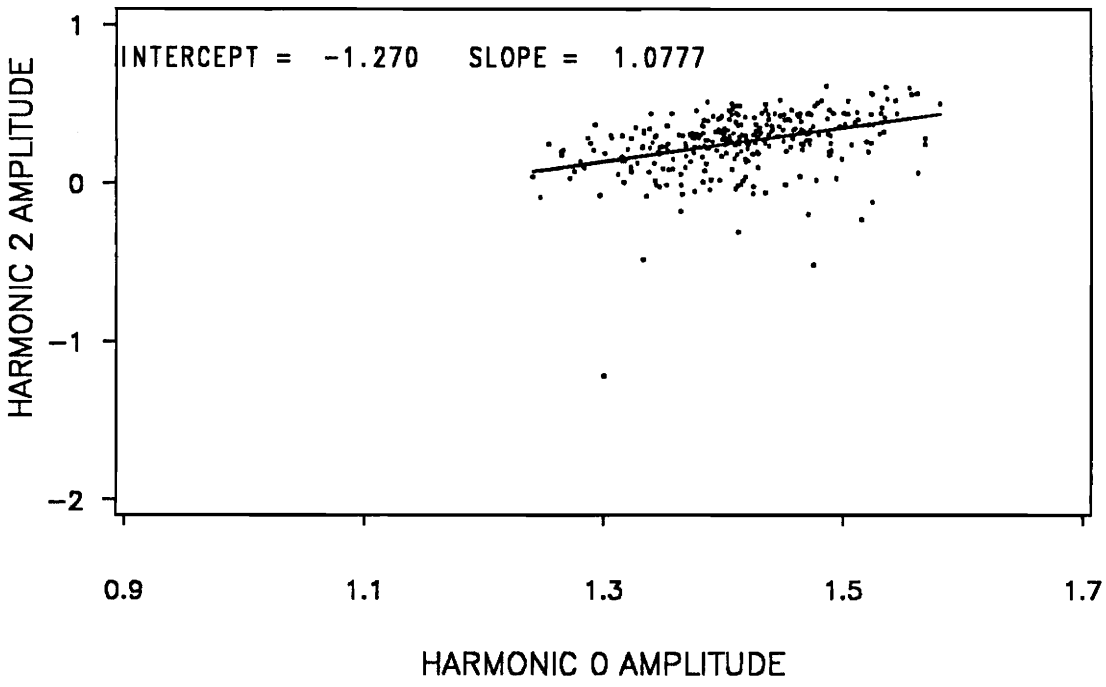

Figure 23. Linear regression of of log-transformed amplitudes of harmonic 0 vs harmonic 2 for all specimens in cluster 4: P = 0.6012; 306 specimens in 35 localities.

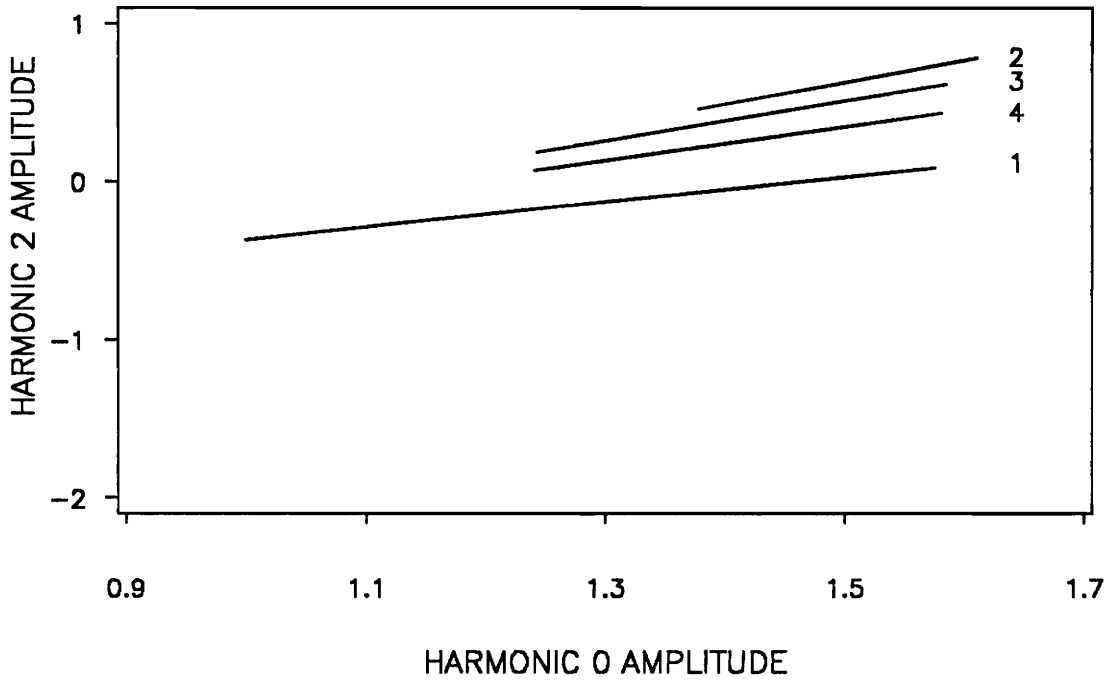

Figure 24. Test for differences among the slopes of clusters 1, 2, 3, and 4: Using log-transformed data for amplitudes of harmonics 0 and 2. P = 0.4955.

Table 12. Test for significant difference among slopes of clusters (clusters 1, 2, 3, and 4).

SOURCE	DF	SUM OF SQUARES	MEAN SQUARE	F VALUE	PR > F
MODEL	7	27.59456365	3.94208052	76.95	0.0001
ERROR	564	28.89314006	0.05122897		
CORRECTED	571	56.48770371			

R-SQUARE	C.V.	ROOT MSE	HAR2 MEAN
0.488506	109.6077	0.22633818	0.20649844

SOURCE	DF	TYPE I SS	F VALUE	PR > F
HAR0	1	10.32859981	201.62	0.0001
CLUSTER	3	17.14336772	111.55	0.0001
HAR0*CLUSTER	3	0.12259611	0.80	0.4955

SOURCE	DF	TYPE III SS	F VALUE	PR > F
HAR0	1	1.46820587	28.66	0.0001
CLUSTER	3	0.01206641	0.08	0.9716
HAR0*CLUSTER	3	0.12259611	0.80	0.4955

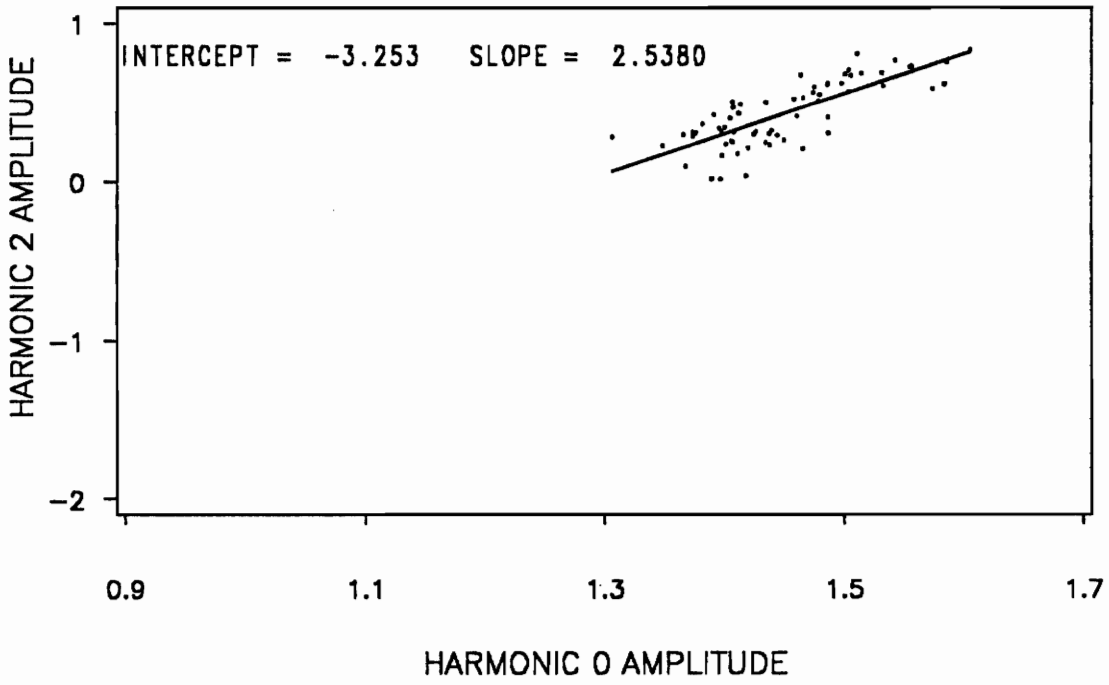

Figure 25. Linear regression of log-transformed amplitudes of harmonic 0 vs harmonic 2 for all specimens in sandstone: P = 0.0001; 65 specimens in 4 localities.

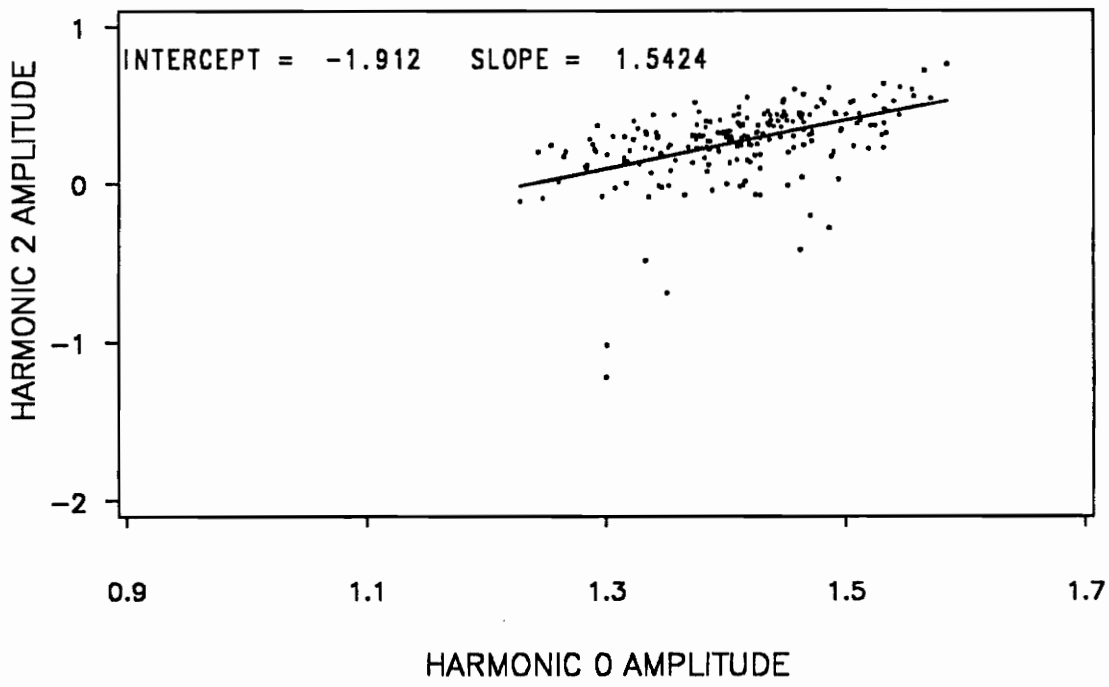

Figure 26. Linear regression of log-transformed amplitudes of harmonic 0 vs harmonic 2 for all specimens in siltstone: P = 0.0070; 213 specimens in 21 localities.

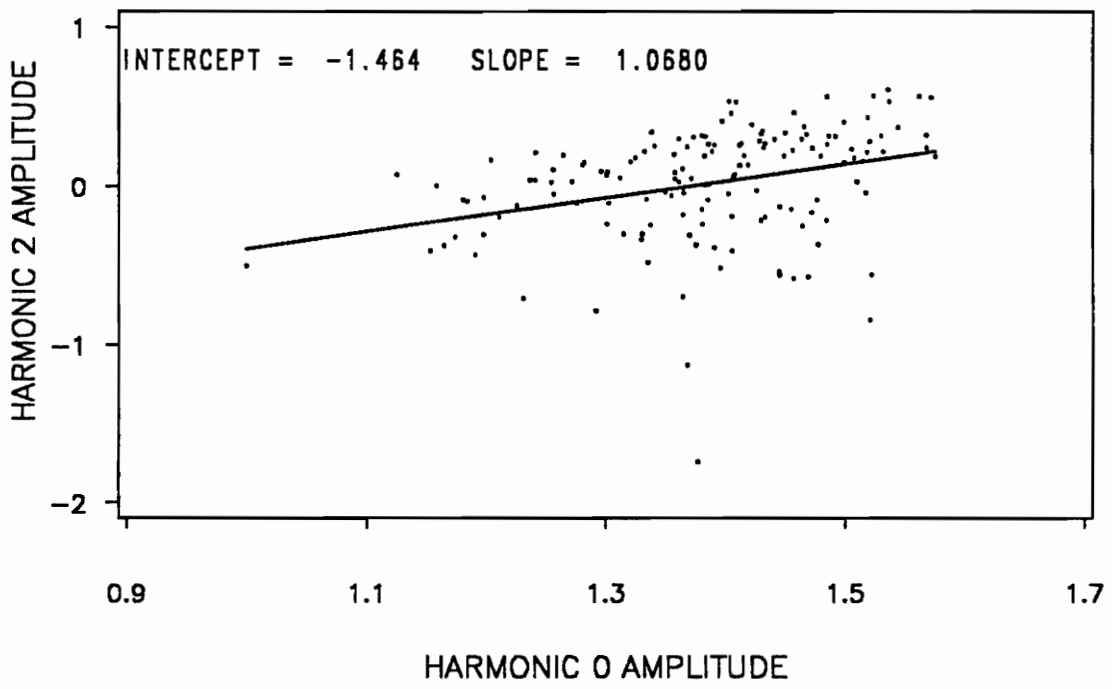

Figure 27. Linear regression of log-transformed amplitudes of harmonic 0 vs harmonic 2 for all specimens in mudstone: P = 0.7943; 148 specimens in 19 localities.

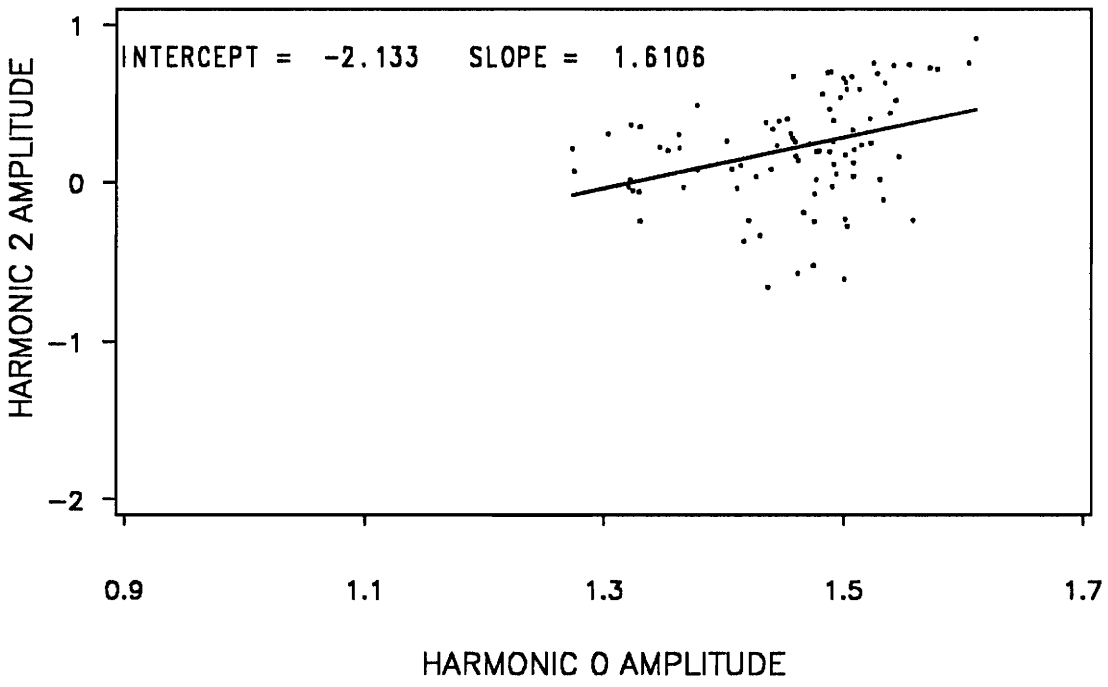

Figure 28. Linear regression of log-transformed amplitudes of harmonic 0 vs harmonic 2 for all specimens in calcareous shale: P = 0.1873; 90 specimens in 10 localities.

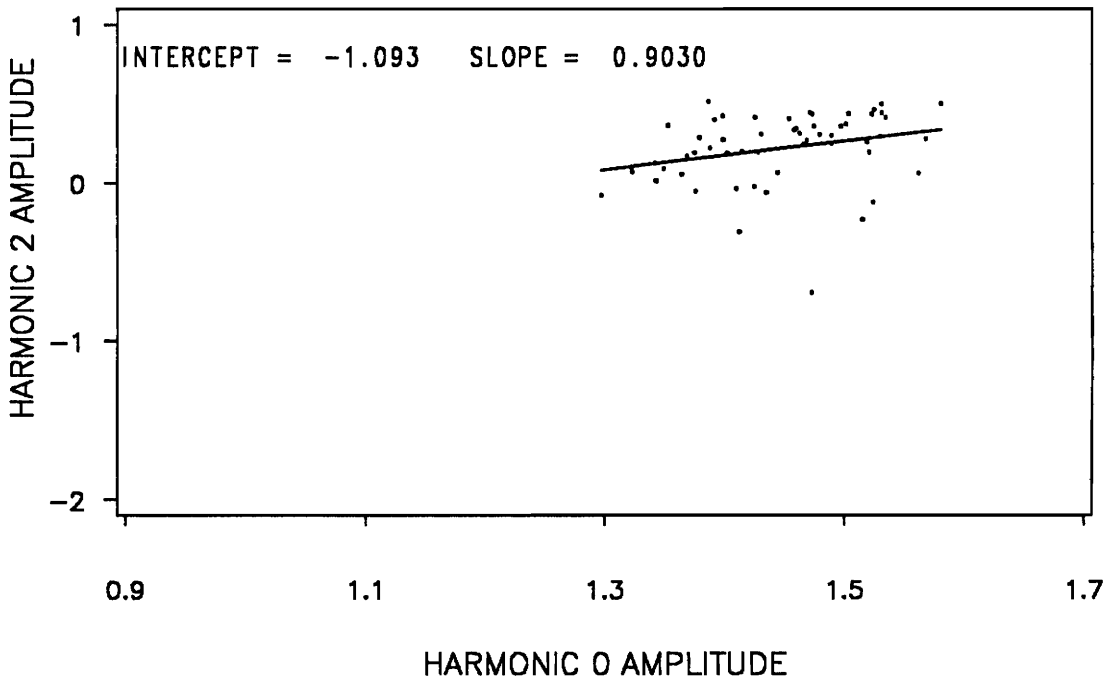

Figure 29. Linear regression of log-transformed amplitudes of harmonic 0 vs harmonic 2 for all specimens in limestone: P = 0.8215; 56 specimens in 9 localities.

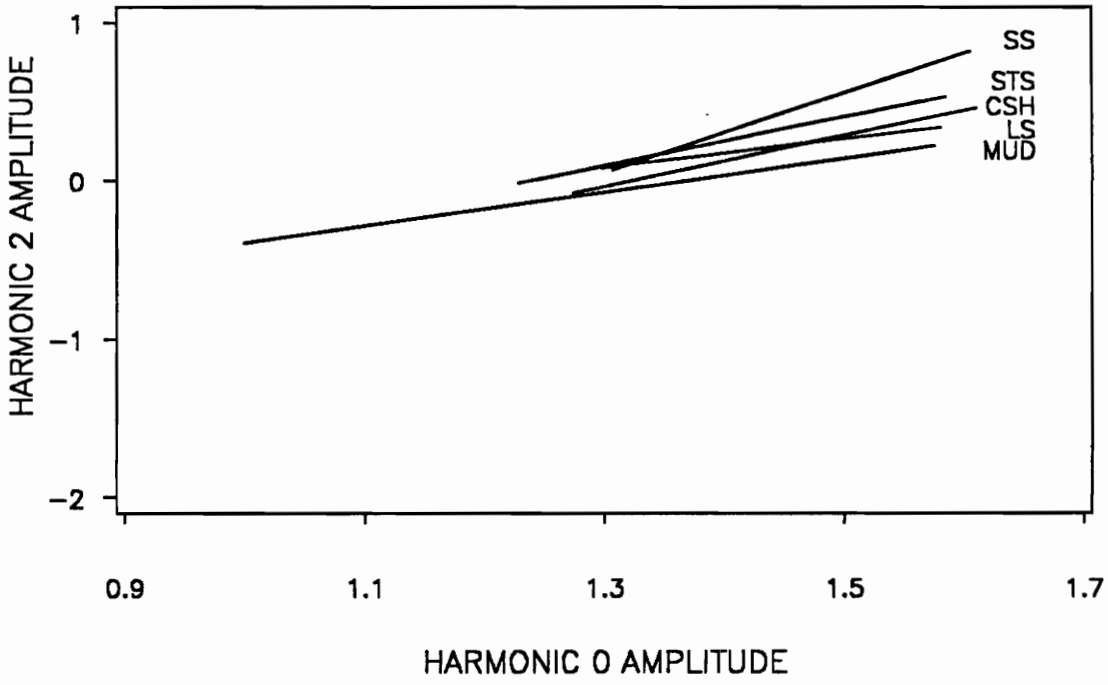

Figure 30. Test for differences among the slopes of the five lithologies: Using log-transformed data for the amplitudes of harmonic 0 and 2. P = 0.0622 at α = 0.05.

Table 13. Test for significant difference among slopes of lithologies (sandstone, siltstone, mudstone, calcareous shale, limestone).

SOURCE	DF	SUM OF SQUARES	MEAN SQUARE	F VALUE	PR > F
MODEL	9	17.23595938	1.91510660	27.42	0.0001
ERROR	562	39.25219355	0.06984376		
CORRECTED	571	56.48815293			

R-SQUARE	C.V.	ROOT MSE	HAR2 MEAN
0.305125	127.9808	0.26427970	0.20649955

SOURCE	DF	TYPE I SS	F VALUE	PR > F
HAR0	1	10.32855731	147.88	0.0001
LITH	4	6.27793425	22.47	0.0001
HAR0*LITH	4	0.62946782	2.25	0.0622

SOURCE	DF	TYPE III SS	F VALUE	PR > F
HAR0	1	5.32838601	76.29	0.0001
LITH	4	0.45401120	1.63	0.1664
HAR0*LITH	4	0.62946782	2.25	0.0622

4, a cluster containing round specimens, and cluster 1, which contains the roundest specimens. Horizons b, c, and d each contain fewer localities from cluster 2 than would be expected. The probability that cluster and horizon are independent of each other was found to be 0.123 using Fisher's exact test, therefore the null hypothesis cannot be rejected. Because the clusters are based only on the mean amplitudes for significant harmonics for each locality, further statistical tests using all specimens were employed to assess the relationship between time and morphology.

Each horizon was assigned a length of 1.25 my based on the total time of deposition of the Hamilton Group and its equivalents (5 my/4 horizons) and was regressed against the amplitudes of harmonic 2 for all specimens (Figure 31). The resulting negative slope of the regression line suggests a trend towards roundness with time, although the magnitude of the slope is rather small (-0.072). The probability of no change of shape occurring with time was determined to be 0.0001 which would lead one to reject the null hypothesis. However, less than 7% of the total variation in amplitudes is explained by the fitted regression line (R^2 = 0.0609) and the relative dispersion about the mean is very high (CV = 47.23935). At best the test is inconclusive and in actuality it indicates that the overall shape encompassed by each horizon overlaps to such an extent that a meaningful trend cannot be detected. Results of an analysis of variance testing for a significant difference among horizons are similar (see Table 15 for R^2 values, coefficients of variation, and probabilities).

Principal component analysis was used to graphically display the relationship among the specimens in the four horizons in order to substantiate the tests above. Plots of all specimens in each horizon for the first and second principal components are shown in Figure 32-Figure 35 and the four are overlain in Figure 36. Principal component 2 accounts for a relatively small proportion of the total variance and the range of scores for axis 2 are fairly similar for each horizon. The differences among horizons rest primarily in the scores for the first principal component. The ranges of scores for principal component 1 for Figure 32-Figure 54 is given in Table 16. Horizon a (Figure 32) spans the length of the first principal component to include very round and very elongate specimens. Horizons b

Table 14. Listing of localities by cluster and horizon used in a Fisher's exact test.

	HORIZON A	HORIZON B	HORIZON C	HORIZON D	TOTAL
CLUSTER 1	4	1	11	1	17
CLUSTER 2	4	0	0	0	4
CLUSTER 3	3	0	2	2	7
CLUSTER 4	8	2	19	6	35
TOTAL	19	3	32	9	63

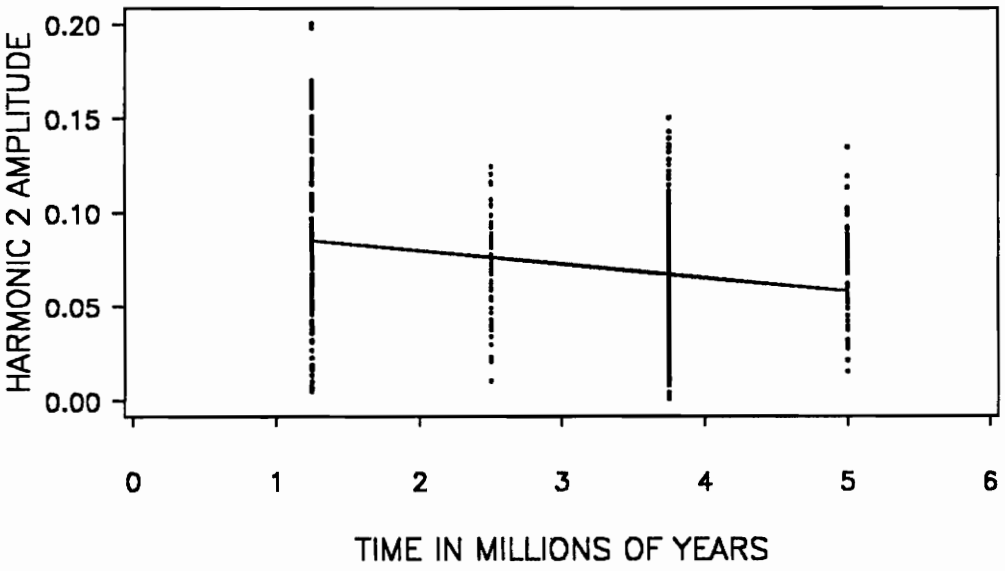

Figure 31. Linear regression of all specimens by horizon: Intercept = 0.095; slope = -0.072; p = 0.0001.

Table 15. Test for significant difference among horizons a, b, c, and d using all specimens.

DEPENDENT VARIABLE: HAR2

SOURCE	DF	SUM OF SQUARES	MEAN SQUARE	F VALUE	PR > F
MODEL	3	0.05284131	0.01761377	15.39	0.0001
ERROR	568	0.64989614	0.00114418		
CORRECTED	571	0.70273745			

R-SQUARE	C.V.	ROOT MSE	HAR2 MEAN
0.075194	47.00318	0.0338258	0.0719649

SOURCE	DF	TYPE I SS	F VALUE	PR > F
HORIZON	3	0.05284131	15.39	0.0001

SOURCE	DF	TYPE III SS	F VALUE	PR > F
HORIZON	3	0.05284131	15.39	0.0001

DEPENDENT VARIABLE: HAR4

SOURCE	DF	SUM OF SQUARES	MEAN SQUARE	F VALUE	PR > F
MODEL	3	0.02818714	0.00939571	49.19	0.0001
ERROR	568	0.10848506	0.00019099		
CORRECTED	571	0.13667220			

R-SQUARE	C.V.	ROOT MSE	HAR4 MEAN
0.206239	52.92451	0.0138201	0.0261128

SOURCE	DF	TYPE I SS	F VALUE	PR > F
HORIZON	3	0.02828714	49.19	0.0001

SOURCE	DF	TYPE III SS	F VALUE	PR > F
HORIZON	3	0.02818714	49.19	0.0001

DEPENDENT VARIABLE: HAR6

SOURCE	DF	SUM OF SQUARES	MEAN SQUARE	F VALUE	PR > F
MODEL	3	0.00630467	0.0021056	44.30	0.0001
ERROR	568	0.02694391	0.00004744		
CORRECTED	571	0.03324859			

R-SQUARE	C.V.	ROOT MSE	HAR6 MEAN
0.189622	47.95140	0.0068874	0.0143633

SOURCE	DF	TYPE I SS	F VALUE	PR > F
HORIZON	3	0.00630467	44.30	0.0001

SOURCE	DF	TYPE III SS	F VALUE	PR > F
HORIZON	3	0.00630467	44.30	0.0001

MANOVA TEST CRITERIA FOR THE HYPOTHESIS OF NO OVERALL TYPE EFFECT

WILKS' CRITERION	F(3,551)	PROB > F
0.70997518	23.13	0.0001
PILLAI'S TRACE	F(3,551)	PROB > F
0.29377202	20.55	0.0001
HOTELLING-LAWLEY TRACE	F(3,551)	PROB > F
0.40322739	25.30	0.0001
ROY'S MAXIMUM ROOT CRITERION	F(3,551)	PROB > F
0.38974854	73.79	0.0001

(Figure 33), c (Figure 34), and d (Figure 35) are quite similar, although horizon c contains both rounder and more elongate specimens than do horizons b and d. The results of principal component analysis confirm the interpretation of linear regression and analysis of variance made above. No horizon occupies a shape domain distinctly different from the others, although horizon a includes a degree of elongateness not present in the other horizons (Figure 36).

ENVIRONMENT

A series of tests were conducted to identify if particular shapes could be correlated with certain environments. An initial test was made to see if lithology is independent of cluster before proceeding with statistical tests using all specimens. The number of localities composed of each lithology for each cluster is given in Table 17. Using the hypothesis that morphological shape is independent of environment, one would expect to find localities of each lithology equally divided among the four clusters. As seen in Table 17, more localities composed of mudstone than would be expected fall in clusters 1 and 4, the two clusters containing the rounder specimens. Localities composed of siltstone are represented to an unusually large extent in cluster 4. The probability that lithology and cluster are independent of each other was found to be only 0.00252 using Fisher's exact test, therefore the null hypothesis must be rejected.

Analysis of variance using all specimens was employed to test the hypothesis that there is no difference among lithologies for overall shape as measured by the amplitudes of harmonics 2, 4, and 6. Based on the resulting probability alone this hypothesis would have to be rejected ($p < 0.0001$). However, less than 20% of the variability is accounted for and the dispersion about the mean approaches 50%, which makes the test inconclusive (see Table 18 for R^2 values and coefficients of variation).

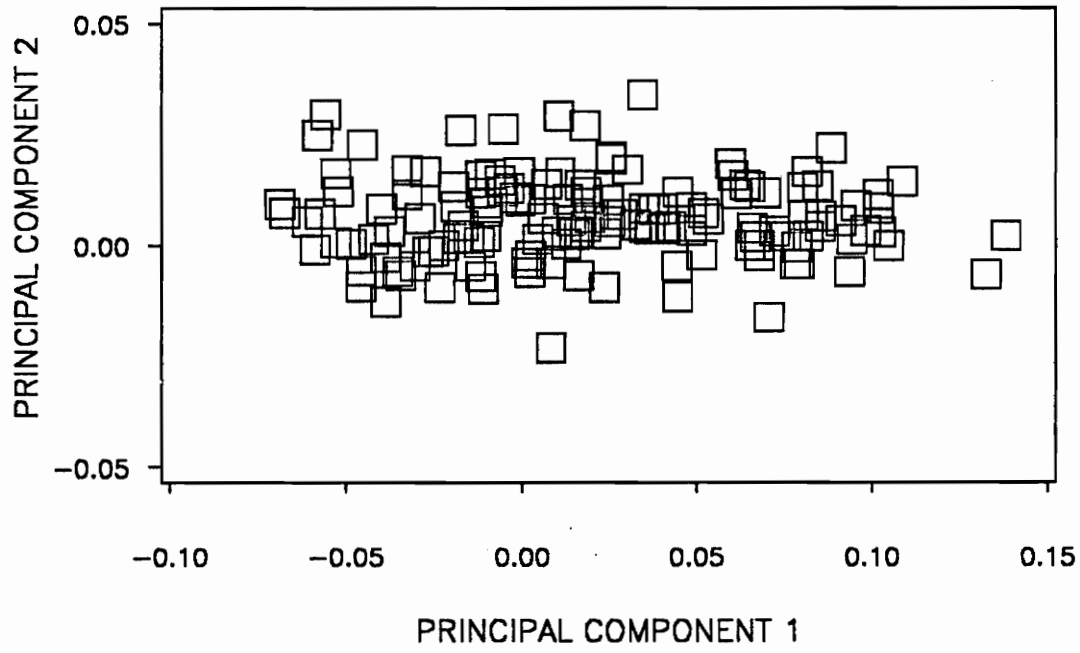

Figure 32. Principal component analysis with all specimens in horizon a.

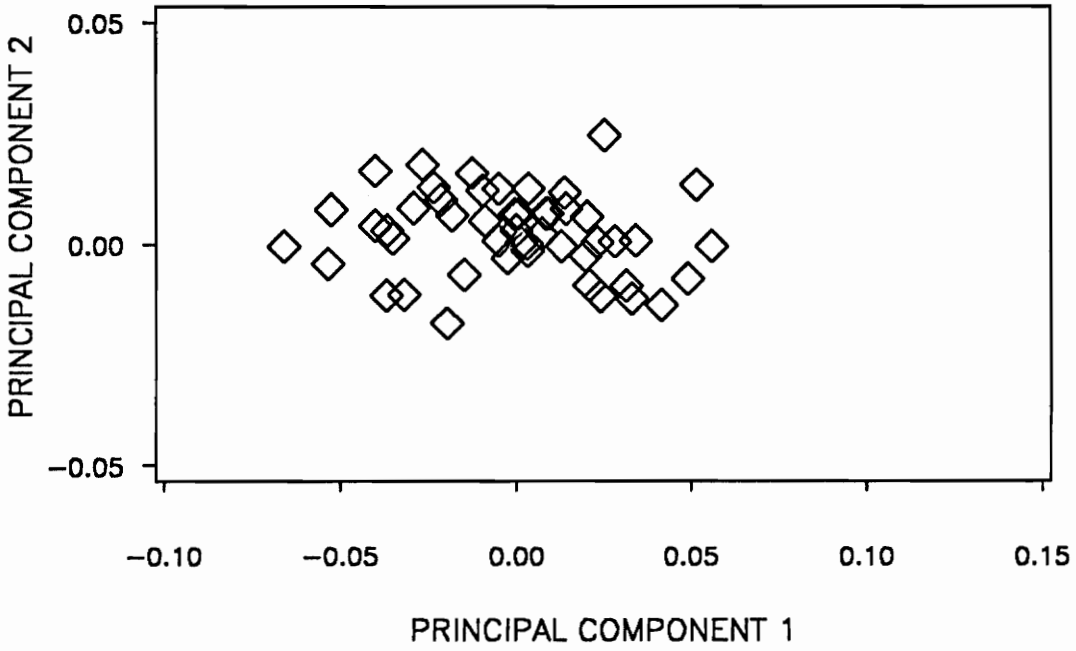

Figure 33. Principal component analysis with all specimens in horizon b.

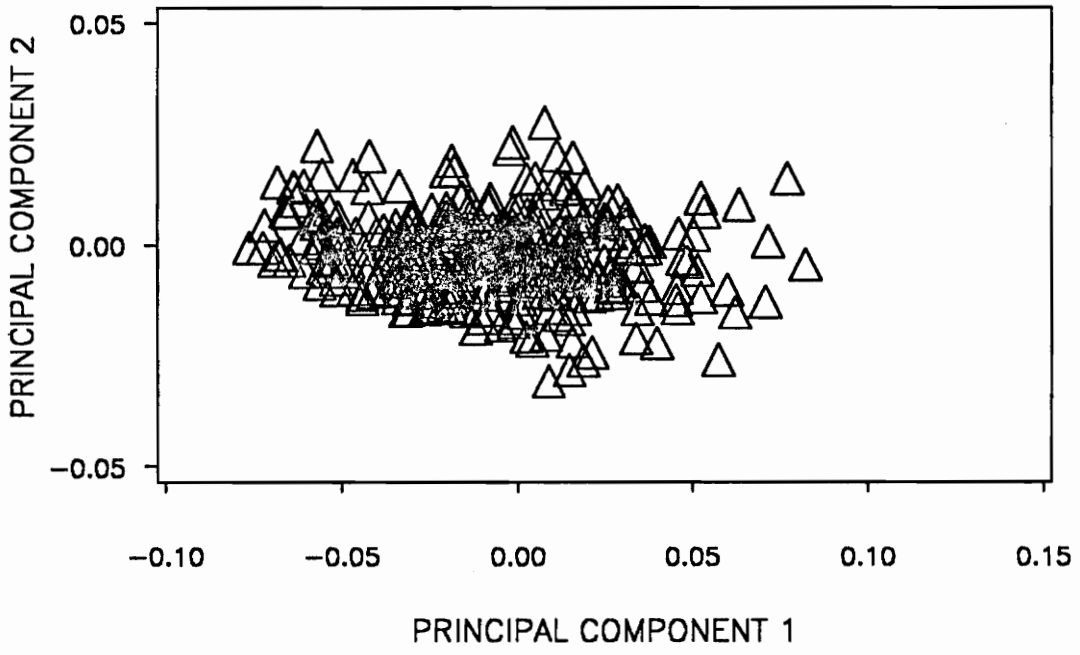

Figure 34. Principal component analysis with all specimens in horizon c.

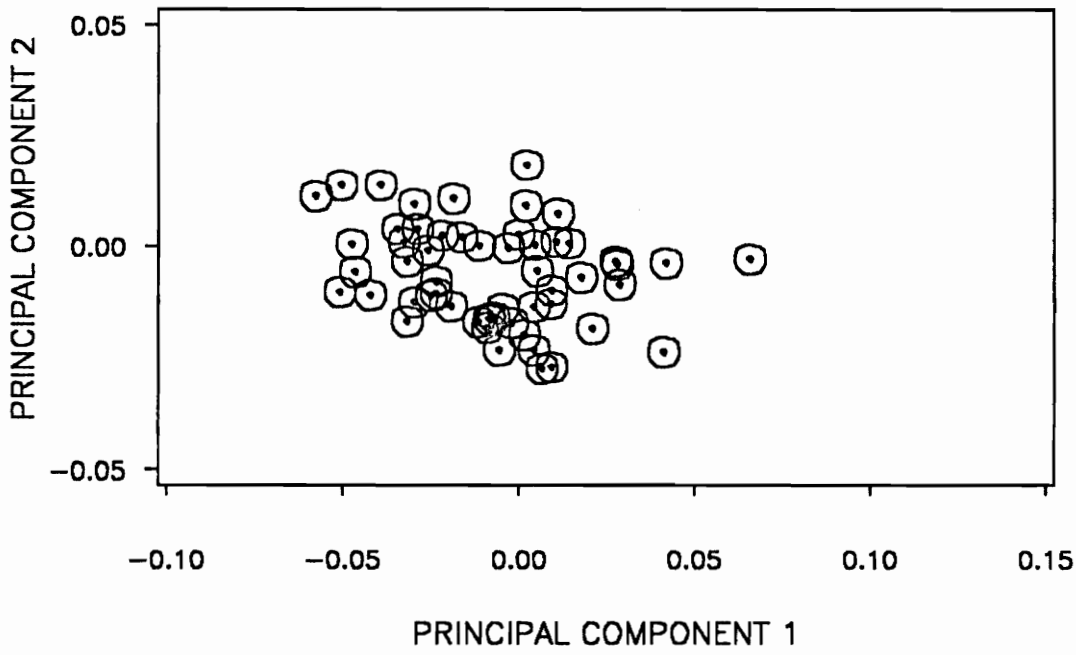

Figure 35. Principal component analysis with all specimens in horizon d.

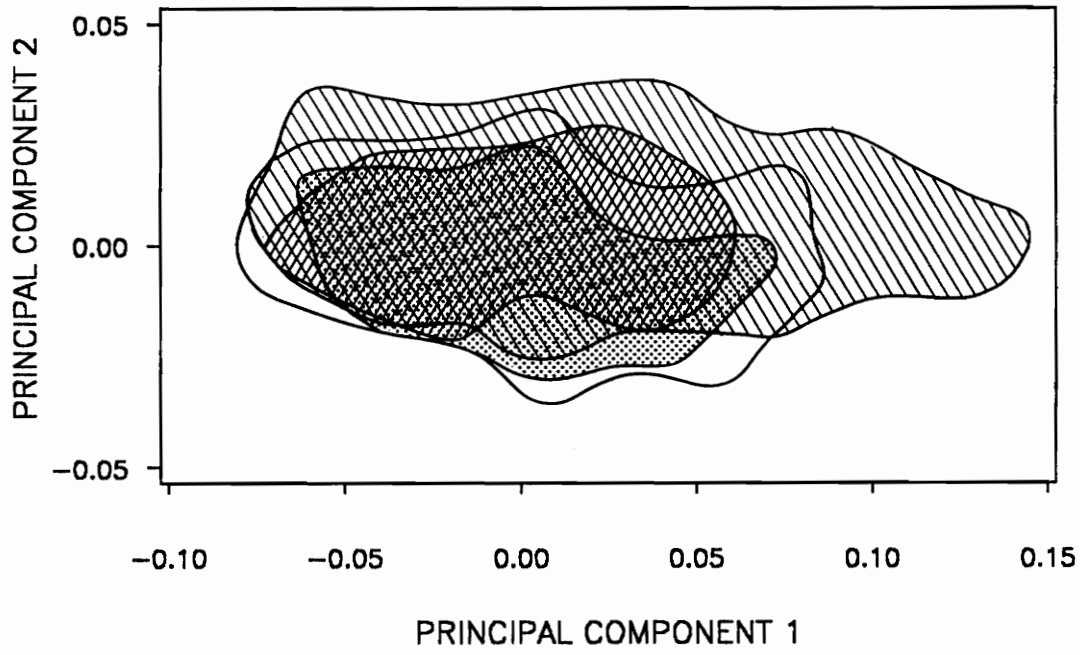

Figure 36. Principal component analysis with all specimens plotted by horizon: Horizon a shown in left line pattern; horizon b in right line pattern; horizon c with no pattern; horizon d in dot pattern.

Table 16. Ranges of scores on principal component axis 1 for lithologies and horizons as depicted in Figures 32-54.

	Sandstone	-0.030354 - 0.132553		Horizon a	-0.068517 - 0.138086
	Calcareous shale	-0.065961 - 0.138086		Horizon b	-0.067142 - 0.055867
	Siltstone	-0.068517 - 0.082293		Horizon c	-0.076161 - 0.082293
	Mudstone	-0.076161 - 0.066724		Horizon d	-0.065961 - 0.066724
	Limestone	-0.067142 - 0.066679			
Horizon a	Sandstone	0.025567 - 0.132553	Sandstone	Horizon a	0.025567 - 0.132553
	Siltstone	-0.068517 - 0.063798		Horizon b	-0.029056 - 0.055867
	Calcareous shale	-0.058541 - 0.138086		Horizon c	-0.030354 - 0.048585
	Limestone	-0.067142 - 0.066679	Siltstone	Horizon a	-0.068517 - 0.063798
Horizon b	Sandstone	-0.029056 - 0.055867		Horizon b	-0.036439 - 0.049044
	Siltstone	-0.036439 - 0.049044		Horizon c	-0.068183 - 0.082293
	Mudstone	-0.065777 - 0.019861		Horizon d	-0.049290 - 0.010073
Horizon c	Sandstone	-0.030354 - 0.048585	Mudstone	Horizon b	-0.065777 - 0.019861
	Siltstone	-0.068183 - 0.082293		Horizon c	-0.076161 - 0.059960
	Mudstone	-0.076161 - 0.059960		Horizon d	-0.056523 - 0.066724
	Calcareous shale	-0.065961 - 0.032750	Calcareous shale	Horizon a	-0.058541 - 0.138086
Horizon d	Siltstone	-0.049290 - 0.010073		Horizon c	-0.065961 - 0.032750
	Mudstone	-0.056523 - 0.066724	Limestone	Horizon a	-0.067142 - 0.066679

Table 17. Listing of localities by cluster and lithology used in a Fisher's exact test.

	MUDSTONE	SILTSTONE	SANDSTONE	CALCAREOUS SHALE	LIMESTONE	TOTAL
CLUSTER 1	10	2	0	4	1	17
CLUSTER 2	0	0	2	2	0	4
CLUSTER 3	2	3	0	1	1	7
CLUSTER 4	7	16	2	3	7	35
TOTAL	19	21	4	10	9	63

Table 18. Test for significant difference among lithologies. The test includes five lithologies (sandstone, siltstone, mudstone, calcareous shale, and siltstone) and 572 observations.

DEPENDENT VARIABLE: HAR2

SOURCE	DF	SUM OF SQUARES	MEAN SQUARE	F VALUE	PR > F
MODEL	4	0.12167218	0.03041804	29.68	0.0001
ERROR	567	0.58106527	0.00102481		
CORRECTED	571	0.70273745			

R-SQUARE	C.V.	ROOT MSE	HAR2 MEAN
0.173140	44.4836	0.03201260	0.07196488

SOURCE	DF	TYPE I SS	F VALUE	PR > F
LITH	4	0.12167218	29.68	0.0001

SOURCE	DF	TYPE III SS	F VALUE	PR > F
LITH	4	0.12167218	29.68	0.0001

DEPENDENT VARIABLE: HAR4

SOURCE	DF	SUM OF SQUARES	MEAN SQUARE	F VALUE	PR > F
MODEL	4	0.02387440	0.00596860	30.00	0.0001
ERROR	567	0.11279780	0.00019894		
CORRECTED	571	0.13667220			

R-SQUARE	C.V.	ROOT MSE	HAR4 MEAN
0.174684	54.0138	0.01410454	0.02611283

SOURCE	DF	TYPE I SS	F VALUE	PR > F
LITH	4	0.02387440	30.00	0.0001

SOURCE	DF	TYPE III SS	F VALUE	PR > F
LITH	4	0.02387440	30.00	0.0001

DEPENDENT VARIABLE: HAR6

SOURCE	DF	SUM OF SQUARES	MEAN SQUARE	F VALUE	PR > F
MODEL	4	0.00637697	0.00159424	33.64	0.0001
ERROR	567	0.02687162	0.00004739		
CORRECTED	571	0.03324859			

R-SQUARE	C.V.	ROOT MSE	HAR6 MEAN
0.191797	47.9292	0.00688423	0.01436332

SOURCE	DF	TYPE I SS	F VALUE	PR > F
LITH	4	0.00688423	33.64	0.0001

SOURCE	DF	TYPE III SS	F VALUE	PR > F
LITH	4	0.00637697	33.64	0.0001

MANOVA TEST CRITERIA FOR THE HYPOTHESIS OF NO OVERALL TYPE EFFECT

WILKS' CRITERION	F(3,551)	PROB > F
0.66444887	20.82	0.0001
PILLAI'S TRACE	F(3,551)	PROB > F
0.36741271	19.78	0.0001
HOTELLING-LAWLEY TRACE	F(3,551)	PROB > F
0.45721188	21.48	0.0001
ROY'S MAXIMUM ROOT CRITERION	F(3,551)	PROB > F
0.30034141	42.57	0.0001

To graphically depict if each lithology can be linked with a morphological shape, the principal component scores of all specimens were plotted by lithology on principal component axes 1 and 2 (Figure 37-Figure 43). As with the plots of horizons, the range of scores for the second principal component are fairly similar for each lithology while the differences among lithologies occur dominantly in the first principal component. Specimens in calcareous shale (Figure 37) exhibit a very wide range of values for axis 1 that includes the most elongate specimens and some of the roundest. The range of scores for the other lithologies is more restricted. Specimens in sandstone tend to be elongate to round (Figure 38). Specimens in siltstone (Figure 39) and limestone (Figure 40) tend to be round, and those in mudstone (Figure 41) tend to be round to very round. Each lithology does not occupy a unique field in the morphological space defined by the first and second principal components. When the three plots for the clastics of the Appalachian Basin are overlain, the extensive overlap among them is apparent (Figure 42). The same is true for the carbonates of the Michigan Basin (Figure 43).

TIME AND ENVIRONMENT

To explore if the apparent lack of relationship between morphology and lithology existed through time, separate principal component plots for each lithology at each horizon were made and overlain by horizon (Figure 44-Figure 49) and by lithology (Figure 50-Figure 54). Separate plots were made of the Appalachian and Michigan basins for horizons a (Figure 44-Figure 45) and c (Figure 47-Figure 48). For the Appalachian Basin in horizon a, which contains samples composed only of sandstone and siltstone, the overlap in range between the two is minor (Figure 44). Most of the specimens in sandstone are more elongate than those in siltstone as was the case when specimens in all horizons were plotted in Figure 42. Included in the sandstone group are specimens in localities N16 and N17 which are two of the four localities in cluster 2, the cluster with the most elongate specimens. The

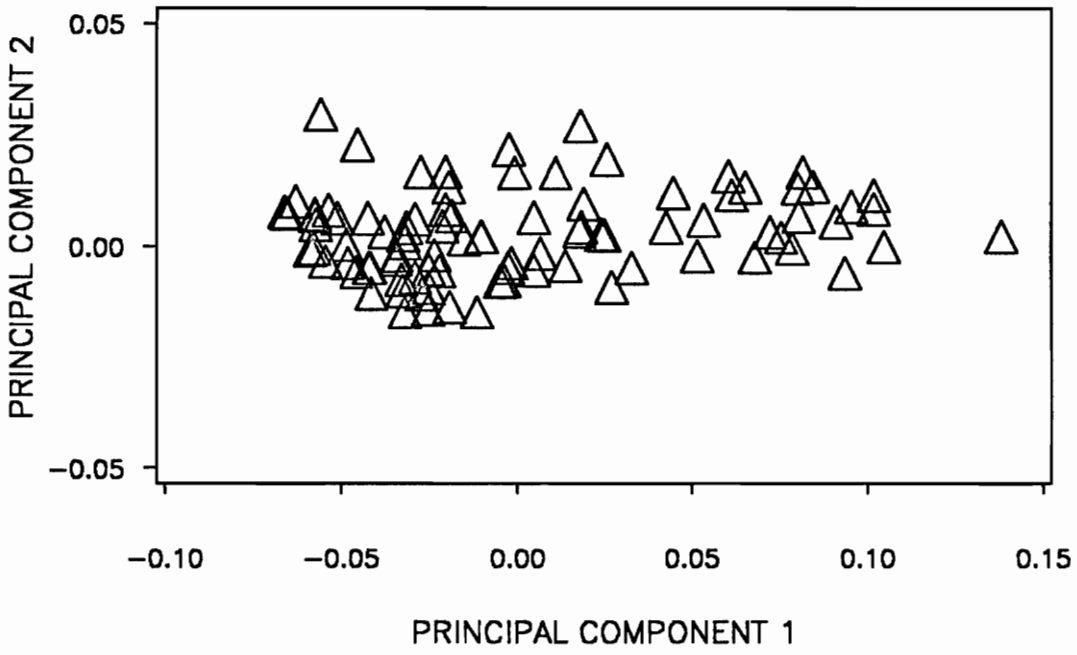

Figure 37. Principal component analysis with all specimens in calcareous shale.

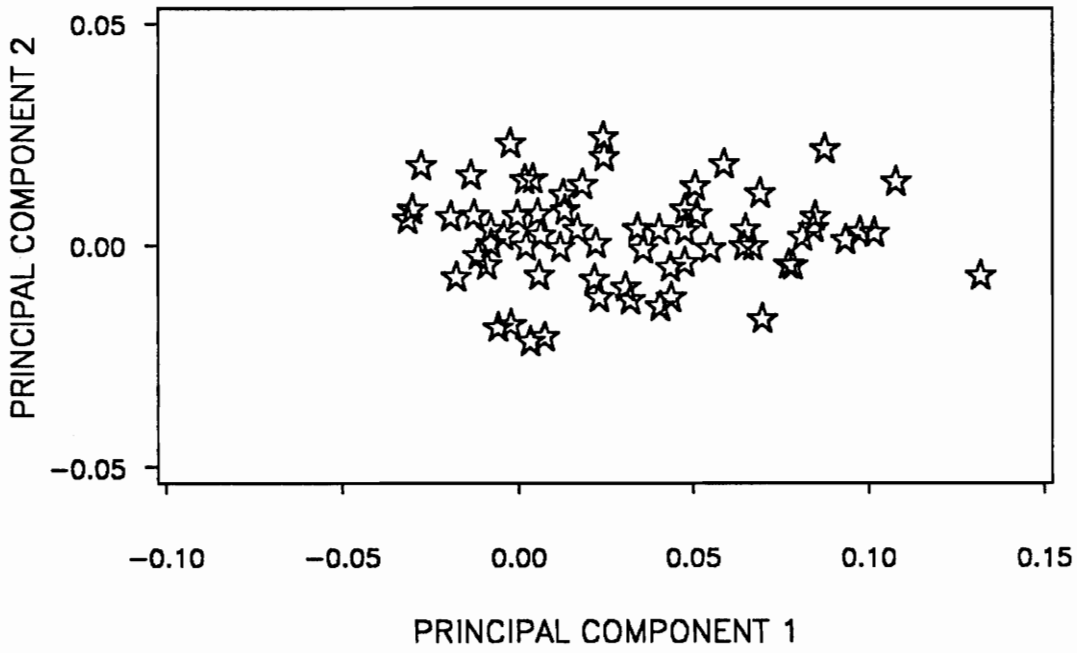

Figure 38. Principal component analysis with all specimens in sandstone.

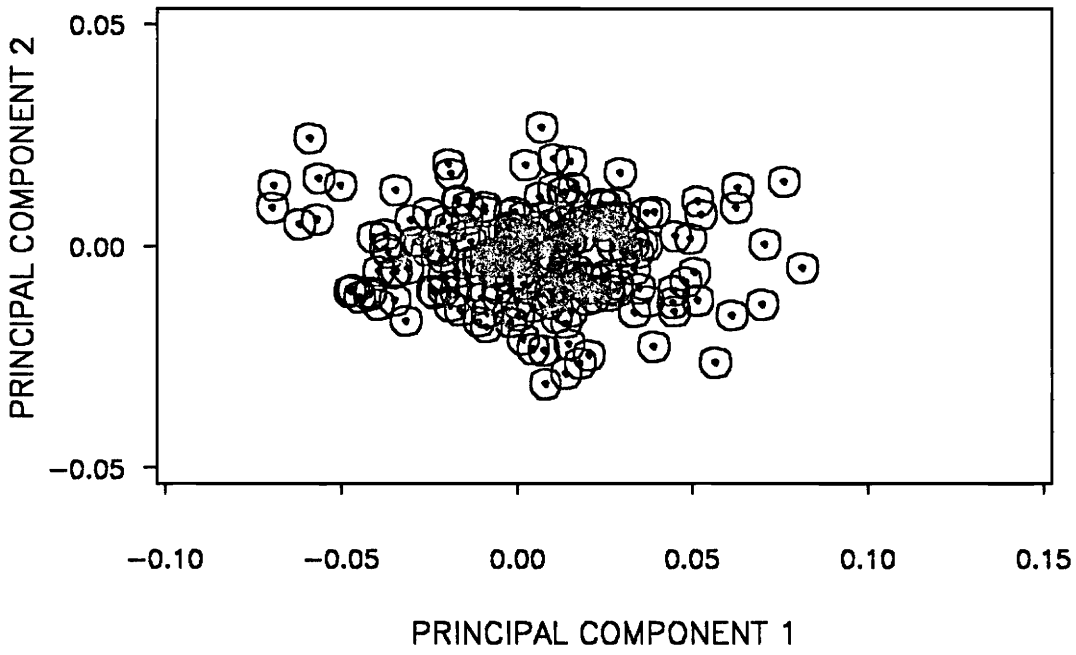

Figure 39. Principal component analysis with all specimens in siltstone.

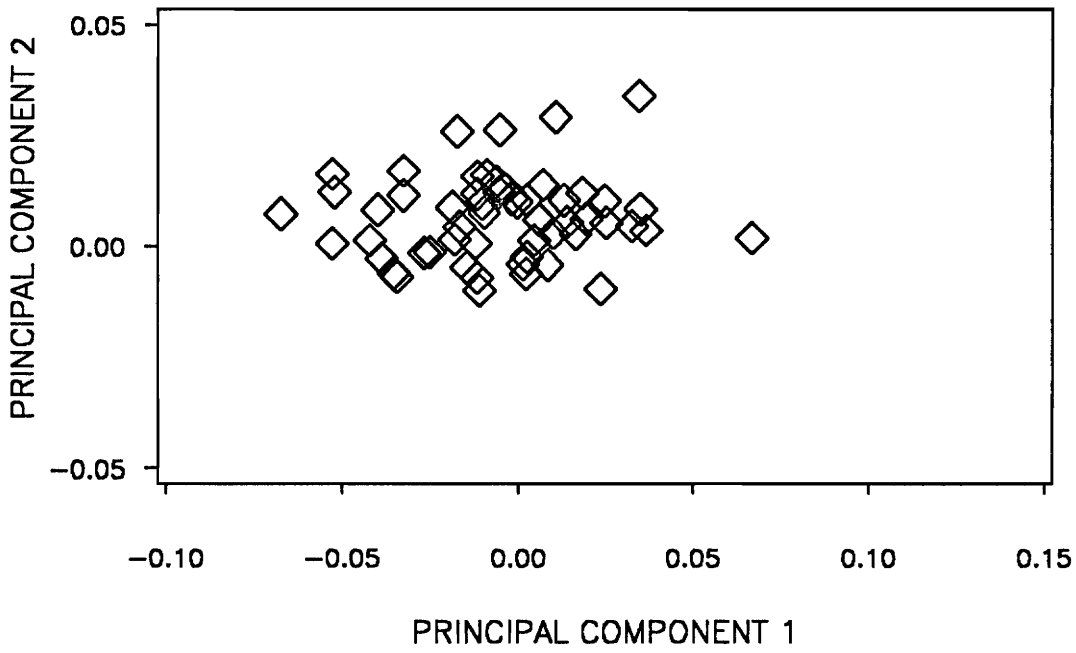

Figure 40. Principal component analysis with all specimens in limestone.

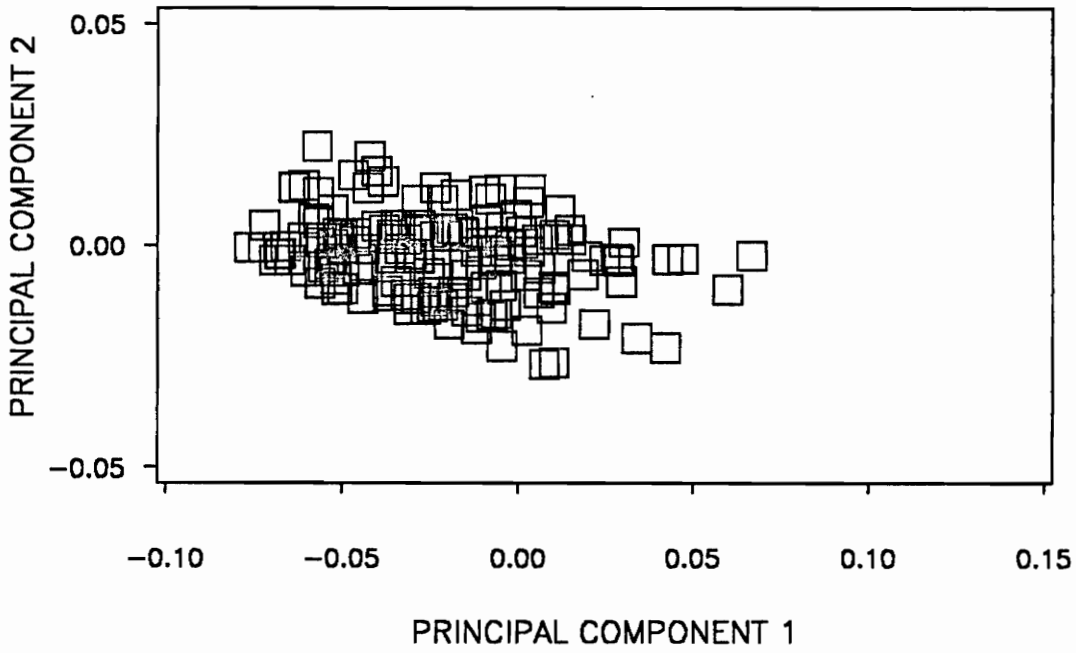

Figure 41. Principal component analysis with all specimens in mudstone.

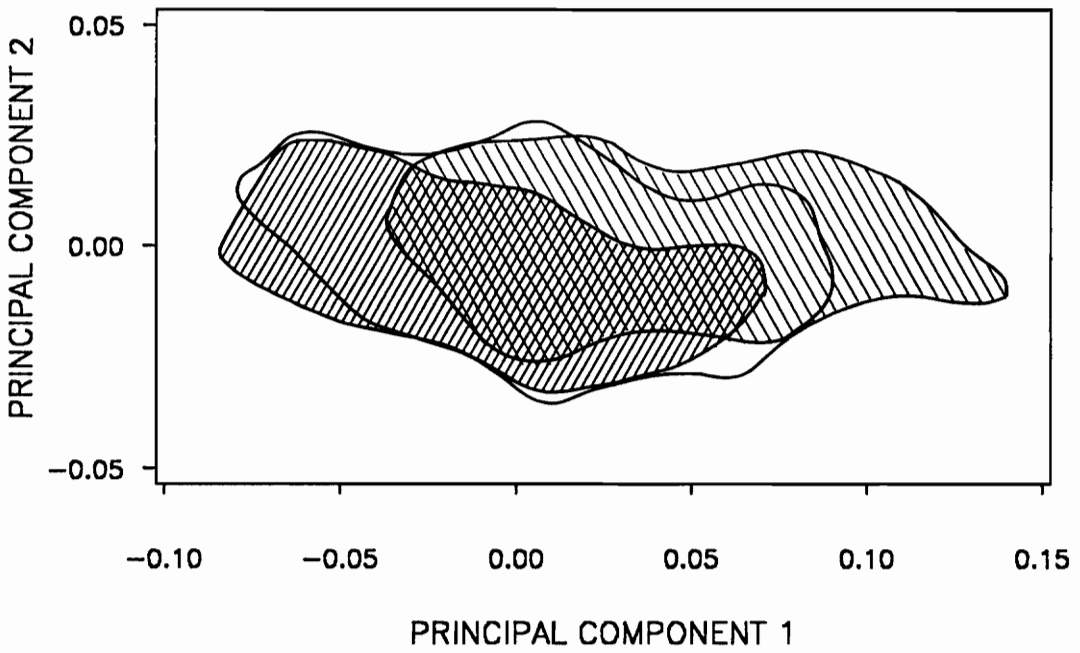

Figure 42. Principal component analysis with all specimens in the Appalachian Basin plotted by lithology: Sandstone shown in left line pattern; siltstone with no pattern; mudstone in right line pattern.

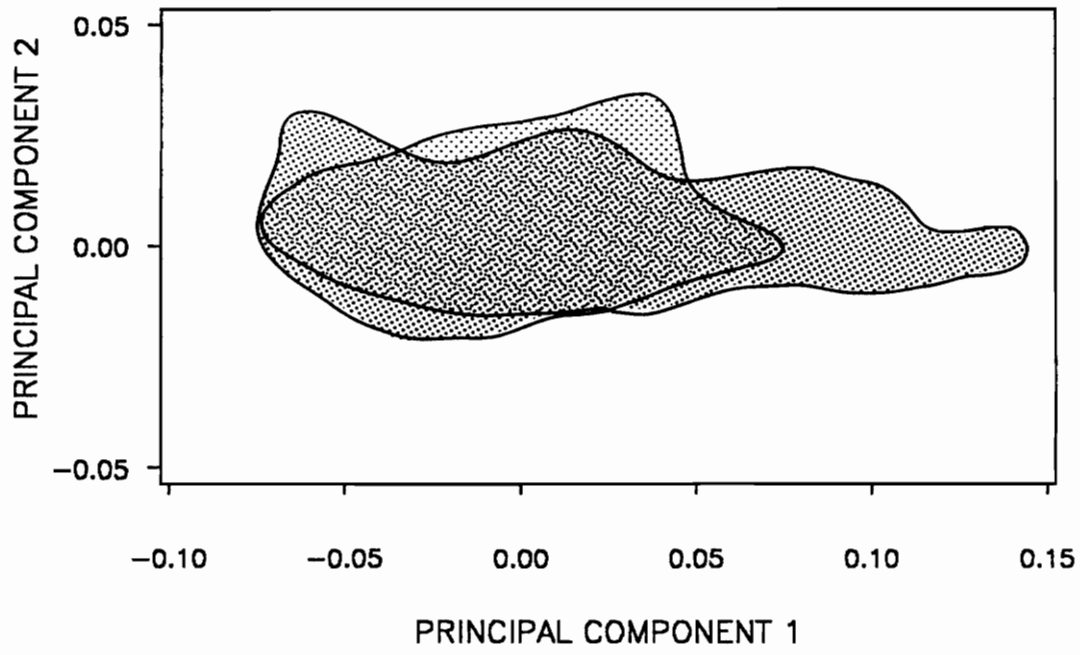

Figure 43. Principal component analysis with all specimens in the Michigan Basin plotted by lithology: Calcareous shale shown in dense dot pattern; limestone in light dot pattern.

range of the field of calcareous shale in the Michigan Basin at horizon a includes all but the roundest specimen in limestone and extends beyond the limestone range to include some of the most elongate specimens, those in localities O01A and O02A (Figure 45). The pattern in Figure 45 is very similar to that for all horizons plotted in Figure 43. For horizon b the pattern shown in Figure 42 is repeated: the three clastic lithologies are ordered on axis 1 with mudstone extending lowest (roundest) and siltstone and sandstone offset from the mudstone field to include more elongate specimens (Figure 46). However, the range of sandstone is much less extensive at this horizon than as a whole, appearing more like the siltstone field in Figure 42. For horizon c in the Appalachian Basin, the range of scores for the sandstone specimens lies within that for siltstone which includes both rounder and more elongate specimens (Figure 47). The fields of siltstone and mudstone overlap considerably, although more specimens in mudstone are rounder and more specimens in siltstone are elongate. Unlike the overall pattern and that for horizons a and b, in horizon c both mudstone and siltstone have more elongate specimens contained in them then does sandstone. For horizon c in the Michigan Basin only specimens in calcareous shale were found. The range of calcareous shale is more restricted here than in horizon a being confined to the rounder specimens (Figure 48). Horizon d is limited to the Appalachian Basin and includes only specimens in siltstone and mudstone. Specimens in siltstone lie within the field for mudstone which includes more elongate specimens, a reversal of the overall situation and that of horizons b and c (Figure 49). The relationship of the shape fields encompassed by each lithology is not consistent from horizon to horizon.

When plots of specimens found in sandstone are grouped by horizon and overlain (Figure 50), there is an apparent shift towards roundness from horizon a to b although the distribution in horizons b and c overlap completely. Only the low end of the field of horizon a overlaps with the high end of the fields of horizon b and c. Specimens in siltstone were collected at all four horizons, although the concentration of specimens in horizon c is much greater than the other three. Horizons a and c have the greatest ranges of scores and include the fields of horizons b and d (Figure 51). Unlike the other three horizons, horizon d is limited

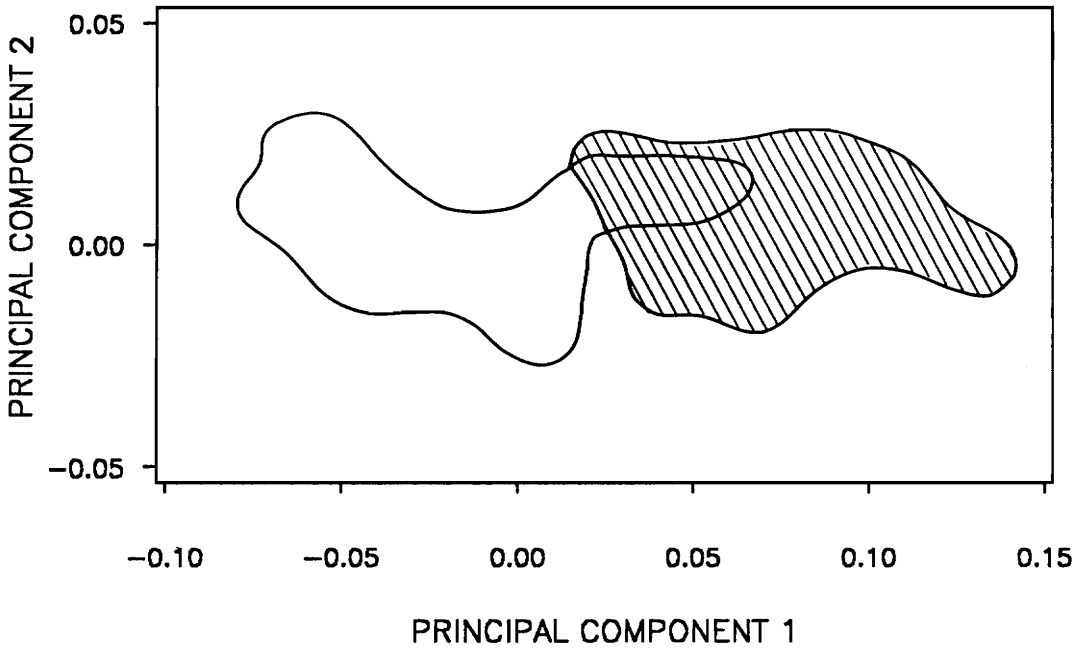

Figure 44. Principal component analysis with all specimens in horizon a in the Appalachian Basin plotted by lithology: Sandstone shown in left line pattern; siltstone with no pattern.

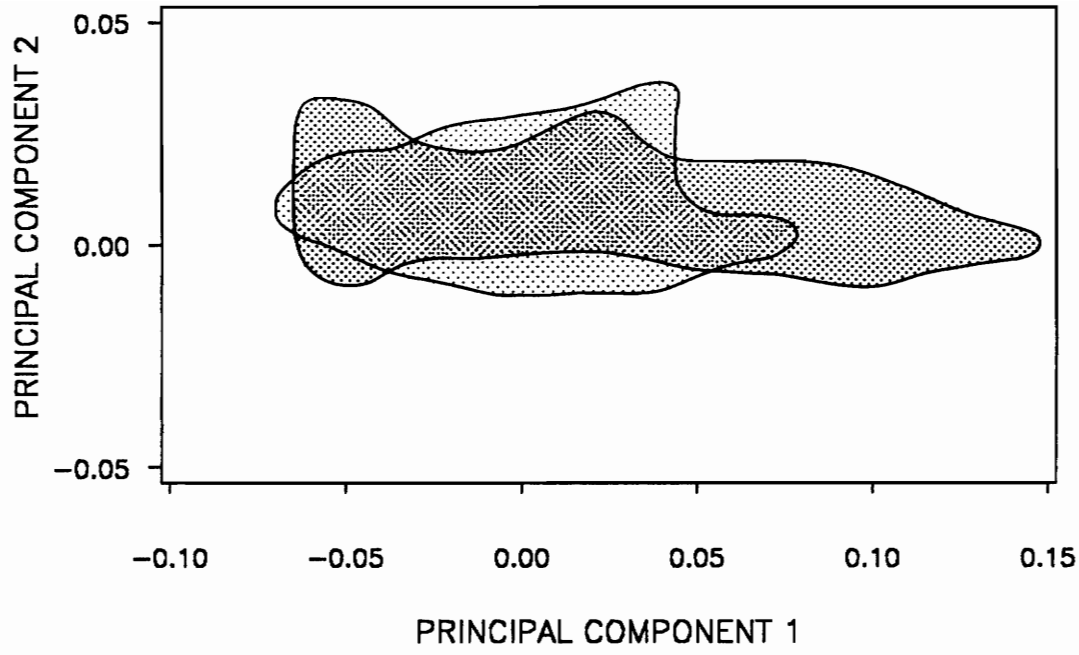

Figure 45. Principal component analysis with all specimens in horizon a in the Michigan Basin plotted by lithology: Calcareous shale shown in dense dot pattern; limestone in light dot pattern.

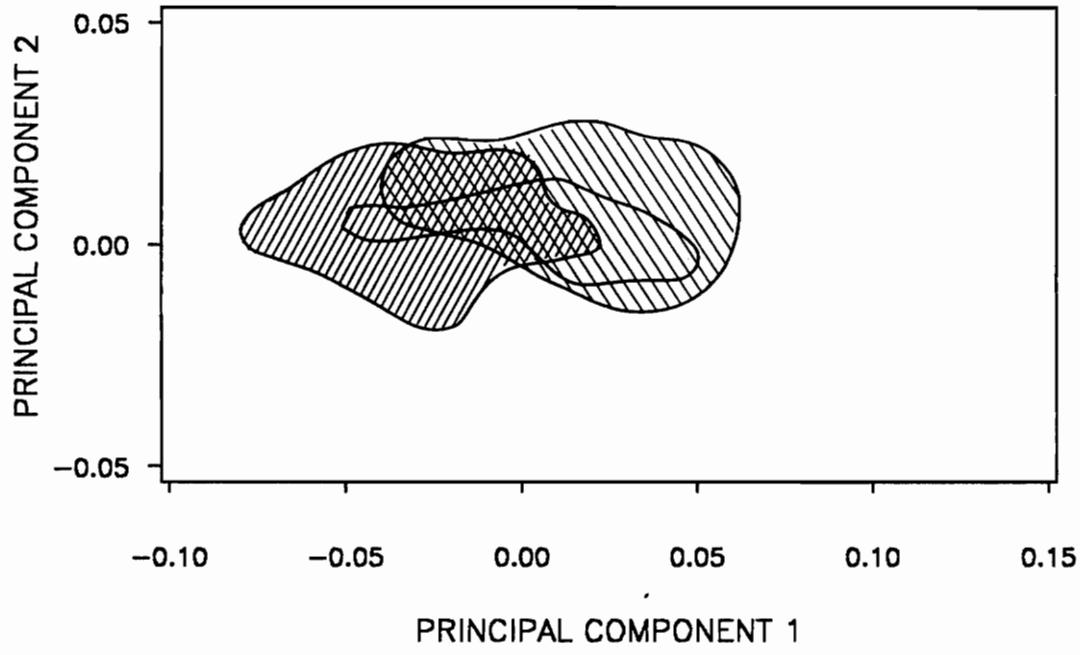

Figure 46. Principal component analysis with all specimens in horizon b plotted by lithology: Sandstone shown in left line pattern; siltstone with no pattern; mudstone in right line pattern.

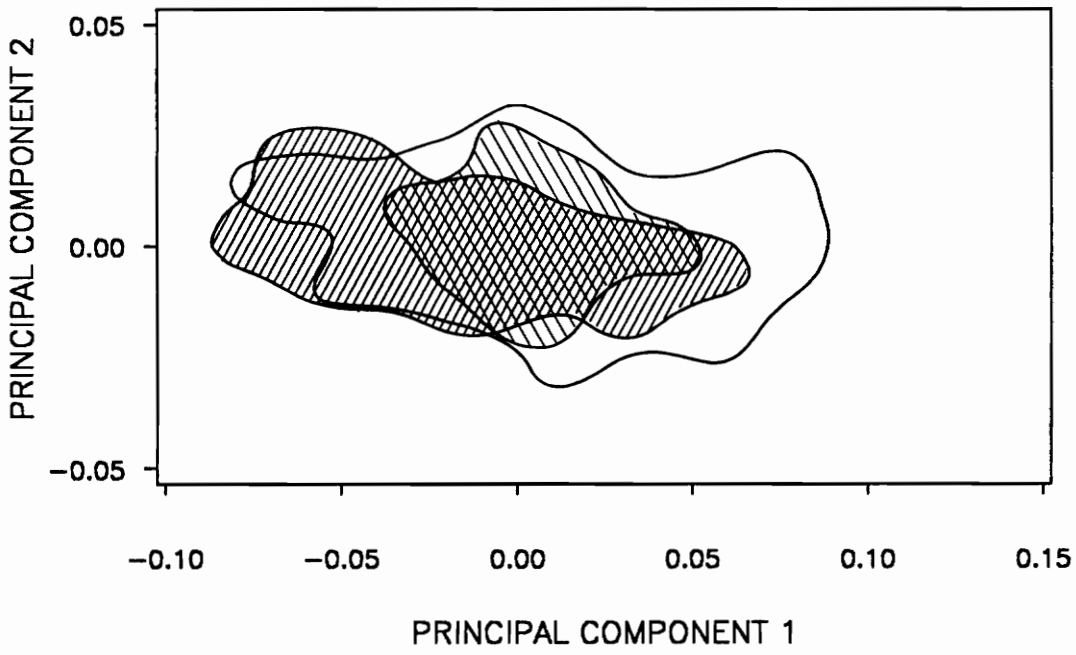

Figure 47. Principal component analysis with all specimens in horizon c in the Appalachian Basin plotted by lithology: Sandstone shown in left line pattern; siltstone with no pattern; mudstone in right line pattern.

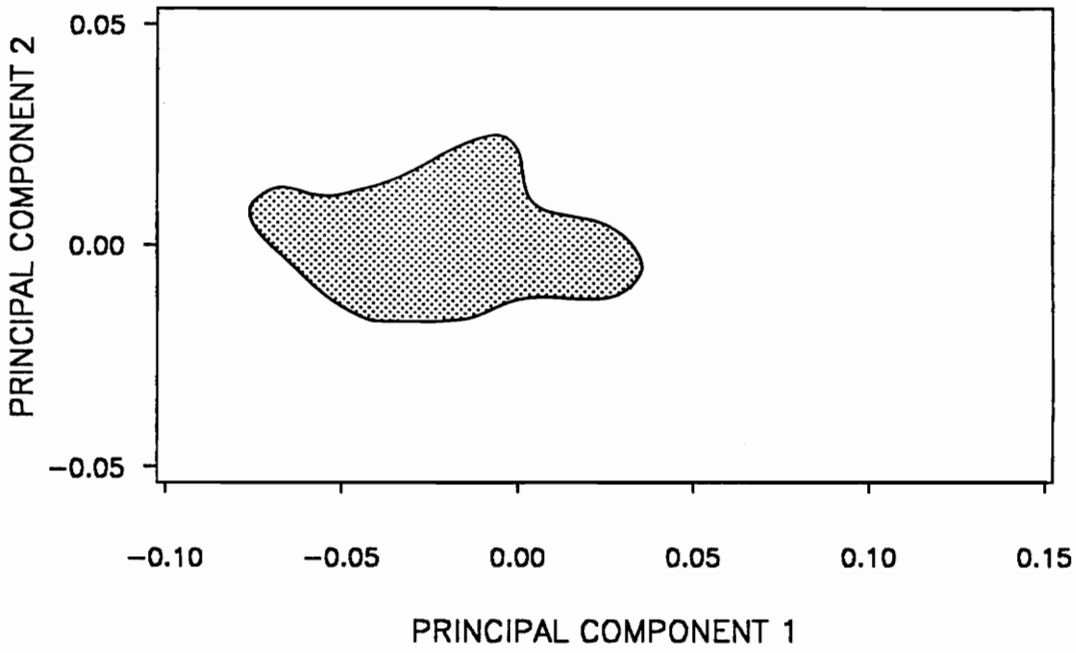

Figure 48. Principal component analysis with all specimens in horizon c in the Michigan Basin plotted by lithology: Calcareous shale shown in dense dot pattern.

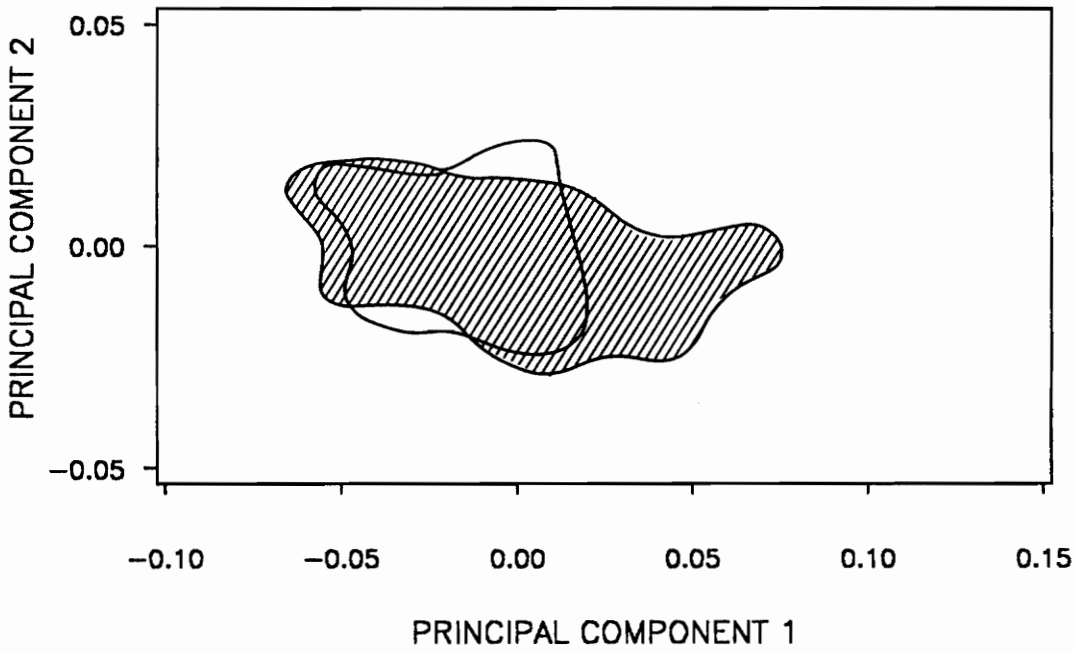

Figure 49. Principal component analysis with all specimens in horizon d plotted by lithology: Siltstone shown with no pattern; mudstone in right line pattern.

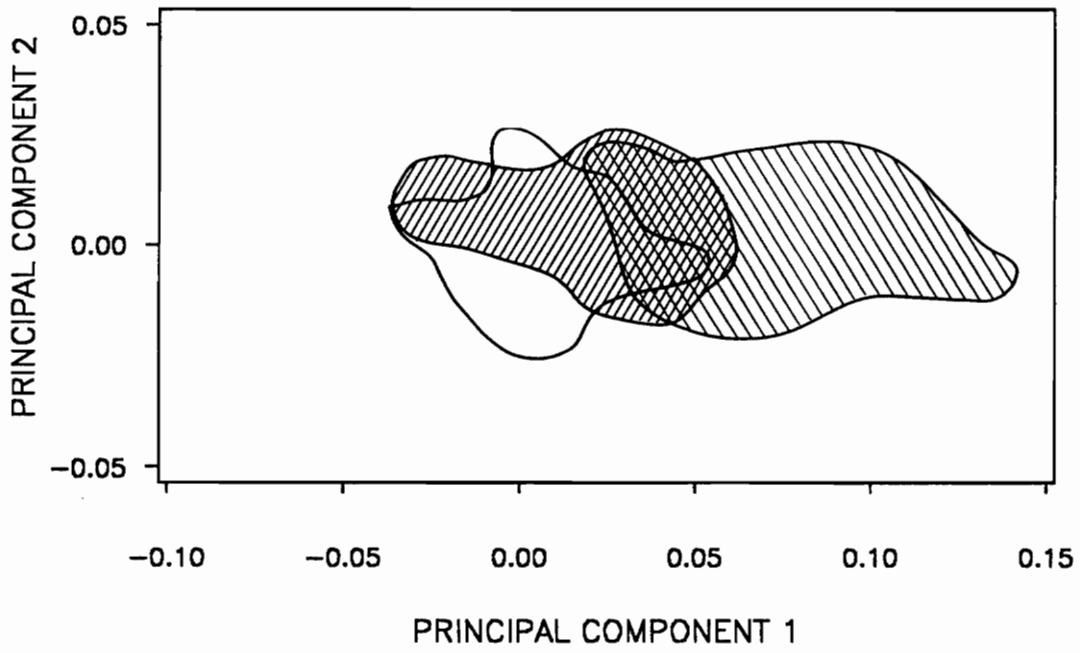

Figure 50. Principal component analysis with all specimens in sandstone plotted by horizon: Horizon a shown in left line pattern; horizon b in right line pattern; horizon c with no pattern.

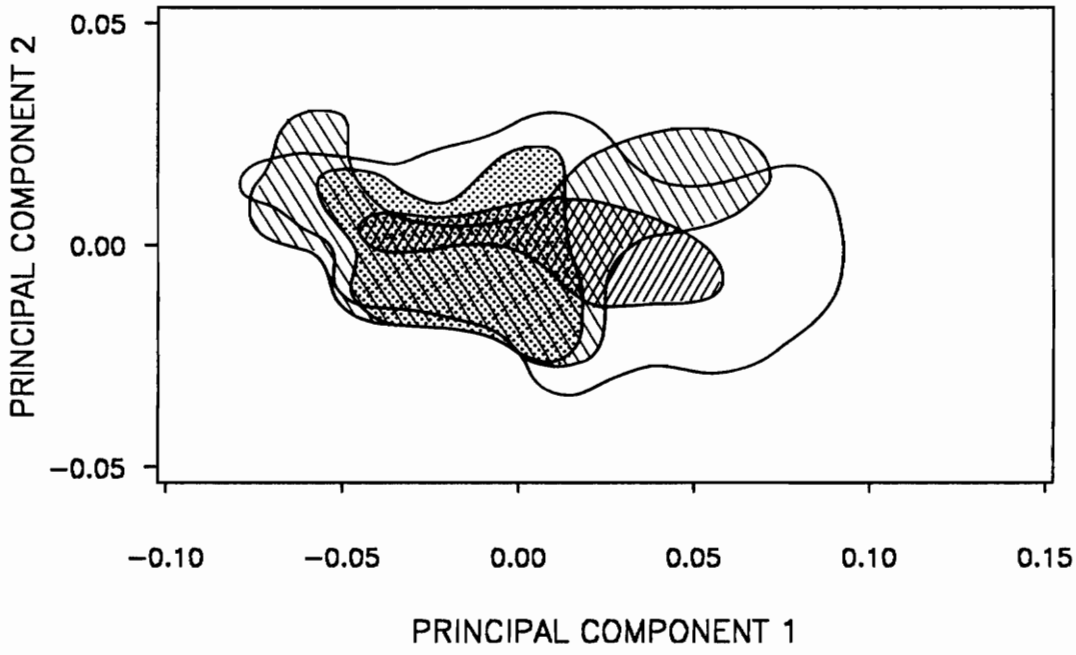

Figure 51. Principal component analysis with all specimens in siltstone plotted by horizon: Horizon a shown in left line pattern; horizon b in right line pattern; horizon c with no pattern; horizon d in dot pattern.

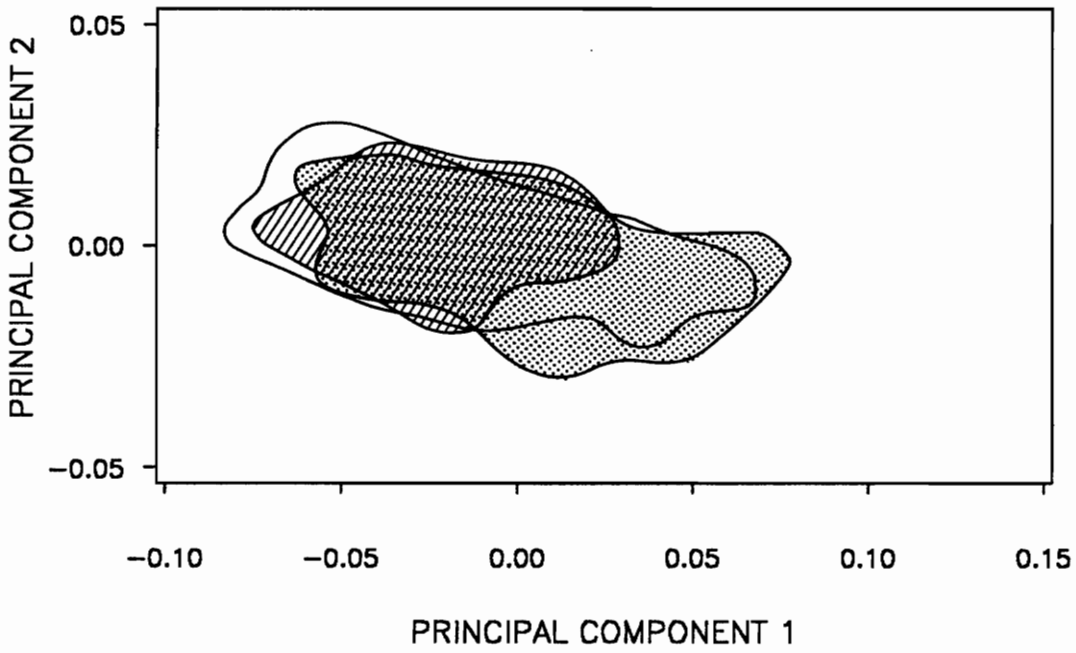

Figure 52. Principal component analysis with all specimens in mudstone plotted by horizon: Horizon b shown in right line pattern; horizon c with no pattern; horizon d in dot pattern.

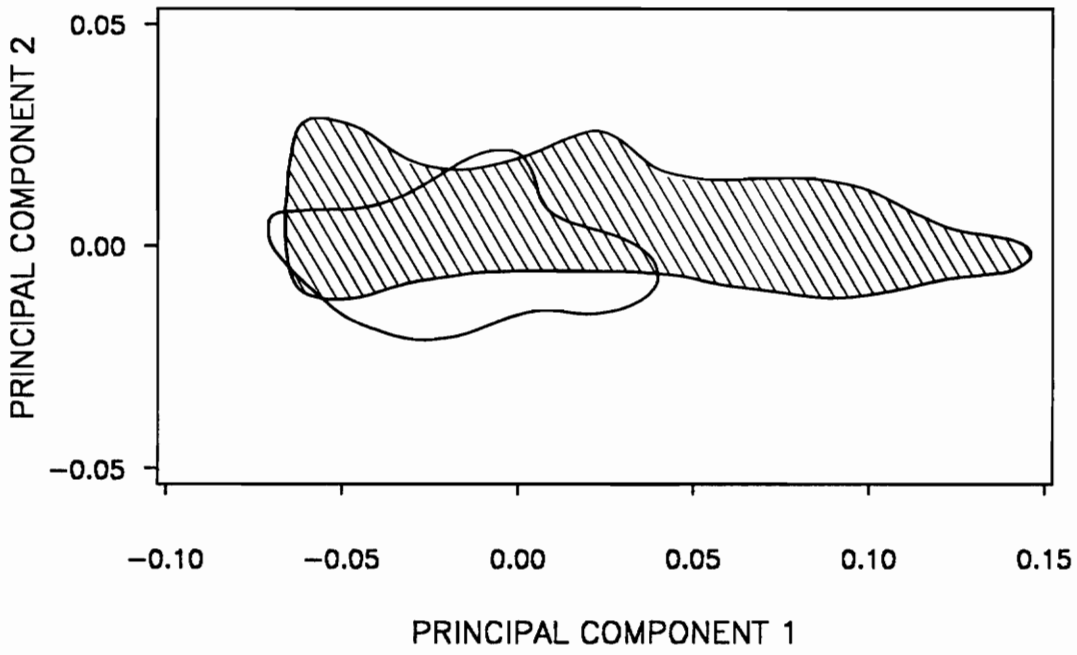

Figure 53. Principal component analysis with all specimens in calcareous shale plotted by horizon: Horizon a shown in left line pattern; horizon c with no pattern.

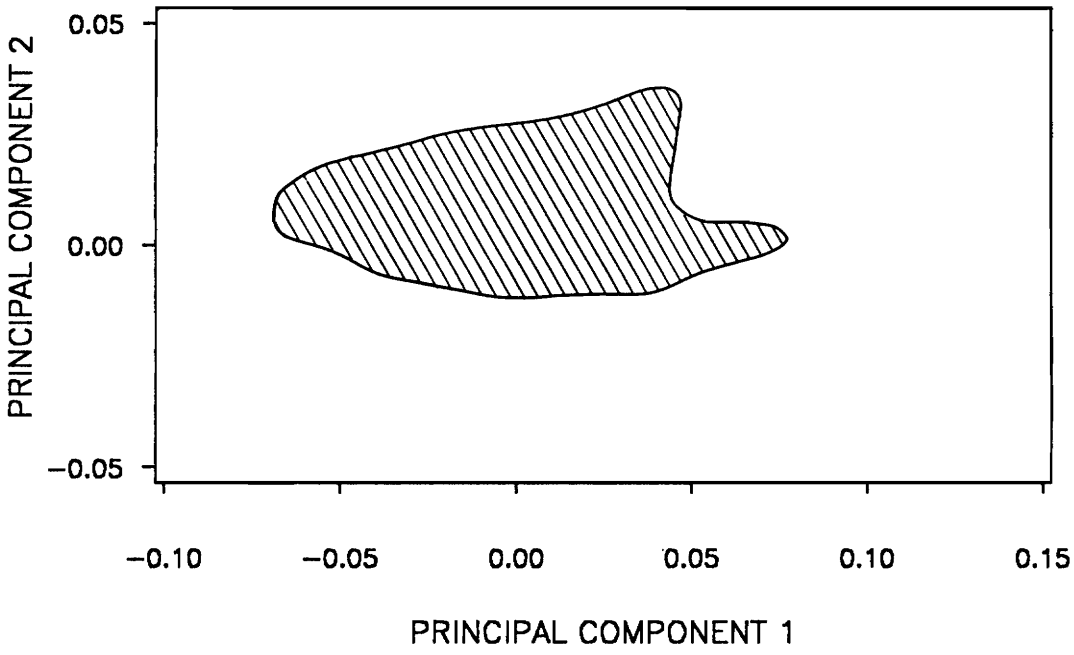

Figure 54. Principal component analysis with all specimens in limestone plotted by horizon: Horizon a shown in left line pattern.

to rounder specimens. Specimens in mudstone in horizon b are contained within the field of horizon c which has a few more elongate specimens and more that are rounder (Figure 52). There appears to be a shift towards elongateness from horizon b to c although the ranges of horizons c and d are similar. The carbonates of the Michigan Basin are restricted to horizons a and c. The field of calcareous shale at horizon a extends much higher on principal component axis 1 than does horizon c, almost entirely due to the presence of very elongate specimens in localities O01A and O02A in horizon a (Figure 53). Specimens in limestone are found solely in horizon a where they range from round to somewhat elongate (Figure 54).

Separate regressions of the amplitudes of harmonic 2 versus time were run for each lithology except limestone which occurs only in one horizon (Figure 55-Figure 61). In testing for no change of shape with time for specimens found in siltstone (Figure 55), the null hypothesis can not be rejected because the slope does not differ significantly from 0 ($p = 0.8282$). This supports the pattern seen in the principal component plot for siltstone (Figure 51). When the amplitudes for harmonic 2 for specimens in mudstone were regressed against time (Figure 56), the probability of finding no shape change with time is only 0.002. The positive slope suggests a trend towards elongateness with time which was also apparent in the principal component plot (Figure 52). However, the magnitude of the slope is very small (0.090), less than 6% of the total variation in amplitudes is explained by the fitted regression line ($R^2 = 0.0571$), and the dispersion about the mean is very high (CV = 52.88406). Tests for specimens in sandstone (Figure 57) and calcareous shale (Figure 58) are both highly significant ($p < 0.0001$). Close to 50% of the variation is accounted for in the sandstone regression ($R^2 = 0.5459$) and 30% for calcareous shale ($R^2 = 0.2906$). Both slopes are negative indicating a trend towards roundness which was also evident in the principal component plots (Figure 50 and Figure 53). However, with each lithology the overlap between horizons is extensive except where specimens in cluster 2 (the most elongate) are present. Because sandstone and calcareous shale are the only lithologies in which cluster 2 specimens are found, these specimens were removed from the analyses and the regressions were run again (Figure 59-Figure 60). With cluster 2 specimens removed the slopes were found to not differ

significantly from 0 (sandstone, $p = 0.1951$; calcareous shale, $p = 0.5788$) and therefore the null hypothesis of no change in shape with time can not be rejected. When linear regression was repeated for all specimens minus those in cluster 2 (Figure 61), the null hypothesis also can not be rejected ($p = 0.5189$). No significant change in shape with time can be detected.

ONSHORE-OFFSHORE TREND

To examine if an onshore-offshore trend in overall shape exists, amplitudes for harmonic 2 were regressed against distance from shoreline for all New York specimens and for New York specimens in horizon c. This analysis was done only for New York because it represents a clearcut transect from source of clastic input to offshore, includes many different environments, covers a large distance (413 km), and is the most complete section. Locality N16 at Berne, New York, is the furthestmost east locality and distances from shoreline for all other localities were measured relative to it. Localities from Berne to central New York (see Figure 7 on page 28) are located on the westward-sloping shelf and are composed predominantly of sand and silt (see Figure 8 on page 30). Localities in western New York are on the eastward-sloping shelf and they are all composed of mudstone. The area in westcentral New York where no samples were collected is the location of the structural basin (between localities N27 and N35).

In the analysis for horizon c, the slope of the regression line was found to be significantly different from 0 ($p < 0.0001$) indicating a correlation between the more elongate forms and nearshore and between the rounder forms and offshore (Figure 62). However, the strength of this relationship is not strong because the total variation in amplitudes that is accounted for by the fitted regression line is only 32% ($R^2 = 0.3164$). Similar results are found when all New York specimens are plotted (Figure 63) ($p < 0.0001$; $R^2 = 0.2976$).

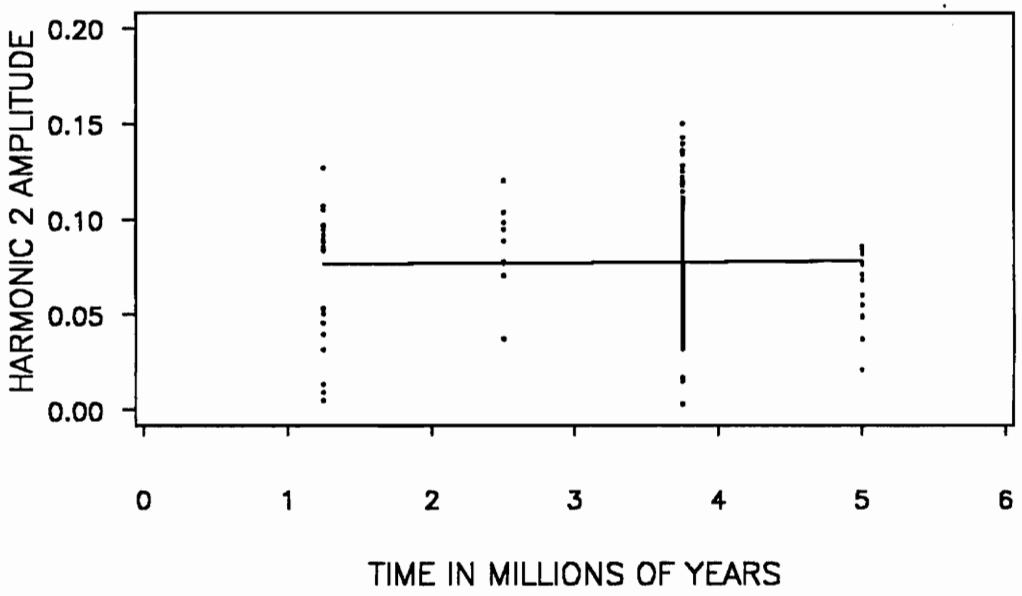

Figure 55. **Linear regression of all specimens in siltstone in each horizon:** Intercept = 0.076; slope = 0.005; P = 0.8282; N = 213 (a: 20; b: 9; c: 171; d: 13).

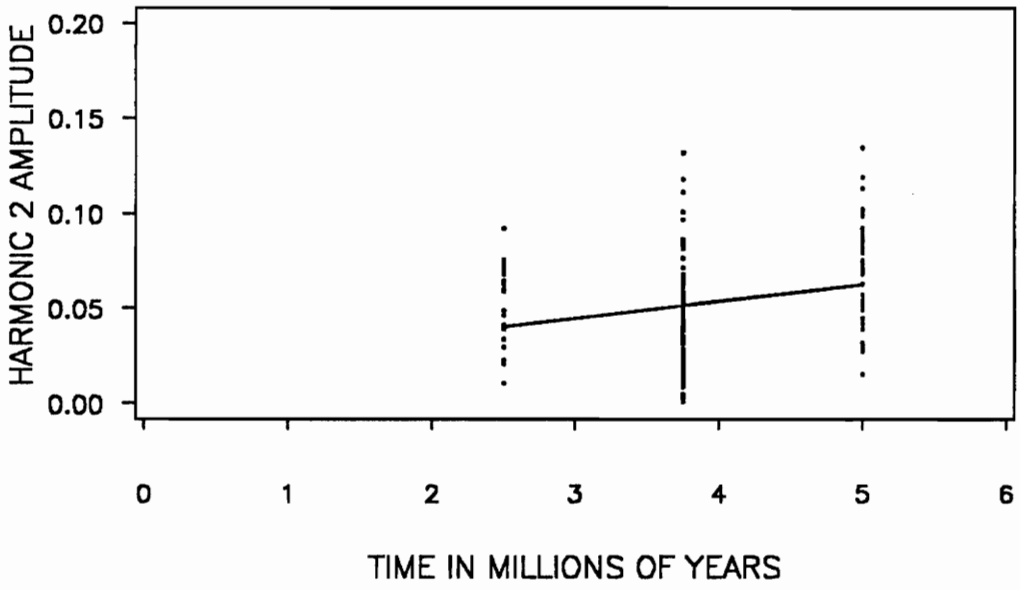

Figure 56. Linear regression of all specimens in mudstone in each horizon: Intercept = 0.018; slope = 0.090; p = 0.0020; N = 148 (b: 22; c: 84; d: 42).

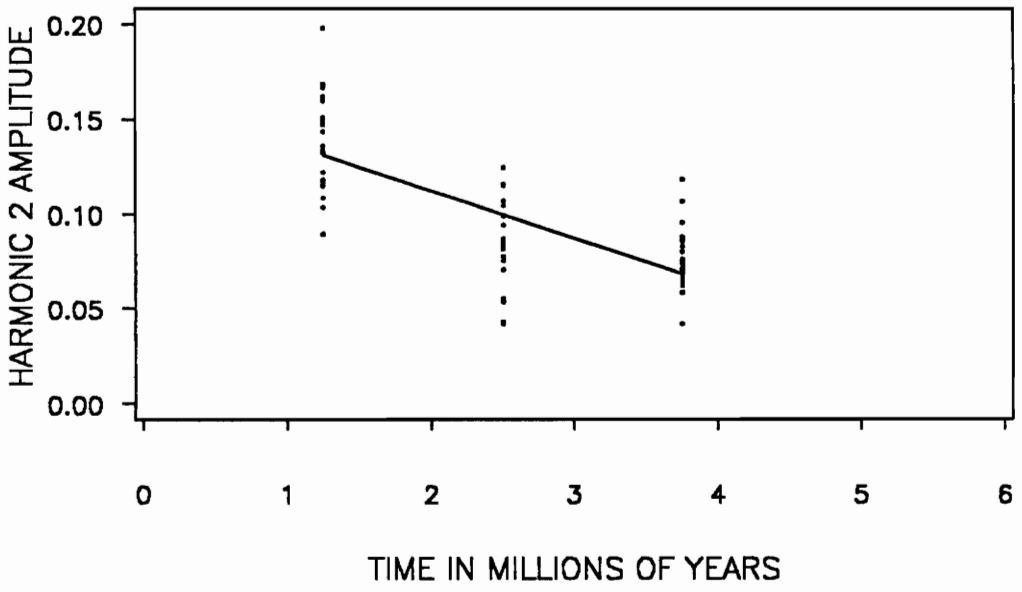

Figure 57. **Linear regression of all specimens in sandstone in each horizon:** Intercept = 0.163; slope = -0.251; $p < 0.0001$; N = 65 (a: 25; b: 18 c: 22).

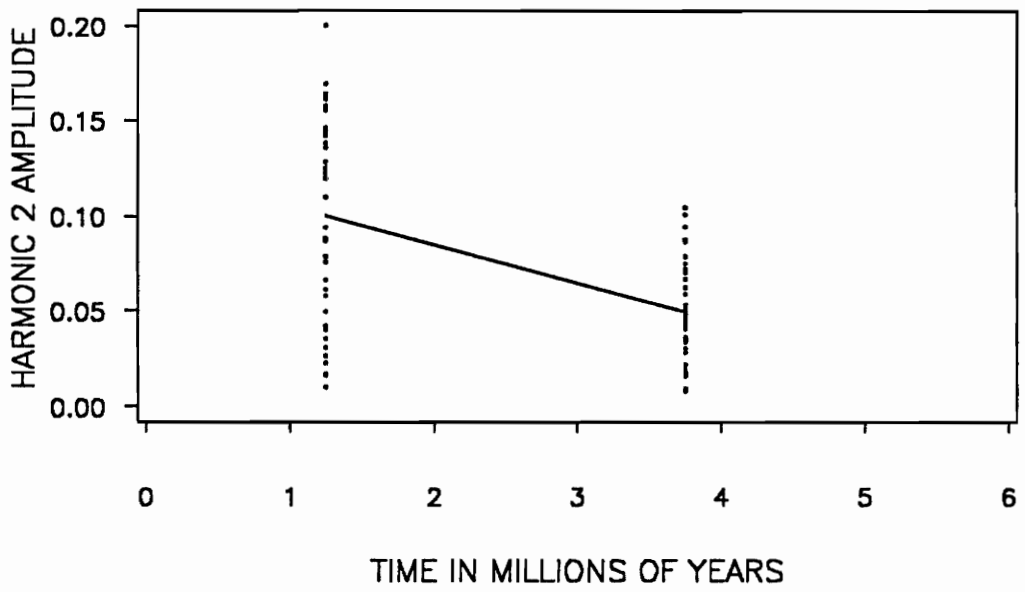

Figure 58. Linear regression of all specimens in calcareous shale in each horizon: Intercept = 0.126; slope = -0.204; $p < 0.0001$; N = 90 (a: 31; c: 49).

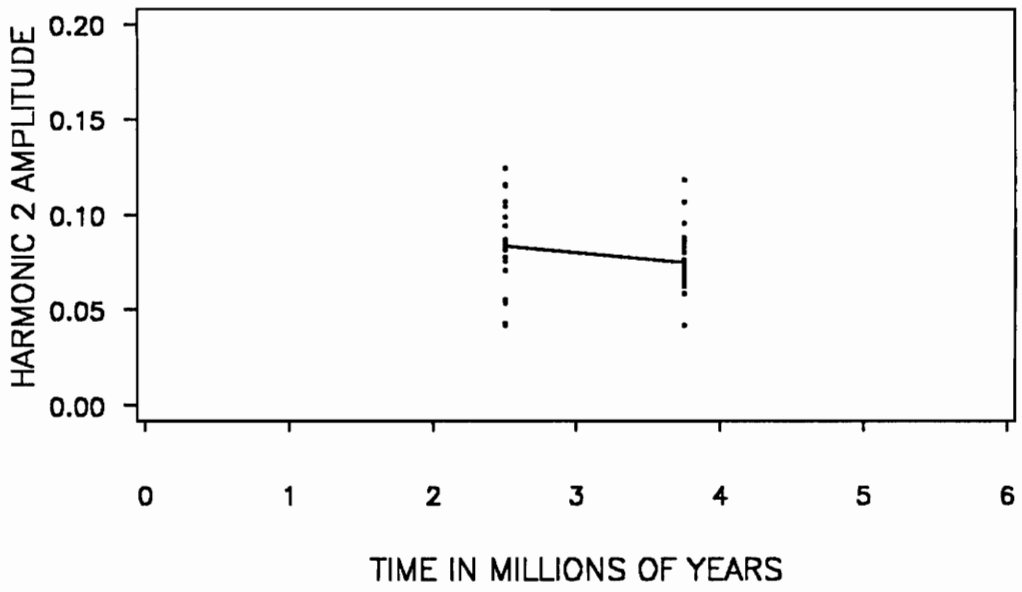

Figure 59. Linear regression of all specimens in sandstone in each horizon minus specimens in localities N16 and N17: Intercept = 0.102; slope = -0.070; p = 0.1951; N = 40 (b: 18; c: 22).

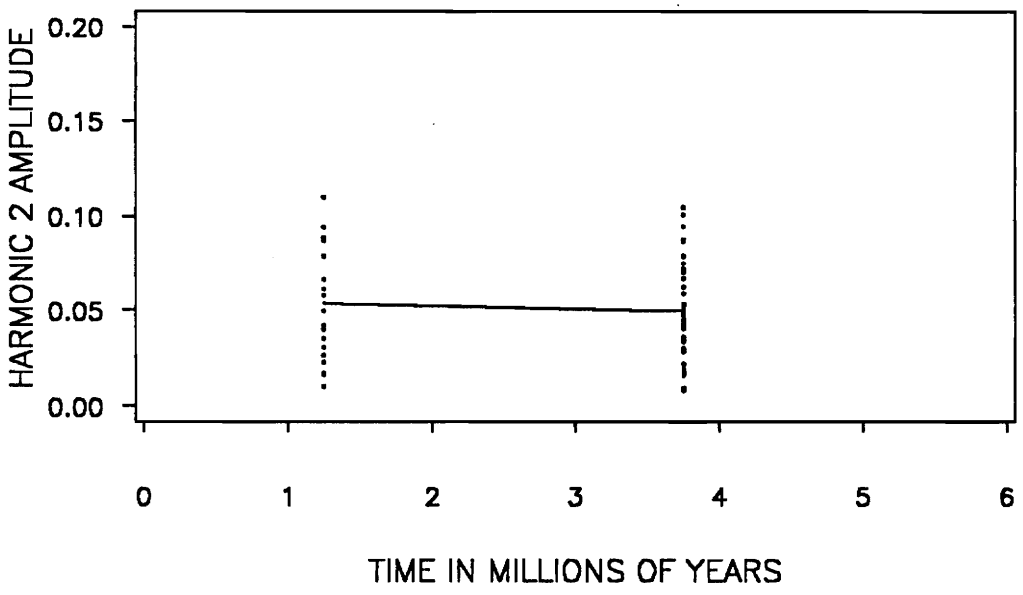

Figure 60. Linear regression of all specimens in calcareous shale in each horizon minus specimens in localities O01A and O02A: Intercept = 0.056; slope = -0.016; p = 0.5788; N = 68 (a: 19; c: 49).

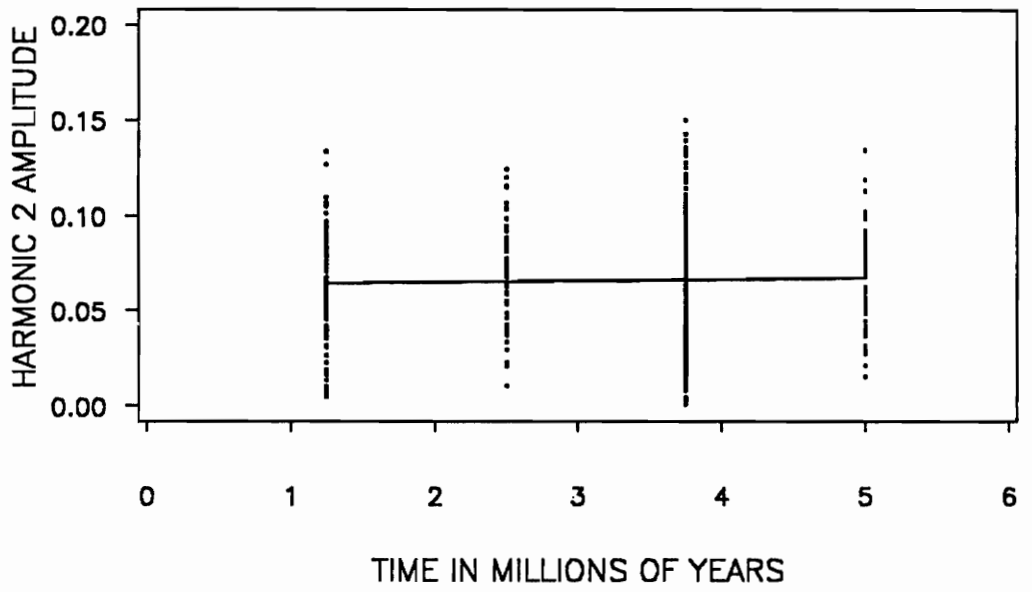

Figure 61. Linear regression of all specimens in each horizon except those in localities N16, N17, O01A, and O02A: Intercept = 0.064; slope = -0.007; p = 0.5530; N = 525.

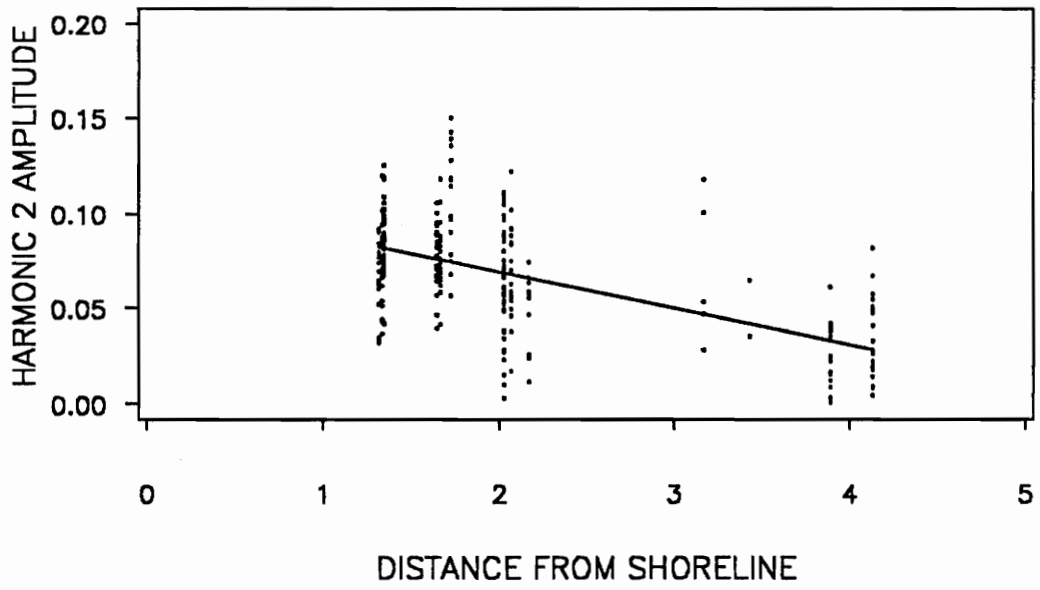

Figure 62. Linear regression of harmonic 2 vs distance from shoreline for all specimens in horizon c of New York: Distance from shoreline given in hundreds of kilometers from Berne, NY. Intercept = 0.108; slope = -0.192; $p < 0.0001$.

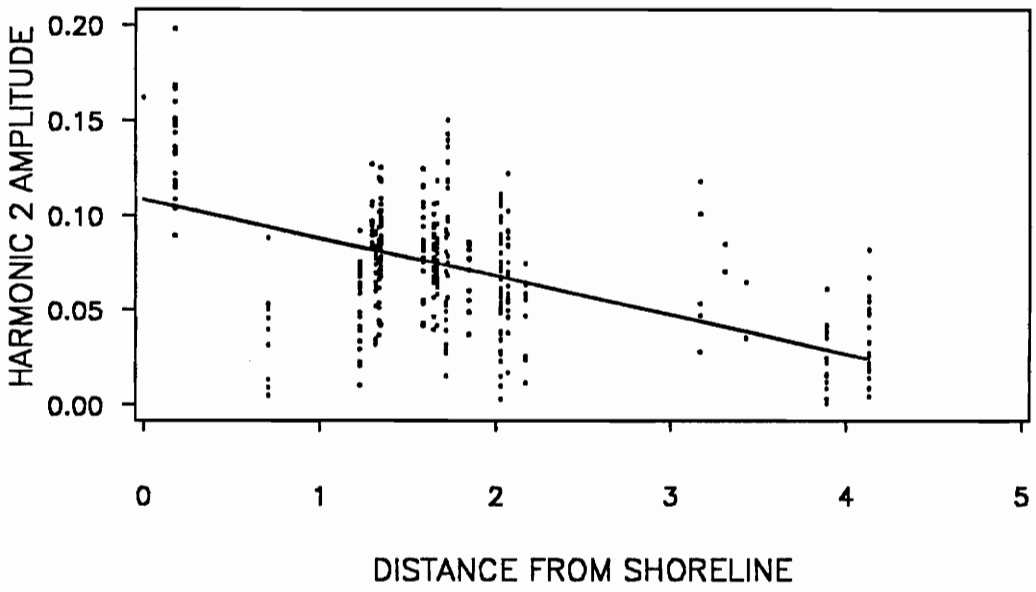

Figure 63. Linear regression of harmonic 2 vs distance from shoreline for all specimens in New York: Distance from shoreline given in hundreds of kilometers from Berne, NY. Intercept = 0.109; slope = -0.203; $p < 0.0001$.

DISCUSSION

ALLOMETRY

Some shape changes can be required by size increase. For example, as a brachiopod grows, its metabolic requirements increase in proportion to its volume. However, its pumping capacity increases in proportion to the surface area of the lophophore filaments. Therefore, as the brachiopod grows the lophophore must increase in surface area in order to meet the metabolic requirements of the animal. Brachiopod species that are small as adults can retain a fairly simple lophophore, whereas species with large adults must have a correspondingly enlarged (and usually more complex) lophophore. Living brachiopods that are spirolophous as adults begin life with a simple trocholophe which becomes a schizolophe with growth and a spirolophe on adulthood (Rudwick, 1970). Shell shape and lophophore complexity are interdependent so that many brachiopod species also exhibit a change in the shell shape over their ontogeny.

Mucrospirifer, whose calcified spiral brachidium indicates that it was spirolophous, exhibits considerable ontogenetic allometry in the shape of its shell. Although comparisons of overall shape in this study were made using only adults, it was necessary to determine if adults in a given population had different shapes due solely to size differences. Comparisons

of overall shape for taxonomic purposes cannot be made unless shape can be shown to be independent of the size of the specimen. Failure to recognize this could lead to unwarranted taxonomic distinctions. The linear regressions performed on size vs shape (harmonic 0 vs harmonic 2) using log-transformed data indicated that no significant allometry is present in the samples used in this study. Therefore, any differences in overall shape identified in subsequent analyses must be attributed to causes other than allometry.

GEOGRAPHICAL VARIATION AND THE POLYTYPIC SPECIES CONCEPT

Geographical variation is "the occurrence of differences among spatially segregated populations of a species" (Mayr, 1970). That species vary geographically has been known since the Linnaean period of the 1700s. However, it was not until the mid-19th century when the ranges of species became better sampled through extensive exploration and increased collecting that the study of geographical variation began in earnest. Biologists now consider it essential to include geographical variation in taxonomic work. Geographical variation is integral to the concept of a polytypic species which consists of many local populations that are more or less different from each other (Mayr, 1970). The typological concept of a species would have us regard all individuals of a species as replicas of the type. However, no two individuals are ever exactly the same, nor are any two populations. Variation occurs both within populations and between populations of a given species. The example of the Song Sparrow is illustrative (Mayr, 1970). In the late 1700s and early 1800s four species of sparrows, including the Song Sparrow (*Passerella melodia*), were recognized in eastern North America. In the middle of the 19th century four additional "species" were identified during exploration of the west. With further exploration, populations intermediate between the four western "species" and the eastern Song Sparrow were discovered. This led ornithologists to combine the five "species" into a single polytypic species. Today the Song Sparrow consists of 34

subspecies and is recognized across North America from Georgia to Mexico and from the Aleutian Islands to Newfoundland.

Species have a complex population structure determined by geographical and ecological factors, genetic and developmental potentials, and past history. Mayr (1970) classifies populations of species into three structural components: clines; geographical isolates; and hybrid belts. A cline is composed of a series of gradually-changing contiguous populations. This mode of geographical variation often results from environmental gradients. A geographical isolate is a population separated from the main body. The frequency of isolates within a species depends on the structure of the environment and on the dispersal capabilities of the species. Hybrid belts are narrow zones of increased variability bordered on either side by uniform groups of populations. Populations within a species are each adapted to the local environment, yet share much of their genetic system with conspecific populations and retain contact with them through gene flow (Mayr, 1970).

Application of the polytypic species concept has proceeded more slowly among the invertebrates, especially for taxa known only from the fossil record. I believe that this is particularly true for brachiopods, which are relatively rare in the modern oceans, but which were among the dominant bottom-dwelling organisms in the Paleozoic. There are only 400 extant species of brachiopods while there are 30,000 recognized as fossils. Undoubtedly brachiopods have declined in abundance, but how many of these 30,000 Paleozoic species would be valid if geographical variation was well studied and the concept of a polytypic species was applied? Articulate brachiopods as a group have many features that predispose them to having polytypic species: they are sedentary; dependent on the substrate; and have nonplanktotrophic larvae. Other animals with low dispersal capabilities, such as snails and flightless insects, commonly show extreme localization of phenotypically distinct populations (Mayr, 1970). Reproductive strategy, such as the length of time marine larvae are in the water column, can also affect dispersal capability. Chuang (1977) reports that larvae of the inarticulates *Lingula* and *Glottidia* have a long planktotrophic existence and that the planktotrophic life of *Discinisca* larvae is shorter. Articulate larvae, on the other hand, have a very short

free-swimming stage and some articulates are known to brood (Chuang, 1977). With this information in mind, one would predict finding localized phenotypically distinct populations when sampling is conducted over a broad geographical range spanning many different environments.

Previous studies of *Mucrospirifer* were limited to portions of its geographical range: New York (Hall, 1867; Raymond, 1904); Ontario (Shimer and Grabau, 1902); Ontario and Michigan (Grabau and Reed, 1910; Mook, 1915); Ontario, Michigan, Ohio (Stumm, 1956; Tillman, 1964); and Ohio (Stewart, 1927). My study is the first that includes a large number of specimens from both the Appalachian and Michigan basins and therefore covers most of the reported geographical range of *Mucrospirifer*. It also has the advantage of being a statistical study that can objectively, and repeatably, quantify the similarities among specimens and test their significance.

Using the two species-discriminating features of Tillman (1964), overall shape of the shell and shape of the fold/sulcus, only one highly variable polytypic species of *Mucrospirifer* can be identified. The shape of the fold/sulcus proved to have no species-level taxonomic value. I could not separate specimens into the two species Tillman (1964) identified using his two subdivisions of the shape of the fold or sulcus. Instead I found the fold/sulcus to be very variable with many intermediates between the two end members. This is one line of evidence for a single polytypic species.

Overall shape also could not distinguish more than one species. If means of amplitudes of significant harmonics for each locality are used rather than amplitudes for each specimen in a locality, then four possible morphs can be discerned as seen in Figure 14-Figure 16. However, using all specimens the variation in shape within a locality is often as great as that between localities, particularly for clusters 1, 3, and 4 (see Figure 18 on page 67). This can also be seen in Figure 17 where the clusters overlap extensively, except for the end members clusters 1 and 2 which have only one specimen in common. If one considers the variation to be similar to the clinal type, it is not surprising to find little overlap between the two end members yet extensive overlap among the transition forms in between.

If the four clusters were indeed separate species, distinguished by differences in overall shape and shape of the fold and sulcus, then each should be readily identifiable. Yet discriminant analysis yields an unacceptably high rate of misclassification (see Table 7 on page 68). An interesting "gradient" of decreasing misclassification is evident when different clusters are grouped together and compared to other clusters: 1 vs 3/4 vs 2; 1/4 vs 3 vs 2; 1/4 vs 2/3; 1/3/4 vs 2 (Table 7). This also suggests variation similar to the clinal type.

Allometric regressions of ontogeny are useful quantitative taxonomic descriptors because each species usually has a significantly different slope (Gould, 1966). I plotted allometric regressions for adulthood since my primary purpose was to determine if adult shape is independent of size, as discussed above. Although not as definitive as ontogenetic allometries for delimiting taxonomic units, allometric regressions of adulthood can still provide insight regarding taxonomy. The allometric regressions of the four clusters are not significantly different from 0, however each has a slight apparent slope (see Figure 20-Figure 23). In comparing the four slopes I found that they did not differ significantly from each other (see Figure 24 on page 81), a fact that can be regarded as evidence for a single species. The fact that the lines of regression differ in intercept in a stepwise fashion suggests clinal variation.

Even so, there is some evidence to indicate that cluster 2 is morphologically more discrete than the other clusters and may represent a subspecies. It is more readily identifiable as a separate grouping, even by cursory observation, than the other clusters. In discriminant analysis, when cluster 2 is contrasted against other clusters or cluster groupings, the percent properly classified ranges from 85.11% to 97.87%, which is higher than the other clusters (see Table 7 on page 68). The range of variation within localities in cluster 2 is low and generally less than most other localities (see Figure 17 on page 64). Cluster 2 is the only cluster limited to just one horizon. It is found in horizon a, then disappears. The other clusters persist from horizon a through horizon d. Removing cluster 2 specimens from the linear regression analysis of horizons significantly changes the slope, suggesting that this cluster is truly different from the others (see Figure 61 on page 131). The fact that the clusters overlap

extensively cannot be ignored. However, the overlap between cluster 2 and the other clusters grouped together is relatively small. Figure 64 shows cluster 2 and clusters 1/3/4 plotted on principal components 1 and 2. An analysis of variance indicates that the means of the two groups are significantly different ($p < 0.0001$), although the proportion of variation explained by the model is less than optimal (see Table 19 for R^2 values). However, when the same plot is constructed for horizon a alone, the only time interval when cluster 2 co-occurs with the other clusters, the extent of overlap is less and the R^2 values are much higher (R^2 for harmonic 2 = 0.634050, Table 20, Figure 65). By definition a subspecies inhabits a geographical subdivision of the range of a species (Mayr, 1970). Yet cluster 2 specimens are not found in a single environment or in a circumscribed geographical area. They occur in New York in sandstone and in Michigan in calcareous shale. I feel that the evidence is too ambiguous to dictate the erection of subspecies at this time.

To retain Tillman's (1964) two species, *Mucrospirifer mucronatus* and *Mucrospirifer thedfordensis*, would require evidence other than that which Tillman himself proposed. To justify the erection of separate species in the future would require information from features not previously studied in depth including internal shell structure and soft part anatomy as evidenced in shell markings (muscle scars, brachidium, genital markings, etc.). Based on overall shape and the shape of the fold and sulcus, a single polytypic species is here identified and named *Mucrospirifer mucronatus*, the first-used species name.

ECOLOGICAL CORRELATIONS

Another question to be addressed is whether different morphological variants of *Mucrospirifer mucronatus* can be associated with particular environmental factors allowing functional explanations to be offered for differences in form. The overall shape of the "body" without the alae was analyzed in this study. The last measurement of the shell outline used was located approximately at the cardinal angle where the alae begin. However, the alae are

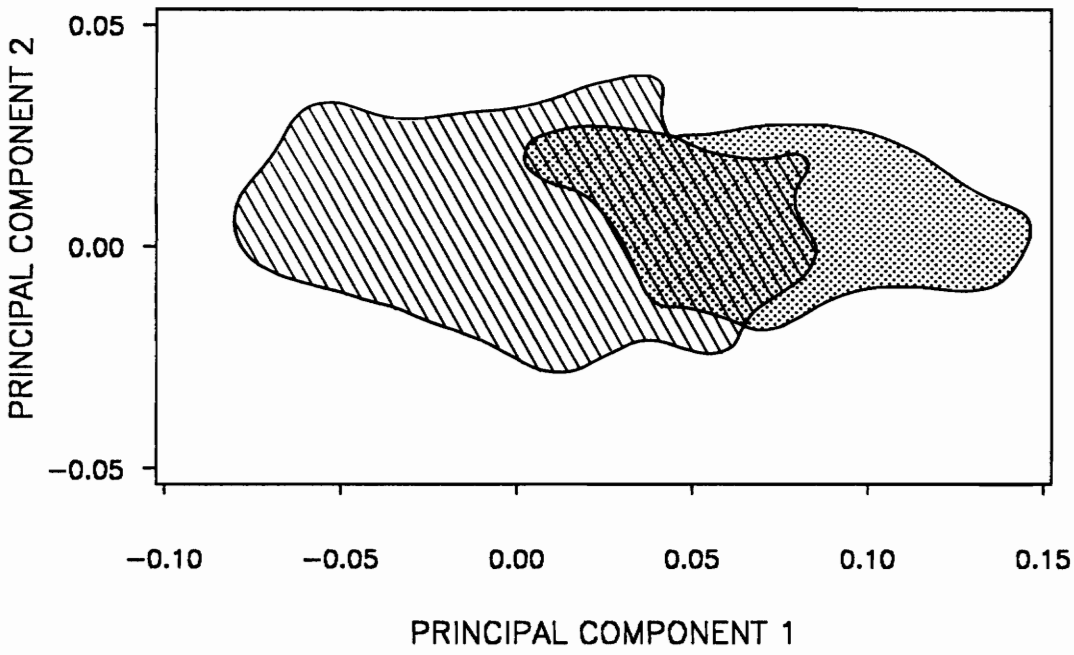

Figure 64. Principal component analysis with specimens in cluster 2 and with specimens in clusters 1, 3, and 4 grouped together for horizons a-d: Cluster 1/3/4 shown in left line pattern; cluster 2 in dot pattern.

Table 19. Test for significant difference between clusters 1, 3, and 4 grouped together and cluster 2 for horizons a-d.

DEPENDENT VARIABLE: HAR2

SOURCE	DF	SUM OF SQUARES	MEAN SQUARE	F VALUE	PR > F
MODEL	1	0.23155460	0.23155460	280.12	0.0001
ERROR	570	0.47118285	0.00082664		
CORRECTED	571	0.70273745			

R-SQUARE	C.V.	ROOT MSE	HAR2 MEAN
0.329504	39.95183	0.0287513	0.0719649

SOURCE	DF	TYPE I SS	F VALUE	PR > F
CLUSTER	1	0.23155460	280.12	0.0001

SOURCE	DF	TYPE III SS	F VALUE	PR > F
CLUSTER	1	0.23155460	280.12	0.0001

DEPENDENT VARIABLE: HAR4

SOURCE	DF	SUM OF SQUARES	MEAN SQUARE	F VALUE	PR > F
MODEL	1	0.04139470	0.04139460	247.64	0.0001
ERROR	570	0.09527750	0.00016715		
CORRECTED	571	0.13667220			

R-SQUARE	C.V.	ROOT MSE	HAR4 MEAN
0.302876	49.51124	0.0129288	0.0261128

SOURCE	DF	TYPE I SS	F VALUE	PR > F
CLUSTER	1	0.04139470	247.64	0.0001

SOURCE	DF	TYPE III SS	F VALUE	PR > F
CLUSTER	1	0.04139470	247.64	0.0001

DEPENDENT VARIABLE: HAR6

SOURCE	DF	SUM OF SQUARES	MEAN SQUARE	F VALUE	PR > F
MODEL	1	0.00745108	0.00745108	164.63	0.0001
ERROR	570	0.02579751	0.00004526		
CORRECTED	571	0.03324859			

R-SQUARE	C.V.	ROOT MSE	HAR6 MEAN
0.224102	46.83781	0.0067275	0.0143633

SOURCE	DF	TYPE I SS	F VALUE	PR > F
CLUSTER	1	0.00745108	164.63	0.0001

SOURCE	DF	TYPE III SS	F VALUE	PR > F
CLUSTER	1	0.00745108	164.63	0.0001

MANOVA TEST CRITERIA FOR THE HYPOTHESIS OF NO OVERALL TYPE EFFECT

WILKS' CRITERION	F(3,568)	PROB > F
0.61427925	118.89	0.0001
PILLAI'S TRACE	F(3,568)	PROB > F
0.38572075	118.89	0.0001
HOTELLING-LAWLEY TRACE	F(3,568)	PROB > F
0.62792412	118.89	0.0001
ROY'S MAXIMUM ROOT CRITERION	F(3,568)	PROB > F
0.62792412	118.89	0.0001

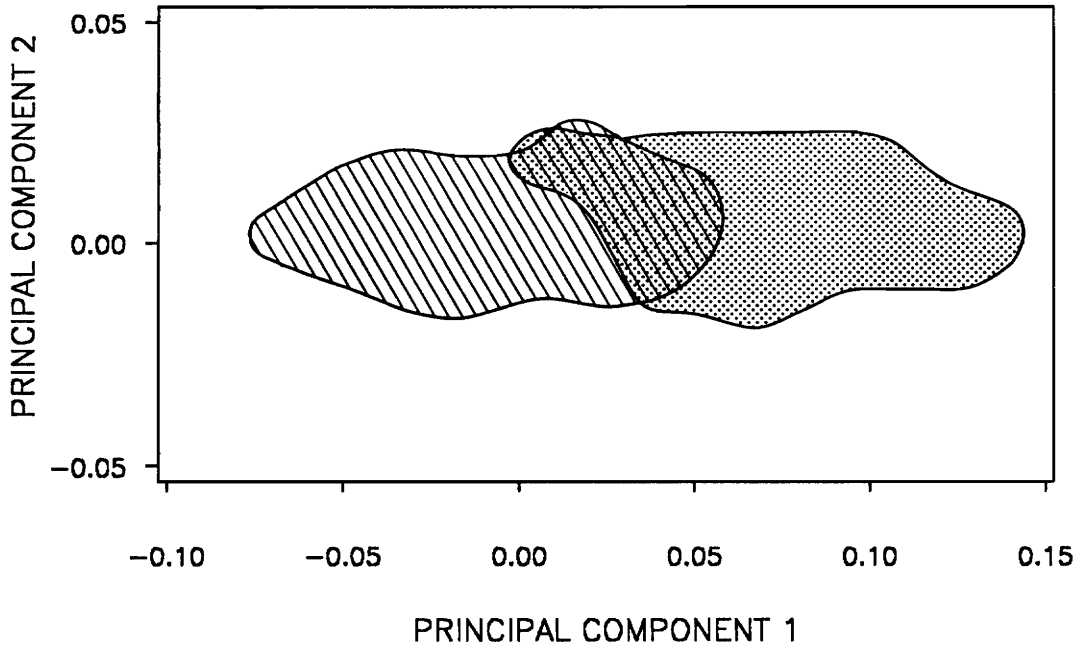

Figure 65. Principal component analysis with specimens in cluster 2 and with specimens in clusters 1, 3, and 4 grouped together for horizon a only: Cluster 1/3/4 shown in left line pattern; cluster 2 in dot pattern.

Table 20. Test for significant difference between clusters 1, 3, and 4 grouped together and cluster 2 for horizon a only.

DEPENDENT VARIABLE: HAR2

SOURCE	DF	SUM OF SQUARES	MEAN SQUARE	F VALUE	PR > F
MODEL	1	0.18038407	0.18038407	242.57	0.0001
ERROR	140	0.10411105	0.00074365		
CORRECTED	141	0.28449512			

R-SQUARE	C.V.	ROOT MSE	HAR2 MEAN
0.634050	30.80035	0.0272700	0.0885378

SOURCE	DF	TYPE I SS	F VALUE	PR > F
CLUSTER	1	0.18038407	242.57	0.0001

SOURCE	DF	TYPE III SS	F VALUE	PR > F
CLUSTER	1	0.18038407	242.57	0.0001

DEPENDENT VARIABLE: HAR4

SOURCE	DF	SUM OF SQUARES	MEAN SQUARE	F VALUE	PR > F
MODEL	1	0.01976224	0.01976224	113.92	0.0001
ERROR	140	0.02428642	0.00017347		
CORRECTED	141	0.04404866			

R-SQUARE	C.V.	ROOT MSE	HAR4 MEAN
0.448646	34.86910	0.0131710	0.0377726

SOURCE	DF	TYPE I SS	F VALUE	PR > F
CLUSTER	1	0.01976224	113.92	0.0001

SOURCE	DF	TYPE III SS	F VALUE	PR > F
CLUSTER	1	0.01976224	113.92	0.0001

DEPENDENT VARIABLE: HAR6

SOURCE	DF	SUM OF SQUARES	MEAN SQUARE	F VALUE	PR > F
MODEL	1	0.00281505	0.00281505	63.11	0.0001
ERROR	140	0.00624462	0.00004460		
CORRECTED	141	0.00905966			

R-SQUARE	C.V.	ROOT MSE	HAR6 MEAN
0.310723	33.23400	0.0066787	0.0200858

SOURCE	DF	TYPE I SS	F VALUE	PR > F
CLUSTER	1	0.00281505	63.11	0.0001

SOURCE	DF	TYPE III SS	F VALUE	PR > F
CLUSTER	1	0.00281505	63.11	0.0001

MANOVA TEST CRITERIA FOR THE HYPOTHESIS OF NO OVERALL TYPE EFFECT

WILKS' CRITERION	F(3,138)	PROB > F
0.36533148	79.91	0.0001
PILLAI'S TRACE	F(3,138)	PROB > F
0.63466852	79.91	0.0001
HOTELLING-LAWLEY TRACE	F(3,138)	PROB > F
1.73724020	79.91	0.0001
ROY'S MAXIMUM ROOT CRITERION	F(3,138)	PROB > F
1.73724020	79.91	0.0001

fairly similar throughout the spectrum of forms identified in this study, while the differences among the forms lie primarily in the shape of the "body." The length of the "body" is the radius from the hingeline at the beak to the commissure at the fold/sulcus and is described as long or short in relation to specimens of the same width. On average, in the cluster 1 form the alae appear more spine-like in relation to the "body," which is relatively round and long (Figure 66). In the form represented by cluster 2, the "body" is fusiform and short and grades into the alae gradually. Cluster 3 specimens are similar to those in cluster 2 in having a short "body," but they are less fusiform. Specimens in cluster 4 resemble cluster 1 specimens but they are not as round and long.

In adulthood the alae often were partitioned off from the rest of the shell and therefore could not function as part of the mantle cavity or be used for any other internal structures (see Figure 5 on page 19). Rudwick (1970) suggested that the alae might have acted like skis to stabilize the shell in soft sediment and Cowen's work (1968) documenting the coincidence of the decline in the size of the pedicle opening with the growth of the alae supports this idea. Another possibility is that the height of the shell above the substrate was related to water turbulence and stability, so that shorter forms existed in more agitated water and longer forms in quieter water. David K. Jacobs (pers. comm., 1990) suggested that the alae may have had a hydrodynamic role in controlling water flow around the animal in order to maximize its filter-feeding capacity. If the alae were an adaptation to soft substrate then one might expect to find forms with spine-like alae more often in mudstones than in coarser-grained rocks. If the height of the shell was an adaptation to amount of turbulence, then short forms would be expected to have lived near shore and long forms further from the shore. Further study would benefit from flow-tank work to analyze current movement around the alae and would also be useful to test the stability hypotheses.

In this project the relationship between morphological shape and lithology was analyzed. No strong correlation emerges between lithology and shape over the entire study area. In the Michigan Basin the most elongate specimens (cluster 2) are confined to calcareous shale, but round specimens can be found in both limestone and calcareous shale. A slight

Figure 66. Example of a specimen from each cluster: (A) Cluster 1, specimen O02C06; (B) Cluster 2, specimen N1722; (C) Cluster 3, specimen M1301; (D) Cluster 4, specimen N1002.

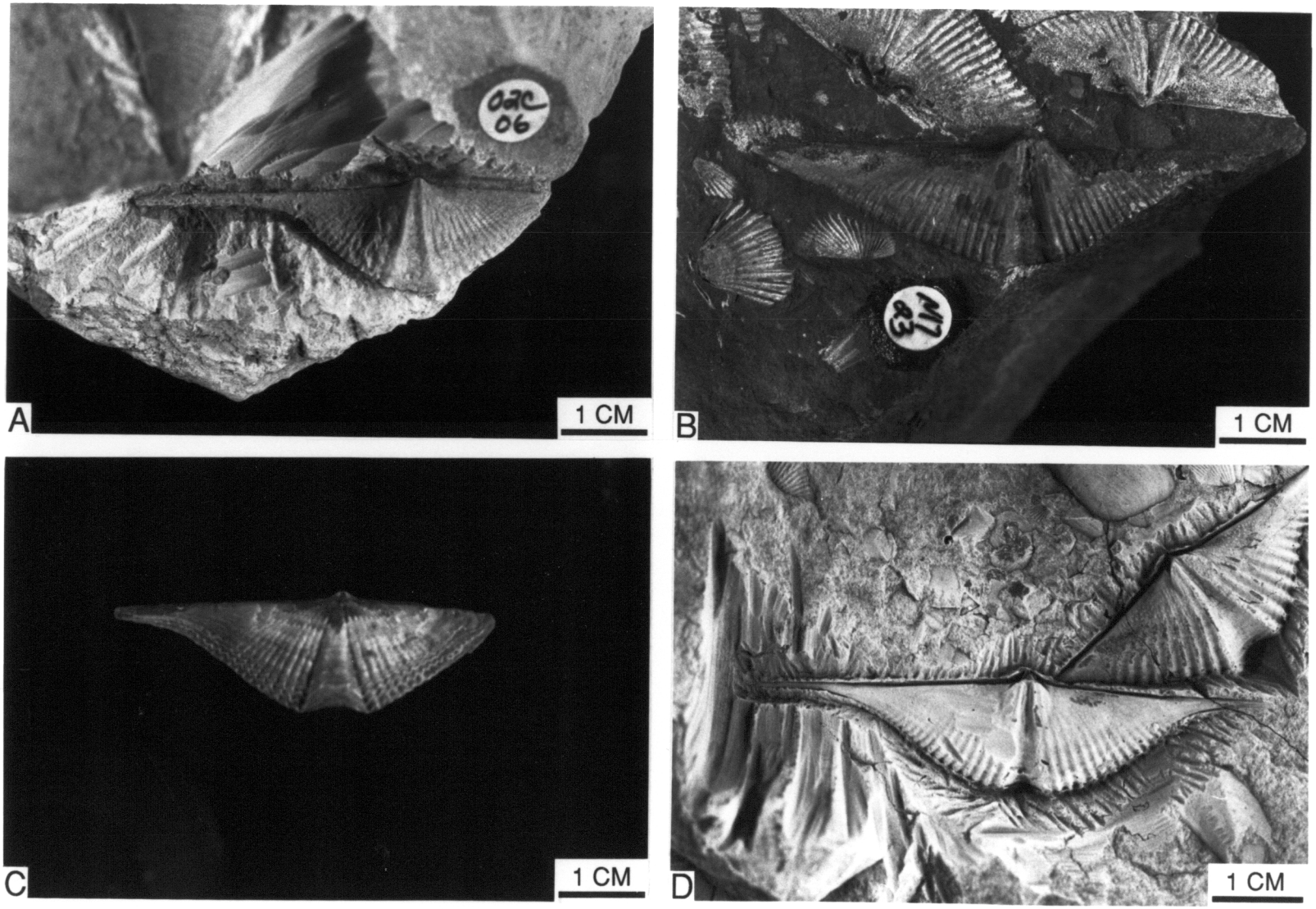
A
1 CM
B
1 CM
C
1 CM
D
1 CM

tendency is apparent in the Appalachian Basin where the roundest specimens are found in mudstone and the most elongate are in sandstone. Specimens of intermediate shape can be found in siltstone as well as in mudstone and sandstone (see Figure 42 on page 109). The extensive overlap among the shape fields of each lithology prohibits definitively assigning a given shape to a rock type. In addition, the tendency that emerges when all horizons are grouped together is not apparent when each horizon is considered separately. In horizon c, for example, both mudstone and siltstone contain more elongate specimens than does sandstone (see Figure 47 on page 116). The fact that the very elongate cluster 2 specimens are found in both fine-grained offshore and coarse-grained nearshore sediments makes a functional determination impossible.

In New York a more definitive trend is evident. As one goes from the nearshore shelf in the east to the offshore shelf in the west there is a corresponding decrease in the elongateness of specimens. The change in shape is more extreme if all New York specimens are analyzed because cluster 2 specimens are easternmost and cluster 1 specimens are westernmost. Examining only horizon c where all but 19 of the 258 specimens are in clusters 1 and 4 whose shape fields overlap most, the shape change is less pronounced yet the trend towards roundness going from east to west is still obvious (see Figure 62 on page 133). A lithological change is also evident going from east to west in horizon c. The sands and silts common in eastern New York are absent in the west where the lithologies are predominantly mudstone. Although the western part of the state was further from the shoreline this does not necessarily imply that the water depth was substantially greater. Brett and Baird (1985) have shown that the structural basin was in westcentral New York and it was flanked on either side by shallower shelves. Further sedimentological and ecological work is necessary to more clearly delineate environments, but it can be said that the mudstones of the west represent less agitated and quieter waters than do the sandstones and siltstones of the east. In New York it appears that my hypothesis correlating shell length (height above the substrate) with water turbulence may apply and that Rudwick's (1970) stability hypothesis may also be appropriate. Further work is necessary before a definitive conclusion can be drawn.

STASIS AND PUNCTUATED EQUILIBRIA

The theory of punctuated equilibria claims that most evolutionary change is concentrated in speciation events that are instantaneous in geological time and that once established, species remain morphologically stable during their geological histories (Eldredge and Gould, 1972). Gould (1982) defined "geologically instantaneous" as 1% or less of the lifespan of a species, which is on average 5-11 million years. Most of the rock record is not sufficiently complete to directly observe events at this scale. With the exception of the use of deep-sea cores, it is difficult to test the phenomenon of the geologically abrupt appearance of new species. It can always be argued that a morphological gap is due to missing section. However, if a species exists for 5-11 million years essentially unchanged, the imperfection of the geological record is immaterial. Stasis can still be documented. Identifying morphological stasis over most of the lifetime of a species, particularly when this includes large amounts of missing section, is integral to and validates punctuated equilibria (Gould and Eldredge, 1977; Gould, 1982).

In this study speciation per se cannot be observed. The stratigraphical resolution over such a large geographical area is inadequate and the ±380 million-year-old Middle Devonian rocks are certainly incomplete. In addition, I have shown above that *Mucrospirifer* appears to be represented by a single species in the study area, rather than the two or more species previously described. Therefore, no speciation of *Mucrospirifer* is observed in this time interval. It is, however, possible to observe whether or not *Mucrospirifer mucronatus* shows directional change in shape through time. The geographical coverage is extensive and different lithologies were sampled which allows facies changes and associated migration to be taken into account.

I tested for potential morphological stasis by comparing all specimens in each horizon and by comparing specimens in a given lithology in each horizon. Using both principal component analysis and linear regression, no significant directional change over time could be

identified even when horizons were examined by each lithology. Going from horizon a to b there is a loss of variation in the most elongate portion of morphospace. But from horizon b through d morphological stasis predominates (see Figure 36 on page 99). Even with the inclusion of cluster 2 specimens the line of regression has only a very slight slope (-0.072, see Figure 31 on page 92). A temporal "trend" is not significant when it is barely detectable compared to the vast geographical variation within and among contemporaneous populations. All evidence accrued in this study indicates that the 5-7 million year history of *Mucrospirifer mucronatus* was characterized by morphological stasis.

The case histories that have been described since the theory of punctuated equilibria was proposed have uncovered both taxonomic and ecological patterns for the frequency of gradualism or punctuated equilibria. Shallow-water marine invertebrates and species in benthic environments exhibit a higher frequency of punctuated equilibria. Oceanic microplankton and species in pelagic environments show a higher frequency of phyletic gradualism (Gould, 1983, 1985). Johnson (1982) attributed these trends to environmental stability, or lack thereof. A changing paleogeography allows peripheral isolates to develop, while a stable paleogeography does not. Pelagic environments are more stable and homogeneous than benthic, hence the prevalence of gradualism in pelagic and punctuated equilibria in benthic environments. However, any explanation is incomplete without taking in account the intrinsic properties of species. Environmental changes alone cannot explain why articulate brachiopods are more speciose than inarticulate brachiopods, for example. Differences in larval dispersal strategy are an important consideration. Scheltema (1982) found that larval dispersal capability correlates directly with geographical range and indirectly with phyletic evolution. He concluded that species with wide geographical dispersal as larvae will tend to have a reduced capacity for allopatric speciation and will evolve slowly.

The same characteristics that predispose articulate brachiopods to having polytypic species--sedentary lifestyle, dependence on the substrate, nonplanktotrophic larvae--also predispose them to speciating via the allopatric (peripheral isolate), founder (founder-flush, genetic transilience), or stasipatric (parapatric) modes, all of which are compatible with

punctuated equilibria. This does not mean that speciation results from geographical variation within a species. Subspecies or clines are rarely incipient species that eventually evolve into full-fledged species (Mayr, 1970). If that were the case then each cluster in this study should show directional change over the 5-7 million year interval covered. But as can be seen in Figure 67-Figure 69, no significant directional change is evident. Stasis persists through millions of years and extensive climatic changes.

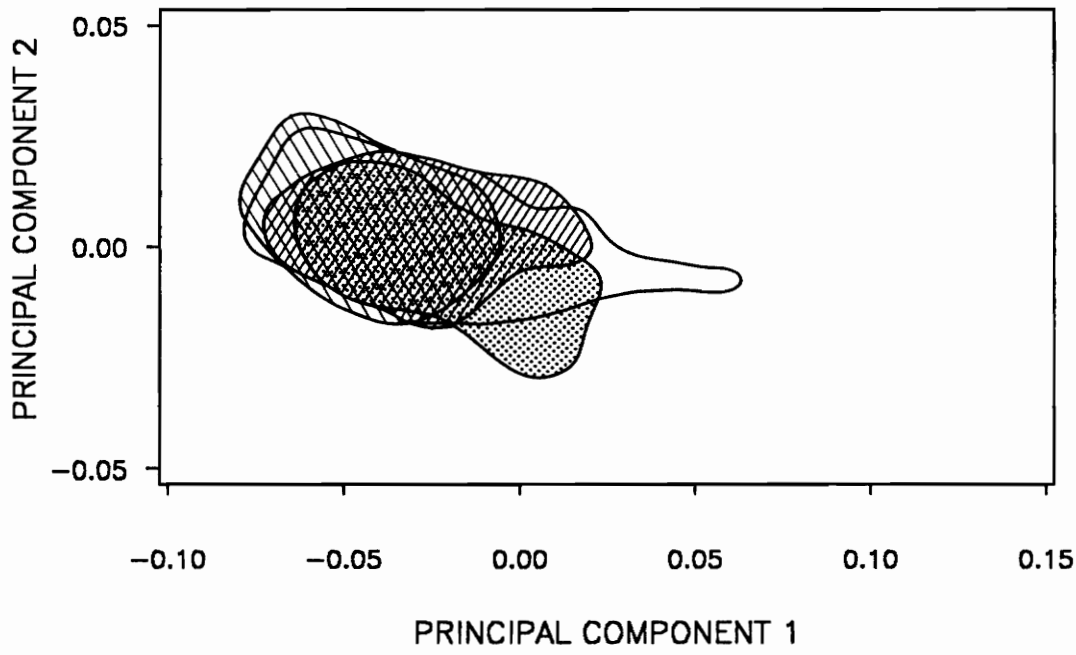

Figure 67. Principal component analysis with specimens in cluster 1 plotted by horizon: Horizon a shown in left line pattern; horizon b in right line pattern; horizon c with no pattern; horizon d in dot pattern.

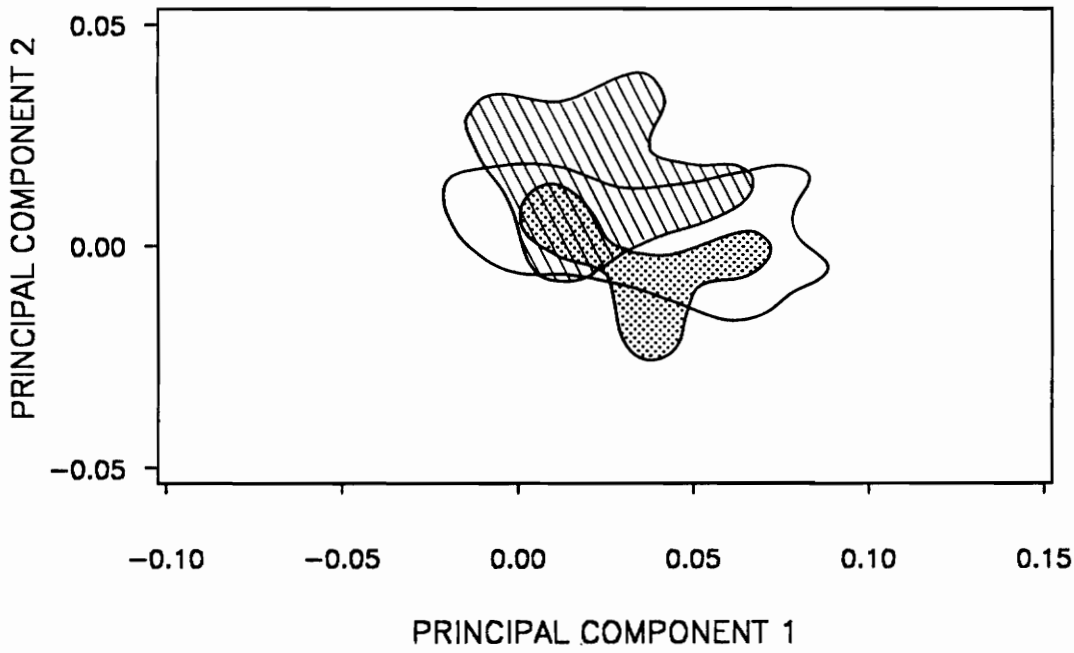

Figure 68. Principal component analysis with specimens in cluster 3 plotted by horizon: Horizon a shown in left line pattern; horizon c with no pattern; horizon d in dot pattern.

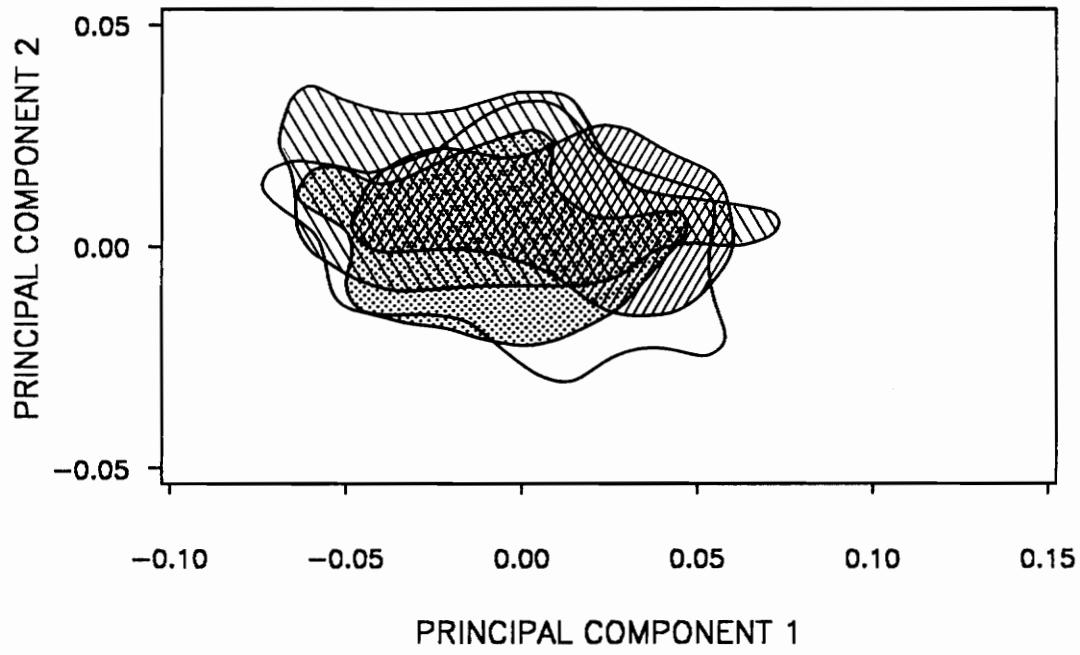

Figure 69. Principal component analysis with specimens in cluster 4 plotted by horizon: Horizon a shown in left line pattern; horizon b in right line pattern; horizon c with no pattern; horizon d in dot pattern.

REFERENCES

Anstey, R. L., and Delmet, D. M. 1973. Fourier analysis of zooecial shapes in fossil tubular bryozoans. Geol. Soc. Amer. Bull., 84: 1753-1764.

Anstey, R. L., and Pachut, J. F. 1980. Fourier packing ordinate: a univariate size-independent measurement of the polygonal packing variation in Paleozoic bryozoans. Math. Geol., 12(2): 139-156.

Baird, G. C. 1979. Sedimentary relationships of Portland Point and associated Middle Devonian rocks in central and western New York. N.Y. State Mus. Bull., 433: 1-24.

Beaumont, C., Quinlan, G. M., and Hamilton, J. 1988. Orogeny and stratigraphy: numerical models of the Paleozoic in the eastern interior of North America. Tectonics, 7: 389-416.

Berg, T. M., McInerny, M. K., Way, T. H., and MacLachlan, D. B. 1983. Stratigraphic correlation chart of Pennsylvania. Penn. Geol. Surv., 4th Ser., Genl. Geol. Rept. 75.

Boon, J. D., III, Evans, D. A., and Hennigar, H. F. 1982. Spectral information from Fourier analysis of digitized quartz grain profiles. Math. Geol., 14(6): 589-605.

Bray, J. R., and Curtis, J. T. 1957. An ordination of the upland forest communities of southern Wisconsin. Ecol. Monogr., 27: 325-349.

Brett, C. E. 1974. Contacts of the Windom Member (Moscow Formation) in Erie County, New York. NY State Geol. Assn., 46th Ann. Mtg., Guidebook, p. C1-C29.

Brett, C. E., and Baird, G. C. 1985. Carbonate-shale cycles in the Middle Devonian of New York: an evaluation of models for the origin of limestones in terrigenous shelf sequences. Geology, 13: 324-327.

Brett, C. E., Baird, G. C., and Miller, K. B. 1986. Sedimentary cycles and lateral facies gradients across a Middle Devonian shelf-to-basin ramp, Ludlowville Formation, Cayuga basin. N.Y. State Geol. Assn., 58th Ann. Mtg., Guidebook, p. 81-127.

Brower, J. C., Nye, O. B., Jr., Belak, R., Carey, E. F., Leetaru, H. H., MacAdam, M., Millendorf, S. A., Salisbury, A., Thomson, J. A., Willette, P. D., and Yamamoto, S. 1978. Faunal assemblages in the Lower Hamilton Group in Onondaga County, New York. New York State Geological Assn., 50th Ann. Mtg. Guidebook, p. 104-123.

Burke, C. D., Full, W. E., and Gernant, R. E. 1987. Recognition of fossil fresh water ostracodes: Fourier shape analysis. Lethaia, 20: 307-314.

Bush, G. 1975. Modes of animal speciation. Ann. Rev. Ecol. Sys., 6: 339-364.

Bush, G. L. 1981. Stasipatric speciation and rapid evolution in animals, p. 201-218. *In* Evolution and Speciation: Essays in Honor of M. J. D. White, W. R. Atchley and D. S. Woodruff, Eds. Cambridge Univ. Press, NY.

Canfield, D. J., and Anstey, R. L. 1981. Harmonic analysis of cephalopod suture patterns. Math. Geol., 13(1): 23-35.

Carson, H. L. 1971. Speciation and the founder principle. Stadler Genet. Symp., 3: 51-70.

Carson, H. L. 1975. The genetics of speciation at the diploid level. Am. Nat., 109: 83-92.

Carson, H. L. 1976. Genetic differences between newly formed species. Bio Science, 26: 700-701.

Carson, H. L., and Templeton, A. R. 1984. Genetic revolutions in relation to speciation phenomenon: the founding of new populations. Ann. Rev. Ecol. Syst., 15: 97-131.

Christopher, R. A. and Waters, J. A. 1974. Fourier series as a quantitative descriptor of miospore shape. J. Paleontol., 48(4): 697-709.

Chuang, S. H. 1977. Larval development in *Discinisca* (Inarticulate brachiopod). Amer. Zool., 17: 39-53.

Cisne, J. L., and Rabe, B. D. 1978. Coenocorrelation: gradient analysis of fossil communities and its applications in stratigraphy. Lethaia, 11: 341-364.

Cooper, G. A. 1957. Paleoecology of the Middle Devonian of eastern and central United States, p. 249-278. *In* Treatise on Marine Ecology and Paleoecology, Part 2, Paleoecology, H. D. Ladd, Ed. Geol. Soc. Amer. Mem. 67.

Cooper, G. A. and others. 1942. Correlation of the Devonian sedimentary formations of North America. Geol. Soc. Amer. Bull., 53: 1729-1794.

Cowen, R. 1968. A new type of delthyrial cover in the Devonian brachiopod *Mucrospirifer* Palaeontology, 11: 317-327.

Davis, J. C. 1986. Statistics and Data Analysis in Geology. 2nd ed. Wiley, NY. 646 pp.

Delmet, D. A., and Anstey, R. L. 1974. Fourier analysis of morphological plasticity within an Ordovician bryozoan colony. J. Paleontol., 48(2): 217-226.

Dennison, J. M., and Textoris, D. A. 1978. Tioga Bentonite time-marker associated with Devonian shales in Appalachian basin, p. 166-182. *In* Proc. First Eastern Gas Shales Symp., Oct. 17-19, 1977, Morgantown, WVA, G. L. Schott, W. K. Overbey, Jr., A. E. Hunt, and C. A. Komar, Eds. U.S. Dept. of Energy, Morgantown Research Center, Publ. MERC/SP-77/5.

Digby, P. G. N., and Kempton, R. A. 1987. Multivariate Analysis of Ecological Communities. Chapman and Hall, NY. 206 pp.

Ehlers, G. M., and Kesling, R. V. 1970. Devonian strata of Alpena and Presque Isle Counties, Michigan. Geol. Soc. Amer. North-Central Section Mtg., Guidebook. 130 pp.

Ehrlich, R., and Weinberg, B. 1970. An exact method for characterization of grain shape. J. Sed. Pet., 40(1): 205-212.

Eldredge, N. 1971. The allopatric model and phylogeny in Paleozoic invertebrates. Evolution, 25: 156-167.

Eldredge, N. 1972. Systematics and evolution of *Phacops rana* (Green, 1832) and *Phacops iowensis* Delo, 1935 (Trilobita) in the Middle Devonian of North America. Bull. Amer. Mus. Nat. Hist., 47: 45-114.

Eldredge, N., and S. J. Gould. 1972. Punctuated equilibria: an alternative to phyletic gradualism, p. 82-115. *In* Models in Paleobiology, T. J. M. Schopf, Ed. Freeman, Cooper & Co., San Francisco.

Ellison, R. L. 1965. Stratigraphy and Paleontology of the Mahantango Formation in South-Central Pennsylvania. Penn. Geol. Surv., 4th Ser., Genl. Geol. Rept. 48.

Ettensohn, F. R. 1985a. The Catskill Delta complex and the Acadian Orogeny: A model, p. 39-49. *In* The Catskill Delta, D. L. Woodrow and W. D. Sevon, Eds. Geol. Soc. Amer. Spec. Pap. 201.

Ettensohn, F. R. 1985b. Controls on development of Catskill Delta complex basin-facies, p. 65-77. *In* The Catskill Delta, D. L. Woodrow and W. D. Sevon, Eds. Geol. Soc. Amer. Spec. Pap. 201.

Faill, R. D. 1985. The Acadian orogeny and the Catskill Delta, p. 15-37. *In* The Catskill Delta, D. L. Woodrow and W. D. Sevon, Eds. Geol. Soc. Amer. Spec. Pap. 201.

Fisher, J. N. 1970. The paleoecology of the Hamilton Group (Middle Devonian) in southeastern New York state. B.A. Honors Thesis, Smith College.

Fisher, J. H., Barratt, M. W., Droste, J. B., and Shaver, R. H. 1988. Michigan Basin, p.361-382. *In* The Geology of North America, Vol. D-2, Sedimentary Cover--North American Craton: U.S. Geol. Soc. Amer.

Foote, M. 1989. Perimeter-based Fourier analysis: a new morphometric method applied to the trilobite cranidium. J. Paleontol., 63(6): 880-885.

Fortey, R. A. 1985. Gradualism and punctuated equilibria as competing and complementary theories. Spec. Pap. Paleontol., 33: 17-28.

Gardner, W. C. 1974. Middle Devonian stratigraphy and depositional environments in the Michigan Basin. Michigan Basin Geol. Soc. Spec. Pap., No. 1. 138 pp.

Gauch, H. G., Jr. 1982. Multivariate Analysis in Community Ecology. Cambridge Univ. Press. 298 pp.

Geary, D. H. 1987. Evolutionary tempo and mode in a sequence of the Upper Cretaceous bivalve *Pleuriocardia*. Paleobiology, 13(2): 140-151.

Gevirtz, J. L. 1976. Fourier analysis of bivalve outlines: implications on evolution and autecology. Math. Geol., 8(2): 151-163.

Gingerich, P. D. 1985. Species in the fossil record: concepts, trends, and transitions. Paleobiology, 11(1): 27-41.

Gould, S. J. 1966. Allometry and size in ontogeny and phylogeny. Biol. Rev., 41: 587-640.

Gould, S. J. 1980. Is a new and general theory of evolution emerging? Paleobiology, 6(1): 119-130.

Gould, S. J. 1982. The meaning of punctuated equilibrium and its role in validating a hierarchical approach to macroevolution, p. 83-104. *In* Perspectives on Evolution, R. Milkman, Ed. Sinauer Assoc., Sunderland, MA.

Gould, S. J. 1983. Punctuated equilibrium and the fossil record. Science, 219: 438-440.

Gould, S. J. 1985. The paradox of the first tier: an agenda for paleobiology. Paleobiology, 11(1): 2-12.

Gould, S. J., and Eldredge, N. 1977. Punctuated equilibria: the tempo and mode of evolution reconsidered. Paleobiology, 3: 115-151.

Gould, S. J., and Eldredge, N. 1986. Punctuated equlibrium at the third stage. Syst. Zool., 35: 143-148.

Grabau, A. W., and Reed, M. 1910. Mutations of *Spirifer mucronatus*. Proc. 7th Internat. Zool. Cong., Boston, Aug. 19-24, 1907, The University Press.

Grasso, T. X. 1970. Paleontology, stratigraphy, and paleoecology of the Ludlowville and Moscow formations (Upper Hamilton Group) in central New York. NY State Geol. Assn., 42nd Ann. Mtg., Guidebook, p. D1-D22.

Grasso, T. X. 1978. Benthic communities of the Ludlowville and Moscow formations (Upper Hamilton Group), in the Tully Valley, Onondaga County. NY State Geol. Assn., 50th Ann. Mtg., Guidebook, p. 143-172.

Grasso, T. X. 1981. Stratigraphy, paleontology, and paleoecology of the Upper Hamilton Group (Middle Devonian), in the Genesee Valley, Livingston County. Natl. Assn. Geol. Teachers--Eastern Section, Field Guidebook for the Geology of Genesee Valley Area of Western New York, p. B1-B36.

Hall, J. 1867. Natural History of New York. Palaeontology: Vol. IV, Part I. Containing Descriptions and Figures of the Fossil Brachiopoda of the Upper Helderberg, Hamilton, Portage, and Chemung Groups. Geological Survey of New York, Albany. 428 pp., 63 pl.

Healy-Williams, N., and Williams, D. F. 1981. Fourier analysis of test shape of planktonic foraminifera. Nature, 289: 485-487.

Hoskins, D. M., Inners, J. D., and Harper, J. A. 1983. Fossil Collecting in Pennsylvania. PA Geol. Surv., 4th Ser., Genl. Geol. Rept. 40.

Johnson, J. G. 1982. Occurrence of phyletic gradualism and punctuated equilibria through geologic time. J. Paleontol., 56(6): 1329-1331.

Kaesler, R. L., and Waters, J. A. 1972. Fourier analysis of the ostracode margin. Geol. Soc. Amer. Bull., 83: 1169-1178.

Kent, D. V., and Van Der Voo, R. 1990. Palaeozoic palaeogeography from palaeomagnetism of the Atlantic-bordering continents, p. 49-56. *In* Palaeozoic Palaeogeography and Biogeography, C. R. Scotese and W. S. McKerrow, Eds. Geol. Soc. Mem. No. 12.

Kesling, R. V., Segall, R. T., and Sorensen, H. O. 1974. Devonian strata of Emmet and Charlevoix counties, Michigan. Mus. Paleontol. Pap. Paleontol. No. 7. 187 pp.

Kesling, R. V., Johnson, A. M., and Sorensen, H. O. 1976. Devonian strata of the Afton-Onaway area, Michigan. Mus. Paleontol. Pap. Paleontol. No. 17. 148 pp.

Lachenbruch, P. A. 1975. Discriminant Analysis. Hafner Press, NY. 128 pp.

Lich, D. L. 1990. *Cosomys primus*: a case for stasis. Paleobiology, 16(3): 384-395.

Mayr, E. 1942. Systematics and the Origin of Species. Columbia Univ. Press, NY, 334 pp.

Mayr, E. 1954. Change of genetic environment and evolution, p. 157-180. *In* Evolution As a Process, J. Huxley, Ed. Allen and Unwin, London.

Mayr, E. 1963. Animal Species and Evolution. Harvard Univ. Press, Cambridge, MA.

Mayr, E. 1970. Populations, Species, and Evolution. Belknap Press, Cambridge, MA. 453 pp.

Miller, A. I. 1988. Spatial resolution in subfossil molluscan remains: implications for paleobiological analysis. Paleobiology, 14(1): 91-103.

Mook, C. C. 1915. Statistical study of variation in *Spirifer mucronatus*. Ann. N.Y. Acad. Sci., 26.

New York State Geological Association. 1956. Guidebook for Field Trips in Western New York State. NY State Geol. Assn., 28th Ann. Mtg., p. 29-38, 92-95, 103-107.

Nunn, J. A., and Sleep, N. H. 1984. Thermal contraction and flexure of intracratonal basins: a three-dimensional study of the Michigan basin. Geophys. J. Roy. Astron. Soc., 76: 587-635.

Oliver, W. A., Jr., deWitt, W., Jr., Dennison, J. M., Hoskins, D. M., and Huddle, J. W. 1969. Devonian of the Appalachian Basin, United States, p. . *In*

Oliver, W. A., Jr., and Klapper, G. 1981. Introduction, p. 1-4. *In* Devonian Biostratigraphy of New York, Part 1. Oliver, W. A. and Klapper, Eds. International Union of Geological Sciences, Subcommission on Devonian Stratigraphy, Washington, D.C.

Patchen, D. G., and Dugolinsky, B. K. 1979. Guidebook Middle and Upper Devonian Clastics Central and Western New York State, U.S. Dept. of Energy--Eastern Gas Shales Project. 170 pp.

Plants, H. F. 1977. Paleoecology of the Martinsburg Formation at Catawba Mountain, Virginia. M.S. Thesis, Virginia Polytechnic Institute and State University, Blacksburg, VA. 216 pp.

Quinlan, G. M. 1987. Models of subsidence mechanisms in intracratonic basins, and their applicability to North American examples. Can. Soc. Pet. Geol., Mem. 12: 463-481.

Quinlan, G. M., and Beaumont, C. 1984. Appalachian thrusting, lithospheric flexure, and the Paleozoic stratigraphy of the eastern interior of North America. Can. J. Earth Sci., 21: 973-996.

Raymond, P. E. 1904. The *Tropidoleptus* fauna at Canandaigua Lake, New York, with the ontogeny of twenty species. Ann. Carnegie Mus., 3: 79-177.

Rickard, L. V. 1975. Correlation of the Devonian rocks in New York State. N.Y. Mus. Sci. Serv., Map & Chart Ser. No. 24.

Rickard, L. V. 1981. The Devonian system of New York, p. 5-21. *In* Devonian Biostratigraphy of New York, W. A. Oliver, Jr. and G. Klapper, Eds. International Union of Geological Sciences Subcommission on Devonian Stratigraphy.

Rickard, L. V. 1984. Correlation of the subsurface Lower and Middle Devonian of the Lake Erie region. Geol. Soc. Amer. Bull., 95: 814-828.

Rohlf, F. J., and Archie, J. W. 1984. A comparison of Fourier methods for the description of wing shape in mosquitoes (Diptera: Culicidae). Syst. Zool., 33: 302-317.

Rollins, H. B., Eldredge, N., and Linsley, R. M. 1972. Paleontological problems of the Hamilton Group (Middle Devonian). NY State Geol. Assn., 44th Ann. Mtg., Guidebook, p. F1-F28.

Rounds, T. R., Jr., 1982. Dinoflagellate biostratigraphy and organic- walled phytoplankton cyst paleoecology of the Demopolis-Ripley transition interval from the Upper Cretaceous Selma Group of Mississippi and Alabama. M.S. Thesis, Virginia Polytechnic Institute and State University, Blacksburg, VA. 612 pp.

Rudwick, M. J. S. 1970. Living and Fossil Brachiopods. Hutchinson and Co. Ltd., London. 199 pp.

SAS Institute. 1988. SAS/STAT User's Guide, Release 6.03 Edition. Cary, N.C. 1028 pp.

Sanford, B. V. 1967. Devonian of Ontario and Michigan, p. 973-999. *In* International Symposium on the Devonian System, Proc. I, Calgary, Alberta, 1967, D. H. Oswald, Ed. Alberta Soc. Petroleum Geol., vol. 1.

Scheltema, R. S. 1982. Dispersal of marine invertebrate organisms: paleobiogeographic and biostratigraphic implications, p. 73-108. *In* Concepts and Methods of Biostratigraphy, E. G. Kauffman and J. E. Hazel, Eds. Dowden, Hutchinson and Ross, Stroudsburg, PA.

Schumann, D. 1967. Die lebensweise von *Mucrospirifer* Grabau, 1931 (Brachiopoda). Palaeogeogr. Palaeoclimatol. Palaeoecol., 3: 381-392.

Schwarcz, H. P., and Shane, K. C. 1969. Measurement of particle shape by Fourier analysis. Sedimentology, 13: 213-231.

Scotese, C. R., and McKerrow, W. S. 1990. Revised World maps and introduction, p. 1-21. *In* Palaeozoic Palaeogeography and Biogeography, C. R. Scotese and W. S. McKerrow, Eds. Geol. Soc. Mem. No. 12.

Scott, G. H. 1980. The value of outline processing in the biometry and systematics of fossils. Palaeontology, 23(4): 757-768.

Sevon, W. D., and Woodrow, D. L. 1985. Middle and Upper Devonian stratigraphy within the Appalachian basin, p. 1-7. *In* The Catskill Delta, D. L. Woodrow and W. D. Sevon, Eds. Geol. Soc. Amer. Spec. Pap. 201.

Shaffer, B. L., and Wilke, S. C. 1965. The ordination of fossil communities; an approach to the study of species interrelationships and communal structure. Pap. Mich. Acad. Sci. Arts Lett., L: 199-214.

Shimer, H. W. and Grabau, A. W. 1902. Hamilton Group of Thedford, Ontario. Bull. Geol. Soc. Amer., 13: 149-186.

Sneath, P. H. A., and Sokal, R. R. 1973. Numerical Taxonomy. Freeman, San Francisco. 573 pp.

Stanley, S. M., and Yang, X. 1987. Approximate evolutionary stasis for bivalve morphology over millions of years: a multivariate, multilineage study. Paleobiology, 13(2): 113-139.

Stewart, G. A. 1927. Fauna of the Silica Shale of Lucas County. Geol. Surv. Ohio, 4th Ser., Bull. 32: 1-76.

Stumm, E. C. 1956. A revision of A. W. Grabau's species of *Mucrospirifer* from the Middle Devonian Traverse Group of Michigan. Contrib. Mus. Paleontol. Univ. Mich., 9(1): 1-44.

Templeton, A. R. 1980. The theory of speciation via the founder principle. Genetics, 94: 1011-1038.

Thayer, C. W. 1981. Ecology of living brachiopods, p. 110-126. *In* Lophophorates, T. W. Broadhead, Ed. Univ. Tenn., Dept. Geol. Sci. Studies in Geol. 5.

Tillman, J. R. 1964. Variation in species of *Mucrospirifer* from Middle Devonian rocks of Michigan, Ontario, and Ohio. J. Paleontol., 38(5): 952-964.

Waters, J. A. 1977. Quantification of shape by use of Fourier analysis: the Mississippian blastoid genus *Pentremites*. Paleobiology, 3: 288-299.

Wei, K-Y., and Kennett, J. P. 1988. Phyletic gradualism and punctuated equilibrium in the late Neogene planktonic foraminiferal clade *Globoconella*. Paleobiology, 14(4): 345-363.

White, M. J. D. 1978. Modes of Speciation. Freeman, San Francisco. 455 pp.

Whittaker, R. H. 1973. Ordination and Classification of Communities, Part V. Handbook of Vegetation Science. Dr. W. Junk, The Hague. 737 pp.

Woodrow, D. L., Fletcher, F. W., and Ahrnsbrak, W. F. 1973. Paleogeography and paleoclimate at the deposition sites of the Devonian Catskill and Old Red facies. Geol. Soc. Amer. Bull., 84: 3051-3064.

Younker, J. L., and Ehrlich, R. 1977. Fourier biometrics: harmonic amplitudes as multivariate shape descriptors. Syst. Zool., 26: 336-342.

Zar, J. H. 1984. Biostatistical Analysis. 2nd ed. Prentice-Hall, Englewood Cliffs. 718 pp.

Appendix A. Locality register.

N02
LOCATION: Hennaberry Rd., north of junction with Pratt Falls Rd., 100 ft uphill from yellow brick house on west side. Stop 8 of Brower et al. (1978). Pompey, Onondaga Cty.
GEOLOGY: Otisco Member, Ludlowville Formation.

N03
LOCATION: Sweet Rd., 0.3 mi north of junction with Burke Rd. Stop 9 of Brower et al. (1978). Pompey, Onondaga County.
GEOLOGY; Centerfield Member, Ludlowville Formation.

N04
LOCATION: Cedar St. (Madison County 101), 2.6 mi north of US 20. Stop 1 of Rollins et al. (1972). Village of Morrisville, town of Eaton, Madison County.
GEOLOGY: Pecksport Member, Marcellus Formation (Brett, pers. comm., 1986).

N05
LOCATION: Soule Rd. From US 20 in Morrisville turn south onto Eaton St. Bear right at junction (103) toward village of West Eaton. Turn left onto NY 26 and take for 0.7 mi to Bradley Brook Rd. Take Bradley Brook Rd. south for 1.5 mi to Soule Rd. Stop 2 of Rollins et al. (1972). Village of Pierceville, town of Lebanon, Madison County.
GEOLOGY: Lower Windom Member, Ludlowville Formation (Brett, pers. comm., 1986).

N06
LOCATION: Deep Spring Rd. From US 20 in Morrisville, turn south onto Eaton St. Bear right at junction (103) toward village of West Eaton. Turn left onto NY 26 and take for 0.7 mi to Bradley Brook Rd. Take Bradley Brook Rd. south for 2.6 mi to village of Lebanon, turn left and go 0.7 mi to Reservoir Rd. Go another 0.9 mi to Deep Spring Rd. Turn right and go 1.1 mi to outcrop on right. Stop 3 of Rollins et al. (1972). Village of Lebanon, town of Lebanon, Madison County.
GEOLOGY: Lower Windom Member, Ludlowville Formation (Brett, pers. comm., 1986).

N07
LOCATION: No. 4 Rd., south of Pompey Center. From US 20 at Pompey Center, take Pompey Center Rd. south to No. 4 Rd. Go east on No. 4 Rd. to borrow pit. From Eldredge (1972). Town of Pompey, Onondaga County.
GEOLOGY: Pompey Member, Skaneateles Formation.

N10
LOCATION: Robert's Rd., near village of West Eaton. From US 20 in Morrisville, go south on Eaton St., bear right at fork (103) and take to West Eaton. Go left (west) on NY 26 to branching road (NY 52) and bear right. Take 1.1 mi to Robert's Rd. Go 0.8 mi on Robert's Rd. to quarry. From Eldredge (pers. comm., 1986). Town of Eaton, Madison County.
GEOLOGY: Ludlowville Formation

N11
LOCATION: Bishop Rd. From US 20 in Madison, turn south on Solsville Rd. (Lake Moraine Rd.), bear right at Y (Frederick Rd.), and turn right at Bishop Rd. (0.8 mi from US 20). Go 1.3 mi to quarry on left. From Eldredge (pers. comm., 1986). Town of Madison, Madison County.
GEOLOGY: Butternut Member, Skaneateles Formation.

N13
LOCATION: On side road off US 80 in community of 5-Mile Point near Cooperstown. Second left going north from 3-Mile Point. "5-Mile Point" cited by Fisher (1970), but no specifics given.
GEOLOGY: Otsego Shale, Marcellus Formation.

N16
LOCATION: Cole Hill Rd. (Albany County Rt. 2), Berne. Take NY 443 south from intersection with NY 30 just past Schoharie. Go 2.6 mi from intersection of NY 443 with NY 156. From Fisher (1970).
GEOLOGY: Otsego Shale, Marcellus Formation.

N17
LOCATION: Gridley Hill Rd., near Middleburgh. Go 2.2 mi on NY 145S from intersection of NY 145S and NY 30N in Middleburgh. Turn left, go 0.4 mi, and then turn right onto Gridley Hill Rd. Quarry is 0.2 mi on left.
GEOLOGY: Otsego Member, Marcellus Formation (Brett, pers. comm., 1986).

N18
LOCATION: Lafayette Rd., Lafayette. From US 20 in Lafayette, turn northwest onto Lafayette Rd. Roadcut is 0.2 mi on left. From Grasso (1970, 1978).
GEOLOGY: Otisco Member, Ludlowville Formation.

N19
LOCATION: NY 80, 0.7 mi south of junction with US 20 near Lafayette. Also is 7.0 mi west of junction of US 11 and US 20 in Lafayette. Known as Lord's Hill. From Grasso (1970).
GEOLOGY: Portland Point Member, Moscow Formation.

N20
LOCATION: US 11N, near Tully. Roadcut is 0.3 mi north of junction of NY 80 and US 11. From Grasso (1970).
GEOLOGY: Upper Windom Member, Moscow Formation.

N22
LOCATION: Portland Point Rd. From Ithaca, take NY 34 to junction with NY 34B. Take NY 34B toward King Ferry for 0.7 mi to Portland Point Rd. For N22A-C go to end of road and walk north up the railroad tracks. Locality N22D is roadside quarry 1.4 mi from junction with 34B. From Patchen and Dugolinsky (1978) and Grasso (1970).
GEOLOGY: Otisco Shale (N22A) and Ivy Point Siltstone (N22B, N22C, N22D), Ludlowville Formation (Brett et al., 1986).

N25
LOCATION: Railroad cut off Francis Rd., near East Bethany. From junction of US 20 and NY 63 go 2.7 mi on NY 63 (northwest). Turn left (west) onto Paul Rd. at edge of settled area. Pass Bethany Center Rd. at 1.5 mi. Pavement ends at 1.8 mi. Road ends at 2.9 mi. Turn left onto Francis Rd. Go 0.6 mi to bridge overpass. From NYGSA (1956).
GEOLOGY: Ledyard-Wanakah Members, Ludlowville Formation.

N26
LOCATION: Little Beard's Creek, near Leicester. At junction of US 20A/NY 39 and NY 36 in Leicester, turn north (right) onto NY 36. Go 0.8 mi on NY 36 to Kingston Rd. and trailer park on right. Turn right onto Kingston Rd. and go 0.4 mi to end of road. Walk to creek and down creek to cliff. From Grasso (1981).
GEOLOGY: Lower Windom Shale, Moscow Formation.

N27
LOCATION: Jaycox Run, near Geneseo. At junction of US 20/NY 5 and NY 39 turn south onto NY 39. Turn right (west) at Nations Rd. and go 1.1 mi to old railroad embankment. This locates you at the bottom of the section. From Grasso (1981). Alternatively, to begin at the top of the section, go 6.5 mi down NY 39S and park on right. Section exposed in stream 0.25 mi west of road. From NYGSA (1956).
GEOLOGY: Wanakah Shale, Ludlowville Formation.

N31
LOCATION: Piarist Fathers Home, Lakeshore Dr., near Wanakah, on Lake Erie shore. Go south on US 5 to Wanakah, then 1.2 mi to traffic light and turn right onto Lakeshore Dr. Go 3.4 mi and turn right at sign for Piarist Fathers just past The Bluffs. Permission from the Piarist Fathers is necessary to collect from the cliff face. From Eldredge (pers. comm., 1986) and Patchen and Dugolinsky (1978).
GEOLOGY: Wanakah Shale, Ludlowville Formation.

N33
LOCATION: Bridge over Cazenovia Creek, Northrup Rd., Spring Brook. At junction of US 20/NY 78 (Transit Rd.) and NY 16 (Seneca St.), take NY 16S for 0.8 mi to junction with Northrup Rd. Go right on Northrup for 0.2 mi to bridge. From Eldredge (pers. comm., 1986) and Brett (1974).
GEOLOGY: Upper Wanakah Shale, Ludlowville Formation.

NY34
LOCATION: Roadcut on NY 38, Cascade, just past Moravia on west side of Owasco Lake. From Brett et al. (1986).
GEOLOGY: Upper Otisco Shale (N34A) and Ivy Point Siltstone (N34B-G), Ludlowville Formation.

N35
LOCATION: King Ferry, on Cayuga Lake. From junction of NY 34B and NY 90 continue west on NY 90 for 1.0 mi to junction of NY 90 and Clearview Rd. Turn west onto Clearview Rd., south of Triangle Diner. Take 1.7 mi to the lakeshore access road. Elmwood Point is exposed 0.6 mi north of junction near dead end sign. Bloomer bed is exposed 1 mi south of junction at end of road. From Brett et al. (1986).
GEOLOGY: Lower Wanakah Member (Elmwood Point) (N35A) and Upper Wanakah Member (Bloomer Creek Bed) (N35B), Ludlowville Formation.

O01A
LOCATION: Hungry Hollow shale pit. At traffic light at 7/79 in Arkona, turn east onto Lambton County Rd. 12 and go 2 mi to road on left (north) (sign for Hungry Hollow preceeds road). Turn left and go 0.5 mi to bridge. Turn left (west) before bridge and follow road to pit on south side of Ausable River. West Williams Township. From NYGSA (1956).
GEOLOGY: Arkona Shale.

O02A
LOCATION: Hungry Hollow, property of Bob Austin, shale pit and banks on north side of the Ausable River. At traffic light at 7/79 in Arkona, turn east onto Lambton County Rd. 12 and go 2 mi to road on left (N) (sign for Hungry Hollow preceeds road). Turn left and go 0.5 mi to bridge. Cross bridge and turn left (west) and go to "Keep Out" sign. Park and proceed to bank and shale pit. West Williams Township.
GEOLOGY: Arkona Shale (O02A) and Widder Formation (O02C).

O04
LOCATION: Rock Glen Falls, Rock Glen Conservation Area. Go north from traffic light in Arkona on 7/79 for 0.9 mi. Turn right (east) at sign for Rock Glen Conservation Area. Go 2 mi to Conservation Area on left. Follow trail to falls. From NYGSA (1956).
GEOLOGY: Lower Widder Formation.

O05
LOCATION: Mystery Falls. At traffic light at 7/79 in Arkona, turn east onto Lambton County Rd. 12. Go 2 mi to road on left (north) (sign for Hungry Hollow preceeds road). Turn left, go past bridge over Ausable, past entrance to Bob Austin's shed, for 2.6 mi. Turn left onto dead end road and go 1.3 mi. Park and walk across field to trees, go down to river, walk downstream to falls (Hungry Hollow Formation). West Williams Township, Middlesex County.
GEOLOGY: Lower Widder Formation.

M01
LOCATION: Dundee Cement Co. (formerly Penn Dixie Cement Corp. and Petoskey Portland Cement Co. before that). Large quarry near shore of Little Traverse Bay off US 31 west of Petoskey. Locality 34-6-3S of Kesling et al. (1974). Emmet County.
GEOLOGY: Gravel Point Formation.

M03
LOCATION: North Allis Highway. From Junction of M68 and M211 in Onaway, take M211 north for 3.6 mi. Turn right (east) onto North Allis Highway and go 1.4 mi. Small roadcut is on right. Approximately locality 35-2E-21N-NE of Kesling et al. (1976). North Allis Township, Presque Isle County.
GEOLOGY: Lower Genshaw Formation.

M08
LOCATION: Ledges below Tower Dam. From M33 and M68 in Tower, turn north at junction with Barclay Rd. Go 0.6 mi on Barclay and turn right just after bridge over creek. Follow road to dam. Locality 34-1E-3C of Kesling et al. (1976). Forest Township, Cheboygan County.
GEOLOGY: Lower Genshaw Formation.

M11
LOCATION: Rainy River Falls, near Onaway. Take M68 west from Onaway and turn north onto Porter Rd. Take Porter Rd. for 2.1 mi. Turn left (west) onto Twin School Highway and go until it ends (0.5 mi). Walk down path to falls. Locality 35-2E-35N-NW of Kesling et al. (1976). North Allis Township, Presque Isle County.
GEOLOGY: Lower Genshaw Formation.

M12
LOCATION: Grand Lake Rd. From Alpena go 8.5 mi north on US 23 to Grand Lake Rd. Turn right and go 1.8 mi to roadcut in ditch on right (east) side of the road. Locality 33-8-35NW of Ehlers and Kesling (1970). Presque Isle County.
GEOLOGY: Lower Genshaw Formation.

M13
LOCATION: Rockport Quarry, near Rockport on Thunder Bay. From Alpena go 8 mi north on US 23. Turn right (east) onto Rockport Rd. (sign for public access at junction). Go 3.5 mi to quarry. Locality 32-9-6NW of Ehlers and Kesling (1970). Alpena County.
GEOLOGY: Bell Shale.

M14
LOCATION: Long Lake Rd. From Alpena go 6 mi north on US 23. Turn left (west) at junction with Long Lake Rd. Take Long Lake Rd. 0.6 mi. Ditch by roadside is not visible from car, by 7770 Long Lake Rd. Locality 32-8-22NE from Ehlers and Kesling (1970). Alpena County.
GEOLOGY: Lower Genshaw Formation.

M15
LOCATION: Huron Portland Cement Co. Quarry, Alpena. Take US 23 north to 2nd Ave. Turn right (northeast) onto 2nd Ave. and take to Hueber. Turn right (southeast) onto Hueber and take to Ford. Take Ford to plant. Locality 31-8-13W of Ehlers and Kesling (1970). Alpena County.
GEOLOGY: Genshaw Formation.

M16
LOCATION: Grand Lake Rd., near Hincka. At junction of US 23 and M65, turn south onto M65. Take M65 for 4.5 mi to Grand Lake Rd. Take Grand Lake Rd. for 0.7 mi to small exposures on each side of the road. Locality 33-6-9NNW of Ehlers and Kesling (1970). Presque Isle County.
GEOLOGY: Killians Member, Genshaw Formation.

M17
LOCATION: County 451. From US 23N about 5 mi south of Rogers City, at junction with East Heythaller, turn east onto East Heythaller Rd. Go 1.5 mi to junction with M451. Take M451 south for 1.9 mi to roadcut on both sides of road. Locality 34-S-8E of Ehlers and Kesling (1970). Presque Isle County.
GEOLOGY: Lower Genshaw Formation.

M19
LOCATION: M65. From junction of US 23 and M65, turn south onto M65. Take M65 2.5 mi to just south of junction with Lake Augusta Highway. Outcrop is on right. Locality 34-6-33NE of Ehlers and Kesling (1970). Presque Isle County.
GEOLOGY: Lower Genshaw.

M20
LOCATION: 4-Mile Dam, outcrop on south side of Thunder Bay River directly below dam. From M32 in Alpena go west to junction with Lake Winyah Rd. Turn right (north) onto Lake Winyah Rd. and take for 2.0 mi to where road turns left. Go straight and drive down below dam. Locality 31-8-7C of Ehlers and Kesling (1970). Alpena County.
GEOLOGY: Norway Point Formation.

M23
LOCATION: Long Lake Rd. From Alpena take US 23 north for 6 mi to Long Lake Rd. Turn left (northwest) onto Long Lake Rd. and take for 4.4 mi to just past Rennsbury Rd. across from 10343. Roadcut and ditch is on left. Locality 32-8-5SW of Ehlers and Kesling (1970). Alpena County.
GEOLOGY: Lower Genshaw.

M24
LOCATION: US 23 just north of junction with M65. Outcrop is on both sides of the road. Locality 34-6-16E of Ehlers and Kesling (1970). Presque Isle County.
GEOLOGY: Lower Ferron Point Formation.

D01
LOCATION: LaVale. Take exit 40 off US 40 at Vocke Rd. Continue on road between the State Police Headquarters and National Jet Corp to outcrop. From Eldredge (pers. comm., 1986).
GEOLOGY: Upper Mahantango Formation.

D02
LOCATION: Near Keyser, WVA. Take US 220 south from Cumberland, and turn left (east) on 21st Lane at hill where southbound lane doubles, about 1 mile north of Keyser, WVA. Go 0.6 mi to railroad tracks. Outcrop is just south of crossing. From Eldredge (pers. comm., 1986).
GEOLOGY: Upper Mahantango Formation.

W01
LOCATION: Romney, 0.5 mi north of junction of US 50 and WVA 28 on WVA 28. From Eldredge (pers. comm., 1986).
GEOLOGY: Lower Mahantango Formation.

P05
LOCATION: Weissport, on the Lehigh Canal. In Weissport take Long Run Rd. north just past Nathan's Hamlet on the left and Ray and Shirl's Tavern on the right to a dirt road that leads downhill to the river. Walk downhill 700 ft to the excavated area. From Hoskins et al. (1983). Carbon County.
GEOLOGY: "Centerfield Fossil Zone," Mahantango Formation.

P07
LOCATION: Deer Lake, 11 mi south of Pottsville. (A) An an abandoned borrow pit on west side of PA 61, 200 ft north of junction of PA 61 and PA 895. (B) An active pit 0.25 mi further north, also on west side of PA 61. From Hoskins et al. (1983). Schuylkill County.
GEOLOGY: Upper Mahantango Formation.

P09
LOCATION: Dalmatia, eastern side of Susquehanna River. From intersection of PA 147 and PA 225 take PA 147 west 1.85 mi to borrow pit. Pit is on south side of PA 147, 2.5 mi northeast of Dalmatia, Lower Mahanoy Township. From Hoskins et al. (1983). Northumberland County.
GEOLOGY: Upper Mahantango Formation.

P10
LOCATION: Newport. Shale pit owned by Harry B. Lesh on southeast side of PA 34, 1 mi southwest of Newport and 500 ft south (behind) Swartz's Car Wash. From Hoskins et al. (1983). Perry County.
GEOLOGY: Upper Mahantango Formation.

P14
LOCATION: Girty's Notch. Roadcut on US 15 on western side of Susquehanna River, 6 mi north of intersection of US 15 with US 22 at Amity Hall. From Ellison (1965).
GEOLOGY: Upper Shale Member, Mahantango Formation.

P15
LOCATION: Millerstown. Railroad cut on western side of the Juniata River. Take PA 17 across the river, then the first right to the road that parallels the railroad. Park at intersection of road paralleling the river and Sugar Run Rd. From Ellison (1965).
GEOLOGY: Montebello Member, Mahantango Formation.

P17
LOCATION: Chaneysville. Take Chaneysville Rd. from US 40 to PA 326 to the roadcut by the Forest Foreman Headquarters. From Ellison (1965).
GEOLOGY: Chaneysville Siltstone, Mahantango Formation.

Appendix B. Fourier-transformed data for harmonics 0, 2, 4, and 6 for all specimens.

SPECIMEN	HAR0	HAR2	HAR4	HAR6	SPECIMEN	HAR0	HAR2	HAR4	HAR6
N0201	24.16359	2.27073	0.25478	0.37080	N0402	27.75351	2.48518	0.68499	0.48817
N0202	26.96457	2.06835	0.27592	0.31981	N0403	32.08017	3.37071	1.49611	0.49366
N0203	23.87924	2.01951	0.78945	0.17169	N0404	27.34125	2.34812	0.94787	0.24442
N0204	21.02391	1.89632	0.83908	0.27212	N0405	30.31633	3.24526	1.43760	0.49829
N0205	26.82057	1.93910	0.41218	0.17330	N0406	37.22209	3.51938	1.51856	0.79623
N0206	24.32735	1.63902	0.31469	0.25239	N0407	25.95355	2.38216	1.12212	0.53599
N0207	26.36563	1.75068	0.58838	0.21184	N0408	34.32524	2.87882	1.04441	0.59077
N0208	24.38412	2.45387	0.26883	0.24718	N0409	19.52119	1.63952	0.89603	0.17879
N0209	26.83710	1.51859	0.69357	0.65292	N0410	29.15456	3.70731	1.73582	0.69667
N0210	26.07710	1.03213	0.38772	0.05415	N0411	21.96414	2.08844	1.16340	0.30250
N0211	24.77509	1.58762	0.52402	0.13343	N05A01	27.99866	3.33877	0.86548	0.26499
N0212	25.96721	2.33894	0.68796	0.51407	N05A02	19.55957	1.58998	0.83776	0.32620
N0213	28.91147	2.70684	0.77472	0.44688	N05A03	20.20857	1.98065	0.50357	0.13407
N0214	25.12004	1.95345	0.82082	0.24548	N05A04	21.52409	2.12738	0.18151	0.22011
N0215	25.67535	1.71720	0.61023	0.25911	N05A05	19.62546	2.31463	0.40523	0.06591
N0216	28.23868	2.50143	0.72007	0.45536	N05A06	21.84557	2.73801	0.71477	0.35766
N0217	26.01167	2.00258	0.39219	0.31382	N05A07	23.74098	1.67121	1.31037	0.31433
N0218	26.81294	1.24462	0.49896	0.29856	N05A08	27.02168	2.75237	0.72414	0.15420
N0219	25.16698	2.06977	0.70895	0.37664	N05A09	31.34470	2.21135	0.81468	0.26433
N0220	36.04109	3.62653	0.97393	0.41703	N05A10	23.96237	1.66214	0.56903	0.39203
N0221	27.23788	2.88354	0.90210	0.44645	N05A11	24.73346	2.08541	0.83241	0.27251
N0222	27.54468	2.30345	0.73515	0.23465	N05A12	29.09286	2.74698	1.11179	0.70509
N0223	21.54939	2.05460	0.08779	0.32732	N05A13	26.23103	1.86340	0.61384	0.50868
N0224	20.66286	1.45350	0.31170	0.36967	N05A14	20.66360	1.96789	0.86561	0.06853
N0225	25.00546	2.12152	0.50126	0.39660	N05A15	33.43164	3.64198	0.99956	0.45996
N0301	25.14665	2.20758	0.90077	0.38024	N05A16	29.92224	3.07389	0.77299	0.64861
N0302	27.40991	1.69827	1.22516	0.84396	N05A17	24.17950	2.48289	0.88162	0.33932
N0303	30.66864	2.02470	0.59819	0.41576	N05A18	28.19505	2.69562	0.63636	0.36722
N0304	30.08345	3.20163	1.10923	0.63892	N05A19	28.58569	1.98893	0.96685	0.41369
N0305	26.28751	1.63318	0.49736	0.60703	N05A20	26.72197	2.33352	0.96838	0.56554
N0306	25.77234	1.50023	0.33410	0.48717	N05B01	18.44789	1.59232	0.52434	0.28022
N0307	25.46307	1.81503	1.04417	0.53005	N05B02	23.97687	1.66861	0.23025	0.31619
N0308	27.20250	1.76479	0.61865	0.61816	N05B03	25.50491	2.69684	0.95092	0.38871
N0309	27.38832	2.00921	0.17830	0.45704	N05B04	26.18071	1.97724	1.26398	0.51162
N0310	25.00667	1.46107	0.69616	0.49425	N05B05	23.35010	1.69857	0.61214	0.20923
N0311	28.16022	1.81542	0.78714	0.30392	N05B06	21.49870	1.68509	0.26258	0.25966
N0312	25.19604	1.72321	0.69463	0.31121	N05B07	25.82350	2.31006	0.92804	0.25913
N0313	23.65430	2.03807	0.19297	0.51434	N05B08	26.16280	2.59630	0.73950	0.42025
N0314	27.50592	2.09334	0.19530	0.67984	N05B09	27.92575	2.27597	0.21333	0.32275
N0315	26.59338	1.99614	0.89721	0.58625	N05B10	22.20776	0.94181	0.24412	0.03948
N0316	24.07788	2.29977	0.61079	0.55106	N05B11	24.35454	1.85036	0.62234	0.18098
N0317	30.66286	2.54309	0.19438	0.53935	N05B12	25.86946	1.74266	0.70568	0.57838
N0318	25.91516	3.06317	0.95881	0.72418	N05B13	19.79021	0.82680	0.17520	0.35405
N0319	25.58365	2.05118	0.53734	0.54231	N05B14	17.92577	1.73649	0.51734	0.12300
N0320	23.78717	2.03515	1.07978	0.41126	N0601	26.68759	2.12332	0.72676	0.04983
N0321	25.53601	1.77791	1.05160	0.36668	N0602	29.60300	2.04915	0.62795	0.01025
N0322	24.93060	1.03997	0.56493	0.18535	N0603	19.44214	1.76516	0.00332	0.24816
N0401	28.93471	2.80550	1.23619	0.39853					

SPECIMEN	HAR0	HAR2	HAR4	HAR6	SPECIMEN	HAR0	HAR2	HAR4	HAR6
N0604	25.15652	2.11001	0.69745	0.20226	N1116	27.82904	0.28750	0.11232	0.21535
N0605	27.38673	2.50758	0.67433	0.34888	N1117	23.41855	0.48690	0.41802	0.01844
N0606	21.27376	1.32758	0.44289	0.09553	N1118	22.94983	1.06090	0.13325	0.13263
N0607	26.29892	1.36535	0.72213	0.01227	N1119	19.96516	1.17119	0.66747	0.38407
N0608	26.56735	0.84870	0.06037	0.11559	N1120	26.01215	1.54738	0.05730	0.37238
N0609	29.16969	1.75107	0.35342	0.23843	N1121	19.13022	1.39342	0.49212	0.40301
N0610	22.05251	1.98399	0.46490	0.31547	N1122	24.29427	1.83566	0.61833	0.39422
N0611	28.28552	0.97303	0.48595	0.00665	N1301	26.81920	0.84580	0.00794	0.53403
N0612	27.29214	1.89169	0.62297	0.18063	N1302	28.97406	0.38282	0.33435	0.16623
N0613	25.26213	1.86309	0.73297	0.20664	N1303	22.42424	0.20436	0.67470	0.26412
N0614	19.22078	1.23600	0.35307	0.25062	N1304	27.18457	2.40256	0.22895	0.15051
N0615	20.87903	1.61584	0.39838	0.31489	N1305	19.98312	0.09541	0.25383	0.10060
N0701	29.21587	1.61038	1.09274	0.35706	N1306	16.88931	0.76824	0.20760	0.13661
N0702	25.51653	3.17497	1.11295	0.56963	N1307	33.03197	1.66493	0.54118	0.86918
N0703	27.21361	3.15513	1.52467	0.49234	N1308	25.29739	1.34540	0.21752	0.41667
N0704	25.54434	2.93748	0.66328	0.59077	N1309	25.15712	0.99313	0.00444	0.40819
N0705	24.98802	2.07998	0.98616	0.25740	N1601	29.10069	4.72026	1.72816	1.06805
N0706	24.88205	2.16353	1.39814	0.65791	N1701	40.28041	6.78907	2.98484	1.37328
N0707	26.18610	1.08904	0.93672	0.13507	N1702	35.98882	5.38012	2.12533	1.12358
N0708	24.50999	1.04316	0.62986	0.08749	N1703	31.48521	4.18944	1.48314	0.74692
N0709	23.21136	1.96916	0.72893	0.18553	N1704	31.68365	4.78137	1.86639	0.59127
N0710	22.29771	1.67609	0.62019	0.24613	N1705	29.23508	3.35233	1.45554	0.59049
N0711	23.65399	1.92820	1.00055	0.29441	N1706	37.48099	3.87354	1.53926	0.75766
N0712	26.69708	2.07394	0.80097	0.53482	N1707	30.60519	4.08896	1.84656	0.65331
N0713	23.32355	1.24145	0.64132	0.15463	N1708	32.43300	6.41894	2.00540	1.21154
N0714	20.25383	1.90899	0.71992	0.19047	N1709	34.00323	4.87560	1.12402	0.86242
N0715	25.82730	2.69135	0.68035	0.63494	N1710	29.78415	3.63717	1.89599	0.55133
N0716	25.39067	2.50706	0.59673	0.34042	N1711	32.70712	4.84217	1.59325	0.63981
N0717	27.80998	1.95385	0.89986	0.48331	N1712	34.10512	4.03608	1.70494	0.68279
N0718	24.60699	2.62572	0.60089	0.56664	N1713	34.87823	5.81977	2.16946	0.96689
N1001	22.55905	1.73958	0.66915	0.29272	N1714	30.16920	3.53466	0.85070	0.82050
N1002	25.77240	3.08339	0.70425	0.50963	N1715	38.52344	5.68451	2.92321	0.94239
N1003	20.78923	1.37494	0.45944	0.33667	N1716	29.85716	3.95124	1.52449	0.69305
N1004	29.15164	2.43481	1.08339	0.26336	N1717	31.90643	3.70679	1.42309	0.73664
N1005	28.00648	2.63824	1.15896	0.21390	N1718	28.87221	2.58181	1.55305	0.46357
N1006	26.17548	1.40603	0.81872	0.26495	N1719	28.72650	3.29895	1.00532	0.73305
N1007	29.46832	2.02504	1.00142	0.24066	N1720	38.34442	4.15819	1.56566	1.21281
N1008	28.55992	2.46872	0.92774	0.60949	N1721	30.65269	4.16279	1.48966	0.63104
N1009	25.69749	2.40952	1.15912	0.25943	N1722	32.03107	4.70787	1.55812	0.57246
N1010	23.73264	2.01222	0.99735	0.24172	N1723	35.86339	5.31092	1.97407	0.83112
N1011	19.98895	1.51870	0.44883	0.10879	N1724	31.89453	5.09750	1.84942	0.85696
N1012	30.88770	1.58286	0.59552	0.37653	N1801	26.62482	2.09058	1.16960	0.22369
N1013	22.78561	1.40362	0.70939	0.32911	N1802	18.18416	1.02699	0.54926	0.28308
N1014	24.20143	1.70281	0.52564	0.02429	N1803	17.48230	1.57666	0.47124	0.15049
N1015	27.28021	2.32608	0.47126	0.72279	N1804	19.23387	1.30433	0.42984	0.26800
N1016	24.93658	2.08206	0.99748	0.47270	N1805	34.68573	3.36187	1.34068	0.37075
N1017	31.64139	2.76083	1.08324	0.15579	N1806	35.08450	4.13777	1.11639	0.66428
N1018	24.83281	2.52317	0.64120	0.74559	N1807	30.18126	3.45550	1.33368	0.50135
N1019	23.19449	0.84814	0.66424	0.11359	N1808	26.16425	3.55711	0.87804	0.31546
N1020	22.06564	0.96932	0.06869	0.32242	N1809	23.66859	3.29955	1.22290	0.34886
N1021	23.83635	2.85734	1.22783	0.36745	N1810	28.66501	3.99032	1.87640	0.68995
N1022	22.49474	0.97051	0.54065	0.04769	N1811	23.76099	2.34952	0.67709	0.44569
N1023	22.47185	1.68148	0.59685	0.17833	N1812	29.22354	2.19134	0.61388	0.41207
N1024	20.67888	1.36192	0.48588	0.02964	N1813	28.02090	3.29972	1.49977	0.53720
N1101	21.10901	1.50293	0.82483	0.31557	N1814	36.76300	5.24632	1.37858	0.74946
N1102	23.15317	0.90214	0.38000	0.17736	N1815	21.03333	2.49702	0.95057	0.36610
N1103	22.72783	1.58059	0.74080	0.30613	N1816	38.39485	5.76418	1.82731	1.17621
N1104	30.51466	1.82756	0.40968	0.62797	N1817	34.00899	4.35635	1.86767	0.82724
N1105	27.57674	1.96165	0.63967	0.25468	N1901	25.36824	1.96780	0.76011	0.18137
N1106	25.55908	1.18285	0.81250	0.14182	N1902	23.95375	1.96822	0.41628	0.05808
N1107	24.25815	0.81431	0.44303	0.08509	N1903	23.53836	2.02340	0.43697	0.22787
N1108	22.35172	0.91673	0.05264	0.32521	N1904	24.22366	1.18638	0.02738	0.16528
N1109	24.09747	1.54098	0.92168	0.07990	N1905	24.23950	1.85748	0.23516	0.36684
N1110	20.91806	1.41366	0.55102	0.16361	N1906	20.74188	1.00737	0.34556	0.33196
N1111	29.61908	0.67653	0.08968	0.48047	N1907	24.45641	0.90327	0.06920	0.21061
N1112	22.76428	1.11099	0.65307	0.25802	N1908	23.53662	1.99148	0.14245	0.34861
N1113	23.97519	0.70649	0.71861	0.07028	N1909	25.64908	1.40969	0.27438	0.07800
N1114	26.39063	2.43293	0.84407	0.16926	N1910	34.02206	2.41366	0.24988	0.29051
N1115	19.76599	1.23484	0.57871	0.14815	N1911	24.11180	1.44869	0.22760	0.06545

SPECIMEN	HAR0	HAR2	HAR4	HAR6	SPECIMEN	HAR0	HAR2	HAR4	HAR6
N2001	15.27356	0.79947	0.36205	0.03759	N3302	18.84564	0.77503	0.27780	0.14644
N2002	16.78668	0.74884	0.23901	0.08052	N3303	25.40445	0.38987	0.29939	0.33963
N2003	16.23383	0.63199	0.30284	0.23241	N3304	24.55672	0.40820	0.26171	0.43584
N2004	15.14306	0.81838	0.20276	0.02454	N3305	25.39223	0.63854	0.33606	0.03661
N2005	9.99514	0.31264	0.06509	0.06532	N3306	28.48033	0.70933	0.21540	0.47531
N2006	29.19250	2.35823	0.24485	0.43447	N3307	24.84726	0.30274	0.02818	0.24489
N2007	15.76105	0.84541	0.14326	0.09089	N3308	20.04750	0.77913	0.21937	0.25032
N2008	18.01682	0.88619	0.10027	0.16377	N3309	23.11368	0.19880	0.01936	0.06328
N2009	13.34756	1.18111	0.04918	0.13727	N3310	21.55554	0.82136	0.37556	0.12016
N2010	14.90895	0.47445	0.41787	0.07698	N3311	23.99376	0.57003	0.15223	0.15069
N2011	14.40099	1.00391	0.35242	0.28652	N3312	26.86140	0.60099	0.22708	0.32003
N2012	17.99768	1.26102	0.12768	0.38114	N3313	23.31709	0.07358	0.15682	0.16081
N2013	14.59327	0.42101	0.01836	0.05826	N3314	24.31708	1.02202	0.15524	0.33640
N2014	21.61255	0.32901	0.41382	0.12641	N3315	15.50326	0.36869	0.04408	0.14125
N2015	14.22590	0.39129	0.14105	0.28471	N3316	23.81322	0.01811	0.01646	0.13058
N2016	15.97932	1.45729	0.09361	0.08122	N3317	25.23361	0.89144	0.42724	0.25673
N2017	17.39955	1.61071	0.48424	0.09192	N34A01	25.74207	2.75855	0.99864	0.51425
N22A01	22.01099	1.94203	0.30676	0.45305	N34A02	27.36353	2.70288	1.16434	0.56050
N22A02	17.62704	0.80689	0.33915	0.10886	N34A03	21.79271	1.64199	0.68035	0.19301
N22A03	22.15294	1.54641	0.69677	0.15129	N34A04	35.91048	3.99152	0.91096	1.03446
N22B01	29.06830	1.09519	0.13008	0.09710	N34A05	26.24564	1.75398	0.57909	0.35951
N22B02	24.03300	2.01219	0.48904	0.12730	N34A06	31.18063	1.06692	0.01706	0.38910
N22B03	24.29243	1.31095	0.77011	0.23304	N34A07	19.15674	1.26874	0.37694	0.39717
N22B04	21.65118	0.82124	0.20160	0.13307	N34A08	34.16403	2.08495	1.09910	0.46515
N22B05	25.30807	2.14152	0.87102	0.26922	N34A09	27.69519	2.74595	1.10242	0.62026
N22B06	26.56082	1.50613	0.30191	0.18333	N34B01	21.20950	2.22911	0.78883	0.59620
N22B07	29.49461	2.71737	0.51679	0.49537	N34B02	32.10913	1.72989	0.82264	0.22362
N22B08	28.32103	1.57320	0.39986	0.26625	N34B03	18.36578	1.47719	0.76602	0.38074
N22B09	29.60403	1.85307	0.23466	0.33792	N34C01	29.93085	0.81350	0.08582	0.51313
N22B10	25.86269	1.93815	1.00770	0.47189	N34C02	32.95227	1.63591	0.68979	0.26231
N22C01	28.08990	2.86581	1.01845	0.46376	N34C03	37.27974	3.60114	1.16946	0.55509
N22C02	28.07393	3.42655	1.05805	0.55752	N34C04	34.98575	2.34579	0.13376	0.52229
N22D01	31.29907	2.14997	0.63079	0.24085	N34C05	33.86903	2.07607	1.13482	0.45187
N22D02	30.95053	2.83126	0.45816	0.49687	N34C06	23.59537	2.02048	0.48911	0.27862
N22D03	30.62871	0.52299	0.39611	0.42649	N34C07	27.84479	0.27413	0.47614	0.51815
N22D04	24.74893	1.69495	0.19665	0.18920	N34C08	31.98260	1.70736	0.75453	0.37229
N22D05	20.29411	0.93410	0.48714	0.42385	N34C09	31.00941	2.04846	0.86775	0.52633
N22D06	34.00153	1.68807	1.23405	0.42247	N34C10	36.95189	2.09693	0.91840	0.27359
N22D07	28.59821	1.67781	0.47177	0.19330	N34C11	19.98415	0.56890	0.28961	0.09544
N2501	27.00598	1.74420	0.55844	0.03413	N34C12	22.60896	0.86859	0.44178	0.17349
N2502	26.64467	0.93744	0.04098	0.03706	N34C13	21.37758	0.49481	0.55894	0.15584
N2601	25.77473	1.80709	0.21017	0.41053	N34D01	24.45897	1.64425	0.37900	0.13438
N2602	24.13364	2.05125	0.50157	0.32732	N34D02	27.07014	0.63090	0.33079	0.18713
N2701	34.31067	4.04939	1.38129	0.34576	N34D03	25.79756	1.34638	0.07814	0.38377
N2702	36.97273	1.73463	0.15442	0.43146	N34E01	19.06491	1.35587	0.32473	0.13927
N2703	22.76451	1.21283	0.53288	0.03950	N34E02	28.56355	1.67111	0.28476	0.35582
N2704	23.12199	0.65607	0.59259	0.06103	N34F01	30.33398	3.30939	0.71085	0.57585
N2705	36.45142	3.67013	1.37019	0.44115	N34F02	26.67323	1.77400	0.58645	0.29730
N3101	30.15073	1.53384	0.37672	0.19445	N34F03	19.95749	0.05922	0.32660	0.23209
N3102	26.85654	0.60451	0.00035	0.13946	N34F04	29.02119	2.61279	0.73266	0.41701
N3103	32.86829	0.90641	0.01833	0.12205	N34F05	23.56088	1.35062	0.55214	0.38372
N3104	33.15115	0.14281	0.05182	0.27595	N34F06	21.75221	1.16590	0.44597	0.02557
N3105	32.32970	1.06781	0.27236	0.09760	N34G01	34.05049	3.00160	0.86509	0.42928
N3106	28.08817	1.53547	0.18632	0.04741	N34G02	25.96257	0.97651	0.36320	0.30172
N3107	33.24687	0.27637	0.59162	0.21874	N34G03	33.88104	2.02032	0.76123	0.61583
N3108	30.60905	2.05534	0.71558	0.30181	N34G04	21.50612	0.32514	0.51109	0.07794
N3109	30.47043	0.60385	0.32853	0.01718	N34G05	22.57309	1.20541	0.36854	0.41194
N3110	29.10341	0.55472	0.21806	0.35177	N34G06	29.64191	2.14809	1.00207	0.40747
N3111	28.61707	0.26076	0.05244	0.19445	N34G07	25.40790	1.90454	0.65159	0.43069
N3112	29.98027	0.42823	0.21955	0.29020	N34G08	23.72327	1.90350	1.16877	0.49986
N3113	33.13600	1.90279	0.26281	0.05052	N34G09	30.76459	1.48404	1.17215	0.37632
N3114	29.42140	0.26624	0.02662	0.40368	N34G10	27.88524	1.96237	0.80492	0.46510
N3115	33.00598	2.70787	0.65183	0.12138	N35A01	32.32007	2.39678	0.67071	0.16625
N3116	37.57526	1.53720	0.16964	0.27585	N35B01	29.65497	1.71580	0.20588	0.62854
N3117	33.99745	1.64701	0.11230	0.10978	N35B02	17.93599	1.05378	0.28432	0.32722
N3118	27.85629	0.73646	0.06766	0.14160	N35B03	20.61919	0.49363	0.22570	0.18338
N3119	23.50868	1.11698	0.36482	0.06717	N35B04	17.21204	1.09042	0.11751	0.23614
N3120	23.70070	0.42396	0.04229	0.04508	N35B05	16.99408	0.19433	0.49735	0.08804
N3301	20.01436	1.22294	0.40158	0.36012	N35B06	21.71594	0.56302	0.67266	0.25911

SPECIMEN	HAR0	HAR2	HAR4	HAR6	SPECIMEN	HAR0	HAR2	HAR4	HAR6
N35B07	32.15776	1.49749	0.46256	0.32276	O0514	23.06511	1.64831	0.48566	0.26989
N35B08	23.10048	1.28270	0.57909	0.07115	O0515	28.80667	1.79839	0.74421	0.20825
O01A01	35.89130	5.58097	2.18313	0.94758	M0101	28.70709	2.14665	0.91448	0.73754
O01A02	37.34178	5.33531	2.40789	0.92083	M0102	21.97766	1.32456	0.65677	0.34702
O01A03	33.75182	4.91322	1.70939	0.92477	M0103	25.68414	0.91818	0.21411	0.61868
O01A04	28.71417	4.72203	1.91310	0.85497	M0104	23.76048	0.88356	0.59154	0.45410
O01A05	34.23018	4.29035	1.91977	0.93389	M0105	25.97610	1.57354	0.92897	0.68622
O01A06	31.76555	4.31945	1.42404	0.89868	M0106	23.92297	1.92110	0.76745	0.40110
O01A07	32.58818	3.92169	1.27759	0.96296	M0107	29.41103	1.84964	0.41469	0.62188
O01A08	33.50758	5.68793	1.97657	1.12753	M0108	25.04663	1.86243	0.55080	0.48733
O01A09	40.78893	8.17172	2.94818	1.47849	M0109	23.35526	1.46538	0.82386	0.39989
O01A10	37.31505	5.31560	2.51732	1.11695	M0110	25.82347	0.48621	0.50875	0.34863
O01A11	30.89935	5.04570	2.13574	0.98832	M0111	25.02286	2.63152	1.03547	0.48847
O01A12	31.61224	4.58078	1.83890	0.86796	M0112	22.02219	1.02884	0.30672	0.52071
O01A13	40.23386	5.71161	2.10364	1.01588	M0113	24.42393	1.64864	0.80850	0.67685
O01A14	33.25609	2.52734	1.43280	0.96275	M0114	27.20793	0.86611	0.35845	0.33772
O01A15	23.85634	3.06527	1.41748	0.59618	M0115	23.11858	1.12967	0.37849	0.30829
O01A16	31.79916	3.90627	1.88632	0.92846	M0116	19.81018	0.83140	0.15833	0.25864
O01A17	31.41946	3.45064	1.62502	0.69067	M0117	22.53630	2.28685	0.98150	0.66209
O01A18	30.36116	3.63413	1.46914	0.74639	M0118	21.01482	1.24832	0.32194	0.45016
O02A01	32.13591	4.70398	2.09192	1.01325	M0119	22.34535	1.22481	0.49210	0.23863
O02A02	30.66284	4.95224	1.55202	0.83923	M0120	23.70390	1.53687	0.29511	0.39021
O02A03	34.81717	5.49452	2.22859	1.23089	M0301	29.71960	2.69920	1.22434	0.94994
O02A04	37.85051	5.23836	1.97155	0.97768	M0302	33.33243	2.70969	0.83269	0.49711
O02C01	27.23958	2.38849	0.94699	0.51085	M0303	29.00499	2.04262	1.03019	0.64761
O02C02	28.99339	1.37237	1.01088	0.42030	M0304	38.06139	3.15847	1.33029	0.83846
O02C03	20.11108	2.02791	0.54335	0.26673	M0305	26.62515	2.58348	0.63908	0.56263
O02C04	30.02176	1.56488	0.76361	0.55579	M0306	26.78824	1.55474	1.01331	0.47187
O02C05	32.17004	2.14909	0.29148	0.25760	M0307	29.82007	2.25976	0.85531	0.48896
O02C06	23.90675	1.19409	0.62718	0.42821	M0801	29.24272	1.73464	0.93036	0.39647
O02C07	21.38594	2.23418	0.69507	0.34249	M0802	31.40195	2.26473	1.77120	0.66285
O02C08	25.95486	1.28004	0.52379	0.79310	M0803	30.83745	1.76073	1.01542	0.51813
O02C09	27.51083	1.20578	0.21724	0.33942	M0804	33.03793	1.80164	0.78943	0.60722
O02C10	31.72308	1.49187	0.03877	0.40389	M1101	26.95116	2.02413	0.86729	0.66849
O02C11	26.35309	0.57159	0.09545	0.42451	M1102	30.83337	1.97986	1.13335	0.48726
O02C12	31.16577	1.13078	0.03871	0.53576	M1103	28.42482	2.52747	1.13060	0.25456
O02C13	36.12601	0.57641	0.47832	0.39313	M1201	36.46156	1.15276	0.72925	0.56122
O02C14	31.70735	0.58554	0.22882	0.17771	M1202	29.58031	2.76983	1.13580	0.68130
O02C15	31.84229	0.52726	0.34536	0.45391	M1203	31.70839	2.34261	1.28892	0.63997
O02C16	30.93733	0.93944	0.56759	0.27422	M1204	31.88643	2.71825	1.36969	0.62140
O02C17	31.04289	1.29686	0.48304	0.46364	M1205	21.02399	1.16805	0.76562	0.38243
O02C18	21.34903	0.87026	0.37199	0.28927	M1301	27.93204	2.43032	0.94422	0.84147
O02C19	29.87645	0.56515	0.46101	0.39358	M1302	28.37149	2.50966	1.41521	1.01398
O02C20	32.22266	1.09033	0.22918	0.42262	M1303	21.00075	2.30507	0.88903	0.61126
O02C21	31.66338	0.24907	0.33631	0.41717	M1304	18.77481	1.63456	0.78179	0.28411
O02C22	26.74437	1.08358	0.32347	0.40827	M1305	34.58138	2.72872	1.88512	1.19228
O0401	18.84467	1.17354	0.83652	0.43225	M1401	34.12833	0.77370	1.16572	0.07925
O0402	23.03293	1.99793	0.62782	0.27809	M1402	33.90289	1.04174	0.15419	0.52976
O0403	22.21756	1.66662	0.77803	0.18415	M1403	30.98642	1.79472	0.73723	0.19839
O0404	27.60010	2.17122	0.64564	0.27427	M1404	26.92793	0.45733	0.13669	0.35056
O0405	25.25470	1.81819	0.56335	0.31170	M1501	27.82162	1.70580	0.65626	0.56629
O0406	30.01085	1.03631	0.22625	0.36058	M1502	20.98674	1.03862	0.67739	0.26013
O0407	29.64325	1.74131	0.21062	0.32513	M1503	26.11641	0.42331	0.37816	0.15026
O0408	33.33025	1.76857	0.12456	0.46243	M1504	25.77689	0.91342	0.40662	0.42267
O0409	30.78348	1.56083	0.50085	0.39494	M1505	21.08160	0.88746	0.42127	0.52234
O0410	25.51633	1.20960	0.26221	0.23718	M1506	23.25499	0.92902	0.70433	0.61384
O0501	30.99988	2.44963	0.84295	0.39714	M1507	21.38737	0.56726	0.22396	0.19262
O0502	20.91464	0.93781	0.12448	0.21505	M1601	33.97308	2.75367	1.36974	0.53226
O0503	32.28140	1.60860	0.38458	0.56595	M1701	33.84827	1.96082	1.63201	0.69534
O0504	35.17030	1.45112	0.44872	0.20928	M1702	33.49176	2.89119	1.12134	0.67763
O0505	29.91403	0.84372	0.19755	0.29700	M1703	24.63625	2.49701	1.02851	0.35663
O0506	32.22353	1.32779	0.62662	0.41141	M1704	33.96098	3.13787	2.29722	1.01994
O0507	30.19711	1.58022	0.31634	0.09327	M1901	30.77573	2.90138	1.16120	0.33200
O0508	27.33855	0.22010	0.35612	0.00152	M1902	29.84581	0.30116	1.08054	0.19903
O0509	28.96075	0.26816	0.39856	0.42457	M1903	28.67366	1.89729	1.20767	0.31997
O0510	28.85974	1.46175	0.23250	0.15385	M2001	34.96831	3.30702	1.26451	0.69210
O0511	32.71391	1.72763	0.40858	0.59101	M2002	22.55481	1.58162	0.38238	0.32935
O0512	28.55205	2.03363	0.51066	0.35253	M2301	34.24428	2.57352	0.84124	0.51539
O0513	29.29475	0.64415	0.44001	0.30707	M2302	36.97446	1.89709	1.01184	0.66007

SPECIMEN	HAR0	HAR2	HAR4	HAR6	SPECIMEN	HAR0	HAR2	HAR4	HAR6
M2303	24.34085	3.25245	1.19726	0.61830	P0504	21.48068	1.64230	0.60674	0.42640
M2304	33.14467	1.55937	1.48344	0.47924	P0505	18.35333	1.54855	0.60164	0.43713
M2305	30.13457	2.01058	1.06640	0.49627	P0506	33.35120	3.70797	0.59752	0.42531
M2306	32.71896	0.58174	0.83683	0.05035	P0701	23.98827	2.06996	0.79152	0.27674
M2307	33.41310	0.75283	0.33366	0.20125	P0702	31.51103	2.51614	1.11416	0.86711
M2308	26.59297	0.94693	0.82507	0.37918	P0703	25.25246	3.40092	1.10841	0.79638
M2309	28.80936	2.20020	0.61960	0.33217	P0901	30.49062	3.63399	0.54029	0.57453
M2310	25.23750	1.52875	0.57487	0.33222	P1001	25.62042	3.37892	0.94524	0.42880
M2401	29.67659	0.20196	0.34763	0.09838	P1002	25.47327	1.14437	0.39320	0.10129
M2402	27.80858	1.15429	0.28232	0.10637	P1003	21.35280	0.45720	0.04661	0.30074
D0101	18.68640	1.06710	0.45037	0.18721	P1004	19.56680	0.16295	0.35786	0.07727
D0102	25.38080	2.87501	0.94346	0.45535	P1005	22.93916	1.97451	0.37732	0.26664
D0103	34.38499	3.40220	0.58699	0.39529	P1006	15.74839	0.49105	0.16179	0.20708
D0201	29.31160	2.10793	1.07691	0.34049	P1401	26.79102	1.92151	0.26600	0.26491
D0202	25.88332	1.84928	0.73150	0.53367	P1402	24.92712	2.55778	0.70348	0.40594
D0203	26.94611	2.21974	0.84192	0.42004	P1403	27.07892	1.84406	0.21847	0.17748
D0204	24.57492	1.80325	0.30785	0.26684	P1404	26.88150	2.13653	0.61316	0.46004
D0205	17.38321	1.08863	0.41699	0.15954	P1405	23.32805	1.75818	0.06593	0.30887
D0206	26.21681	1.35436	0.79706	0.41595	P1406	31.50989	1.40818	0.67559	0.30947
D0207	28.62749	2.88603	0.94162	0.37349	P1407	23.14267	0.96831	0.37970	0.31725
W0101	25.81577	0.96150	0.47305	0.09236	P1408	24.13242	1.01113	0.62823	0.29223
W0102	31.00787	2.75343	1.17819	0.62685	P1409	21.78539	2.18605	0.74258	0.18755
W0103	22.73013	2.73433	0.77904	0.52286	P1501	29.53990	0.62743	0.70373	0.18993
W0104	25.70839	2.43564	0.62277	0.42655	P1502	22.17932	1.50790	0.96061	0.55149
W0105	32.51010	2.50975	1.11721	0.72222	P1601	29.04599	1.96537	0.63068	0.22148
W0106	33.15596	2.32772	0.89580	0.87478	P1602	32.67210	1.43262	0.63283	0.38950
W0107	31.89288	3.30402	1.19890	0.68494	P1701	33.44228	2.33785	0.95870	0.43102
W0108	19.33075	1.90082	0.69864	0.31785	P1702	32.45676	2.79692	0.62335	0.48308
W0109	35.03766	2.72735	1.22073	0.72307	P1703	27.98587	2.67468	1.25743	0.50890
P0501	21.89046	1.78362	0.71611	0.22853	P1704	30.60823	4.10404	0.58456	0.81841
P0502	28.14819	2.15517	0.58401	0.34651	P1705	29.15550	2.17537	0.79442	0.37034
P0503	20.49609	1.12465	0.15878	0.07490					

Appendix B. Fourier-transformed data for harmonics 0, 2, 4, and 6 for all specimens.

Appendix C. FORTRAN programs used to transform data.

```
C*************************************************************************
C
C THIS PROGRAM COMPUTES A FAST FOURIER TRANSFORM FOR ALL SPECIMENS
C IN A LOCALITY USING THE IMSL SUBROUTINE 'FFTRF.'
C
C BY DELPFINE E. WELCH AND JOHN COSTAIN
C
C*************************************************************************
C
      DIMENSION F(1000),X(1000),CANDS(1000),AN(1000),C(501),S(501),
     *DATA(1000),DATA2(1000),DATA3(1000)
      REAL N2
      INTEGER SPECIMEN,N,P,N1,DTHETA
      CHARACTER*80 TITLE,FMTIN,FMTOUT
C-------------------------------------------------------------------------
C     READ IN NUMBER OF SPECIMENS (P)
      READ(5,*)P
      WRITE(12,120)P
  120 FORMAT(I3)
C-------------------------------------------------------------------------
C     READ INPUT (FTMIN) AND OUTPUT (FMTOUT) FORMAT OF DATA
      READ(80,130)FMTIN
C     WRITE(8,130)FMTIN
      READ(80,130)FMTOUT
C     WRITE(8,130)FMTOUT
  130 FORMAT(A80)
C-------------------------------------------------------------------------
      DO 50 SPECIMEN=1,P
C        READ IN SAMPLING INTERVAL (DTHETA)
         READ(5,*)DTHETA
C        WRITE(8,5)DTHETA
    5    FORMAT(I2)
C        READ IN SPECIMEN ID# (TITLE)
         READ(5,100)TITLE
C        WRITE(8,100)TITLE
  100    FORMAT(A80)
C-------------------------------------------------------------------------
C        READ IN NUMBER OF DATA POINTS FOR HALF VALVE(N)
         READ(5,110)N
C        WRITE(8,110)N
  110    FORMAT(I3)
C-------------------------------------------------------------------------
C        READ IN NUMBER OF DATA POINTS FOR WHOLE VALVE(N1)
C        (DATA IS OUTPUT FROM PROGRAM "MIRROR" WHICH CREATES A MIRROR
C        IMAGE OF HALF A VALVE)
         READ(5,110)N1
C        WRITE(8,110)N1
```

```
C-----------------------------------------------------------------------
C        READ IN DATA SET
         READ(5,FMTIN) (X(I),F(I),I=1,N1)
C        WRITE(8,FMTOUT) (X(I),F(I),I=1,N1)
C-----------------------------------------------------------------------
C        ACCESS THE PROGRAM TO COMPUTE THE FAST FOURIER TRANSFORM FROM
C        THE IMSL LIBRARY
         CALL FFTRF(N1,F,CANDS)
         N2=REAL(N1)/2
C        NORMALIZE
         DO 13 I=1,N1
   13       CANDS(I)=CANDS(I)/N2
C-----------------------------------------------------------------------
C        COMPUTE THE HARMONIC AMPLITUDES, AN, FROM THE C'S AND THE S'S
         J=0
         C(1)=CANDS(1)
         S(1)=0
         DO 16 I=2,N1,2
            J=J+1
C-----------------------------------------------------------------------
C           THE C'S (THE COSINE TRANSFORM) ARE IN I
            C(J)=CANDS(I)
C-----------------------------------------------------------------------
C           THE S'S (THE SINE TRANSFORM) ARE IN I+1
   16       S(J+1)=CANDS(I+1)
         AN(1)=CANDS(1)
         J=1
C-----------------------------------------------------------------------
C        ALL AMPLITUDES ARE DIVIDED BY THE VALUE FOR HARMONIC 0 TO
C        NORMALIZE FOR SIZE
         DO 15 I=2,N1,2
            J=J+1
   15       AN(J)=SQRT(CANDS(I)**2+CANDS(I+1)**2)/AN(1)
         AN(1)=AN(1)/AN(1)
C        WRITE(9,20) (CANDS(I),I=1,N1)
   20    FORMAT(8(F8.3,2X))
         WRITE(12,100)TITLE
         WRITE(12,26) (AN(I),I=1,N1/2+1,2)
   26    FORMAT(8(F7.5,2X))
   27    FORMAT(3(A11,1X,F7.5,1X,I3,1X))
   50    CONTINUE
         STOP
         END



C*********************************************************************
C
C THIS PROGRAM COMPUTES A FAST FOURIER TRANSFORM FOR EACH SPECIMEN
C USING THE IMSL SUBROUTINE 'FFTRF.'  IT THEN RECONSTRUCTS AND
C PLOTS THE SPECIMEN ADDING EACH HARMONIC SERIALLY USING THE IMSL
C SUBROUTINE 'FFTRB.'
C
C BY DELPFINE E. WELCH AND JOHN COSTAIN
C
C*********************************************************************
C
      DIMENSION F(1000),X(1000),CANDS(1000),AN(1000),C(501),S(501),
     *DATA(1000),DATA2(1000),DATA3(1000),CANDSP(1000),
     *FP(1000),XCART(1000),YCART(1000)
      REAL N2
      INTEGER SPECIMEN,N,P,N1,H
      CHARACTER*80 TITLE,FMTIN,FMTOUT
C-----------------------------------------------------------------------
C     READ IN NUMBER OF SPECIMENS (P)
      READ(80,120)P
C     READ IN SAMPLING INTERVAL IN DEGREES (DTHETA)
```

```
      READ(5,*) DTHETA
C     WRITE(8,120)P
  120 FORMAT(I3)
C-----------------------------------------------------------------------
C     READ INPUT (FMTIN) AND OUTPUT (FMTOUT) FORMAT OF DATA
      READ(80,130)FMTIN
C     WRITE(8,130)FMTIN
      READ(80,130)FMTOUT
C     WRITE(8,130)FMTOUT
  130 FORMAT(A80)
C-----------------------------------------------------------------------
      DO 50 SPECIMEN=1,P
C        READ IN SPECIMEN ID# (TITLE)
         READ(5,100)TITLE
C        WRITE(8,100)TITLE
  100    FORMAT(A80)
C-----------------------------------------------------------------------
C        READ IN NUMBER OF DATA POINTS FOR HALF VALVE(N)
         READ(5,110)N
C        WRITE(8,110)N
  110    FORMAT(I3)
C-----------------------------------------------------------------------
C        READ IN NUMBER OF DATA POINTS FOR WHOLE VALVE(N1)
C        (DATA IS OUTPUT FROM PROGRAM "MIRROR" WHICH CREATES A MIRROR
C        IMAGE OF HALF A VALVE)
         READ(5,110)N1
C        WRITE(8,110)N1
C-----------------------------------------------------------------------
C        READ IN DATA SET
         READ(5,FMTIN) (X(I),F(I),I=1,N1)
C        WRITE(8,FMTOUT) (X(I),F(I),I=1,N1)
C-----------------------------------------------------------------------
C        ACCESS THE PROGRAM TO COMPUTE THE FAST FOURIER TRANSFORM FROM
C        THE IMSL LIBRARY
         CALL FFTRF(N1,F,CANDS)
         N2=REAL(N1)/2
C        NORMALIZE
         DO 13 I=1,N1
   13       CANDS(I)=CANDS(I)/N2
C-----------------------------------------------------------------------
C        COMPUTE THE HARMONIC AMPLITUDES, AN, FROM THE C'S AND THE S'S
         J=0
         C(1)=CANDS(1)
         S(1)=0
         DO 16 I=2,N1,2
            J=J+1
C-----------------------------------------------------------------------
C              THE C'S (THE COSINE TRANSFORM) ARE IN I
               C(J)=CANDS(I)
C-----------------------------------------------------------------------
C              THE S'S (THE SINE TRANSFORM) ARE IN I+1
   16          S(J+1)=CANDS(I+1)
         AN(1)=CANDS(1)
         J=1
C-----------------------------------------------------------------------
C        ALL AMPLITUDES ARE DIVIDED BY THE VALUE FOR HARMONIC 0 TO
C        NORMALIZE FOR SIZE
         DO 15 I=2,N1,2
            J=J+1
   15       AN(J)=SQRT(CANDS(I)**2+CANDS(I+1)**2)/AN(1)
         AN(1)=AN(1)/AN(1)
         WRITE(9,20) (CANDS(I),I=1,N1)
   20    FORMAT(8(F8.3,2X))
         WRITE(12,27) (SPECIMEN,AN(I),I-1,I=1,N1/2+1)
   27    FORMAT(4(I3,2X,F7.5,2X,I3,1X))
C-----------------------------------------------------------------------
C        INITIALIZE PLOTTER (ONLY ONCE)
```

```
      CALL PLOTS(0,0,50)
C     SET THE ORIGIN, OFFSET, PLOT SIZE, PAGE SIZE
      X0=2.0
      Y0=8.00
      DX=2.50
      DY=-1.0
      HT=0.50
      XMAX=8
C-----------------------------------------------------------------------
C     ACCESS THE SUBROUTINE TO TURN ON GRAPHICS FOR A PARTICULAR
C     TERMINAL
      CALL TEK4105(0)
C     CALL YTERM(0)
C     CALL VT340(0)
C-----------------------------------------------------------------------
      PI=4*ATAN2(1.0,1.0)
      SCL=0.0
      X1=X0
      Y1=Y0
C-----------------------------------------------------------------------
C     ACCESS THE SUBROUTINE TO WRITE THE SPECIMEN ID ON EACH PLOT
      CALL SYMBOL(X1,Y1,0.1,TITLE,0.0,80)
C-----------------------------------------------------------------------
      DO 567 I=1,J,2
         Y1=Y1+DY
         IF(Y1.LT.2.0) X1=X1+DX
         IF(Y1.LT.2.0) Y1=Y0
C-----------------------------------------------------------------------
C        ACCESS THE SUBROUTINE TO ZERO OUT THE PARTIAL HARMONIC ARRAY
         CALL ZERO(N1,CANDSP)
C-----------------------------------------------------------------------
C        INSERT THE DESIRED HARMONICS (STARTING FROM THETA = 0 DEG)
         CANDSP(1)=CANDS(1)
         IF(I.EQ.1) GO TO 721
         DO 568 H=2,(I-1)*2,2
            CANDSP(H)=CANDS(H)
 568        CANDSP(H+1)=CANDS(H+1)
C-----------------------------------------------------------------------
C        ACCESS THE PROGRAM TO COMPUTE THE REVERSE FAST FOURIER
C        TRANSFORM FROM THE IMSL LIBRARY
 721     CALL FFTRB(N1,CANDSP,FP)
C-----------------------------------------------------------------------
C        ACCESS THE SUBROUTINE TO SCALE THE SPECIMENS
         CALL SCALE(N1,FP,HT,SCL)
C        WRITE(60,*) 'H=',I-1,(FP(N),N=1,N1)
C        PLOT AND LOOK AT SHAPES AS EACH HARMONIC IS ADDED.
C-----------------------------------------------------------------------
C        DETERMINE CARTESIAN COORDINATES FROM THE POLAR COORDINATES
         DO 459 K=1,N1
            XCART(K)=FP(K)*COS((K-1)*DTHETA*PI/180.)
 459        YCART(K)=FP(K)*SIN((K-1)*DTHETA*PI/180.)
C           WRITE (70,*) XCART(K),YCART(K)
C-----------------------------------------------------------------------
C        SET A NEW ORIGIN FOR EACH FOSSIL PLOT
         CALL PLOT(X1,Y1,3)
         CALL PLOT(X1,Y1,2)
         CALL PLOT(X1+XCART(1),Y1+YCART(1),3)
         XSYMB=X1-HT/2.
         YSYMB=Y1-HT/2.
C-----------------------------------------------------------------------
C        ACCESS THE SUBROUTINE TO WRITE THE HARMONIC NUMBER ON EACH
C        PLOTTED SPECIMEN
         CALL NUMBER(XSYMB,YSYMB,0.15,FLOAT(I-1),0.0,-1)
C-----------------------------------------------------------------------
         CALL PLOT(X1+XCART(1),Y1+YCART(1),3)
         DO 460 K=1,N1
 460        CALL PLOT(X1+XCART(K),Y1+YCART(K),2)
```

```
            CALL PLOT(X1+XCART(1),Y1+YCART(1),2)
  567       CONTINUE
   50     CONTINUE
C-------------------------------------------------------------------------
C         EMPTY THE BUFFER  (THROUGH PLOTTING)
          CALL PLOT(0.0,0.0,999)
C-------------------------------------------------------------------------
C         ACCESS THE SUBROUTINE TO RETURN TO TEXT MODE
          CALL TEK4105(1)
C         CALL YTERM(1)
C         CALL VT340(1)
C-------------------------------------------------------------------------
          STOP
          END
C-------------------------------------------------------------------------
C SUBROUTINE TO SET TEK4105 TERMINAL IN AND OUT OF GRAPHICS MODE
C-------------------------------------------------------------------------
      SUBROUTINE TEK4105(INDEX)
      IF(INDEX.EQ.0) THEN
C     SET TERMINAL IN GRAPHICS MODE
      WRITE (6,*) CHAR(39),'%!0'
      ELSE
C     SET TERMINAL TO TEXT MODE
      WRITE (6,*) CHAR(39),'%!1'
      ENDIF
      RETURN
      END
C-------------------------------------------------------------------------
C SUBROUTINE TO SET YTERM IN AND OUT OF GRAPHICS MODE
C-------------------------------------------------------------------------
      SUBROUTINE YTERM(INDEX)
      IF(INDEX.EQ.0) THEN
C     SET TERMINAL IN GRAPHICS MODE
      WRITE (6,*) CHAR(39),CHAR(173),CHAR(76),CHAR(241),CHAR(136)
      ELSE
C     SET TERMINAL TO TEXT MODE
      WRITE (6,*) CHAR(39),CHAR(24)
      ENDIF
      RETURN
      END
C-------------------------------------------------------------------------
C SUBROUTINE TO SET VT340 TERMINAL IN AND OUT OF GRAPHICS MODE
C-------------------------------------------------------------------------
      SUBROUTINE VT340(INDEX)
      IF(INDEX.EQ.0) THEN
C     SET TERMINAL IN 401X MODE
      WRITE(*,*) CHAR(39),'[?38h'
      ELSE
C     GET TERMINAL OUT OF 401X MODE
      WRITE(*,*) CHAR(39),'[?38l'
C     SET KEYPAD TO APPLICATION MODE
      WRITE(*,*) CHAR(39),'='
      ENDIF
      RETURN
      END
C-------------------------------------------------------------------------
C SUBROUTINE TO ZERO OUT THE PARTIAL HARMONIC ARRAY
C-------------------------------------------------------------------------
      SUBROUTINE ZERO(N,X)
      DIMENSION X(N)
      DO 1 I=1,N
    1    X(I)=0.0
      RETURN
      END
C-------------------------------------------------------------------------
C SUBROUTINE TO SCALE THE SIZE OF THE PLOTTED SPECIMEN
C-------------------------------------------------------------------------
```

```
      SUBROUTINE SCALE(N,Y,HT,SCL)
      DIMENSION Y(N)
      IF(SCL.NE.0.0) GO TO 10
      YMAX=ABS(Y(1))
      DO 50 I=1,N
   50 YMAX=AMAX1(YMAX,ABS(Y(I)))
      IF(YMAX.EQ.0.0) RETURN
      SCL=HT/YMAX
   10 DO 51 I=1,N
   51 Y(I)=Y(I)*SCL
      RETURN
      END


C*********************************************************************
C
C THIS PROGRAM CREATES A NEW DATA SET AT A SPECIFIED SAMPLING INTERVAL
C FROM DATA FOR A HALF VALVE DIGITIZED IN STREAM MODE, CREATES A
C MIRROR IMAGE FOR THE OTHER HALF OF THE VALVE, AND THEN A MIRROR IMAGE
C OF THE WHOLE VALVE.
C
C*********************************************************************
C
      DIMENSION F(1000),X(1000),Z(1000)
      INTEGER N,P,THETA
      CHARACTER*11 TITLE
C---------------------------------------------------------------------
C     READ IN SAMPLING INTERVAL (THETA)
      READ(9,106)THETA
      WRITE(4,106)THETA
  106 FORMAT(I2)
C---------------------------------------------------------------------
C     READ IN SPECIMEN ID$ (TITLE)
      READ(2,100)TITLE
      WRITE(4,100)TITLE
  100 FORMAT(A11)
C---------------------------------------------------------------------
C     READ IN NUMBER OF DATA POINTS AS MEASURED (M)
      READ(9,111)M
      WRITE(4,111)M
  111 FORMAT(I3)
C---------------------------------------------------------------------
C     READ IN NUMBER OF DATA POINTS FOR HALF VALVE (N)
      READ(9,111)N
      WRITE(4,111)N
C---------------------------------------------------------------------
C     COMPUTE NUMBER OF DATA POINTS FOR WHOLE VALVE (N2)
      N2=(N-1)*4
      WRITE(4,111)N2
C---------------------------------------------------------------------
C     READ IN DATA MATRIX
      READ(2,10) (X(I),F(I),I=1,M)
      WRITE(7,10) (X(I),F(I),I=1,M)
   10 FORMAT(F9.5,6X,F8.5)
C---------------------------------------------------------------------
C     SELECT DATA CLOSEST TO SAMPLING INTERVAL
      K=0
      DO 400 I=90,180,THETA
         V=90
         K=K+1
         DO 300 J=1,M
            IF(ABS(X(J)-I).LT.V)THEN
               F(K)=F(J)
               Z(K)=I
               V=ABS(X(J)-I)
            ENDIF
```

```
300     CONTINUE
400 CONTINUE
    WRITE(8,12) (Z(J),F(J),J=1,N)
 12 FORMAT(F9.5,6X,F9.5)
    J=N
    DO 120 I=1,N
        WRITE(4,13) Z(J),F(J)
 13     FORMAT(F9.5,6X,F9.5)
        J=J-1
120     CONTINUE
    WRITE(4,12) (Z(I),F(I),I=2,N-1)
    J=N
    DO 130 I=1,N
        WRITE(4,13) Z(J),F(J)
        J=J-1
130     CONTINUE
    WRITE(4,12) (Z(I),F(I),I=2,N-1)
    STOP
    END
```

Appendix D. Principal component analysis scores for means of harmonics 2, 4, and 6 for all localities.

LOCALITY	PRIN1	PRIN2	PRIN3	LOCALITY	PRIN1	PRIN2	PRIN3
N02	0.003588	-0.007502	-0.000678	N35B	-0.031319	0.002347	0.001598
N03	0.002685	-0.000265	0.004527	O01A	0.074146	0.005157	-0.000381
N04	0.027551	0.005468	-0.004916	O02A	0.085557	0.002277	0.000414
N05A	0.019977	-0.004687	-0.003661	O02C	-0.030163	0.001387	0.004836
N05B	0.002909	-0.004706	-0.001035	O04	-0.012857	-0.002646	0.000849
N06	-0.007544	-0.006991	-0.004142	O05	-0.029983	-0.001511	0.001096
N07	0.013003	0.002672	-0.002894	M01	-0.012572	0.003731	0.006121
N10	0.003669	0.000482	-0.003680	M03	0.009163	0.004337	0.003722
N11	-0.020863	0.002000	-0.001296	M08	-0.007402	0.013760	0.000075
N13	-0.038501	-0.000728	0.005177	M11	0.006583	0.007665	-0.001519
N16	0.097505	0.001263	0.005696	M12	-0.000622	0.011052	0.001622
N17	0.068767	0.001009	-0.002517	M13	0.024561	0.013124	0.006747
N18	0.039136	-0.001869	-0.003888	M14	-0.041934	0.005255	0.000259
N19	-0.012320	-0.012329	-0.000298	M15	-0.033193	0.008407	0.005261
N20	-0.022788	-0.006265	0.000274	M16	0.012433	0.009113	-0.003918
N22A	-0.006875	-0.003713	-0.001225	M17	0.019125	0.016001	-0.001255
N22B	-0.011641	-0.004849	-0.001529	M19	-0.011534	0.015051	-0.008006
N22C	0.040338	-0.004833	-0.001883	M20	0.009160	-0.003013	0.002072
N22D	-0.017558	-0.001607	0.001087	M23	-0.012410	0.007236	-0.001132
N25	-0.028801	-0.008918	-0.006178	M24	-0.052257	0.001329	-0.002807
N26	0.000187	-0.012523	0.004033	D01	0.015205	-0.007407	-0.001941
N27	-0.004465	-0.001231	-0.006200	D02	0.000887	0.000645	-0.001174
N31	-0.044819	-0.004233	-0.000180	W01	0.013990	0.000823	0.001874
N33	-0.050551	0.001203	0.003718	P05	0.006090	-0.006234	0.000011
N34A	0.007609	-0.000627	0.002348	P07	0.030522	0.001589	0.003552
N34B	0.009890	0.005636	0.000733	P09	0.040455	-0.024244	0.004848
N34C	-0.022726	0.002005	0.000544	P10	-0.021586	-0.002942	0.000511
N34D	-0.029928	-0.006521	0.001521	P14	-0.006173	-0.006459	0.000271
N34E	-0.012747	-0.009970	0.000371	P15	-0.023558	0.016980	0.000030
N34F	-0.010930	-0.001367	-0.000096	P16	-0.018723	-0.000387	-0.001656
N34G	-0.011504	0.005725	0.000166	P17	0.018571	-0.005612	0.001075
N35A	-0.002415	-0.008541	-0.006955				

Appendix E. Principal component analysis scores for harmonics 2, 4, and 6 for all specimens.

SPECIMEN	PRIN1	PRIN2	PRIN3	SPECIMEN	PRIN1	PRIN2	PRIN3
N0201	0.015690	-0.021844	0.002096	N0402	0.016414	-0.006875	0.002156
N0202	-0.001028	-0.016733	-0.000039	N0403	0.037829	0.007936	-0.004937
N0203	0.013168	0.001158	-0.009158	N0404	0.015140	0.002453	-0.007813
N0204	0.021395	0.006409	-0.005106	N0405	0.040070	0.008133	-0.004184
N0205	-0.004173	-0.011204	-0.005919	N0406	0.026827	0.006932	0.002726
N0206	-0.009090	-0.011236	-0.001302	N0407	0.024939	0.010039	0.001774
N0207	-0.007247	-0.002512	-0.005161	N0408	0.012920	0.000351	0.001191
N0208	0.021432	-0.024396	-0.003583	N0409	0.017045	0.013568	-0.009413
N0209	-0.013243	0.006381	0.010940	N0410	0.063798	0.013583	-0.000408
N0210	-0.035556	-0.001122	-0.007784	N0411	0.030318	0.017002	-0.006911
N0211	-0.010134	-0.003177	-0.007384	N05A01	0.045261	-0.012350	-0.009045
N0212	0.017778	-0.005065	0.003974	N05A02	0.014464	0.012684	-0.001300
N0213	0.020668	-0.006597	-0.000598	N05A03	0.023050	-0.011071	-0.009258
N0214	0.006987	0.003488	-0.006069	N05A04	0.018924	-0.026181	-0.002916
N0215	-0.006066	-0.001040	-0.003425	N05A05	0.039931	-0.022293	-0.013159
N0216	0.015597	-0.005989	0.000649	N05A06	0.052419	-0.011777	-0.003010
N0217	0.000835	-0.012292	-0.000705	N05A07	0.007830	0.027411	-0.006044
N0218	-0.026789	0.001285	-0.000037	N05A08	0.027154	-0.010764	-0.010765
N0219	0.010376	-0.001507	-0.000500	N05A09	-0.002114	-0.000460	-0.005704
N0220	0.026801	-0.009319	-0.004959	N05A10	-0.002958	-0.001030	0.002559
N0221	0.034312	-0.004766	-0.001662	N05A11	0.013611	0.002336	-0.005483
N0222	0.010385	-0.004257	-0.006677	N05A12	0.026226	0.004976	0.005983
N0223	0.014852	-0.028348	0.002965	N05A13	-0.001115	-0.001505	0.005475
N0224	-0.004660	-0.009201	0.005496	N05A14	0.025541	0.005191	-0.015259
N0225	0.010287	-0.009818	0.001599	N05A15	0.035811	-0.009173	-0.003906
N0301	0.018082	0.003733	-0.002081	N05A16	0.029667	-0.009733	0.005026
N0302	-0.001268	0.022984	0.013621	N05A17	0.032119	-0.000906	-0.004332
N0303	-0.007822	-0.004232	0.000787	N05A18	0.020842	-0.011545	-0.002402
N0304	0.036657	-0.000790	0.002410	N05A19	0.000282	0.007993	-0.001064
N0305	-0.010455	-0.002115	0.010528	N05A20	0.018549	0.005123	0.003812
N0306	-0.016594	-0.006903	0.007730	N05B01	0.014300	-0.002632	-0.000619
N0307	0.005012	0.014984	0.003801	N05B02	-0.007739	-0.014705	0.001888
N0308	-0.006683	0.000447	0.009303	N05B03	0.035397	-0.001015	-0.003506
N0309	-0.004768	-0.018374	0.005592	N05B04	0.011187	0.020118	0.000976
N0310	-0.011445	0.006975	0.005972	N05B05	0.000080	-0.000919	-0.005381
N0311	-0.006878	0.003765	-0.003291	N05B06	0.001208	-0.015431	-0.000287
N0312	-0.003131	0.002293	-0.001974	N05B07	0.019045	0.002564	-0.007221
N0313	0.008402	-0.020501	0.009346	N05B08	0.026480	-0.007059	-0.000667
N0314	-0.000987	-0.017643	0.013179	N05B09	0.002582	-0.020816	-0.000227
N0315	0.006347	0.007107	0.005992	N05B10	-0.034202	-0.005736	-0.007608
N0316	0.022902	-0.007530	0.006813	N05B11	0.002707	-0.002860	-0.007000
N0317	0.004269	-0.021674	0.005818	N05B12	-0.002929	0.003772	0.007982
N0318	0.048585	-0.003751	0.008122	N05B13	-0.033457	-0.005262	0.008632
N0319	0.006901	-0.006600	0.007013	N05B14	0.023291	-0.006987	-0.009635
N0320	0.019375	0.013693	-0.001453	N0601	0.005907	-0.003296	-0.013010
N0321	0.002697	0.014806	-0.002454	N0602	-0.005932	-0.005578	-0.012714
N0322	-0.030354	0.006140	-0.004037	N0603	0.009014	-0.030761	0.001583
N0401	0.028749	0.006832	-0.005264				

SPECIMEN	PRIN1	PRIN2	PRIN3	SPECIMEN	PRIN1	PRIN2	PRIN3
N0604	0.010893	-0.003452	-0.007346	N1116	-0.065777	-0.000425	0.001758
N0605	0.017677	-0.008297	-0.002742	N1117	-0.052362	0.007876	-0.008220
N0606	-0.011929	-0.003037	-0.008090	N1118	-0.031800	-0.011296	-0.003053
N0607	-0.020102	0.006149	-0.012440	N1119	-0.009479	0.012020	0.004473
N0608	-0.046515	-0.009917	-0.002817	N1120	-0.019468	-0.017982	0.005010
N0609	-0.016514	-0.009803	-0.002793	N1121	0.001538	0.000273	0.006592
N0610	0.015234	-0.010826	-0.000471	N1122	0.003390	-0.001582	0.001690
N0611	-0.039892	0.002535	-0.009621	N1301	-0.045578	-0.009436	0.012838
N0612	-0.004531	-0.003227	-0.006844	N1302	-0.060893	0.005286	-0.001717
N0613	0.001835	0.001221	-0.006705	N1303	-0.057948	0.024772	0.001285
N0614	-0.009858	-0.004772	0.000596	N1304	0.008525	-0.023277	-0.006769
N0615	0.002890	-0.008288	0.001537	N1305	-0.068517	0.009143	-0.002010
N0701	-0.012392	0.015938	-0.002857	N1306	-0.030097	-0.004697	-0.001857
N0702	0.055867	-0.000506	0.001004	N1307	-0.021870	-0.000026	0.014974
N0703	0.051408	0.013335	-0.004698	N1308	-0.023032	-0.009580	0.006462
N0704	0.041396	-0.013585	0.005545	N1309	-0.038639	-0.012769	0.008674
N0705	0.014396	0.008005	-0.007122	N1601	0.098206	0.003281	0.009674
N0706	0.025340	0.024536	0.005557	N1701	0.108608	0.014426	0.004097
N0707	-0.026493	0.018052	-0.008536	N1702	0.085494	0.006544	0.005262
N0708	-0.029056	0.008137	-0.008417	N1703	0.065266	-0.000009	0.001152
N0709	0.012983	-0.000365	-0.008103	N1704	0.085194	0.004167	-0.007150
N0710	0.003137	0.000021	-0.003789	N1705	0.048457	0.008262	-0.001450
N0711	0.013974	0.011522	-0.005379	N1706	0.035014	0.004018	0.000889
N0712	0.007334	0.002456	0.004479	N1707	0.069769	0.011765	-0.003512
N0713	-0.018084	0.006599	-0.006491	N1708	0.132553	-0.006537	0.007333
N0714	0.023325	0.000471	-0.008114	N1709	0.070590	-0.016365	0.004464
N0715	0.031585	-0.009359	0.007679	N1710	0.059733	0.018380	-0.006056
N0716	0.024127	-0.011693	-0.002405	N1711	0.079312	-0.004215	-0.004288
N0717	0.000812	0.006810	0.001999	N1712	0.051939	0.007171	-0.001925
N0718	0.033109	-0.012213	0.006311	N1713	0.102355	0.003050	0.000031
N1001	0.005801	0.001350	-0.002345	N1714	0.044658	-0.011681	0.008999
N1002	0.045763	-0.014372	0.001675	N1715	0.088299	0.021895	-0.004163
N1003	-0.006533	-0.001489	0.002910	N1716	0.065811	0.003837	0.000017
N1004	0.013748	0.005585	-0.007988	N1717	0.048550	0.003326	0.002182
N1005	0.024954	0.005672	-0.010854	N1718	0.025567	0.020014	-0.004398
N1006	-0.015957	0.010433	-0.003756	N1719	0.044481	-0.004802	0.006334
N1007	-0.001266	0.007556	-0.007217	N1720	0.041146	0.003653	0.011781
N1008	0.016516	0.001957	0.004706	N1721	0.067934	0.000001	-0.002378
N1009	0.026064	0.009633	-0.009055	N1722	0.078074	-0.004151	-0.005859
N1010	0.016664	0.009832	-0.007785	N1723	0.081861	0.002160	-0.001845
N1011	0.001449	-0.006020	-0.008416	N1724	0.094281	0.001419	0.000433
N1012	-0.021910	0.000409	0.000541	N1801	0.011182	0.013495	-0.009425
N1013	-0.008075	0.008210	-0.000052	N1802	-0.013031	0.009258	0.001585
N1014	-0.004616	-0.005402	-0.012246	N1803	0.016633	-0.006231	-0.007107
N1015	0.011127	-0.011064	0.012502	N1804	-0.005172	-0.002142	0.000527
N1016	0.015894	0.009621	0.001273	N1805	0.027001	0.002632	-0.007579
N1017	0.015774	0.001015	-0.011783	N1806	0.045523	-0.009736	0.000192
N1018	0.029665	-0.008196	0.013299	N1807	0.046016	0.002616	-0.003990
N1019	-0.033547	0.013099	-0.007192	N1808	0.062103	-0.015219	-0.008152
N1020	-0.033720	-0.011789	0.006254	N1809	0.071568	0.000811	-0.008916
N1021	0.053287	0.007421	-0.006817	N1810	0.077037	0.015001	-0.002135
N1022	-0.029238	0.006185	-0.009593	N1811	0.026557	-0.006346	0.001970
N1023	0.002021	-0.001458	-0.006592	N1812	0.001144	-0.005812	0.000411
N1024	-0.008201	-0.002152	-0.011810	N1813	0.052435	0.010532	-0.003332
N1101	0.003567	0.012388	-0.001621	N1814	0.070769	-0.012699	-0.001141
N1102	-0.034933	0.001300	-0.002527	N1815	0.050406	0.002215	-0.003681
N1103	-0.000281	0.006724	-0.001829	N1816	0.082293	-0.004420	0.006630
N1104	-0.014655	-0.006805	0.009177	N1817	0.063221	0.009030	0.000741
N1105	-0.002375	-0.003138	-0.004466	N1901	0.005595	0.000658	-0.008156
N1106	-0.023341	0.012807	-0.007798	N1902	0.005223	-0.013266	-0.010945
N1107	-0.039907	0.004278	-0.006537	N1903	0.010073	-0.012448	-0.004292
N1108	-0.036712	-0.011508	0.006537	N1904	-0.030612	-0.016439	-0.001416
N1109	-0.004961	0.012475	-0.012380	N1905	-0.000864	-0.016742	0.003271
N1110	-0.004861	0.000793	-0.006151	N1906	-0.024793	-0.000581	0.004931
N1111	-0.053311	-0.004446	0.009364	N1907	-0.041129	-0.010500	0.000912
N1112	-0.021258	0.009872	-0.001764	N1908	0.005390	-0.022901	0.003018
N1113	-0.040018	0.016482	-0.008848	N1909	-0.022374	-0.010110	-0.007221
N1114	0.019861	-0.002553	-0.010284	N1910	-0.007794	-0.017915	-0.002383
N1115	-0.008736	0.005224	-0.006610	N1911	-0.018026	-0.013073	-0.007694

SPECIMEN	PRIN1	PRIN2	PRIN3	SPECIMEN	PRIN1	PRIN2	PRIN3
N2001	-0.020679	0.002788	-0.009862	N3302	-0.033428	-0.000977	-0.002284
N2002	-0.030703	-0.003044	-0.005364	N3303	-0.057844	0.005854	0.005580
N2003	-0.033394	0.004322	0.003627	N3304	-0.056469	0.004981	0.009987
N2004	-0.022541	-0.007494	-0.009017	N3305	-0.049695	0.002185	-0.007091
N2005	-0.045490	-0.005441	-0.001355	N3306	-0.049840	-0.000875	0.008889
N2006	0.002569	-0.019410	0.002955	N3307	-0.064722	-0.003465	0.004213
N2007	-0.023790	-0.010775	-0.004165	N3308	-0.036195	-0.003077	0.003175
N2008	-0.028686	-0.012067	0.000027	N3309	-0.069069	-0.003508	-0.002472
N2009	0.007686	-0.027060	-0.001298	N3310	-0.035675	0.002240	-0.004693
N2010	-0.038165	0.014188	-0.006489	N3311	-0.052626	-0.003071	-0.001040
N2011	-0.001949	0.000015	0.005885	N3312	-0.052534	0.000151	0.004222
N2012	-0.007098	-0.016086	0.010138	N3313	-0.071730	0.004404	0.000980
N2013	-0.049794	-0.009849	-0.002772	N3314	-0.034537	-0.008210	0.005056
N2014	-0.056523	0.011690	-0.003076	N3315	-0.053388	-0.005936	0.002346
N2015	-0.046221	0.000886	0.011555	N3316	-0.076121	-0.000591	0.000808
N2016	0.010279	-0.026683	-0.006979	N3317	-0.037850	0.003372	0.000109
N2017	0.018726	-0.006699	-0.010699	N34A01	0.037816	0.000567	0.000785
N22A01	0.012074	-0.015995	0.007054	N34A02	0.031246	0.006990	0.001225
N22A02	-0.027808	0.001398	-0.004962	N34A03	0.004139	0.002825	-0.006536
N22A03	-0.001235	0.004645	-0.008172	N34A04	0.038308	-0.012037	0.011504
N22B01	-0.040557	-0.009967	-0.004602	N34A05	-0.006213	-0.002109	0.000422
N22B02	0.008013	-0.010635	-0.008745	N34A06	-0.043922	-0.011155	0.005304
N22B03	-0.015653	0.010664	-0.004367	N34A07	-0.006663	-0.003136	0.007783
N22B04	-0.038396	-0.005160	-0.002702	N34A08	-0.008375	0.009256	-0.000998
N22B05	0.014092	0.002887	-0.006010	N34A09	0.030944	0.004584	0.003560
N22B06	-0.020039	-0.009541	-0.003671	N34B02	0.036390	0.000917	0.009196
N22B07	0.016416	-0.014525	0.002439	N34B03	-0.018044	0.004676	-0.005887
N22B08	-0.019908	-0.006244	-0.001611	N34B04	0.013805	0.012502	0.002934
N22B09	-0.015058	-0.014122	0.000932	N34C01	-0.049179	-0.005947	0.009983
N22B10	0.007453	0.011471	0.001371	N34C02	-0.023416	0.001901	-0.003785
N22C01	0.031738	-0.000517	-0.001814	N34C03	0.024865	-0.003441	-0.002166
N22C02	0.051400	-0.005551	-0.000211	N34C04	-0.011779	-0.018969	0.004785
N22D01	-0.005848	-0.005358	-0.005283	N34C05	-0.007722	0.010371	-0.001525
N22D02	0.014828	-0.016937	0.002222	N34C06	0.010738	-0.010021	-0.002553
N22D03	-0.055783	0.006400	0.005798	N34C07	-0.060623	0.013400	0.010199
N22D04	-0.010006	-0.016638	-0.003197	N34C08	-0.018583	0.003613	-0.000902
N22D05	-0.024173	0.007791	0.008640	N34C09	-0.004599	0.004113	0.002660
N22D06	-0.017853	0.016801	-0.002065	N34C10	-0.015549	0.003043	-0.005527
N22D07	-0.016543	-0.005464	-0.004842	N34C11	-0.045752	0.002690	-0.004268
N2501	-0.010329	-0.004365	-0.011396	N34C12	-0.034421	0.004395	-0.003022
N2502	-0.044098	-0.012110	-0.005829	N34C13	-0.046634	0.015694	-0.003448
N2601	-0.007378	-0.015848	0.004794	N34D01	-0.009014	-0.009487	-0.006529
N2602	0.010384	-0.009515	-0.000798	N34D02	-0.051058	0.002637	-0.001411
N2701	0.047225	-0.003152	-0.009973	N34D03	-0.025970	-0.014643	0.005940
N2702	-0.030941	-0.012224	0.002966	N34E04	-0.004632	-0.009140	-0.005288
N2703	-0.019983	0.002097	-0.010586	N34E05	-0.018106	-0.010681	0.001904
N2704	-0.042496	0.012782	-0.008299	N34F01	0.034517	-0.014514	0.002334
N2705	0.030368	0.000558	-0.006281	N34F02	-0.006857	-0.002421	-0.002048
N3101	-0.025196	-0.006575	-0.003889	N34F03	-0.068183	0.014081	0.003965
N3102	-0.055992	-0.008681	-0.000921	N34F04	0.016653	-0.006962	-0.001141
N3103	-0.051248	-0.010105	-0.002834	N34F05	-0.014356	0.002769	0.003410
N3104	-0.072153	-0.000596	0.003191	N34F06	-0.020699	-0.000795	-0.010654
N3105	-0.043672	-0.004753	-0.005269	N34G01	0.014721	-0.006418	-0.002762
N3106	-0.024138	-0.013983	-0.007819	N34G02	-0.036486	0.000063	0.001880
N3107	-0.063349	0.012884	-0.001626	N34G03	-0.012264	0.001353	0.005268
N3108	-0.005969	-0.001527	-0.003602	N34G04	-0.055400	0.015699	-0.006060
N3109	-0.055597	0.001602	-0.007147	N34G05	-0.020090	-0.002221	0.006851
N3110	-0.055925	0.000412	0.004804	N34G06	0.002897	0.006898	-0.001977
N3111	-0.067759	-0.002196	0.001297	N34G07	0.002983	-0.001091	0.002406
N3112	-0.060765	0.001548	0.002809	N34G08	0.016126	0.019642	0.001967
N3113	-0.021160	-0.013736	-0.008409	N34G09	-0.018612	0.018937	-0.002475
N3114	-0.067244	-0.002073	0.008269	N34G10	-0.000307	0.003430	0.001911
N3115	0.006030	-0.010842	-0.010110	N35A01	-0.000847	-0.007022	-0.008284
N3116	-0.037012	-0.010472	-0.000913	N35B01	-0.018588	-0.012059	0.011060
N3117	-0.030856	-0.014742	-0.005281	N35B02	-0.015232	-0.004493	0.006540
N3118	-0.051536	-0.007787	-0.001732	N35B03	-0.050631	0.001518	0.000709
N3119	-0.027813	-0.003113	-0.007701	N35B04	-0.014421	-0.015078	0.003339
N3120	-0.060162	-0.005919	-0.004128	N35B05	-0.056862	0.022294	-0.005222
N3301	-0.011693	-0.001415	0.005394	N35B06	-0.041874	0.019884	0.000070

SPECIMEN	PRIN1	PRIN2	PRIN3	SPECIMEN	PRIN1	PRIN2	PRIN3
N35B07	-0.028160	-0.002850	-0.000383	O0514	-0.002451	-0.004897	-0.001701
N35B08	-0.017165	0.003060	-0.009720	O0515	-0.009928	0.001993	-0.006272
O01A01	0.091095	0.005467	-0.000212	M0101	0.005934	0.005964	0.009923
O01A02	0.080233	0.012921	-0.001649	M0102	-0.009558	0.007690	0.001586
O01A03	0.078606	-0.000471	0.003253	M0103	-0.038493	-0.002814	0.015243
O01A04	0.101795	0.008278	0.001457	M0104	-0.032391	0.011394	0.007370
O01A05	0.061394	0.011459	0.003644	M0105	-0.006017	0.014534	0.010982
O01A06	0.067839	-0.002487	0.005828	M0106	0.010055	0.003041	0.000728
O01A07	0.051509	-0.002211	0.009167	M0107	-0.011555	-0.007127	0.009396
O01A08	0.104768	-0.000092	0.006205	M0108	0.001548	-0.003938	0.005550
O01A09	0.138086	0.002194	0.004252	M0109	-0.005321	0.012053	0.001776
O01A10	0.081463	0.016573	0.003040	M0110	-0.051996	0.012038	0.004083
O01A11	0.101795	0.011297	0.003278	M0111	0.036725	0.003592	0.000027
O01A12	0.080439	0.006753	0.002052	M0112	-0.026451	-0.001421	0.013042
O01A13	0.075484	0.001985	0.001116	M0113	-0.000233	0.009881	0.012215
O01A14	0.011134	0.016433	0.011087	M0114	-0.042070	0.001382	0.003214
O01A15	0.065143	0.013170	0.000588	M0115	-0.024951	-0.001321	0.002348
O01A16	0.060345	0.015592	0.005146	M0116	-0.034167	-0.006800	0.004024
O01A17	0.044771	0.011955	0.000310	M0117	0.035214	0.008244	0.009599
O01A18	0.053268	0.005857	0.002734	M0118	-0.014395	-0.004763	0.009709
O02A01	0.084581	0.013262	0.004740	M0119	-0.017873	0.001531	-0.001674
O02A02	0.093533	-0.005939	0.002084	M0120	-0.010853	-0.009979	0.004946
O02A03	0.095422	0.008884	0.007860	M0301	0.024793	0.010052	0.013306
O02A04	0.072156	0.003094	0.001976	M0302	0.008441	-0.004157	0.000064
O02C01	0.018096	0.003301	0.001675	M0303	0.002613	0.010384	0.006300
O02C02	-0.020228	0.016561	0.000381	M0304	0.014162	0.005529	0.005203
O02C03	0.027221	-0.009158	-0.003315	M0305	0.023660	-0.009567	0.005213
O02C04	-0.018297	0.006721	0.005615	M0306	-0.008836	0.016095	0.002152
O02C05	-0.011183	-0.014978	-0.002905	M0307	0.004667	0.001370	0.001280
O02C06	-0.020150	0.008112	0.005044	M0801	-0.010102	0.009496	-0.000871
O02C07	0.032750	-0.004918	-0.001827	M0802	0.010837	0.029045	0.001351
O02C08	-0.021111	0.004468	0.018565	M0803	-0.011411	0.011747	0.002276
O02C09	-0.032544	-0.007619	0.003199	M0804	-0.016558	0.004440	0.005583
O02C10	-0.031666	-0.014866	0.004513	M1101	0.006225	0.006028	0.008971
O02C11	-0.054211	-0.003521	0.009236	M1102	-0.003628	0.012743	0.000117
O02C12	-0.041173	-0.010558	0.009662	M1103	0.019652	0.006169	-0.008900
O02C13	-0.057115	0.006646	0.002838	M1201	-0.039672	0.008219	0.004968
O02C14	-0.057384	-0.000543	-0.001481	M1202	0.025401	0.005241	0.004820
O02C15	-0.056905	0.004690	0.006521	M1203	0.007252	0.013673	0.003049
O02C16	-0.042203	0.006200	-0.001069	M1204	0.018572	0.011847	0.001153
O02C17	-0.031649	0.000564	0.004568	M1205	-0.011545	0.015711	0.003145
O02C18	-0.032175	0.002447	0.002953	M1301	0.018587	0.004216	0.013069
O02C19	-0.053341	0.007992	0.004494	M1302	0.025878	0.019453	0.015679
O02C20	-0.042066	-0.004838	0.004820	M1303	0.042553	0.004245	0.008950
O02C21	-0.065260	0.007290	0.006134	M1304	0.019290	0.009394	-0.003030
O02C22	-0.033915	-0.002186	0.005586	M1305	0.018272	0.026839	0.014323
O0401	-0.002068	0.021494	0.005943	M1401	-0.045108	0.022611	-0.009687
O0402	0.013933	-0.004292	-0.003513	M1402	-0.045496	-0.005806	0.007953
O0403	0.004983	0.006394	-0.007732	M1403	-0.014923	0.001519	-0.006409
O0404	0.004843	-0.005435	-0.004353	M1404	-0.058541	-0.000989	0.006285
O0405	-0.001467	-0.003826	-0.001328	M1501	-0.010052	0.002124	0.007084
O0406	-0.041419	-0.004828	0.003605	M1502	-0.019309	0.013124	-0.001386
O0407	-0.018998	-0.013629	0.000920	M1503	-0.057125	0.006997	-0.002434
O0408	-0.025051	-0.014420	0.004762	M1504	-0.037339	0.003125	0.006421
O0409	-0.023323	-0.002112	0.001732	M1505	-0.028672	0.005938	0.013442
O0410	-0.028798	-0.007052	-0.000458	M1506	-0.027133	0.016481	0.013395
O0501	0.006767	-0.001621	-0.002220	M1507	-0.048353	0.000209	0.000725
O0502	-0.032490	-0.010064	0.001442	M1601	0.013296	0.010292	-0.001839
O0503	-0.024963	-0.005213	0.007169	M1701	-0.005193	0.026200	0.003232
O0504	-0.034179	-0.003116	-0.003737	M1702	0.016598	0.002769	0.003450
O0505	-0.047920	-0.003834	0.002181	M1703	0.032648	0.004529	-0.004714
O0506	-0.031192	0.004072	0.001802	M1704	0.034621	0.033823	0.006701
O0507	-0.024904	-0.009410	-0.006945	M1901	0.024231	0.002694	-0.007131
O0508	-0.065961	0.007638	-0.007184	M1902	-0.055688	0.029404	-0.004866
O0509	-0.062750	0.009942	0.006942	M1903	-0.000634	0.016410	-0.005512
O0510	-0.026983	-0.010774	-0.004203	M2001	0.025136	0.002389	0.001960
O0511	-0.021913	-0.005614	0.007384	M2002	-0.004677	-0.007856	0.001958
O0512	-0.003614	-0.007675	-0.000495	M2301	0.002571	-0.002425	0.000714
O0513	-0.050935	0.006188	0.001703	M2302	-0.018512	0.008699	0.004689

SPECIMEN	PRIN1	PRIN2	PRIN3	SPECIMEN	PRIN1	PRIN2	PRIN3
M2303	0.066679	0.001968	0.002401	P0504	0.005590	0.001223	0.004695
M2304	-0.017282	0.025845	-0.001357	P0505	0.014986	0.003288	0.007238
M2305	-0.001636	0.010707	0.000833	P0506	0.033891	-0.021215	-0.002977
M2306	-0.052577	0.016193	-0.008611	P0701	0.015309	0.001123	-0.004999
M2307	-0.052626	0.000706	-0.001842	P0702	0.012054	0.007744	0.010748
M2308	-0.032491	0.016955	0.001655	P0703	0.066724	-0.002464	0.009276
M2309	0.002276	-0.006177	-0.002299	P0901	0.042092	-0.023279	0.002465
M2310	-0.011915	0.000620	0.000216	P1001	0.059960	-0.010082	-0.003842
M2401	-0.067142	0.007289	-0.003664	P1002	-0.030126	-0.002148	-0.006401
M2402	-0.035060	-0.005924	-0.005384	P1003	-0.055197	-0.005048	0.007512
D0101	-0.015125	0.002588	-0.002849	P1004	-0.063500	0.012975	-0.004298
D0102	0.042768	-0.003311	-0.001376	P1005	0.009745	-0.014179	-0.002028
D0103	0.021985	-0.018005	-0.003178	P1006	-0.043528	-0.000989	0.004491
D0201	0.003056	0.009515	-0.004538	P1401	-0.006051	-0.015585	-0.001563
D0202	0.001004	0.003045	0.005809	P1402	0.029650	-0.008224	-0.000685
D0203	0.011583	0.001386	-0.000434	P1403	-0.010470	-0.016546	-0.004260
D0204	-0.003528	-0.013599	-0.001181	P1404	0.006317	-0.005250	0.002732
D0205	-0.010093	0.000486	-0.004052	P1405	-0.004515	-0.022962	0.002699
D0206	-0.017449	0.011120	0.002193	P1406	-0.027656	0.004323	-0.001691
D0207	0.029073	-0.003720	-0.004539	P1407	-0.031471	0.001162	0.003208
W0101	-0.036439	0.003092	-0.006743	P1408	-0.028491	0.009861	-0.000040
W0102	0.020380	0.006127	0.002477	P1409	0.028463	-0.003064	-0.009075
W0103	0.049044	-0.007695	0.003594	P1501	-0.049290	0.014060	-0.003751
W0104	0.021013	-0.009216	0.000880	P1502	0.003186	0.018809	0.007615
W0105	0.008577	0.006978	0.005907	P1601	-0.006314	-0.003565	-0.005539
W0106	0.000164	0.003119	0.011771	P1602	-0.028851	0.002979	0.000791
W0107	0.034278	0.000875	0.002723	P1701	-0.001281	0.002872	-0.001744
W0108	0.028232	0.000620	-0.001597	P1702	0.011137	-0.011189	0.000687
W0109	0.009134	0.006986	0.004226	P1703	0.028720	0.009976	-0.001217
P0501	0.010568	0.002340	-0.005683	P1704	0.057502	-0.025975	0.008914
P0502	0.002315	-0.006843	-0.001415	P1705	0.002639	-0.000077	-0.002021
P0503	-0.023340	-0.012736	-0.006103				

Vita

DELPFINE E. WELCH

Education

PhD, Virginia Polytechnic Institute and State University, Geological Sciences, February 1991. GPA 3.89. Dissertation title: Geographical Variation and Evolution in the Middle Devonian Brachiopod, *Mucrospirifer*.

B.S. with Distinction, University of Wisconsin-Milwaukee, Geological Sciences, 1983. GPA 3.67 overall, 3.73 geology.

Emmanuel College, Boston, 1967-1969.

Professional Experience

Exploration Geologist, ARCO Oil and Gas Co., Houston, TX, start date March 4, 1991.

Geological Intern, BP Exploration, Houston, TX, 1989 (summer). Studied the effects of salt tectonics on the deposition and structure of the Wilcox Group in the western margin of the Houston salt diapir province.

Coordinator of Teaching Assistants, Department of Geological Sciences, VPI & SU, 1985, 1987, 1988. Prepared class materials and supervised teaching assistants of introductory laboratories.

Teaching Assistant, Department of Geological Sciences, VPI & SU, 1983-1989. Taught laboratory sections of Introductory Physical Geology, Introductory Economic Geology, Geology for Engineers, upper-level Invertebrate Paleontology, and upper-level Paleobotany.

Geological Intern, Sohio Petroleum Co., Dallas, TX, 1985 (summer). Used subsurface well information in a stratigraphic study of the Simpson Group sands in the Wichita Mountain Front of Oklahoma.

Secretary to the Director, Center for Great Lakes Studies, UW-Milwaukee, 1978-1983. Assisted the Director with administrative duties and coordinated office functions.

Departmental Technical Typist, Department of Chemistry, UW-Milwaukee, 1975-1978. Technical preparation of manuscripts and grant proposals.

Grants, Honors, and Memberships

Graduate Student Assembly Travel Fund Award, 1990-1991
Virginia Commonwealth Fellow, 1987-1988
Geological Society of America Research Grant, 1986-87, and 1987-88.

Graduate Research Development Project Award, VPI & SU, 1986-1987.
Sigma Xi Grant-in-Aid of Research, 1986-1987.
C. G. Tillman Award for Outstanding Teaching Performance by a Graduate Teaching Assistant, 1985.
National Association of Geology Teachers Summer Field Training Program Scholarship, 1983
Union Oil Company Foundation Scholarship, 1982-1983.
Elected to membership, Phi Kappa Phi, 1983.
Member, Paleontological Society.

Publications

Welch, D. E. 1990. Geographic variation and evolution in the shape of the Middle Devonian brachiopod, *Mucrospirifer*. Geol. Soc. Amer. Abstr. Prog., 22(7): A304.

Welch, D. E. 1990. Geographic variation and evolution in the shape of the Middle Devonian brachiopod, *Mucrospirifer*. Appalachian Basin Industrial Associates, 17: 278-297.